ASSESSING DIAGNOSTIC AND THERAPEUTIC TARGETS IN OBESITY-ASSOCIATED LIVER DISEASES

Noemí Cabré Casares

Assessing Diagnostic and Therapeutic Targets in Obesity-Associated Liver Diseases

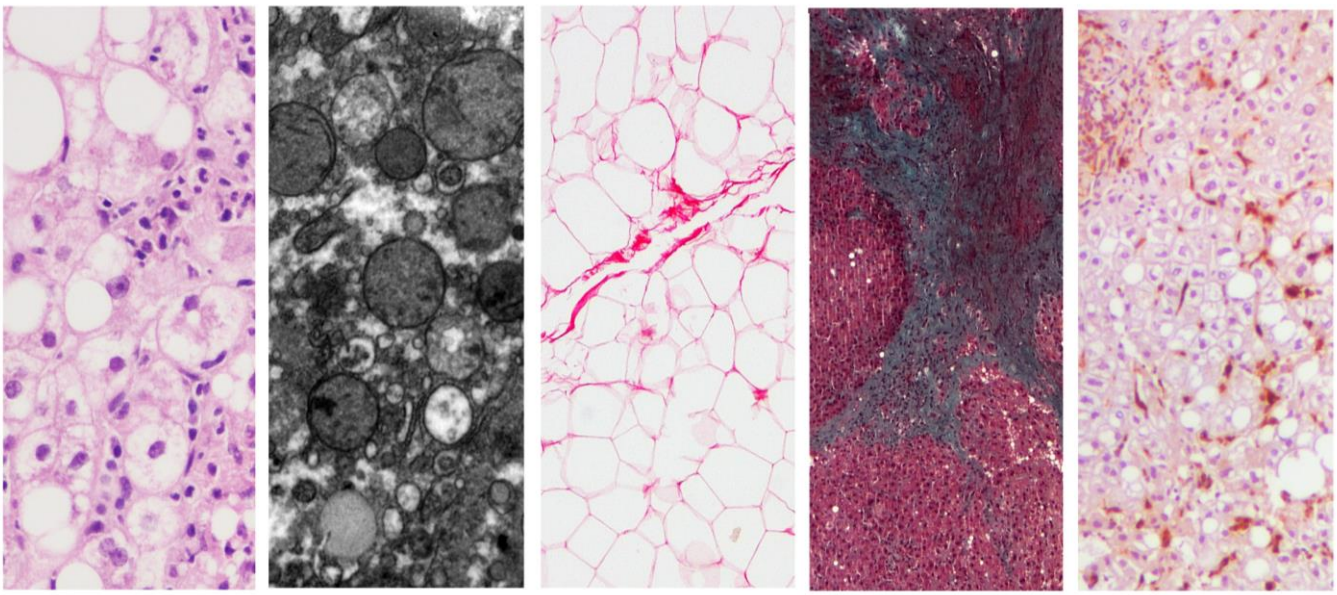

Noemí Cabré Casares

Doctoral Dissertation, 2019

UNIVERSITAT ROVIRA i VIRGILI

UNIVERSITAT ROVIRA I VIRGILI
ASSESSING DIAGNOSTIC AND THERAPEUTIC TARGETS IN OBESITY-ASSOCIATED LIVER DISEASES
Noemí Cabré Casares

UNIVERSITAT ROVIRA I VIRGILI
ASSESSING DIAGNOSTIC AND THERAPEUTIC TARGETS IN OBESITY-ASSOCIATED LIVER DISEASES
Noemí Cabré Casares

UNIVERSITAT ROVIRA I VIRGILI
ASSESSING DIAGNOSTIC AND THERAPEUTIC TARGETS IN OBESITY-ASSOCIATED LIVER DISEASES
Noemí Cabré Casares

Noemí Cabré Casares

Assessing Diagnostic and Therapeutic Targets in Obesity-Associated Liver Diseases

Doctoral Dissertation

Supervised by

Dr. Jorge Joven Maried

Department of Medicine and Surgery

UNIVERSITAT
ROVIRA i VIRGILI

Reus
2019

UNIVERSITAT ROVIRA I VIRGILI
ASSESSING DIAGNOSTIC AND THERAPEUTIC TARGETS IN OBESITY-ASSOCIATED LIVER DISEASES
Noemí Cabré Casares

UNIVERSITAT ROVIRA i VIRGILI

FACULTAT DE MEDICINA I CIÈNCIES DE LA SALUT
DEPARTAMENT DE MEDICINA Y CIRUGIA

Carrer Sant Llorenç, 21
43201 Reus
Tel. 977 759 306
Fax. 977 759352

TO WHOM IT MAY CONCERN

I STATE that the present study, entitled **"Assessing Diagnostic and Therapeutic Targets in Obesity-Associated Liver Diseases"**, presented by **Noemí Cabré Casares** with the purpose of obtaining the degree of Doctor, has been carried out under my supervision at the **Department of Medicine and Surgery** of this University.

Reus, 1th June 2019

Doctoral Thesis Supervisor

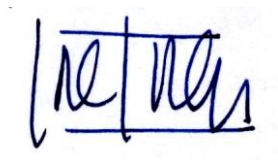

Prof. Jorge Joven Maried

UNIVERSITAT ROVIRA I VIRGILI
ASSESSING DIAGNOSTIC AND THERAPEUTIC TARGETS IN OBESITY-ASSOCIATED LIVER DISEASES
Noemí Cabré Casares

"Be the best you can be. Today the competition is fierce, the funds are tight, and the only way you can do something is by being extremely good at what you do."

Elizabeth Neufeld, PhD
Originally appeared in Albert and Mary Lasker Foundation

UNIVERSITAT ROVIRA I VIRGILI
ASSESSING DIAGNOSTIC AND THERAPEUTIC TARGETS IN OBESITY-ASSOCIATED LIVER DISEASES
Noemí Cabré Casares

A la meva família,

UNIVERSITAT ROVIRA I VIRGILI
ASSESSING DIAGNOSTIC AND THERAPEUTIC TARGETS IN OBESITY-ASSOCIATED LIVER DISEASES
Noemí Cabré Casares

Acknowledgements

UNIVERSITAT ROVIRA I VIRGILI
ASSESSING DIAGNOSTIC AND THERAPEUTIC TARGETS IN OBESITY-ASSOCIATED LIVER DISEASES
Noemí Cabré Casares

En primer lloc m'agradaria agrair el suport a totes aquelles persones que, en major o menor mesura, m'han acompanyat durant aquesta apassionant aventura. Cada granet de sorra ha estat imprescindible per a què, finalment, aquest manuscrit hagi agafat forma i, a hores d'ara se'l pugui anomenar la "tesi".

Al Prof. Joven, el meu mentor, la primera persona que va veure "quelcom" en mi el mateix dia que ens vam conèixer, ara fa 8 anys... Durant tot aquest temps s'ha esforçat en inculcar-me una sèrie de valors resumits en frases com: "net i polit", "no te fíes ni de tu padre", "has entès aquesta lliçó?", "les coses s'han de fer bé a la primera"... que amb el pas dels anys he après a valorar i entendre millor. Gràcies per la seva paciència i per haver-me donat l'oportunitat de créixer en aquest món tan sacrificat com és el de la ciència.

Al Dr. Camps, sempre disposat a ajudar-nos. Sóc incapaç de comptar la quantitat d'hores que has passat amb mi ajudant-me a elaborar el que avui és el fruit de tant de temps invertit en mi. Moltes gràcies pel teu suport incondicional. M'has animat a seguir endavant amb tota la força i il·lusió possibles, tot i les dificultats que hem anat trobant pel camí, que no han estat poques.

Al Dr. Durán, todavía recuerdo el primer día que leí su nombre, y la consecuente insistencia para conseguir contactar con él. No habría imaginado que poco después formara parte de esta aventura siendo un referente indiscutible tanto en el ámbito conceptual como profesional. Muchas gracias por la sabiduría que me ha transmitido.

Al Dr. Vendrell i la Dra. Fernández, i en general a tots els membres del DIAMET, pels consells rebuts i l'ajuda prestada, però sobretot per l'oportunitat de participar i defensar el treball del dia a dia en aquelles tardes de dimecres. Hem viscut molt bons moments junts.

Al Prof. Domingo i al Dr. Nadal, gràcies per l'oportunitat de deixar-me endinsar en el món dels elements traça i guiar-nos durant aquests anys.

Al Salva i la Anna, els post-docs del grup, heu estat un dels pilars fonamentals durant aquesta etapa. Tinc molt present els dies amb el "Salvi al Cuelpo" i les inacabables classes de metabolòmica...quina aventura! No podré agrair-vos suficientment, en especial a l'Anna, tota la dedicació emprada en mi mentre era la seva "nena de pràctiques". Moltes gràcies als dos.

Al Gerard i la Eli, les noves generacions. Sabeu que confio en vosaltres i estic convençuda que heu après a ser crítics a l'hora de prendre decisions. Sé que la vostra aventura té molt de recorregut per endavant i que la portareu a terme amb il·lusió i energia. Moltes gràcies per totes aquelles tardes de riures, plors i, com no, de reflexions intentant idealitzar un món millor.

.

Als meus alumnes, els meus nens, heu aconseguit que aquests anys no tan sols hagi descobert la meva passió per la ciència sinó també per la docència. M'enorgulleixo recordant la vostra evolució del primer dia al últim. No us podeu imaginar quin canvi!

A tots els que han format part de la meva aventura americana, Dr. Vondriska, Manuel, Doug, Max and Yuki. First, Dr. Vodnriska, I greatly appreciate the opportunity you gave me to join your team as member of your lab. Thank you very much for teaching and guiding me during these 3 months. Doug, my mentor of bioinformatics, and the best student in Catalan culture I have ever seen. Thank you for everything. Manuel, mi guía incondicional incluso meses antes de que cruzara el charco. Gracias por tu apoyo y asesoramiento, aunque sea desde la distancia, sé que siempre estás disponible para solucionar todos "mis pequeños y no tan pequeños desastres".

A la Fedra, la meva siamesa, companya de feina i amiga. Ambdós sabem que sense haver-nos tingut l'una a l'altra no ho hauríem aconseguit. Ens hem complementat per seguir endavant tot i les dificultats. Mai tindré prou paraules per agrair-te que hagis format part d'aquesta etapa que ara tanquem. Estic convençuda que això només ha estat el principi de molts èxits que ens han d'acompanyar.

A tots els meus amics que, tot i ser conscients de la complexitat dels engranatges que configuren aquest món de la ciència, m'heu donat el vostre suport sempre que l'he necessitat.

Finalment, la meva família. En totes i cada una de les paraules que conformen aquest escrit hi ha una mica de la vostra essència. Aquests quatre anys que s'iniciaven en forma d'una vertadera muntanya russa d'emocions han acabat transformant-se en una interminable marató d'obstacles. El denominador comú en la superació de cada entrebanc heu estat vosaltres. M'heu empès a reflexionar i a cercar la motivació quan ja no sabia ni on més buscar. El vostre suport, la vostra esperança i el vostre amor estan en cada pàgina.

Moltes gràcies a tots!

Contents

UNIVERSITAT ROVIRA I VIRGILI
ASSESSING DIAGNOSTIC AND THERAPEUTIC TARGETS IN OBESITY-ASSOCIATED LIVER DISEASES
Noemí Cabré Casares

Abbreviations

UNIVERSITAT ROVIRA I VIRGILI
ASSESSING DIAGNOSTIC AND THERAPEUTIC TARGETS IN OBESITY-ASSOCIATED LIVER DISEASES
Noemí Cabré Casares

α -KG: α-Ketoglutarate

α-SMA: α smooth muscle actin

β-HB: β-Hydroxybutyrate

1-C: One carbon

4EBP1: Eukaryotic translation initiation factor 4E-binding protein 1

4-HNE: 4-hydroxy-2-nonenal

5-hmC: 5-hydroxymethilcytosine

5-mC: 5-methylcytosine

5-mTHF: 5-methyltetrahydrofolate

ACC: Acetyl-CoA carboxylase

AFLD: Alcoholic fatty liver disease

AKT: Protein kinase B

ALT: Alanine aminotransferase

AMPK: AMP activate protein kinase

AP-1: Activator protein 1

AST: Aspartate aminotransferase

ATG: Autophagy related protein

ATGL: Adipose triglyceride lipase

ATP: Adenosine triphosphate

B2M: Beta-2-Microglobulin

BC: Bariatric surgery

BHMT: Betaine-homocysteine methyltransferase

BMI: Body mass index

CaMKK: Calmodulin-dependent protein kinase

CCL2: C-C motif ligand 2

CCR2: C-C motif chemokine receptor type 2

CD163: Cluster of differentiation molecule 163

ChREBP: Carbohydrateresponsive element-binding protein

CMA: Chaperone-mediated autophagy

DAG: Dialcyl-glyceol

DHF: Dihydrofolate

DNL: de novo lipogenesis

DNMT: DNA methyltransferases

Drp: Dynamin relate protein

ECM: Extracellular matrix

ER: Endoplasmic reticulum

FAD: Flavin adenine nucleotide

FAO: Fatty acid oxidation

FASN: Fatty acid synthase

FAT: Fatty acid translocase

FATP: Fatty acid transport protein

FFA: Free fatty acid

FH: Fumarate hydratase

FOXO1: Forkhad box protein O1

G-CSF: Granulocyte colony-stimulating factor

GDP: Guanosine diphosphate

GLUT-4: Glucose transporter 4

GPCRs: G-protein-coupled cell surface receptors

GSH: Reduced glutathione

GSSG: Glutathione disulfide

H2O2: Hydrogen peroxide

HATs: Histone acetyltransferases

HCC: Hepatocellular carcinoma

HDL: High density lipoprotein

HIF-1α: Hypoxia-inducible factor-KB

HSC70: Heat shock cognate 71 protein

HSCs: Hepatic stellate cells

IDH: Isocitrate dehydrogenase

IFN-α: Interferon alpha

IKK: IkB kinase

IL: Interleukin

IP3: Phosphatidylinositol 1.4.5 triphosphate

IRS: Insulin receptor substrate

JNK: Protein N-terminal kinase

KC: Kupffer cell

LAMP2A: lysosome associated membrane protein type 2

LC3: Microtubule-associated protein 1A/1B-light chain 3

LDL: Low density lipoprotein

LKB1: Liver kinase B1

LPL: Lipoprotein lipase

LPS: Lipopolysaccharide

LSG: Laparoscopic sleeve gastrectomy

MDA: Malondialdehyde

Mfn2: Mitofusin 2

MRC: Mitochondrial respiratory chain

mTOR: Mammalian target of rapamycin

NAD: Adenine dinucleotide

NADPH: Nicotinamide adenine dinucleotide

NAFL: Non-alcoholic fatty liver

NAFLD: Non-alcoholic fatty liver disease

NASH: Non-alcoholic steatohepatitis

NCD: Non-communicable disease

NEFAs: Non-esterified fatty acids

NF-κB: Nuclear factor κB

NO: Nitric oxide

NRF2: NF-E2 related factor 2

OPA1: Optic atrophy protein

OXPHOS: Oxidative phosphorylation

PDGF: Platelets derived growth factor

PI3K: Phosphatidylinositol 3 kinase

PINK1: Protein kinase 1

PIP2: Phosphatidylinositol 4.5 diphosphate

PIP3: Phosphatidylinositol triphosphate

PKC: Protein kinase C

PLC: Phospholipase

PNPLA3: Patatin-like phospholipase domain-containing protein 3

PON: Paraoxonase

PUFA: Polyunsaturated fatty acids

Ractor: Regulatory associated protein of mTOR

Rictor: Rapamycin-insensitive companion

ROS: Reactive oxygen species

RYGB: Roux-en-Y gastric bypass

S6K: S6 kinase

SAH: S-adenosylhomocysteine

SAM: S-adenosylmethionine

SDH: succinate dehydrogenase

SGK: Serum/glucocorticoid regulated kinase

SNP: Single-nucleotide polymorphism

SOD: Superoxide dismutase

SREBP-1: Sterol regulatory element-binding protein 1

STAT3: Signal transducer and activator of transcription 3

T2DM: Type 2 diabetes mellitus

TAG: Triglyceride

TCA or CAC: Tricarboxylic acid cycle or citric acid cycle

TET: Ten- Elven translocation

TFEB: Transcription factor EB

TFG-β: Transforming grow factor

THF: Tetrahydropholate

TLRs: Toll-like receptor

TM6SF2: Transmembrane 6 superfamily member 2

TNFR: Tumor necrosis factor receptor

TNFα: Tumor necrosis factor alfa

TSC: Tuberous sclerosis complex

ULK1: Unc-51 like kinase 1 complex

VLDL: Very low-density lipoproteins

Abstract

UNIVERSITAT ROVIRA I VIRGILI
ASSESSING DIAGNOSTIC AND THERAPEUTIC TARGETS IN OBESITY-ASSOCIATED LIVER DISEASES
Noemí Cabré Casares

Overnutrition and decreased physical activity promote obesity and associated diseases, which are currently leading causes of morbidity and mortality worldwide. High prevalence and heterogeneity of obesity-related metabolic consequences, collectively known as the metabolic syndrome, is a global epidemic associated with a wide variety of comorbidities. A hallmark of type III obesity (BMI > 40 kg/m^2) is a failed attempt to adapt to metabolic perturbations caused by increased food intake. In this context, the role of the liver is crucial. The liver is particularly susceptible to the metabolic perturbations caused by obesity. Most patients with severe obesity have some degree of non-alcoholic fatty liver disease (NAFLD). If untreated or undetected, NAFLD often progresses to non-alcoholic steatohepatitis (NASH) and other subsequent life-threatening diseases with poor prognosis (e.g., cirrhosis or hepatocellular carcinoma). In NASH patients with obesity-associated metabolic disorders, NASH is a serious and underdiagnosed condition. The absence of non-invasive markers for its diagnosis hampers clinical practice and the development of pharmacological treatments.

The prevalence of NAFLD increases almost linearly with body mass index (BMI) and remains closely associated with type 2 diabetes mellitus (T2DM). The mechanisms linking these conditions remain unexplained. The scenario is not completely understood, but the hepatic alterations caused by oxidative stress, mitochondrial dysfunction and hepatocellular death are likely to be critical. Thus, NAFLD may be considered *per se* a multisystemic disease with important contributions to maladaptive responses of multiple regulatory pathways.

There are no specific pharmacological interventions approved for NAFLD/NASH treatment, and targeting obesity remains the cornerstone of clinical management, as weight loss appears associated with improvement in histologic features of NASH. Lifestyle modifications and/or currently approved anti-obesity medications rarely accomplish the objective and maintain the necessary amount of weight loss. Obese patients, however, might represent a unique research opportunity in searching for noninvasive biomarkers of liver alterations. In particular, these patients are likely candidates for bariatric surgery (BS) that can achieve rapid weight loss and/or resolve comorbidities, including NASH.

Oxidative stress is related to the onset and development of liver diseases. Excessive nutrient intake impairs the redox status in the liver, which stimulates inflammation. The molecular mechanisms

accounting for these alterations involve alterations of enzyme activity, post-translational modifications of proteins and activation of nuclear receptors; the consequence is a global modification of metabolic networks. In our **first study** we investigated the molecular mechanisms underlying the presence of hepatic alterations and its remission after BS. We analyzed changes in the circulating levels and hepatic expression of markers of oxidative stress and inflammation in patients with morbid obesity. Results showed that one year after BS liver histology features improved in all patients and that this improvement was greater in severe cases of NAFLD including those with steatohepatitis, bridging fibrosis or cirrhosis. Significant pre-surgery differences in plasma and liver markers of oxidative stress and inflammation (chemokine C-C motif ligand 2, paraoxonase-1, galectin-3, and sonic hedgehog, among others) were observed between patients with, and those without, NASH. Patients showed a consistent improvement of oxidative stress and inflammatory processes and these data encourage the use of BS as a therapeutic option to improve or resolve NAFLD.

NASH is often asymptomatic and laboratory or imaging techniques may help to suspect the disease. However, discrimination of obese patients with or without NASH ultimately requires liver biopsy, an invasive procedure with potential difficulties. Equally, the accurate assessment of pharmacologic approaches requires repeated liver biopsies, which are unrealistic. The choice of potential therapeutic targets needs to consider that NASH is a multisystem disease with an important mitochondrial contribution to the defective metabolic responses. Mitochondrial dysfunction eventually perturbs energy and one-carbon (1-C) metabolism. In the **second study** we hypothesized that plasma levels of metabolites from these pathways would highlight the prominent role of liver disease in regulating metabolic changes, and might provide clinically useful biomarkers. We performed measurements in samples from type III obese patients undergoing BS to identify specific metabolic patterns and to test the diagnostic ability to distinguish between patients with and without NASH. We confirmed that plasma mitochondrial metabolites could mitigate the need for liver biopsy to evaluate the effectiveness of therapies in NASH patients. Targeted plasma metabolic profiles identified connections between human liver metabolism and morbid obesity. Combined models of single or paired plasma measurements of α-ketoglutarate (α-KG), β-hydroxybutyrate, pyruvate and oxaloacetate reduced the uncertainty in clinical diagnosis of NASH and predicted NASH remission.

In the **third study** we provided evidence that mitochondrial dysfunction is at the center of the transition from relatively benign hepatic steatosis to NASH. Hepatic accumulation of α-KG via glutaminolysis appears to be a crucial checkpoint for NASH development, underscoring the signaling functions of mitochondrial metabolites in hepatocytes under stress conditions. We demonstrated that α-KG is a key metabolite of energy homeostasis that modulates hepatocyte death in NASH patients through mammalian TORC1 (mTORC1). However, after BS, the mitochondrial oxidative metabolism and the autophagy-lysosomal function compromised in NASH patients were also completely restored. AMPK activation in hepatocytes abrogated the effects of glutaminolysis and/or α-KG in modulating cell death through mTORC1-driven pathways, supporting the potential use of mTORC1 inhibitors and the future assessment of glutaminase and/or α-KG dehydrogenase as potential therapeutic targets. Finally, we confirm that metabolites may promote epigenetic changes affecting DNA methylation and likely post-translational modifications on enzymes regulating liver energy metabolism. Our data indicated the plausible importance of altered DNA methylation in the pathogenesis of NASH and we propose the significant hypermethylation of TDRD6 promoter in NASH livers and the significant hypomethylation of ACP5, C1orf54 and HDAC9 promoters as potential candidates in future research.

Introduction

UNIVERSITAT ROVIRA I VIRGILI
ASSESSING DIAGNOSTIC AND THERAPEUTIC TARGETS IN OBESITY-ASSOCIATED LIVER DISEASES
Noemí Cabré Casares

1. Obesity: an epidemic disease

Obesity, considered by many as a 21st century epidemic, is one of the greatest public health diseases worldwide (1). At present time, obesity is defined as a disproportionate body weight with an excessive accumulation of adipose tissue that is usually accompanied by mild, chronic or systemic inflammation. Obesity is a major risk factor for developing a number of metabolic or non-communicable diseases (NCDs), including cardiovascular diseases, cancer and diabetes mellitus, thus representing the leading causal factor for death and premature disability (2).

The most common method for classifying obesity degree is an increase in fat mass, named body mass index (BMI). Even though the BMI is an unreliable measure of obesity, it is still the most commonly used. BMI grossly estimates adiposity and identifies overweight and obesity based on weight of the individual expressed in kilograms (Kg) and divided by the square of the height in meters (m^2). The World Health Organization (WHO) defines obese as having a BMI more than 30 kg/m^2. Moreover, obesity is also divided in three different degrees: class I (30.0 > BMI > 34.9), class II (35 > BMI > 39.9) and class III (BMI > 40) (3, 4).

According to the WHO, more than 2.1 billion adults were estimated to be overweight or obese globally in 2016. Furthermore, there is also an alarming increase in globally prevalence rates of overweight and obesity among children and adolescent population. In 2013, 42 million of children under the age of 5 were overweight or obese (5, 6).

Although overweight and obesity are considered a problem of developed countries, their prevalence is increasing in lower and middle-income countries, particularly in urban surroundings. In these developing countries with emerging economies, the rate of this health problem is around 30% higher than in developed countries (3). Therefore, obesity is a risk factor of increasing magnitudes, with clinical importance, which should be monitored systematically and rigorously. Future can be very worrying, if remedy is not provided, as the WHO extrapolation of existing data suggests that by 2025 obesity levels could reach 45–50 % in the US and Western Europe, 30–40 % in Australia, and over 20 % in India (7).

The increasing prevalence of obesity is influenced by an inverse interaction between obesity and socioeconomic class. It seems to be related to genetic, metabolic, behavioral, environmental and economic changes, inherent to modern society (Figure 1) (8, 9). Overall, these factors create an obesogenic environment. This term has been coined to express the sum of influences, opportunities, or conditions of the environment in which one is more susceptible to gain weight (10).

In the past 3 decades, globalization and modernization have promoted growing availability of abundant, cheap, energy-rich and highly palatable foods, together with highly pervasive and persuasive marketing, creates a "*push effect*" that drives overconsumption of calories. At the same time, energy expended in physical activities has decreased as people spend more time doing sedentary life style. Finally, hereditary factors (genetics, family history, racial/ethnic differences), epigenetic fluctuations and our sociocultural system have been shown to influence the risk of obesity. Nowadays, it is increasingly recognized that people are driven to become more overweight and obese as a result of this obesogenic environment (11, 12).

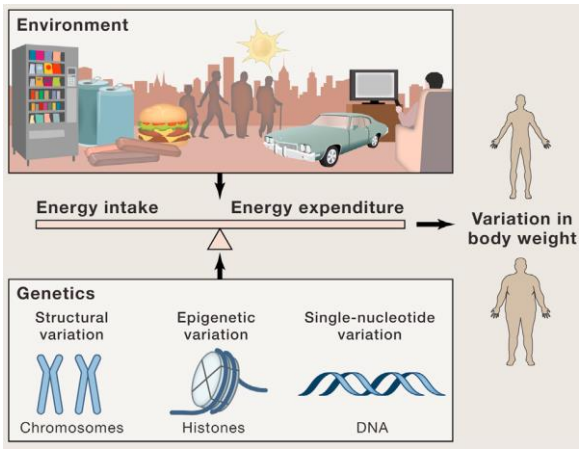

Figure 1. Obesogenic environment contributes to weight gain. The present environment potently facilitates the development of obesity. The increment of human adiposity is influenced by complex interactions between genetic and epigenetic influences. Excessive energy intake has a major impact on energy expenditure, whereas numerous other environmental factors, such as television watching, leisure activities, and transport, negatively affect energy expenditure. Variations in body fat and BMI in large part influenced by genetic alterations modulate energy homeostasis by either decreasing energy expenditure or increasing energy intake. Picture from van der Klaauw AA *et al.* (12)

At a social level, obesity is associated with disability, mortality, and substantial health costs. Nevertheless, at an individual level, severe obesity is often associated with a multitude of clinical problems, including metabolic perturbations, sleep disturbances, respiratory difficulties, mobility issues, as well as considerable social stigma, which can affect quality of life (13).

1.1. Obesity-related comorbidities and mortality

Obese patients have an increased risk of developing many health complications, known as comorbidities. By definition, comorbidity is the presence of two or more additional disorders coexisting with a primary disease, which can contribute to premature death. In the context of obesity, there are metabolic diseases (for example type 2 diabetes mellitus [T2DM]) and fatty liver diseases), cardiovascular diseases (hypertension, stroke and atherosclerosis), Alzheimer's disease and some types of cancer (for example in breast, liver, pancreas, ovarian, kidney and colon) (14-17).

Although obesity is associated with several metabolic disturbances, all obese humans are not equal and approximately 20% of patients with severe obesity have a normal metabolic profile. The authors define these obese individuals as "*metabolically healthy*" obese. However, most obese patients are "*metabolically unhealthy*". Nowadays, the reason of these two phenotypes is unknown. Differences in glucose tolerance, inflammatory response, adipose tissue distribution, adipokine secretion and age may be an explanation to this phenomenon. Thus, obesity is a heterogeneous disorder with variable risk profile (18).

Obesity can be considered an inflammatory disease nature, characterized by a chronic systemic low-grade inflammation, where different kinds of cytokines are involved. In obese individuals, adipose tissue releases increased amounts of non-esterified fatty acids, glycerol, hormones, pro-inflammatory cytokines and other factors that are involved in the development of insulin resistance, which is a major trigger for T2DM. Evidence from several studies indicates that obesity and weight gain are associated with an increased risk of diabetes and many of these metabolic changes in obesity seem to be associated with insulin resistance (19, 20).

Dramatic changes in diet and lifestyle of the worldwide population are triggering obesity as a global epidemic. Obesity is associated with a major risk factor for metabolic organs, and the relationship between obesity and liver disease was described several decades ago (21). Furthermore, the prevalence of obesity-related liver diseases has also certainly increased, becoming the most common cause of chronic liver disease in adults and children (22).

2. Nonalcoholic Fatty Liver Disease: a spectrum of clinical and pathological severity

The liver is a vital organ that is involved in a wide range of functions that are important to metabolic homeostasis. Accordingly, liver diseases can promote a high number of pathologies (23). In 1980, Ludwig described the status of a group of patients who, without significant alcohol consumption, showed the same histopathological changes than those who had a liver disease associated with alcoholism. Therefore, this find is known to be the first histopathologic description of Nonalcoholic Fatty Liver Diseases (NAFLD) (24).

By definition, NAFLD disorder is characterized by a broad spectrum of hepatic derangements ranging from simple steatosis and non-alcoholic steatohepatitis (NASH) to liver cirrhosis and hepatocellular carcinoma (HCC) (25). Whereas simple steatosis remains a benign process in most affected individuals, the presence of liver inflammation (as observed in NASH) is the driving force for the development of fibrosis and cirrhosis (26).

In the past 30 years, NAFLD was the leading cause of chronic liver disease in developing countries (27). The prevalence of NAFLD is constantly increasing. It rose from an estimated 15 % in 2010 to a 25% in 2015, and likewise, the rate of NASH in the same timeframe has almost doubled, where the overall NASH prevalence estimated among biopsied NAFLD patients was 59.1% in 2015 versus 33% estimated in 2010. NAFLD is widespread in all continents, but the highest rates are reported from South America (31%), followed by Asia (27%), the USA (24%) and Europe (23%), whereas NAFLD is less common in Africa (14%) (28, 29).

During the last two decades, approximately one-quarter of the European population is has been affected by NAFLD. In this context, a 2016 meta-analysis reported an average prevalence of 23.71% in Europe, with a variability ranging from 5% to 44% in different countries (27, 30). Along the same line, epidemiological data from Spain describe similar results, with a NAFLD prevalence of 25.8% in the adult population (31). The data of incidence rates and trends in the global NAFLD pandemic are unknown. NAFLD is now more common than alcoholic fatty liver disease and it is thought that NAFLD is set to replace viral hepatitis as the primary cause of end-stage liver disease and liver transplantation over the next decade (32).

2.1 Pathogenesis and mechanism of NAFLD progression

NAFLD is a spectrum of liver disorders (Figure 2). It is defined by the presence of lipid accumulation, also known as steatosis, in the absence of excessive alcohol consumption (25, 33). NAFLD comprises the benign non-alcoholic fatty liver (NAFL), and a more severe form referred to as NASH. NASH is characterized by the presence of steatosis, hepatocellular ballooning, lobular and portal inflammation, apoptosis, necrosis and almost always hepatic fibrosis. To regenerate new cells, NASH progresses to cirrhosis, where the hepatocytes are replaced by scar tissue made of type I collagen produced by stellate cells. Lastly, cirrhosis is an end-stage phase with organ failure that requires liver transplantation or may lead to the development of HCC and liver failure (34, 35).

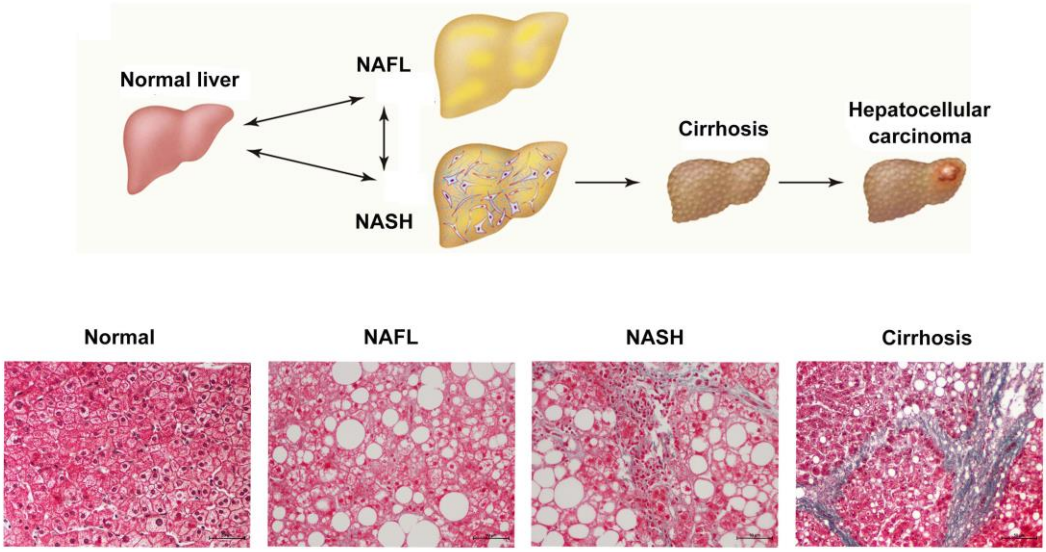

Figure 2. NAFLD disease spectrum. Schematic representation of NAFLD progression. The benign form of NAFLD, progresses to NASH with or without fibrosis. NASH leads to cirrhosis and eventually hepatocellular carcinoma (HCC). NASH may progress to HCC without going through the cirrhosis stage. Histological sections illustrating normal liver, steatosis, NASH, and cirrhosis. Picture modified from Cohen *et al*. (34).

The pathophysiology of NAFLD has not been resolved and, nowadays the mechanisms leading to NAFLD are still unclear. Several mechanisms have been proposed, but insulin resistance seems to have crucial importance in the development and progression of NAFLD (36). The pathological progression of NAFLD follows tentatively a "*three-hit*" process namely: steatosis, lipo-toxicity and inflammation. Overall, fat accumulation on the liver (1st hit) augments vulnerability to oxidative stress (2st hit), which triggers inflammation, endoplasmic reticulum (ER) stress, mitochondrial

dysfunction and the incapacity of hepatocytes to synthesize endogenous antioxidants (3rd hit). However, the existence of various parallel factors acting in synergy and the growing evidence of genetic predisposition of some individuals made evident that this view was too simplistic to recapitulate the complexity of this disease (37). Thus, a "*multiple-hit*" hypothesis was developed and substituted the outdated hypothesis for the origin and progression of NAFLD (36, 38).

2.2.1 Genetics and NAFLD

Although NAFLD is typically characterized by an obesity-related excess of adiposity and insulin resistance, seems that genetic factors are important determinants for the NAFLD condition. Genome-wide association studies have identified novel loci associated with disease severity (39-42). To this day, modifications in 2 two genes have been shown to influence NAFLD predisposition and progression. The first single-nucleotide polymorphism (SNP) has been identified in PNPLA3 (encoding patatin-like phospholipase domain-containing protein 3) (39). PNPLA3 (rs738409; c.444 C>G; p.I148M) is a non-synonymous cytosine to guanine nucleotide transversion mutation that results in an isoleucine to methionine amino acid change at codon 148. PNPLA3 variant have been associated with the severity of NASH and fibrosis. It is expressed in white adipose tissue and liver, and its expression is nutritionally regulated, and it increases with obesity (43). The second of these genes encodes transmembrane 6 superfamily member 2 (TM6SF2), with a non-synonymous SNP (rs58542926; c.449 C>T; p.E167K) (41). TM6F2 variant is also associated with progressive NAFLD and acts as a regulator of liver triglyceride content and plasma total cholesterol levels (44).

Genetic predisposition must be placed in the context of environmental factors. Even though major advances uncovering the genetic basis for the heritability of NAFLD have been done, heritable mechanisms not encoded in the DNA sequence are emerging. Discordant NAFLD in genetically identical twins has been explained by microRNAs (45), and epigenetic factors might also be a mechanism through which environmental exposures exert a heritable effect on disease risk (46). Genetic endowment and epigenetic modifications have an important effect in the liver fat content, enzymatic processes, and the liver inflammatory environment, hence influencing the progressing of NALFD to NASH or persisting in a stable stage. Therefore, the pathogenesis of NAFLD seems to be a vicious cycle resulting in intricate alterations in the histopathological and biochemical features of the liver.

2.1.2 Pathophysiology of NAFLD

The liver has a remarkable metabolic plasticity that performs important biochemical functions necessary for metabolic homeostasis, and it is one of the principal regulators of glucose and lipid metabolism. In NAFLD, numerous disorders modify the liver's capacity to process lipids and it has been linked to multifactorial alterations in peripheral tissues, including skeletal muscle and adipose tissue (26).

The initial stage of NAFLD involves over-accumulation of various lipids or lipid droplets, mostly observed in cases of obesity. Most lipids that accumulate in the liver are derived from increased uptake of circulating free fatty acids (FFA) and upregulated endogenous synthesis of FFAs. Dietary intake affects the metabolism of the human body and plays an important role in the development of NAFLD. Therefore, the amount of lipids present in hepatocytes represents a complex interaction among: 1) hepatic fatty acid uptake of plasma FFA released from lipolysis in adipose tissue and from the hydrolysis of circulating triglycerides, 2) *de novo* lipogenesis (DNL), 3) decreased fatty acid oxidation (FAO), and 4) reduction of hepatic lipid exportation via very low-density lipoproteins (VLDL) (Figure 3) (47, 48).

Adipose tissue has an important role in the accumulation of hepatic lipids in the settings of obesity-associated NAFLD (49). Adipose tissue has several functions in the organism, and the principal is to accumulate energy as triglycerides (TAG), that are released as FFA when other tissues need them. In normal conditions, insulin stimulates glucose transporter 4 (GLUT-4) in adipose tissue and promotes re-esterification of FAA into TAG storage. However, obese patients have an excess of FFA and if the caloric excess persists, the fat depots reach their maximum storage capacity and appears to trigger a cascade of different events (50). First, weight gain is associated with a marked expansion of adipose tissue, which leads to adipocyte's growth in size (hypertrophy) and they accumulate more fat by the activation of lipoprotein lipase (LPL). Second, there is a differentiation of pre-adipocytes into new adipocytes (adipogenesis). Subsequently, it leads to an increase of the number of adipocytes (hyperplasia), which results in the dysfunction and eventual adipocyte death (51).

Insulin resistance is one of the key factors in the development of steatosis/NASH (52). Insulin resistance compromises the ability of adipocytes to store fat and TAG in adipocytes are mobilized through lipolysis releasing FFA into circulation and they are transported to other tissues, for

example, liver or muscle (53, 54). Fatty acids are primarily delivered to the liver from blood following lipolysis of TAG in adipose tissue, a process that is regulated by actions of insulin on adipocytes. Hepatocytes take up these FFA via fatty acid transport proteins (FATPs) and fatty acid translocase (FAT/CD36). FFA accumulation in hepatocytes promotes the synthesis of triglycerides; during this process, the production of diacyl-glycerols (DAGs) has been implemented as a cause of hepatic insulin resistance and the conversion from TAG to DAG is mediated by adipose triglyceride lipase (ATGL). DAG activates protein kinase Cε (PKCε) membrane translocation to inhibit insulin receptor kinase and decrease insulin signaling (55-57).

Hepatic lipids that are not esterified also induce endoplasmic reticulum stress, leading to the activation of c-Jun N-terminal kinases (JNKs) and nuclear factor – kappaβ (NF-κβ). JNKs and NF-κβ are two major regulators of inflammatory pathways that also inhibit phosphorylation of insulin receptor substrate-1 (IRS-1), aggravating hepatic insulin resistance and increasing intra-hepatic cytokine production. The synthesis of DAGs is intimately related to inflammatory pathways, and DAGs may also contribute to hepatic production of inflammatory cytokines [e.g., tumor necrosis factor-α (TNF-α), interleukin (IL)-6, IL-1] (47, 52, 58). These cytokines meditate inflammation in NASH through the recruitment and activation of Kupffer cells (resident hepatic macrophages) (59).

Moreover, the liver itself can contribute to hepatic steatosis by producing lipid from carbohydrate in DNL process. In healthy liver, DNL is not a main source of hepatic lipid, but in the setting of obesity and hyperinsulinemia, DNL can contribute as much as 25% of total hepatic lipid stores, and is considered an important factor in the development of NAFLD (60, 61). The enzymes for DNL are upregulated by insulin and glucose through the action of two transcription factors, sterol regulatory element-binding protein 1 (SREBP-1c), which transcriptionally activates most genes required for lipogenesis, and carbohydrateresponsive element-binding protein (ChREBP) (62). ChREBP, also regulated by glucose, which induces gene expression of liver-type pyruvate kinase, a key regulator enzyme in glycolysis (63).

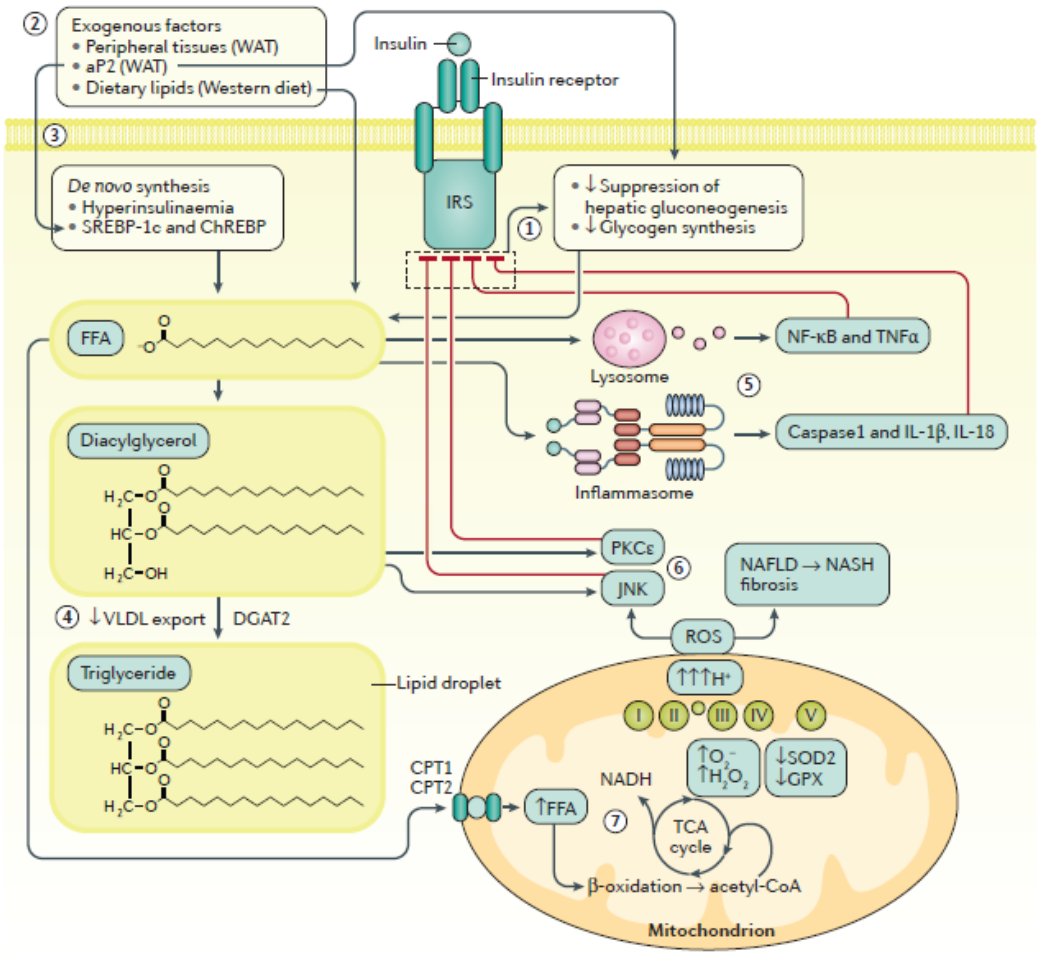

Figure 3. Pathophysiological aspects in NAFLD: role of lipids and insulin resistance in energy metabolism.
NAFLD is associated with hepatic and peripheral insulin resistance, resulting in an insufficient suppression of hepatic gluconeogenesis, decreased glycogen synthesis and increased lipid accumulation (1). High amounts of free fatty acids (FFA) are attributed to an increased delivery from white adipose tissue. Levels of FFAs are further augmented by the availability of dietary lipids (2). *De novo* synthesis of FFA (DNL) is driven by sterol regulatory element binding-protein 1c (SREBP-1c) and carbohydrate response element binding-protein (ChREBP) and is characterized by hyperinsulinaemia and hyperglycaemia (3). However, lipid export through VLDL is decreased (4). FFA induces insulin resistance, causing lysosomal instability by induction of the NF-κB–TNFα pathway, or by activating the caspase-1–IL-1β/IL-18 pathways through the inflammasome (5). Diacylglycerol (DAG) promotes insulin resistance through the activation of protein kinase C (PKCε) and c-Jun N-terminal kinase (JNK) (6). The hepatocyte attempts to limit FFA by increasing mitochondrial β-oxidation, increased oxidative stress and mitochondrial dysfunction, leading to aggravation of insulin resistance and progression to NASH and fibrosis (7). Picture from Tilg H *et al*. (47)

Moreover, the excess of FFA in the liver induces oxidative stress, which is initially compensated by cellular antioxidant mechanisms. Nevertheless, the overloading of FFA generates reactive oxygen species (ROS) causing lipid peroxidation, increased levels of iron, activation of cytochrome P450, increased mitochondrial β-oxidation and stimulation of lipo-oxygenase (64, 65). Furthermore, ROS, through polyunsaturated fatty acids (PUFA), promotes the release of 4-hydroxy-2-nonenal (4-HNE) and malondialdehyde (MDA), which are involved in the pathogenesis of liver damage due to direct toxicity, and can intervene in the formation of Mallory bodies and increase collagen synthesis due to stellate cells (66). Consequently, increased hepatic inflammation and fibrosis and results in an increased risk of developing cirrhosis and HCC.

2.2 The role of oxidative stress and inflammation in NAFLD

Oxidative stress is considered an imbalance between production of free radicals and reactive oxygen species (ROS), and their elimination by protective mechanisms, referred to as antioxidants is an important process to maintain body's homeostasis. This imbalance leads to damage of important biomolecules and cells, with potential impact on the whole organism. Organisms produce ROS as a by-product of cellular metabolism and in response to intra and extracellular environmental factors (67).

ROS includes the superoxide anion (O_2^-), hydrogen peroxide (H_2O_2), hydroxyl radicals (OH^-), nitric oxide (NO), hypochlorite and peroxynitrite ($ONOO^-$, the result of a reaction from O_2^- and NO), all of which have inherent chemical properties that confer reactivity to different biological targets (68, 69). Low concentrations of free radicals, ROS and other nitrogen species are necessary for normal cell redox status, cell function and intracellular signaling. However, in some disease states, free radicals are produced in excess. High concentrations of ROS and free radicals can damage DNA, proteins, carbohydrates and lipid constituents, and compromise cell function (70).

ROS are by-products of aerobic metabolism, and most are generated in the cells by mitochondrial respiratory chain (MRC) (71). Free radicals and ROS can be generated by enzymes in the cytosol, such as amino acids oxidases, cyclooxygenases, lipoxygenase, NO synthase and xanthine oxidase, which generate superoxide anion or other derived ROS. These enzymes link the generation of ROS with specific signaling pathways involved in particular pathological processes (72).

Cells have developed a range of antioxidant strategies to protect the organism from the constant generation of free radicals and reactive species with a complex system of endogenous enzymatic antioxidants:

- Superoxide dismutase (SOD): It is an enzyme that catalyzes the dismutation of the superoxide anion to hydrogen peroxide, which is then decomposed by catalases primarily located in the peroxisomes. Two forms of SOD are known: SOD-1 contains copper and zinc and is also known as Cu-ZnSOD. This enzyme is primary located in the cytosol but also in the nucleus and is an homodimeric protein. Copper is essential for the catalytic reaction, while zinc is important for maintaining the structure of the protein; SOD-2, also known as manganese-dependent superoxide dismutase MnSOD, is found in the mitochondrial matrix (73).

- Catalase: It is located in the liver, erythrocytes, kidneys and central nervous system. The principal function of this enzyme is to convert H_2O_2 to water and molecular oxygen.

- Glutathione peroxidase: It is an important enzyme in cellular antioxidant defense system, detoxifying peroxides and hydroperoxides. Its function is to reduce H_2O_2 to water, oxidizing two molecules of glutathione (GSH) to glutathione disulphide (GSSG), which is converted back to GSH by the enzyme glutathione reductase using NADPH (74).

- Paraoxonases (PON): It is a family of three enzymes termed PON1, PON2 and PON3. They have multifunctional roles in various biochemical pathways such as protection against oxidative damage and lipid peroxidation, contribution to innate immunity, detoxification of reactive molecules, bio-activation of drugs, modulation of ER stress and regulation of cell proliferation/apoptosis (75, 76).

The role of oxidative stress in the initiation and progression of NAFLD from simple steatosis to NASH has not been yet robustly established. Nevertheless, increased levels of ROS and lipid peroxidation products (MDA and HNE), decreased levels of antioxidants enzymes (SOD and catalase), and low levels of antioxidant compounds such as glutathione, have been observed in patients with NAFLD/NASH (64). Various mechanisms have been reported to cause lipid peroxidation (77, 78). Pro-oxidant system such as cytochrome P450, lipoxygenase and cyclooxygenase along with free radical products have been synergistically implicated in the emergence of oxidative stress in NAFLD.

Similarly, the inflammation leading to NASH has been discussed in relation to alterations in metabolic and pro-inflammatory transcription factors expression like CYP4A1 and CYP2E (isoforms of cytochrome P450).

Chronic inflammation is associated to elevated ROS levels, because loss oxidative equilibrium in cells, tissues and organs potentiates inflammatory responses, which can potentially trigger NAFLD (79). For example, anti-inflammatory cascades are linked to diminished ROS concentrations, increased oxidative stress triggers inflammation, and redox balance inhibits cellular response to inflammation (80). Whether oxidative stress and inflammation represent the cause or the consequences of cellular pathology is unknown, but evidence suggests that both processes contribute considerably to the pathogenesis of NAFLD (81, 82) .

Inflammatory cells also produce soluble mediators, such as cytokines (IL-1, IL-6, TNF-α, interferon alpha [IFN-α]), chemokine (C-C motif chemokine ligand 2 [CCL2]), prostaglandins, and leukotrienes (molecules derived from arachidonic acid), which act by further recreating inflammatory cells to the site of damage and producing more reactive species (83). These key sensors can activate signal transduction cascades as well as inducing changes in transcriptional factors, for example: nuclear factor-KB (NF-KB), signal transducer and activator of transcription 3 (STAT-3), hypoxia-inducible factor-1α (HIF-1α), activator protein-1 (AP-1), nuclear factor of activated T cells, and NF-E2 related factor-2 (Nrf2), which regulate cellular stress responses (84).

Adipokines and cytokines play an important role in mediating pathological interactions between adipose tissue and the liver. Adipokines have pro- and anti-inflammatory functions, so an imbalance can promote injuries in the liver tissue. Several studies showed that alterations in plasma levels of adipokines correlates with insulin resistance and liver inflammation, for these reason high levels of TNF-α and low levels of plasma adipokines are possible diagnostic markers to differentiate NAFL and NASH patients (85, 86).

In the liver injury tissue, the metabolic response and inflammation are closely related to NASH. Chronic low-grade systemic inflammation and fibrosis influence the proliferation and activation of a type of macrophages, especially because liver tissue homeostasis is maintained through an adequate balance of oxidative and pro- and anti-inflammatory state (87, 88).

2.2.1 The role of tissue macrophage-mediated inflammation on NAFLD

Macrophages are bone marrow-derived cells that play an important role in the elimination of pathogens and regulation of inflammatory and immune responses. Macrophages are in a continuous functional state (proliferation and activation), which depends directly on the microenvironment where they are found, and whose regulation is very important since they are critical in the initiation and increase of immune responses. Resident hepatic macrophages received the name of Kupffer cells (KCs) and are localized in the periportal zone. The liver comprises the largest population of resident macrophage in the body, representing 80-90% of total fixed macrophages and 35% of the liver non-parenchymal cells (89, 90).

Another important feature of macrophages is the plasticity. It allows their adaptation according to environmental changes, which lead to the activation of KCs and their consequent differentiation into M1 or "classically activated" and M2 or "*alternatively activated*" in the liver of obese mice as well as humans (91-93). Inflammatory cytokines and microbial products, such as lipopolysaccharide (LPS), can induce differentiation of KCs in a M1 profile. M2 profile can be induced by IL-4, IL-10, IL-13, IL-33, transforming grow factor (TFG-β), and granulocyte colony-stimulating factor (G-CSF). M1 macrophages are the key factor cells for the elimination of pathogens, and are characterized for the production of IL-12, IL-23, NO and production of ROS. However, M2 macrophages are usually related to tissue repair and resolution, and produce IL-10, TFG-β and extracellular matrix components (94-96).

Dysregulation of M1/M2 phenotypic balance is emerging as an important mechanism that promotes pathogenesis of chronic inflammatory disease (Figure 4) (97). KCs are known to control the inflammatory responses in NAFLD (98, 99). In early stages of the disease, KCs expand rapidly and secrete cytokines and chemokines such as IL-1, TNF-α and CCL2, contributing to a paracrine activation or apoptotic signaling pathways in hepatocytes and the recruitment of other immune cells. Evidences suggest that KCs can activate hepatic stellate cells (HSCs) through the production of profibrotic cytokine TFG-β and platelet-derived growth factor (PDGF) (100). Upon liver injury, HSCs sense hepatocyte damage and immune cell signaling and respond by transdifferentiation into active myofibroblast like cells that express alpha-smooth muscle actin (α-SMA) and migrate activating a fibroinflammatory response (101). Contrarily, KCs can promote multiple matrix metalloproteinases (MMPs) that promote extracellular matrix degradation and thus favor the resolution of fibrosis

(102). Recent studies have demonstrated the antifibrotic properties of KCs, which acting as M2 macrophages can produce a variety of MMPs, enhancing extracellular matrix (ECM) degradation.

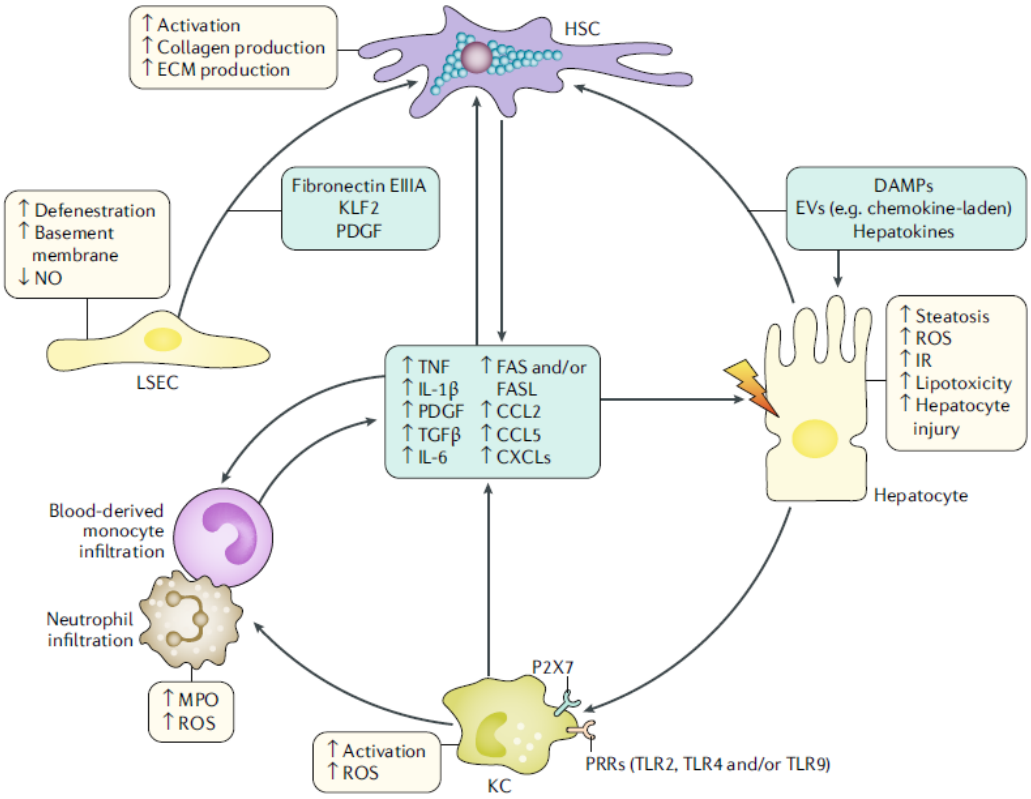

Figure 4. Modulation of macrophages in Kupffer cells during NAFLD. Activated Kupffer cells (KCs) induce lipotoxicity, steatosis, cell death and insulin resistance in hepatocytes by releasing a variety of cytokines and chemokines. Hepatic stellate cells (HSCs) can be activated by DAMPs derived from damaged and stressed hepatocytes or by chemokines and cytokines. HSC activation is characterized by increased collagen production and extracellular matrix (ECM) organization and by the release of pro- inflammatory and profibrogenic cytokines. Picture from Schuster S. *et al.* (103)

Finally, changes in the activation state of macrophages involve coordinated regulation at both the metabolic and transcriptional levels (104). During inflammation, macrophages are metabolically characterized by an increased glycolysis and, lactate production and decreased oxidative phosphorylation (OXPHOS), to reduce for example microorganisms. In contrast, anti-inflammatory and profibrotic macrophages show increased oxygen consumption, mitochondrial respiration, and fatty acid oxidation, as well as decreased glycolysis (105, 106).

2.3 Mitochondrial dysfunction and NAFLD

Mitochondria are essential organelles that play a central role in cellular metabolism, for example, supplying the cell with energy and synthesizing key molecules (107). Mitochondria regulate apoptosis through the intrinsic pathway triggered in response to cellular stress signal, and apoptosis-related proteins influence mitochondrial respiration (108). Therefore, whether cells live or die is a process in which mitochondria play an important role. For this, it is not surprising, that mitochondrial diseases are often associated with metabolic components and, consequently, mitochondrial defects would be expected under inflammatory conditions, in obesity, and other energy-dependent disturbances, such as liver disorders (109).

Mitochondria are dynamic organelles which fuse and divide in response to environmental stimuli, developmental stage, and energy requirements (Figure 5A). The main dynamic activities are fusion (the joining of two organelles into one), fission (the division of a single organelle into two), transport (directed movement within a cell), and mitophagy (targeted destruction via the autophagic pathway) (110, 111). Under "*normal*" conditions, a shift toward fusion contributes to a rapid provision of energy whereas a shift toward fission produces numerous mitochondrial fragments.

Mitochondrial fusion (Figure 5B) is an evolutionary conserved process that is mediated by three GTPases of dynamic superfamily, mitofusin 1 (Mfn1), Mfn2, and optic atrophy 1 (Opa1). Because mitochondria have double membranes, mitochondrial fusion is a two-step process requiring outer-membrane fusion followed by inner-membrane fusion. Fusion process plays an important role for OXPHOS activity, particularly through the regulation of mitochondrial DNA (mtDNA) levels. As a complement to fusion, fission of mitochondria is equally critical for cellular and organismal physiology (Figure 5C). Mitochondrial division is mediated by dynamin-related protein 1 (Drp1), a GTPase that is recruited to the mitochondria via receptors proteins (Mff, Fis1, MiD49, and Mi50). Besides influencing mitochondria morphology, fission has been implicated in multiple functions, including mitochondrial transport, mitophagy, and apoptosis (107, 112-114).

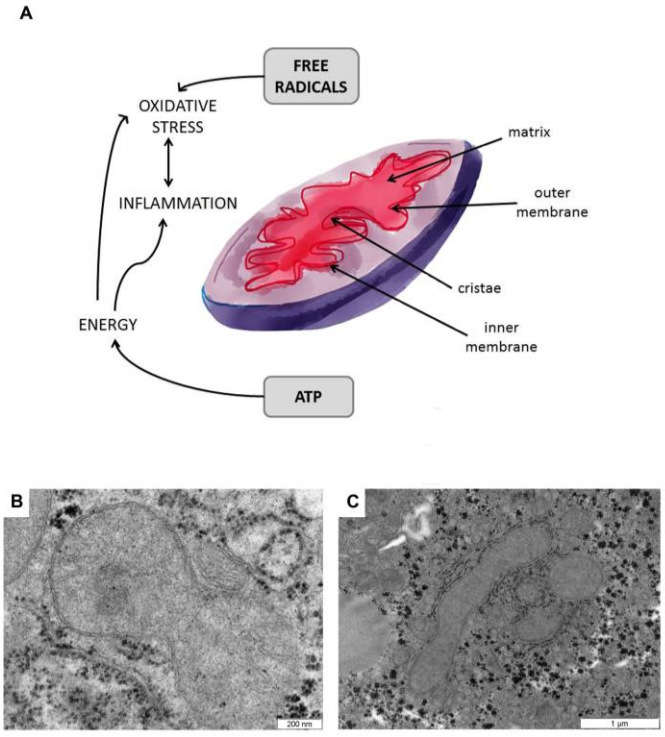

Figure 5. Mitochondrial metabolism and dynamics. Mitochondria are double membrane-bound organelles with characteristic inner membrane folds, termed cristae (A). Mitochondria are essential organelles since their most prominent role is to supply the cell with metabolic energy in the form of ATP through oxidative phosphorylation. Mitochondrial dynamic is determined by fission (B) and fusion (C) processes which are crucial for mitochondrial inheritance and for the maintenance of mitochondrial functions. Picture obtained from Camps J. *et al.* (115)

Mitochondria play a critical role in the production of energy in the form of adenosine triphosphate (ATP). In humans, ATP is produced by three different processes to generate ATP: the tricarboxylic acid (TCA) cycle, OXPHOS and FAO. The TCA cycle oxidizes acetyl-CoA, derived from sugars, fats and amino acids to generate nicotinamide adenine dinucleotide (NADH) and flavin adenine dinucleotide (FADH), which can be used by the OXPHOS system to generate ATP (116, 117).

Mitochondrial dysfunction is a central feature in patients with obesity who have T2DM and/or NAFLD. Mitochondrial dysfunction has a pivotal role during the transition from NAFL to NASH (118, 119). One of the principal drivers of mitochondrial deterioration in NASH is increased of FAA oxidation and lipotoxicity (120). A constant flux of FFA through mitochondria and elevated TCA cycle activity generates harmful ROS, which in turn can damage the protein complexes of the MRC and the mtDNA. Several studies showed that MCR complex activities were decreased in liver tissue from

patients with NASH (119, 121). Of note, mitochondria are not the only source of FAA oxidation; microsomes and peroxisomes also metabolize FAA and contribute to ROS production in NASH (122). Over time, mitochondria become progressively more dysfunctional, triggering oxidative stress, ATP depletion and loss of mitochondrial integrity, which all contribute to hepatocyte death.

2.4 Energy metabolism-related aspects in liver homeostasis

The liver is a key metabolic organ that governs energy metabolism. It acts as a hub to metabolically connect to various tissues, including skeletal muscle and adipose tissue (23). Nutrients are digested in the gastrointestinal tract, and glucose, fatty acids, and amino acids are absorbed into the bloodstream and transported to the liver through the portal vein circulation system. Liver can use glucose to diverse purposes: catabolism via glycolysis and the TCA cycle to produce ATP, storage as glycogen (glycogenogenesis), utilization as a carbon precursor for the biosynthesis of metabolites and generation of NADPH as reducing power via the pentose phosphate pathway. The liver also plays a central role in both glycogenolysis (the breakdown of glycogen) and gluconeogenesis (the synthesis of glucose from carbohydrate precursors), both of which contribute to the supply of blood glucose to deliver to other tissues (48).

In the postprandial state, glucose is condensed into glycogen and/or converted into fatty acids or amino acids in the liver. In hepatocytes, free fatty acids are esterified with glycerol-3-phosphate to generate TAG. TAG is stored in lipid droplets in hepatocytes or secreted into the circulation as very low-density lipoprotein (VLDL) particles. Amino acids are metabolized to provide energy or used to synthesize proteins, glucose, and/or other bioactive molecules. In the fasted state or during exercise, fuel substrates are released from the liver into the circulation and metabolized by muscle, adipose tissue, and other extrahepatic tissues. Alanine, lactate, and glycerol are delivered to the liver and used as precursors to synthesize glucose (gluconeogenesis). Non-esterified fatty acids (NEFAs) are oxidized in hepatic mitochondria through FAO and generate ketone bodies (ketogenesis). Liver-generated glucose provides essential metabolic fuels for extrahepatic tissues during starvation and exercise (48, 123, 124).

Liver energy metabolism is tightly controlled. Multiple nutrients, hormones, and neuronal signals are known to regulate glucose, lipid, and amino acid metabolism in the liver. For these reason, dysfunction of liver signaling, and metabolism causes or predisposes to T2DM or NAFLD. (125).

2.4.1 AMPK guardian of metabolism

Eukaryotes have evolved a very sophisticated system to sense low cellular ATP levels via the AMP-activated protein kinase (AMPK) complex. AMPK is a heterodimeric serine/threonine kinase formed by three subunits, two regulatory (β and γ) and one catalytic (α), and it is the fuel sensor par excellence. AMPK is activated by phosphorylation subunit α at threonine 172 (126). In absence of phosphorylation, AMPK is inactive. AMPK is activated by hypoxia, hyperosmolality, ROS, hypoglycemia, and stimulation of signaling pathways. In addition, adiponectin activates AMPK through two independent pathways; on the one hand through liver kinase B1 (LKB1) and on the other hand though Ca^{2+}/calmodulin-dependent protein kinase (CaMKK). When AMP/ATP ratio increases, AMPK is phosphorylated. Once activated, AMPK acts by promoting catabolic pathways in order to restore energy homeostasis, resulting in ATP generation, and downregulating anabolic pathways that consume ATP (127).

During energy stress, AMPK directly phosphorylates key factors involved in the multiple pathways to restore energy imbalance (Figure 6). The effect of AMPK on metabolism can be broadly divided into two categories: the inhibition of anabolism to minimize ATP consumption and the activation of catabolism to stimulate ATP production (126).

One of the key AMPK functions is the inhibition of acetyl-coenzyme A (CoA) carboxylase (ACC), a rate-limiting enzyme in de novo lipogenesis. ACC suppression by AMPK lowers malonyl-CoA production, thus increasing the long chain fatty acids oxidation and inhibiting insulin-mediated lipid synthesis (128). Moreover, AMPK inhibits hepatic cholesterol synthesis by inhibiting SREBP-1. SREBP-1, in turn, controls the expression of genes involved in triglyceride synthesis and accumulation, such as fatty acid synthase (FASN) and ACC. In contrast, AMPK inhibits the mechanistic target of rapamycin complex 1 (mTORC1), which stimulates lipogenesis and protein synthesis (129, 130).

Lastly, AMPK is closely related to insulin resistance and liver lipid content. Experimental studies also confirmed that phosphorylated AMPK protein expression level in high-fat-diet-induced NAFLD mice was significantly lower than in normal control group, which suggested that AMPK was involved in the pathological process of NAFLD (131).

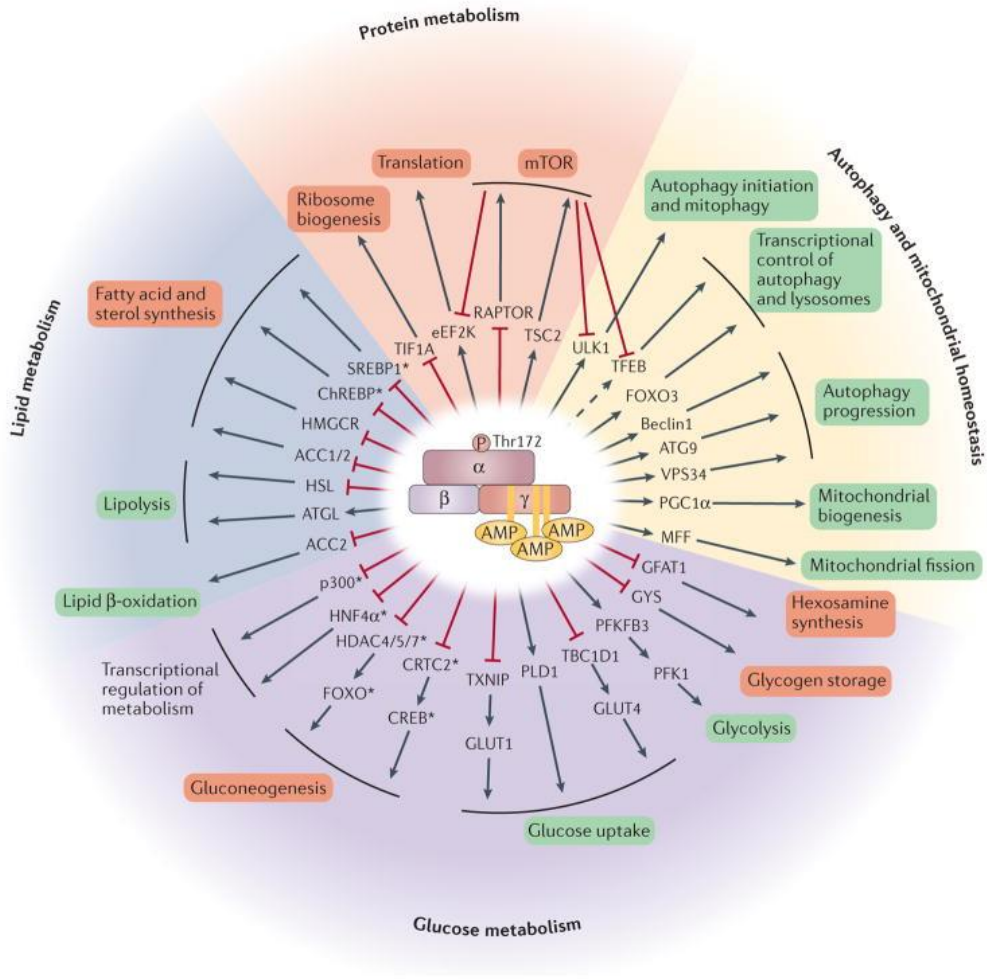

Figure 6. AMPK regulates a variety of metabolic processes. Once activated, AMPK complex phosphorylates key targets to rewire metabolism. The direct targets of AMPK are shown in the first concentric circle. The pathways modulated by AMPK are grouped into four general categories: protein metabolism, lipid metabolism, glucose metabolism, and autophagy and mitochondrial homeostasis. Picture from Schuster Herzig S. *et al.* (126)

2.4.2 The game of mTOR

Another key player in maintaining energy homeostasis is the mechanistic (formerly "*mammalian*") target of rapamycin (mTOR). mTOR is an atypical serine/threonine kinase in the phosphoinositol 3-phosphate kinase (PI3K)-related kinase (PIKK) family, highly conserved from yeast to humans. In the early 2000s were several studies published by Hall and Sabatini, to demonstrate that mTOR existed in two highly conserved, large molecular complex, termed mTOR complex 1 (mTORC1) and mTOR complex 2 (mTORC2) (132, 133).

mTORC1 is defined by mTOR and the core components, Raptor (Kog1), and mLST8 (mammalian lethal with Sec13 protein 18, also known as Lst8). This complex regulates protein synthesis, ribosome biogenesis, transcription factors, lipid synthesis, nucleotide biosynthesis, and nutrient uptake, while inhibit catabolic process like autophagy in response to growth factors, amino acids, and cellular energy (134). mTORC2 comprises mTOR, Rictor (Avo3), Sin1 (Avo1), and mLST8 (Lst8). Its function regulates many cellular processes via the AGC kinase family members , such as protein kinase B (Akt), serum/glucocorticoid regulated kinase (SGK), and protein kinase C (PKC) (135). It is to phosphorylate several AGC kinases in response to growth factors (Figure 7A).

mTOR is activated by nutrients, growth factors, and cellular energy, and is inhibited by the rapamycin. Rapamycin-FKBP12 complex directly inhibits mTORC1, but mTORC2 is characterized by its insensitivity to acute rapamycin treatment. However, long-term treatment with rapamycin can also suppress mTORC2 (136).

Well characterized down-streams targets of mTORC1 are ribosomal protein S6 kinase (S6K), eukaryotic translation initiation factor 4E (Eif4e) binding proteins (4E-BPs), and the autophagy activating kinase ULK1. mTORC1 positively regulates anabolic processes (Figure 7B).

mTORC1 and mTORC2 play a key role in the liver lipid metabolism, and this process has already been extensively reviewed (137, 138). mTORC1 promotes de *novo* lipid synthesis through the SREBP transcription factor, which control the expression of metabolic genes involved in fatty liver and cholesterol biosynthesis. Also, mTORC1 signaling in the liver affects systemic glucose and insulin homeostasis, as we showed in the liver of specific tuberous sclerosis 1 (TSC1) knockout (L-TSC1 KO)

and raptor knockout mice, modulating Akt signaling (139, 140). However, hyperactivation of mTORC1 signaling upon fasting causes metabolic stress due to systemic and hepatic glutamine depletion and, thereby inability of glutaminolysis to sustain TCA cycle (141).

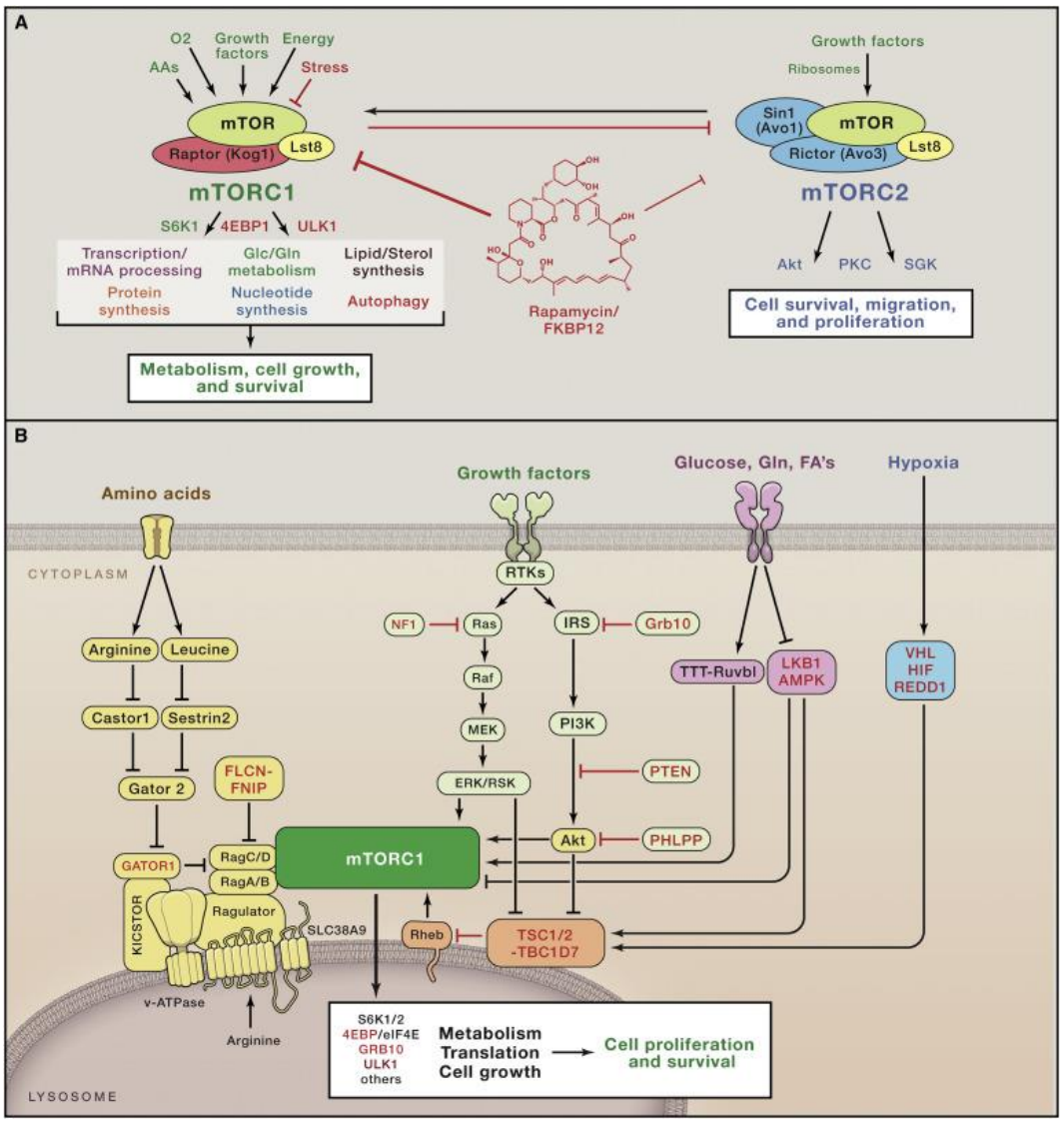

Figure 7. mTOR activation pathways. (A) The core components of mTOR complex 1 (mTORC1) and mTORC2. (B) Schematic detailing the key molecular players in the nutrient sensing branch upstream of mTORC1. mTORC1 promotes several cellular anabolic processes, such as ribosome biogenesis and, lipid synthesis, whereas it blocks autophagy and other catabolic processes. Picture from Blenis J. *et al* (142).

2.4.2.1 Amino acids activate Rag-mTORC1 signaling

A variety of environmental signals regulates mTORC1 activity, including growth factors, cellular stress, and energy and amino acids levels (143). mTORC1 activity is particularly sensitive to leucine and arginine levels, whereas yeast mTORC1 responds best to the amino acid and nitrogen source glutamine (144).

The Rag GTPases, members of the Ras GTPase superfamily, activate mTORC1 in response to some amino acids, such as leucine and glutamine (Figure 8A) (145). The Rheb and Rag GTPases reside on the lysosomal surface and coordinate mTORC1 activity in response to environmental conditions. The Rag GTPases consist of a constitutive heterodimer of RagA or RagB bound to RagC or RagD. In the presence of nutrients RagA/B interacts with RagC/D to form a heterodimer that is anchored to the surface of the lysosome. This active conformation of the Rag GTPases induces the translocation of mTORC1 to the lysosomal surface (146). Once on the lysosome, the growth factors-stimulated GTP-loaded form of the small GTPase Rheb binds and activates mTORC1. Grow factors stimulate lysosomal Rheb through the PI3K/PDK1/Akt pathway. AKT phosphorylates and inactivates tuberous sclerosis complex 2 (TSC2) by inducing its release from the lysosome. TSC2 otherwise associates with TSC1 and TBC1D7 to form the TSC complex that functions as GAP (GTPases activating protein) (144). Nevertheless, mTORC1 inactivation is an active process that requires translocation of TSC2 to the lysosome to inhibit Rheb. For example, hypoxia inhibits mTORC1 signaling as a result of activation of AMPK (147).

Glutamine is the most abundant amino acid in the blood, and is especially important in cell growth and metabolism. Glutamine is transported into cells through one of many transporters, such as the solute carrier family 1 neutral amino acid transporter member 5 (SLC1A5) (148). Glutamine is metabolized via a process termed glutaminolysis (Figure 8B), which consists of two deamination steps. First, there is a conversion of glutamine to glutamate catalyzed by the enzyme glutaminase (GLS). The second step involves the conversion of glutamate to α-ketoglutarate (α-KG) catalyzed by glutamate dehydrogenase (GDH), which enters the TCA cycle to generate ATP through production of NADH and $FADH_2$ (149, 150). Incorporation of α-KG intro de TCA cycle is a major anaplerotic step in proliferating cells and it is critical for the production of oxaloacetate which reacts with acetyl-CoA (generated by glycolysis) to produce citrate. However, the conversion of citrate to α-KG is not reversible. α-KG enters into mitochondria, where it can be used to provide the cell energy and

biosynthetic substrates through TCA cycle. Changes in the α-KG/citrate ratio could be the principal driving force for the switch from oxidative glucose to reductive glutamine metabolism by isocitrate dehydrogenases (IDHs) in the non-canonical reverse reaction to form citrate, promoting the use of glutamine as the primary carbon source for citrate synthesis (151).

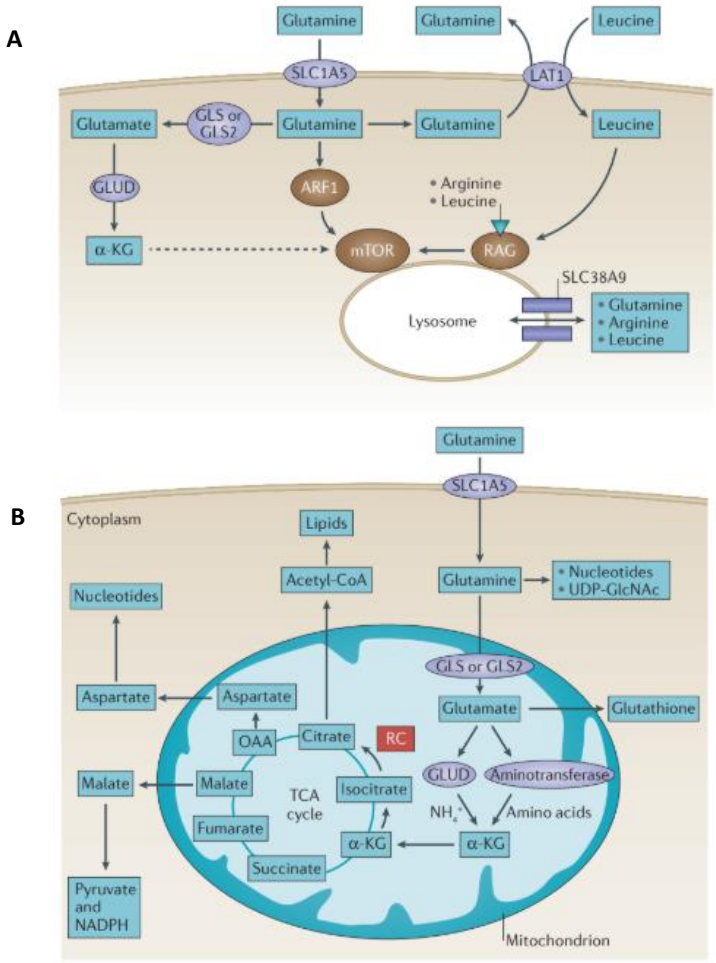

Figure 8. Glutamine controls mTORC1 activity. (A) Glutamine enters into the cell by SLC1A5 transporter and is converted to glutamate by glutaminase (GLS or GLS2). Glutamate can contribute to the synthesis of glutathione or is converted to α-ketoglutarate (α-KG) through glutamate dehydrogenase (GLUD). α-KG enters the tricarboxylic acid (TCA) cycle and can provide energy for the cell. Alternatively, α-KG can proceed backwards through the TCA cycle, in a process called reductive carboxylation (RC) to produce citrate, which supports synthesis of acetyl-CoA and lipids. (B) Amino acids stimulate the mTOR pathway, and amino acid pools rely on glutamine to be maintained. Glutamine can contribute to mTORC1 activation by being exchanged for essential amino acids, including leucine, through the large neutral amino acid transporter 1 (LAT1; a heterodimer of SLC7A5 and SLC3A2) antiporter17. This RAG-dependent regulation of mTOR is probably dependent on the lysosomal amino acid transporter SLC38A9, which transports glutamine, arginine and leucine as substrates. Picture from Altman BJ. *et al.* (151).

Glutaminolysis is correlated with mTORC1 activity (149). The enzymes mediating glutaminolysis sense leucine and glutamine directly. Leucine is an essential amino acid that directly binds to and activates glutamate dehydrogenase, and glutamine is the substrate for glutaminase. Thus, glutaminolysis accounts for an actual sensing mechanism, for at least leucine and glutamine, which ultimately leads to GTP loading of Rag and mTORC1 activation (Figure 8). In addition, glutaminolysis is necessary for GTP loading of RagB and activation of mTORC1 signaling. α-KG, the product of glutaminolysis, is sufficient to stimulate recruitment of mTORC1 to the lysosome (144).

Finally, glutaminolysis promotes cell growth and inhibits autophagy via regulation of mTORC1. Combined, these findings suggest that glutaminolysis is upstream of the Rag GTPase and mTORC1, and that Rag, and thus mTORC1, senses glutamine and leucine via glutaminolysis.

2.5 The influence of Autophagy in NAFLD

Autophagy (term derived from the Greek meaning "*eating of self*") is an evolutionarily conserved cellular degradation process that involves the delivery of cytoplasmic cargo (macromolecules or organelles) to the lysosome. This process degrades long-lived, unnecessary, or damaged proteins and organelles to maintain intracellular homeostasis. Autophagy can be subdivided into three classes: macroautophagy, microautophagy and chaperone-mediated autophagy (CMA) (152, 153). Variations of these autophagic pathways have been described according to the type of cytosolic component preferentially degraded. For example, selective degradation of mitochondria by macroautophagy is now termed mitophagy or for lipids named lipophagy (154).

Macroautophagy is the main route for the incorporation of cytoplasmatic components into lysosomes. During macroautophagy entire cellular organelles such as mitochondria, lipid droplets, or protein aggregates, are sequestered in a double membrane structure known as autophagosome. The autophagosome fuses to a lysosome resulting in the degradation of the autophagosome contents by the hydrolytic enzymes of the lysosome (155). During this process, there are different genes generically known as autophagy-related genes (Atg), which encode for protein products involved in the execution and regulation of macroautophagy (156).

Mechanisms underlying the different steps of macroautophagy are complex (Figure 9). Briefly, Atg proteins organize in functional complexes that mediate each of the steps of macroautophagy: initiation, nucleation, membrane elongation, cargo recognition, sealing and fusion with lysosomes.

First, the complex known as UNC-51-like kinase 1 (ULK1)-Atg13-FIP200-(Atg101) initiates phagophore formation. The activity of this complex is controlled by mTORC1, the main inhibitor of autophagy, and is negatively regulated by AMPK (157, 158). Upon mTOR inhibition, ULK1 dissociates from the complex and starts autophagosome formation. Then, nucleation of the phagophore requires the Beclin-1 vacuolar protein sorting 34 and 15 (Vps34, Vps15, class III PI3K). The synthesis of phosphatidylinositol-3-phosphate (PI3P) by Vps34 is an important trigger for the elongation and closure of the autophagosome by two ubiquitin-like conjugation systems, Atg5-Atg12 and LC3 (Atg8)- phosphatidylethanolamine (PE) complex. The last phases of the autophagic process mediate the autophagy degradation. The processes of autophagosome-lysosome fusion and the lysosomal biogenesis, activation, reformation, and turnover are tightly regulated. The cargoes are selectively recognized by autophagy adaptors, such as p62, also called sequestosome 1, which is a protein that contains an LC3-interacting region and allows selective degradation of the ubiquitinated cargo by autophagy. Moreover, an important regulator of lysosomal biogenesis and autophagy is the transcription factor EB (TFEB). TFEB coordinates the cellular responses to different stresses, such as nutrient starvation, metabolic stress, and lysosomal stress, in order to maintain cellular homeostasis (153, 159-161).

Similar sequestration of a region of the cytosol occurs in microautophagy, but in this case the lysosomal membrane invaginates to surround the cargo, which is then internalized into the lysosomal lumen in single membrane vesicles. Endosomal microautophagy involves selection of protein cargo by the heat shock cognate 71 kDa protein (HSC70).

Selective autophagy has been associated with CMA. In CMA, a pentapeptide motif in the amino acid sequence of cytosolic proteins targeted for degradation is identified by the chaperone HSC70 (162). Once the chaperone-substrate complex reaches the lysosomal membrane, the substrate protein binds to the lysosome-associated membrane protein type 2A (LAMP-2A) and drives its oligomerization into a translocation complex that transports the substrate into the lysosomal lumen for degradation. LAMP-2A is the only one of three spliced variants of the *lamp2* gene that

participates in CMA. Therefore, CMA activity is determined by the levels of LAMP-2A at the lysosomal membrane and by its efficiency of assembly and disassembly in this compartment. CMA has been extensively studied in the liver where it is induced in order to mediate selective removal of damaged proteins. CMA is usually activated by nutritional changes such as starvation or in response to lipid overload (163-166).

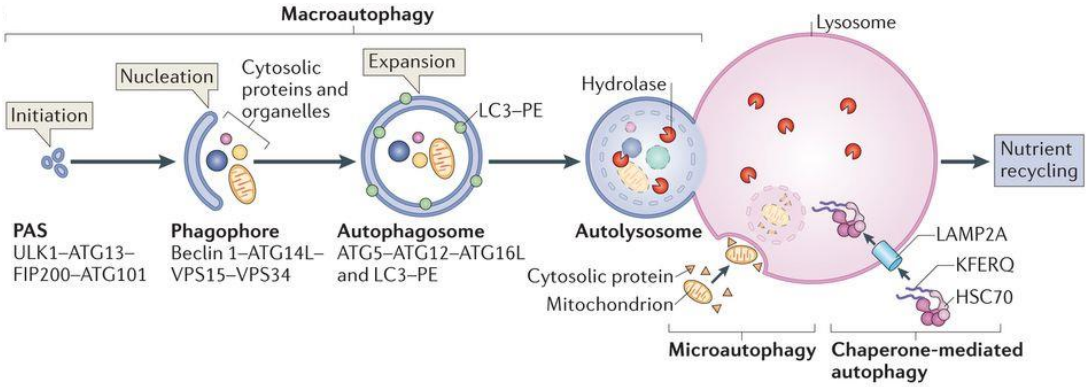

Figure 9. Autophagosome formation. In macroautophagy, the initiation is mediated by the UNC51-like kinase 1 (ULK1) complex, which consists of ULK1, autophagy-related protein 13 (Atg13), FAK family kinase interacting protein of 200 kDa (FIP200) and ATG101. Further nucleation requires the class III PI3K complex, which is composed of the vacuolar protein sorting 34 (VPS34) PI3K, along with its regulatory subunits ATG14L, VPS15 and beclin 1 (Atg6 in yeast). Phagophore membrane elongation and autophagosome completion requires two ubiquitin-like conjugation pathways. The first produces the ATG5–ATG12 conjugate, which forms a multimeric complex with ATG16L, whereas the second results in the conjugation of phosphatidylethanolamine (PE) to LC3 (the microtubule-associated protein 1 light chain 3). In microautophagy, substrates are directly engulfed at the boundary of the lysosomal membrane. In chaperone-mediated autophagy, substrates with the pentapeptide motif KFERQ are selectively recognized by the heat shock cognate 70 kDa protein (HSC70) chaperone and translocated to lysosomes in a LAMP2A-dependent manner. Picture from Kaur J. *et al.* (159)

The best-characterized example of selective autophagy is the process called mitophagy, in which depolarized mitochondria are selectively surrounded by autophagosomes and degraded (Figure 10). Mitophagy is regulated by serine/threonine protein kinase 1 (PINK1), p62 and receptors such as protein Bcl-2 nineteen-kilodalton interacting protein 3 (BNIP3), NIP3-like protein X (NIX) and FUN14 domain-containing protein 1 (FUNDC1). Mitophagy is an important process in cellular quality control, because it regulates the mitochondria status, the size and fusion and fission processes (154, 159).

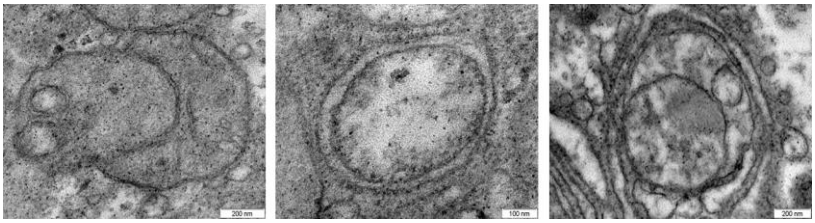

Figure 10. Mitophagy process. Transimission electron micrographies of mitophagy in liver of patients with NAFLD.

Autophagy helps to maintain a positive energetic balance in the liver. A growing number of liver pathologies, such as NAFLD, have been associated with autophagy dysfunctions. Several studies in mice showed that obesity-associated NAFLD results in decreased macroautophagy and CMA in the liver (161). A number of possible mechanisms for the inhibition of autophagy in fatty liver have been suggested including deceased expression of autophagy gens, reduced levels of lysosomal enzymes, and impaired fusion of autophagosome with the lysosome (167-169).

The human beings have two major lipid metabolism pathways, the lipolysis pathway and the lipophagy pathway (170). Lipolysis consists of the gradual degradation of intracellular lipid droplets into FFAs and glycerol by the cytoplasmic lipases. Once released, these FFAs are then transported into the mitochondria, where they undergo β-oxidation to form Acetyl-CoA. During lipophagy lipid droplets are wrapped by a double membrane and sent for degradation to the lysosomes as autolysosomes. Lipophagy ensures the degradation of excessive lipid droplets present in cells, and the maintenance of cellular homeostasis (171).

Lipolysis and lipophagy both play important roles in the degradation of lipid droplets. There is a general consensus that autophagy is up-regulated during the early stage of NAFLD as an attempt to prevent lipid accumulation. However, as NAFLD progresses, it seems that the autophagy process is blocked. Studies conducted with animal models and NAFLD patients have reported that autophagy flux was suppressed, and that restoring autophagy balance could help to restore liver histology to a healthy state. Short-term inhibition of autophagy in NAFLD might be induced via the mTOR complex; while long-term inhibition could be regulated by the transcription factors such as Forkhead box protein O1 (FOXO1) and Transcription factor EB (TFEB), since they control the transcription of autophagic genes. In a fatty liver, mTORC1 could be over-activated, possibly due to excessive food consumption and/or hyperinsulinemia (159, 161, 172, 173).

2.6 One-carbon metabolism and DNA methylation

Studies in diverse organisms, including humans, have suggested the important role of nutrients in regulating epigenetics in normal and disease states. Chronic diseases, such as obesity, T2DM, cancer, heart disease and aging, have been linked to metabolic and epigenetic factors that play an important role in pathogenesis (174-176).

The emerging field of epigenetics, an inheritable phenomenon that can affect gene expression without altering the DNA sequence, provides a new perspective on the pathogenesis of liver diseases. Animal studies have demonstrated that hepatic steatosis can be induced by the derangement of one-carbon (1-C) metabolism. (177, 178).

One-carbon metabolism utilizes a variety of nutrients such as glucose, vitamins, and amino acids, to produce 1-C units that fuel a diversity of metabolic pathways. These pathways include nucleotide metabolism, maintenance of cellular redox status, lipid biosynthesis, and methylation metabolism (179). Two major components of 1-C metabolism are the folate and methionine cycles (Figure 11), which function to transfer single-carbon units to acceptor substrates. Importantly, the methionine cycle provides a link to histone methylation through the generation of S-adenosylmethionine (SAM). Histones can be mono-, di-, or trimethylated at lysines and arginines by histone methyltransferases (HMTs), which transfer the methyl group from SAM to the histone substrate, generating S-adenosylhomocysteine (SAH) (180).

Folic acid is a B vitamin provided by the diet and it is essential to start the folate cycle. Folic acid is reduced first to dihydrofolate (DHF) and then tetrahydrofolate (THF) before it can enter to the folate cycle. THF can be interconverted between different oxidation states, including 5,10-methylene-THF, 5-methyl-THF, and 10-formyl-THF each supporting distinct biosynthetic functions. 5-methyl-THF is used for the homocysteine re-methylation to generate methionine during methionine cycle. (181). Thus, the folate cycle coupled to the methionine cycle constitutes a bi-cyclic metabolic pathway that circulates carbon units.

The methionine cycle is crucial in the epigenetic reaction for the generation of SAM through the adenylation of methionine, an essential amino acid sourced from diet, by methionine adenosyltransferase (MAT) (182). The liver plays a crucial role because is the site where nearly half

of the methionine metabolism and 85% of all methylation takes place (183). Nutritional factors, e.g. methionine, influencing the metabolism of SAM and SAH, may impact on DNA methylation status. The establishment of epigenome is vulnerable to nutritional factors especially in disease such as obesity, T2M and liver disorders (184).

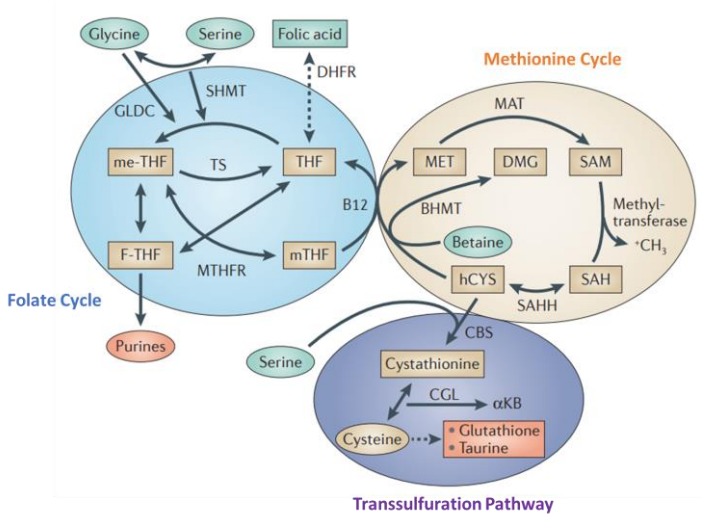

Figure 11. One-carbon metabolism and epigenetics. SAM is produced from methionine by methionine adenosyltransferase (MAT). Methyl-transferases utilize SAM to donate a methyl group to histone or DNA, producing SAH. SAH is converted to homocysteine (hCys) via S-adenosylhomocysteine hydrolase (SAHH) and recycled by transsulfuration pathway. SAH can be remethylated to regenerate methionine by donation of a methyl group from 5-methyltetrahydrafolate (5-mTHF) via folate cycle or from betaine via betaine–homocysteine S-methyltransferase (BHMT). Picture modified from Locasale JW. *et al.* (179)

SAM is considered the universal methyl donor and uses methyltransferases to methylate metabolites, RNA, DNA, and proteins, including histones. After the methyl group is transferred from SAM to an acceptor substrate, SAH is produced. In turn, SAH is hydrolyzed by S-adenosylhomocysteine hydrolase (SAHH) to adenine and homocysteine. Homocysteine enters the trans-sulphuration pathway and condenses with serine to generate cystathionine in an irreversible reaction by cystathionine β-synthase. In addition, betaine-homocysteine methyltransferase (BHMT) transfers a methyl group from betaine, an intermediate in choline metabolism, to regenerate methionine and produce dimethylglycine. 5-methyltetrahydrofolate-homocysteine methyltransferase (MTR) regenerates methionine by the transfer of 5-methyl-THF to homocysteine, producing THF (180, 181, 185).

2.6.1 DNA methylation

DNA methylation is an epigenetic mark of gene regulation that is generally associated with transcriptional repression when present at the promoter regions of genes. It works in concert with histone modifications to regulate the activity of genes, and these regulatory mechanisms help guide levels of gene transcription in all tissues (186). DNA methylation changes are known to modulate susceptibility to obesity, a major risk factor for NAFLD (187).

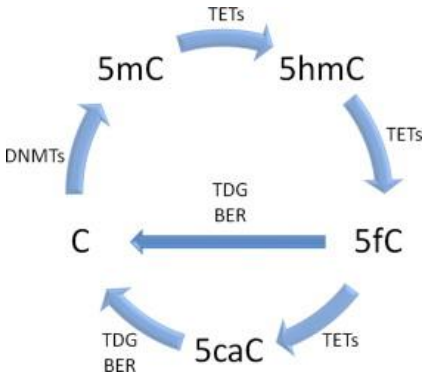

Figure 12. DNA methylation cycle.
DNMTs regulate DNA methylation generating 5-mC modifications, which are then potentially substrates for TET-regulated step-wise demethylation via the functional (5hmC epigenetic mark). TDG (thymine DNA glycosylase) and BER (base excision repair) are involved in active demethylation. Picture modified from Mann DA. *et al* (118)

DNA can be covalently modified and the best-known modification is methylation of the C-5 position of a cytosine adjacent to a guanine residue (CpG dinucleotides), which normally leads to gene suppression. The enzymes that instruct DNA methylation (DNA methyltransferases, DNMT) and demethylation (ten-eleven translocation enzymes (TET1-3) are beginning to be functionally defined (188). DNMT1 is the responsible of DNA stability, *de novo* methylation is regulated by, DNTM3a and DNMT3b, and the TET enzymes catalyze the oxidation of 5-methylcystosine (5-mC) via three intermediate chemical states (5-hydroxymethylcytosine (5hmC), 5-formylcytosine (5fC) and 5-carboxylcytosine (5caC)) to its demethylated form which is then again available for re-methylation by DNMTs (Figure 12) (189).

DNA methylation is critical in gene regulation. Under most circumstances, methylation is related to a decrease in transcription. Liver disorders strongly correlate with abnormal gene expression and transcription factors play an important role in altering the transcriptome during steatohepatitis (187, 190). Furthermore, changes in global DNA methylation are also an essential component of liver diseases (191, 192).

2.6.2 Metabolites modulate epigenetics

Several metabolites generated by energy metabolism are implicated in the regulation of chromatin remodeling (Figure 13). The enzymes involved in the DNA and histone methylation/demethylation (DNMTs, DNA hydroxylases (DNHDs), histone acetyltransferases (HATs), HMTs and histone demethylases (HDMs)) are sensitives to the nutrients and metabolic fluctuations (193). As extensively reviewed (194-196), some of these enzymes utilize metabolites as a substrate or cofactor, derived from diverse metabolic pathways including: 1-C metabolism, TCA cycle, β-oxidation and glycolysis that can modify gene expression. For example, SAM and the ratio of SAM/SAH haven shown to be influenced by multiple dietary and environmental factors.

Glucose enters the cells and the major proportion can be converted to acetyl-CoA trough glycolytic pathways, along with the decreased NAD+/NADH ratio. Acetyl-CoA is an essential substrate of HATs and behaves as an essential acetyl group donor in histone lysine acetylation reactions. Metabolites that accumulate in physiological conditions can also inhibit chromatin-modifying enzymes. For instance, fasting-induced increased circulating levels of the ketone body beta-hydroxybutyrate inhibit histone deacetylases (HDCAs) in multiple tissues and induce expression of genes associated with resistance to oxidative stress (197, 198).

α-KG is a key metabolite to modulate the removal of methylation marks by HDMs and TET enzymes (199). For example, JmjC domain-containing histone demethylase (JHDM) proteins are important in the context of energy homeostasis because they depend on FAD^+ and α-KG to regulate histone methylation. In the context of DNA methylation, TET proteins depend on Fe (II) and α-KG. Although it is not clear whether TET proteins sense α-KG, it is known that the TCA cycle intermediates, fumarate and succinate, can act as competitive inhibitors of JHDMs and TETs. Mechanistically, enzymes succinate dehydrogenase (SDH) and fumarate hydratase (FH) regulate DNA and histone methylation counteracting α-KG -dependent enzymes. This suggests that the relative concentrations of TCA cycle intermediates may regulate TET and DNMT enzymes activity (178, 197).

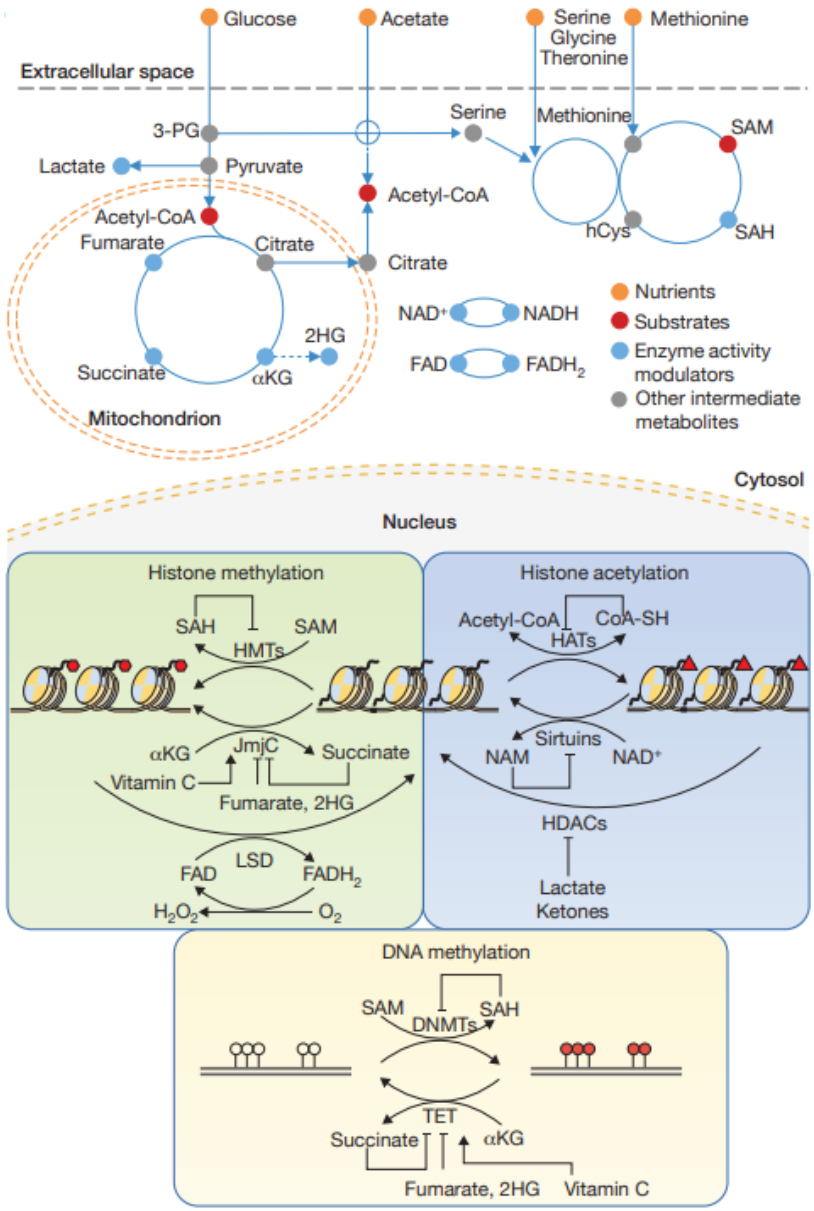

Figure 13. Metabolic pathways provide substrates for enzymes that modify chromatin. Metabolic pathways implicated in the generation of 1-C metabolism required for methylation, acetylation, or demethylation of chromatin. TCA cycle metabolites serve to provide carbon units for both acetylation and demethylation via α-KG. Chromatin modification reaction requires intermediary metabolites, such as α-KG, SAM, SAH, succinate, fumarate and acetyl-CoA. Picture obtained from Reid MA. *et al.* (195)

2.7 Diagnosis of NAFLD

NAFLD is usually an asymptomatic disease and, consequently, it is often diagnosed accidentally following a routine blood test or an imaging study done for other reasons. Early diagnosis and treatment of NAFLD can prevent it is development into more progressive NAFLD, such as NASH, liver fibrosis, cirrhosis and HCC. Most patients with NAFLD are asymptomatic or complain about non-specific symptoms. Although liver biopsy is the reference method to diagnose hepatic steatosis and its progressive stages, there are several non-invasive methods to use in the clinical practice (200, 201). Nevertheless, in the present time, any specific marker for the diagnosis of NAFLD exists.

2.7.1 The noninvasive diagnosis of NAFLD

Liver test can show mild increases in the levels of alanine aminotransferase (ALT), aspartate aminotransferase (AST), and gamma-glutamyl transferase (GGT), but these levels remain normal in the majority of people with NAFLD (80%) (202). Consequently, they are considered as poor markers for the diagnosis of NAFLD due to their low specificity, sensitivity and prognostic value. Ferritin may be increased in up to 60% of patients, but is mainly a marker of subclinical inflammation, given that iron overload is uncommon in NAFLD. However, high ferritin levels have been associated with more-advanced disease (203). For these reasons, other diagnostic methods are needed to confirm the suspected diagnosis of NAFLD.

Nowadays, different indices or biomarkers are validated for the diagnosis NAFLD patients. The best-validated biomarkers are the Fatty Liver Index, the SteatoTest© and the NAFLD liver fat score (Table 1) (25). There are also other scoring systems that predict NAFLD, such as NAFLD Liver Fat Score, Hepatic Steatosis Index, Visceral Adiposity Index and Triglyceride-Glucose Index. According to European guidelines, the best externally validated scores are Fatty Liver Index, Steatotest© and NAFLD Liver Fat Score but the weakness of these and other scores is that they predict reliably only the presence of steatosis, not its severity (200).

Other different serum markers of fibrosis seem to have a better performance, particularly the NAFLD Fibrosis Score (NFS), Fibrosis-4 (FIB-4) and commercially available panels, such as FibroTest©, FibroMeter© and the Enhanced Liver Fibrosis (ELF) test (25).

Table 1. Scores predicting NAFLD and NAFLD severity (NASH)

Score	Components	Cut-off value	AUROC	Sensitivity (%)	Specificity (%)
NAFLD					
Fatty Liver Index	BMI, WC, TG and GGT	>60	0.85	61	86
NAFLD liver fat score	MetS, T2DM, AST and ALT	-0.640	0.86	86	71
SeatoTest©	GGT, ALT, BG, TG and CHOL	>0.69	0.80	38	81
Fibrosis					
NAFLD Fibrosis Score	Age, BG, BMI, platelets, albumin, and AST or ALT	>0.676	0.84	43	96
Fibro-Test©	GGT, BIL, haptoglobin, apoAI and α2-macroglobulin	>0.30	0.81	92	71
FIB-4 index	Age, ALT, AST and platelets	>2.67	0.80	33	98
BARD	BMI, AST or ALT and T2DM	2-4	0.81	NA	NA
Hepascore	Age, gender, α2 macroglobulin, HA, BIL and GGT	>0.37	0.81	75	84
Enhanced Liver Fibrosis	HA, TIMP1 and PIINP	>0.35	0.90	80	90
AST/platelet ratio index	AST levels and platelet counts	>0.91	0.87	66	91

AUROC, area under the curve of the receiver-operating characteristic plot; HA, hyaluronic acid; MetS, metabolic syndrome; PIIINP, amino-terminal propeptide of type III collagen; TIMP1, tissue inhibitor of metalloproteinase 1. Table obtained from Brunt EM. *et al*.(25)

The imaging technologies are of wide interest as a possible non-invasive method the evaluation and diagnosis of NAFLD. Due to it is low cost and high availability without radiation exposure, ultrasound is commonly used as a first-line imaging method in the clinical practice. The increased liver-kidney contrast showing an echogenic (bright) liver is a widely accepted criterion to set the diagnosis of NAFLD (204). However, the intra-observer and inter-observer repeatability in grading the NAFLD with ultrasound is shown to be highly limited (205). Thus, the drawback with ultrasound is the relatively low sensitivity, especially when steatosis is less than 20% or it is use with in individuals-with very high body mass index (BMI, >40 kg/m^2) (200).

Computed tomography (CT), magnetic resonance imaging (MRI) and ^{1}H-MRS are the best non-invasive tools to quantify liver steatosis. The leading quantitative MRI biomarker for hepatic steatosis is proton density fat fraction (PDFF) (206). MRI measures the quantity of steatosis directly by differentiating protons in fat from those in water. This enables the accurate quantification of hepatic steatosis. However, patients with morbid obesity did not typically fit into the apparatus (207).

2.7.2 The non-invasive diagnosis of NASH

The European guidelines state very clearly that NASH must be diagnosed only by a liver biopsy showing steatosis, hepatocyte ballooning and lobular inflammation (200). Some biochemical

measures such as cytokeratin-18, various cytokines (TNF-α, IL-6) and chemokines (for example CCL2), imaging studies or scoring systems have been proposed to diagnose NASH or distinguish NASH from simple steatosis (52, 201, 208). However, up to date, none of them have been proved accurate enough or externally validated to the degree that they would be generally accepted.

The emergent field of metabolomics is increasingly being applied towards the identification of biomarkers for disease diagnosis, prognosis and risk prediction. Metabolomics involves the quantification of a large number of low molecular weight compounds in plasma and tissue samples. Recent developments in robust statistical analysis have allowed to detect changes in cellular and tissue metabolism related to some metabolic diseases such as obesity, T2DM, cancer, and more recently, NAFLD (209-212).

2.8 Novel therapeutic options for treating NAFLD and NASH

Lifestyle modifications with weight reduction, physical activity and diet control in overweight or obese people, are one of the first steps in the management of NAFLD. It has been demonstrated that lifestyle modifications leading to weight reduction and/or increased physical activity consistently reduces fat accumulation in the liver. However, these habits are rarely maintained in a long-term. At present, the pharmacotherapeutic agents available for NAFLD are scarce, but some potential new drugs are seen in the horizon. These agents are targeting insulin resistance, weight reduction and fibrotic or inflammatory processes. Bariatric surgery or liver transplantation may be used for selected patients (26, 213).

2.8.1 Pharmacotherapy

The recommendations of pharmacotherapy in NAFLD guidelines are unestablished (200). However, there are some interesting therapeutic targets with potential action. For instance, vitamin E is an antioxidant with several targets. It has been shown that vitamin E induces resolution of NASH more often than placebo but without improvement of fibrosis (214). Apoptosis in NASH and other chronic liver diseases promote tissue injury and fibrosis, which establishes a rationale for inhibiting apoptosis as a therapeutic strategy. Emricasan, a pancaspase inhibitor, reduces apoptosis that can attenuate inflammation and fibrosis; it is also currently in phase 2B clinical trials for NASH (215, 216).

Metformin is a biguanide widely used for the treatment of T2DM which action is mediated by the activation of AMPK, a regulator of energy metabolism, is able to stimulate ATP-producing catabolic

pathways (glycolysis, fatty acid oxidation, and mitochondrial biogenesis) and to inhibit ATP-consuming anabolic processes (gluconeogenesis, glycogen, fatty acid, and protein synthesis). Metformin effectively improves both hepatic and peripheral insulin resistance and decreases endogenous glucose production by various mechanisms resulting from primary inhibition of complex I of the mitochondria respiratory chain (217, 218). Several clinical trials have supported the beneficial role of metformin in patients with NAFLD. Most of these studies have evaluated the effect of various doses of metformin on liver biochemistry (aminotransferase profile), histology, and metabolic syndrome features (219-221).

Glucagon-like peptide-1 (GLP-1) is an intestinal hormone generated through the processing of proglucagon that stimulates insulin secretion and inhibits secretion of glucagon. GLP-1 is also an insulin sensitizer with additional metabolic effects that contribute to its anti-NASH activity (222). GLP-1 analogues, liraglutide and semaglutide, are promising in NASH treatment due to their potential to induce weight loss and insulin sensitivity, which may have a direct beneficial hepatic effect leading to decreasing hepatocyte triglyceride accumulation and fibrosis (223). However, more extensive and long-term studies are necessary to establish the role of GLP-1 in the treatment of NASH.

Cenicriviroc is a selective inhibitor of C-C motif chemokine receptors 2 and 5 (CCR2-CCR5), which are expressed on the surface of Kupffer cells, macrophages and hepatic stellate cells. Originally, cenicriviroc was developed as an anti-HIV agent, but several studies revealed that it has an important role as antifibrotic and anti-inflammatory in the liver diseases (224). There have not been any safety concerns with cenicriviroc and it has been well tolerated. The large double-blind, randomized, multinational phase 2b CENTAUR trial is currently ongoing. The first results will be presented in one year (225, 226). After 2 years of treatment, however, the fibrosis stage in those patients undergoing active therapy was not significantly different from that of patients on placebo. This molecule is also being evaluated in a phase 3 trial (58).

Silymarin, a standardized extract from *Silybum marianum*, or milk thistle, and its major active compound silybinin or sylibin have been used since the time of ancient physicians, to treat liver diseases (227). Several studies in vitro and animal models have credited the silymarin therapeutic role treating NAFLD due to its anti-inflammatory, antioxidant, and antifibrotic properties. Recently,

silymarin extract tablets treated fatty liver disease in several clinical trials, whose results showing decreased hepatic enzymes levels in serum, especially ALT, indicated that silymarin could partially restore the liver's function and mitigate NASH patients' symptoms. Furthermore, there were few side effects when administrating with therapeutic dosage. Therefore, silymarin could be a promising herbal remedy to treat NAFLD patients (228-230).

2.8.2 Bariatric surgery

Bariatric surgery is the third-line approach recommended when the multiple attempts at weight loss through lifestyle interventions and/or pharmacotherapy are not successful. Today, bariatric surgery is indicated for patients with severe or complex obesity whose BMI is at least 35 Kg/m^2 with co-morbidities or at least 40 Kg/m^2 without co-morbidities) (231, 232). At present, the most widely used procedures are Roux-en-Y gastric bypass (RYGB) and laparoscopic sleeve gastrectomy (LSG) (233, 234) (Figure 14).

- LSG procedure is characterized by the reduction of the stomach to about 15% of its original size, leaving a thin tube of lesser curve (banana shape). This procedure is not reversible.

- In the RYGB technique the stomach is divided to create a small pouch. The smaller stomach is joined directly to a loop of jejunum around one meter distal to the duodenal-jejunal flexure, bypassing the rest of the stomach and the upper portion of the small intestine (duodenum). The redundant stomach and jejunum are then re-anastomosed to the jejunum at a variable distance downstream where digestive juices join food. In normal digestion, food passes through the stomach and enters the small intestine where most of the nutrients and calories are absorbed. Thus, with this surgery, food is not absorbed, and the amount of food is restricted by limited size of gastric pouch.

Classically, bariatric surgery has been described as 1) restrictive, which aimed to reduce food intake by limiting gastric volume, or 2) restrictive with some malabsorption, which reduces stomach size and creates a physiological condition of malabsorption. The first group includes LSG and the second includes RYGB.

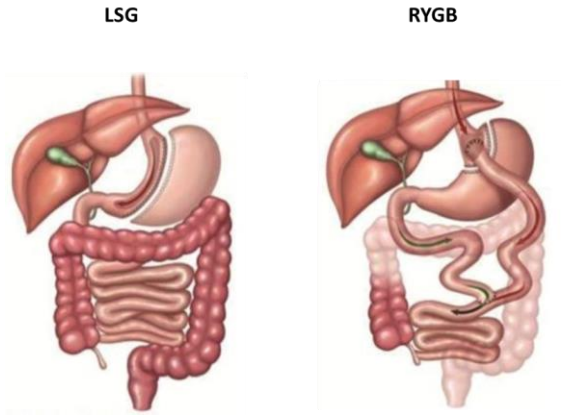

Figure 14. Commonly performed surgical methods for bariatric surgery. LSG stomach is transected vertically creating a gastric tube and leaving a pouch of 100 to 200 mL. In RYGB an upper gastric pouch, of 15 to 30 mL in volume, and a lower gastric remnant are formed from the stomach.

Bariatric surgery is the most radical therapy for the metabolic syndrome and NASH, leading typically to massive weight loss, and improvement of liver histology. The impact of bariatric surgery in NAFLD regression is consistent, as seen by several studies (235-239). These studies have shown that surgery-induced weight loss is also associated with improved hepatic histology including reduced steatosis, steatohepatitis, and fibrosis by ameliorating some factors that contribute to the pathogenesis of NAFLD (improvement of insulin sensitivity and inflammation). The beneficial effects are probably mediated by an enhanced of adipose tissue function, an improvement of insulin sensitivity and a decrease of inflammation and oxidation. All together could modify the course of NAFLD.

Hypothesis and Aims

UNIVERSITAT ROVIRA I VIRGILI
ASSESSING DIAGNOSTIC AND THERAPEUTIC TARGETS IN OBESITY-ASSOCIATED LIVER DISEASES
Noemí Cabré Casares

Hypothesis

Oxidative stress, mitochondrial dysfunction and cell death responses are implicated in the obesity-associated liver diseases via metabolic reprogramming. Understanding the role of metabolites in cell fate outcomes may provide therapeutic strategies and potential disease biomarkers.

Aims

- ✓ To assess the hepatic markers of oxidative stress and inflammation in obese patients undergoing bariatric surgery.
- ✓ To discover blood-based diagnostic markers and contributing factors to NASH onset.
- ✓ To evaluate how weight loss affects liver and plasma metabolic reprogramming.
- ✓ To investigate the impact of AMPK/mTORC1 driven-pathways in NASH remission.

UNIVERSITAT ROVIRA I VIRGILI
ASSESSING DIAGNOSTIC AND THERAPEUTIC TARGETS IN OBESITY-ASSOCIATED LIVER DISEASES
Noemí Cabré Casares

Materials and Methods

UNIVERSITAT ROVIRA I VIRGILI
ASSESSING DIAGNOSTIC AND THERAPEUTIC TARGETS IN OBESITY-ASSOCIATED LIVER DISEASES
Noemí Cabré Casares

STUDY I

Bariatric surgery reverses non-alcoholic fatty liver disease in morbid obesity and while reducing oxidative stress and inflammation

UNIVERSITAT ROVIRA I VIRGILI
ASSESSING DIAGNOSTIC AND THERAPEUTIC TARGETS IN OBESITY-ASSOCIATED LIVER DISEASES
Noemí Cabré Casares

Study design and participants

This was a prospective, 12 months follow-up, longitudinal study including 436 patients with severe obesity who underwent laparoscopic sleeve gastrectomy at the Hospital Universitari Sant Joan de Reus. Patients provided 12-hours fasting blood samples immediately before surgery together with an intraoperative wedge-liver biopsy. Written informed consent was obtained according to the procedures approved by our Institutional Review Board (OBESPAD/14-07-31proj3 project) and the ethical guidelines of the 1975 Declaration of Helsinki. Exclusion criteria were age <25 years, alcohol abuse, infectious diseases, primary sclerosing cholangitis, autoimmune diseases, and cancer. One hundred and twenty patients agreed to have a second blood extraction and a liver biopsy at 12 months post-surgery, and signed fully informed consent (OM-NAFLD, ESO3/18012013 project). Biopsies were performed by ultrasound-guided, percutaneous needle puncture. Patients were classified according to the non-alcoholic fatty liver score (NAS) system. The scales included the unweighted sum of steatosis (0-3), lobular inflammation (0-3) and ballooning (0-2) scores. Values assigned were ≤ 2 for non-NASH, >2 and ≤4 for uncertain NASH, and ≥5 for definite NASH. Information for fibrosis included the absence of fibrosis (F0), mild to moderate fibrosis (F1 and F2), bridging fibrosis (F3) and cirrhosis (F4) (240). Liver biopsies were assessed by a single experienced pathologist who was blinded with respect to the provenance of the samples.

For comparisons, we used sera of healthy non-obese controls (n=404) in which NAFLD diagnosis was discarded using imaging procedures (INFLAMET/15-04/4proj7 project). These subjects were participants in a population-based study conducted in our geographical area. They had no clinical or analytical evidence of renal insufficiency, hepatic damage, or neoplasia. The samples (stored at –80ºC) were obtained from the Biological Samples Bank of our Institution. A detailed description of this population has been published (241).

Measurement of circulating levels of selected biochemical parameters

Serum and EDTA-plasma samples were collected after centrifugation and stored at -80ºC for batched analyses. Serum PON1 concentrations were determined using an in-house ELISA with antibodies specific of PON1 (242). Serum PON1 lactonase and esterase activities were determined using synthetic substrates. Lactonase activity was measured as the hydrolysis of 5-thiobutyl butyrolactone (TBBL), and paraoxonase (esterase) activity was determined as the rate of hydrolysis of paraoxon (242). Plasma concentrations of CCL2, IL-10, TNF-α and galectin-3 were measured by ELISA (PeproTech, London, UK; and R&D Systems, Minneapolis, MN, USA). Serum alanine

aminotransferase (ALT) and aspartate aminotransferase (AST) activities, and cholesterol, HDL-cholesterol, LDL-cholesterol, triglycerides, glucose, C-reactive protein (CRP), and insulin concentrations were analyzed using standard tests in a Roche Modular Analytics P800 system (Roche Diagnostics, Basel, Switzerland).

Immunohistochemical analyses in hepatic biopsies

Procedures were performed essentially as previously reported (243). To assess differences in oxidation and inflammation, we analyzed the hepatic immunohistochemical expression of 4-hydroxy-2-nonenal (a marker of lipid peroxidation), cluster of differentiation 68 (CD68, a marker of macrophages), PON1, CCL2, C-C chemokine receptor type 2 (CCR2), IL-10, TNF-α, and galectin-3. The appropriate primary and secondary antibodies and other reagents are described in Supplementary Table 2. Positive staining was quantified using the Image J software (National Institutes of Health, Bethesda, MD, USA).

Western blotting of liver tissue

Western blot was performed by denaturing 50 µg of protein from frozen liver tissues were subjected to 8%–14% sodium dodecyl sulfate polyacrylamide gel electrophoresis. The resolved proteins were transferred to polyvinylidene difluoride membranes (Thermo Fisher, Barcelona, Spain) using bovine serum albumin at 5% in Tris-buffered saline, 0.1% Tween-20 (pH = 7.4) as blocking agent. Membranes were incubated with the corresponding primary and secondary antibodies for PON1, galectin-3, TNF-α, IL-10, CD163 (a marker of anti-inflammatory macrophages), signal transducer and activator of transcription 3 (STAT-3) and its phosphorylated form (pSTAT-3), which regulate multiple metabolic processes (244), α-smooth muscle actin (α-SMA), and sonic hedgehog (Shh); these last two proteins being associated with liver fibrosis. Technical details and reagents are reported in Table 2. Fumarylacetoacetate hydrolase (FAH) was used as a reference (control) protein. Protein bands were visualized using SuperSignal West Femto chemiluminescent substrate (Pierce, Rockford, IL, USA) and analyzed with a ChemiDoc system using Image Lab 2.0 software (Bio-Rad Laboratories, Hercules, CA, USA).

Statistical analyses

Kolmogorov-Smirnov test was used to assess the distribution characteristics of variables. Student's t-test (parametric) or Mann-Whitney U- test (non-parametric) were used to assess differences between any two groups of variables. Analyses were performed with the SPSS 22.0 package (IBM Corp., Armonk, NY, USA). Statistical significance was set at $p < 0.05$.

Table 2: Antibodies and relevant technical information for immunohistochemistry and western blotting

Antigen	Name	Primary antibody and source	Dilution	Secondary antibody and source	Dilution
Immunohistochemistry					
CD68	Cluster of differentiation 68	Anti-CD68, Clone KP1 (Dako, Santa Clara, CA, USA)	Ready-to-use	Horse anti-mouse IgG, BA-9400 (Vector, Burlingame, CA, USA)	1:200
Gal-3	Galectin-3	Anti-Gal-3, R2D AF1154 (R&D Systems, Minneapolis, MN, USA).	1:400	Rabbit anti goat IgG, BA-5000 (Vector, Burlingame, CA, USA)	1:200
TNF-α	Tumor necrosis factor alpha	Anti-TNF-α, ab6671 (Abcam, Cambridge, UK)	1:200	Goat anti-rabbit IgG, BA-1000 (Vector, Burlingame, CA, USA)	1:200
CCL2	Chemokine (C-C motif) ligand 2 (CCL2)	Anti-CCL2, ab9669 (Abcam, Cambridge, UK)	1:200	Goat anti-rabbit IgG, BA-1000 (Vector, Burlingame, CA, USA)	1:200
CCR2	Chemokine (C-C motif) receptor 2	Anti-CCR2, abcam 21667 (Abcam, Cambridge, UK)	1:500	Goat anti-rabbit IgG, BA-1000 (Vector, Burlingame, CA, USA)	1:200
IL-10	Interleukin-10	Anti-IL-10, ab34843 (Abcam, Cambridge, UK)	1:200	Goat anti-rabbit IgG, BA-1000 (Vector, Burlingame, CA, USA)	1:200
PON-1	Paraoxonase-1	In-house	1:50	Goat anti-rabbit IgG, BA-1000 (Vector, Burlingame, CA, USA)	1:200
HNE	4-hydroxy-2-nonenal	Anti-HNE, MHN-100P (Genox, Baltimore, MD, USA)	1:1000	Goat anti-rabbit IgG, BA-1000 (Vector, Burlingame, CA, USA)	1:200
Western Blotting					
Gal-3	Galectin-3	Anti-Gal-3, R2D AF1154 (R&D Systems, Minneapolis, MN, USA).	1:1000	Rabbit anti-goat IgG, BA-5000 (Vector, Burlingame, CA, USA)	1:5000
TNF-α	Tumor necrosis factor alpha	Anti-TNFα #3707 (Cell signaling, Danvers, MA, USA)	1:1000	Goat α-rabbit HRP, P0448 (Dako, Santa Clara, CA, USA)	1:5000
CD163	CD163 molecule	Anti-CD163, ab182422 (Abcam, Cambridge, UK)	1:1000	Goat α-rabbit HRP, P0448 (Dako, Santa Clara, CA, USA)	1:5000
IL-10	Interleukin-10	Anti-IL-10, ab34843 (Abcam, Cambridge, UK)	1:1000	Goat α-rabbit HRP, P0448 (Dako, Santa Clara, CA, USA)	1:5000
pSTAT-3	Phospho-signal transducer and activator of transcription 3	Anti-pSTAT3, ab76315 (Abcam, Cambridge, UK)	1:1000	Goat α-rabbit HRP, P0448 (Dako, Santa Clara, CA, USA)	1:5000
STAT-3	Signal transducer and activator of transcription 3	Anti-STAT3, ab68153 (Abcam, Cambridge, UK)	1:1000	Goat α-rabbit HRP, P0448 (Dako, Santa Clara, CA, USA)	1:5000
PON-1	Paraoxonase-1	In-house	1:200	Goat α-rabbit HRP, P0448 (Dako, Santa Clara, CA, USA)	1:5000
α-SMA	α-smooth muscle actin	Anti α –SMA, ab5694 (Abcam, Cambridge, UK)	1:1000	Goat α-rabbit HRP, P0448 (Dako, Santa Clara, CA, USA)	1:5000
Shh	Sonic hedgehog	Anti Shh, ab53281 (Abcam, Cambridge, UK)	1:1000	Goat α-rabbit HRP, P0448 (Dako, Santa Clara, CA, USA)	1:5000

STUDY II

NASH modulates circulating metabolites from energy and one-carbon metabolism in obesity: implication in NASH remission

UNIVERSITAT ROVIRA I VIRGILI
ASSESSING DIAGNOSTIC AND THERAPEUTIC TARGETS IN OBESITY-ASSOCIATED LIVER DISEASES
Noemí Cabré Casares

Participants

Among patients referred to the Bariatric Surgery Unit at the Hospital Universitari Sant Joan de Reus 270 patients with homogeneous ethnic origin consented to participate according to current guidelines and to the procedures (207, 245) approved by our Institutional Review Board and Ethics Committee (OBESPAD/14.07-31proj3 and INFLAMET/15-04/4proj7) and provided written informed consent to an intraoperative liver biopsy and donation of a preoperative fasting blood sample. Histologic discrimination was based on the non-alcoholic fatty liver score (NAS) system with care to avoid excluding advanced cases with low steatosis (200, 240, 246). Only patients at both sides of the clinical spectrum classified as non-NASH (n=130) i.e., with only minor liver alterations, or NASH (n = 53) were included. NASH patients also agreed to undergo blood donation, and a second biopsy was performed by ultrasound guided, percutaneous needle puncture (OM-NAFLD, ESO3/18012013) at 12 months post-surgery. Relevant data were extracted from clinical records. Healthy age- and sex-matched nonobese controls (n=50) were recruited among participants in a previous population-based study (247) in whom liver alterations were excluded via liver imaging techniques and laboratory assessment (207). The BMI was calculated as the weight in kilograms divided by the square of the height in meters. A similar time of fasting (at least 10 hours) was considered essential for collecting blood samples, and EDTA-plasma aliquots were immediately stored at -80 °C for batched analyses. Readily available laboratory measurements were analyzed using standard tests in a Roche Modular Analytics P800 system (Roche Diagnostics, Basel, Switzerland). Homeostatic model assessment for insulin resistance (HOMA-IR) was calculated as described (248).

Liver Biopsies

Portions of the liver were obtained with wedge resection during the surgical procedure, and paired biopsies in NASH patients were obtained with needle devices 12 months after surgery, which required cooperation from trained pathologists, radiologists and surgeons (249, 250) Histologic features in sections stained with hematoxylin and eosin, Masson's trichrome and Sirius red dyes were evaluated by the scores for steatosis (0-3), lobular inflammation (0-3), and ballooning (0-2), for a total (unweighted) score ranging from 0 to 8. Non-NASH patients scored ≤ 2, and NASH patients scored ≥ 5. Liver fibrosis was assessed considering the scale defined as F0, normal; F1a or F1b, mild or moderate focal pericellular fibrosis in zone 3; F1c, portal fibrosis; F2, perivenular and pericellular

fibrosis confined to zones 2 and 3, with or without portal or periportal fibrosis; F3, bridging or extensive fibrosis with architectural distortion; and F4, cirrhosis (200, 240, 251).

Quantitative targeted metabolomics platform

To quantitate metabolites involved in energy generation and 1-C metabolism, a chromatographic separation followed by mass spectrometry detection were performed. Metabolite extraction and chromatographic and mass spectrometer conditions have been previously described (252-254). Briefly, 400 μL of methanol containing selected internal standards (Cambridge Isotope Laboratories, Tewksbury, MA, USA) were added to 100 μL of plasma. The use of internal standards ensures to maximize technical precision during the injection and recovery during the extraction procedures. After protein precipitation, samples were centrifuged at 14000 rpm at 4 ºC during 10 minutes and supernatant was collected, dried in a Savant SPD2010 SpeedVac rotatory vacuum system (Thermo Fischer, USA) and stored at -80 ºC until analysis. Calibration curves containing internal standards were prepared immediately before each analysis using commercially available standards (Sigma-Aldrich, Madrid, Spain).

For the quantitation of intermediates of energy generation, dried samples were derivatized with methoxyamine dissolved in pyridine (40 mg/mL) and N-Methyl-N-trimethylsilyltrifluoroacetamide (TMS) as described (254). Then, samples were placed in chromatographic vials and injected into a 7890A gas chromatograph (GC) coupled with an electron impact (EI) source to a 7200 quadrupole time-of-flight mass spectrometer (QTOF-MS) equipped with a J&W Scientific HP-5MS column (30 m × 0.25 mm, 0.25 μm) (Agilent Technologies, Santa Clara, CA, USA). Parameters and conditions for GC-EI-QTOF-MS equipment are detailed in Riera-Borrull *et al.* (252). For the quantitation of metabolites belonging 1-C metabolism, samples were dissolved in 100 μL of methanol:H2O (8:2 v/v) and injected into a 1290 Infinity ultra-high performance liquid chromatograph (UHPLC) coupled with an iFunnel electrospray ionization (ESI) source to a 6490 triple quadrupole mass spectrometer (QqQ-MS) (Agilent Technologies) equipped with an Acquity UPLC HSS T3 column (2.1 x 150 mm, 1.8 μm) (Waters Corporation, Mildford, MA, USA) working in Multiple Reaction Monitoring (MRM) and positive ionization modes. Detailed parameters of UHPLC-ESI-QqQ-MS and transitions for each metabolite were already described (253, 254).

Metabolites were identified and quantitated using MassHunter Qualitative and Quantitative Analysis B.07.00 software (Agilent Technologies), respectively.

Global DNA methylation

RNA-free DNA from peripheral blood leukocytes was prepared and purified using the QIAamp DNA Blood Mini Kit (Qiagen, Barcelona, Spain) dissolving DNA in RNase-free water. DNA quantitation and purity were assessed using a Nanodrop 1000 spectrophotometer (Thermo, Madrid, Spain). Total 5-methylcytosine (5-mC) and 5-hydroxymethylcytosine (5-hmC) content were detected in genomic DNA using an acid hydrolysis followed by a LC-MS-based method. DNA was hydrolyzed following a published protocol (255). Briefly, 200 µL of 88% formic acid was added to dry DNA (2.5 µg) and incubated at 140 ºC for 90 minutes in sealed glass vials. Samples were cooled at room temperature and evaporated under N_2, resuspended in 100 µL of 0.1% formic acid and placed into chromatographic vials. Detection of 5-mC, 5-hmC and guanine (G) was carried out by injecting 5 µL of hydrolyzed DNA into the UHPLC-ESI-QqQ-MS system (Agilent Technologies) equipped with an Acquity UPLC HSS T3 column (2.1 x 150 mm, 1.8 µm) (Waters Corporation) and operating in MRM and positive ionization modes. Transitions used were as follow: for 5-mC, 126 → 109 and 126 → 83; for 5-hmC, 142 → 124 and 142 → 90; for G, 152 → 135 and 152 → 110. Metabolites were detected and quantitated using MassHunter Qualitative and Quantitative Analysis B.07.00 (Agilent Technologies), respectively. Quantitation was performed attending to the standard calibration curves to calculate the proportions of methylated and hydroxymethylated DNA related to the total guanine content.

Statistical analysis

The employed statistical software included the program 'R' (http://cran.rproject. org), the SPSS 25.0 package (IBM, Madrid, Spain) and the MetaboAnalyst 4.0 (256) (https://www.metaboanalyst.ca/). Significantly altered metabolites, which were corrected for multiple testing, were defined using a p-value < 0.05 and a predesigned false discovery rate (257). We used Welch's t-test and/or Wilcoxon's rank sum test for pairwise comparisons and repeated- measurement analysis of variance for some calculations. We used multivariate statistics to improve the analysis of complex raw data and for pattern recognition. Random forests were used as a supervised classification technique to provide an unbiased estimate of prediction accuracy of classification and to select variables with the largest impacts (258). Heatmaps were used to visualize metabolomic data indicating the relative abundance of metabolites with color intensity. We also used linear discriminant analysis as a method of classification and principal component analysis as an unsupervised data analysis method to segregate the compared groups according to metabolomic data. Finally, logistic regression

analysis and receiver operating characteristic (ROC) curves described and assessed binary classifications (259). For this purpose, we also used confusion matrix and predicted class probabilities of each sample across 100 Monte-Carlo cross-validations.

STUDY III

α-Ketoglutarate regulates AMPK/mTOR-driven pathways in NASH remission: therapeutic perspectives through rewiring metabolism and epigenetics

UNIVERSITAT ROVIRA I VIRGILI
ASSESSING DIAGNOSTIC AND THERAPEUTIC TARGETS IN OBESITY-ASSOCIATED LIVER DISEASES
Noemí Cabré Casares

Study design and participants

We included morbidly obese patients consecutively referred to the bariatric surgery unit at the Hospital Universitari Sant Joan de Reus with age > 30 years, BMI > 40 kg/m2, resistance to medical therapy based on lifestyle variations and without medical or psychological contraindications for LSG. The indication was confirmed according to guidelines currently used in preoperative evaluation (260). The ensuing clinical assessment excluded patients with current or past history of daily consumption of alcohol (>25 g / d) (n =12), long-term consumption of hepatotoxic drugs (n = 6) and positive testing for chronic liver diseases (n = 4). We finally included 62 patients that provided 12-hours fasting blood samples before surgery and written informed consent according to the procedures approved by our Institutional Review Board and Ethic Committee (OBESPAD/14.07-31proj3), which included intraoperative wedge-liver biopsy. Histology features were classified according to the non-alcoholic fatty liver score (NAS) system. Patients without NASH (n = 31; NAS ≤ 2) or with proven NASH (n = 31) agreed to follow-up blood samples being taken during their involvement in a 1-year prospective longitudinal study and signed an additional fully informed consent (INFLAMET/15-04/4proj7). Those patients with NASH also agreed to a second biopsy to be performed at 12 months post-surgery by ultrasound-guided, percutaneous needle puncture (OM-NAFLD, ESO3/18012013).

Cell culture experiments

HepG2 cells were maintained in complete cell culture medium obtained by supplementing DMEM high glucose (4.5 g/L) (Lonza Ibérica) with 1% L-glutamine (Lonza Ibérica), 1% penicillin/ streptomycin–EDTA (Sigma), 1% nonessential amino acids (Sigma), and 10% fetal bovine serum (Sigma). Cells were seeded in either 6 well plates at a concentration of 200,000 cells/mL in complete cell culture medium. Standard starvation medium was EBSS (GIBCO) containing 4.5 gl-1 of glucose. The activation of glutaminolysis was performed by adding the permeable α-KG (dimethyl-α-ketoglutarate, DMKG) (Sigma). When indicated, DMKG was added to a final concentration of 0.2-2mM for 72h. Inhibitor metformin (10mM final concentration) (Sigma) were used to concomitantly with the activation of glutaminolysis. After the respective treatments cells were washed two times with phosphate-buffered saline (PBS) and stored at -80ºC until extraction and quantification of metabolites. For immunoblot assays, media were replaced with RIPA solution, lysis buffer containing a cocktail of protease inhibitor (P8340 Sigma), inhibitor of phosphatases (P0044Sigma) and PMFS 1mM.

Flow cytometry

After treatment, cells were stained with annexin V and propidium iodide (PI) (Annexin V—early apoptosis detection kit, #6592 Cell Signaling Technology) following the manufacturer's instructions. Then, cells were analysed using BDFACS Canto BD-Biosciences flow cytometer. The analysis of the data was performed using the software FlowJo.

Laboratory measurements

Blood samples were obtained after an overnight fast. Serum and plasma samples were collected after centrifugation and were stored at -80ºC until the day of analysis. Serum cholesterol, high-density lipoprotein (HDL) cholesterol, triglycerides, glucose, albumin, and insulin concentrations were analyzed by standard tests in a Roche Modular Analytics P800 system (Roche Diagnostics, Basel, Switzerland). Low- density lipoprotein (LDL) concentration was estimated by the Friedewald formula (261).

Histological analysis

Liver biopsies were obtained from NAFLD patients undergoing bariatric surgery (n=62). Biopsies from normal individuals were not collected due to ethical considerations. To minimize the variability between individuals, samples were obtained from the same location and by the same specialist. Biopsies were processed conventionally for diagnostic purposes, histological grading, and staging, as described (262). All liver specimens were evaluated by an experienced pathologist, blinded to clinical data, using the NAFLD histology scoring system. The severity of steatosis was graded from 0 to 3, inflammation from 0 to 3, hepatocellular ballooning between 0 or 1, and fibrosis from 0 to 4. Each liver specimen was assessed for the presence or absence of NASH by using the NAFLD activity score (NAS score), defined as the sum of steatosis, inflammation and hepatocyte ballooning. Those patients with a NAS score of ≥ 5 were classified as having NASH (240).

Transmission electron microscopy (TEM)

The samples used or TEM was prepared following the protocol described (263). Briefly, small pieces of the liver were fixed in a 2% glutaraldehyde solution in 0.1M cacodylate buffer, pH 7.4. Post fixed, the sample were included in osmium tetroxide (OsO_4) and dehydrated in sequential steps of acetone prior to impregnation in increasing concentrations of the resin in acetone. Small sections (500nm) were stained with 1% toluidine blue. Ultrathin sections (70nm) were subsequently cut

using a diamond knife, double-stained with uranyl acetate and lead citrate, and examined using a transmission electron microscope (Hitachi, Tokyo, Japan).

Immunoblotting analysis

Previously frozen liver tissue (20 mg) was homogenized in 300 µl of a lysis buffer (0.25M sucrose, 1mM Pefabloc, and phosphatase Inhibitor cocktail (Roche), using a sonicator (Branson Sonifer 150, Thistle Scientific, Glasglow, United Kingdom). Cells were harvested and homogenized with RIPA solution. Lysis buffer containing 2% sodium dodecyl sulfate (SDS), 50 mM Tris-HCl (pH 6.8), 10 mM dithiothreitol (DTT), 10% glycerol, 0.002% bromphenol blue, and freshly added protease inhibitors. 50 µg of protein from total homogenates at 100 °C for 5 min in Laemmli sample buffer (LSB) and β-mercaptoethanol. For the protein separation, 8%-14% SDS-polycrilamide gel was used and transferred to a PVDF or nitrocellulose membrane (Thermo Fisher, Barcelona, Spain). Membranes were blocked with non-fat milk or bovine serum albumin at 5% in Tris, sodium chloride and 1% Tween-20. The following antibodies (Table 3) were used pAMPK, AMPK, pAKT, AKT, pMTOR, MTOR, pS6, p4EBP1, p62, FASN, LC3, Tom20, Casp 8 and Casp 3, pSTAT-3, STAT-3 (1/1000, Cell Signaling), IL-10, MFN2, OXPHOS and LAMP2A (1/1000, Abcam), β-actin and Casp 9 (1/1000, Sigma) and FAA (1/2000, Millipore). Secondaries peroxidase-conjugated antibodies diluted 1:5000 (Dako). Immunoreactive bands were visualized using SuperSignal West Femto chemiluminescent substrate (Pierce, Rockford, IL, USA) and the analysis was performed with a ChemiDoc system (Bio-Rad Laboratories, Madrid, Spain). Bands were analyzed and quantified using the software Image Lab 2.0 (Bio-Rad Laboratories).

Targeted metabolomics analysis

Metabolite extraction from liver tissue (20 mg) was performed adding 500 µL of methanol/water (8:2) containing internal standards and disrupting the tissue using a Precellys 24 system (Izasa, Barcelona). After centrifugation at 14,000 rpm for 10 min at 4°C, supernatants were collected, and the homogenization step was repeated. To avoid interferences in the analysis, non-polar compounds such as lipid species were further removed adding 2 mL of chloroform and following the Folch protocol (264). Polar phase was collected, filtered using 0.22 µm filters, dried in a rotatory vacuum system and stored at -80 ºC until analysis. Sample preparation and equipment settings for the analysis of metabolites involved in energy and 1-C metabolism were performed as described in Study II and in previously published data (252-254). Raw data was processed and compounds were

detected and quantitated using the MassHunter Qualitative and Quantitative Analysis B.07.00 software (Agilent Technologies), respectively.

RNA extraction

Total RNA was isolated from human liver tissue using the Qiagen RNeasy Lipid Tissue Mini Kit, and RNA concentration was quantified on a NanoDrop ND-1000 spectrophotometer (Nanodrop Technologies Inc., Wilmington, NC). An RNA integrity number (RIN) was calculated using a RNA2100 Bioanalyzer (Agilent Technologies, Santa Clara, CA) with the RNA 6000 Nano Kit.

Gene expression microarray

For microarray investigation of gene expression, 100 ng of total RNA were prepared using the Agilent One-Color Microarray-Based Gene Expression Analysis Low Input Quick Amp Labeling Kit (cat. no. 5190-2943), and were then hybridized to the Agilent SurePrint G3 Human Gene Expression 8x60k v2 microarray following the manufacturer's instruction. In short, an input of 100 ng of entire RNA was used to generate cDNAs, followed by in vitro transcription and incorporation of Cy3 into the nascent cDNAs. The cy3-labeled cDNAs were fragmented and hybridized to the array for 17 h at 65ºC in an Agilent hybridization oven (cat. no. G2545A) Arrays were scanned on an Agilent G2565CA microarray scanner at 5 µM resolution. The raw data were extracted using the Agilent Feature Extraction 10.7.3.1 Software.

Gene expression analysis

One microgram of RNA was transcribed to cDNA with random primers using the Reverse Transcription System (Applied Biosystems, Foster City, CA). Quantitative gene expression was evaluated by Real-time PCR (qPCR) on a 7900HTFast Real-Time PCR System using the TaqManR Gene Expression Assay (Applied Biosystems). All measurements (Table 4) were normalized to 18S.

DNA Extraction

Liver tissues were dissolved in 200 µL lysis buffer from the Qiagen QIAmp DNA Micro Kit (cat. no. 56304), and incubated with proteinase K overnight at 56°C. DNA concentration was determined using a NanoDrop ND-1000 spectrophotometer (Nanodrop Technologies Inc., Wilmington, NC).

Global DNA methylation

Total 5-mC and 5-hmC content were detected and quantitated in genomic DNA as previously described in Study II.

DNA methylation microarray

To detect methylation differences in individual cytosine-guanine dinucleotides (CpGs) between NASH and Non-NASH patients, we performed array-based DNA methylation analysis. Bisulfite-converted DNA was analyzed using the Illumina Infinium Human MethylationEPIC BeadChip Array technology (San Diego, CA), which explores more than 850,000 CpGs in the human genome.

Statistical analysis

The Kolmogorov-Smirnov test was used to assess the normal distribution of our variables. Wilcoxon rank-sum tests (nonparametric) were used to determine significant differences between groups according to the distribution of variables and considered statistically significant when $p < 0.05$. The chi-squared test use to compare categorical variables. All results are shown as the mean ± SEM unless otherwise stated. Statistical analyses were carried out using the SPSS 22.0 package and R version 3.4. MetaboAnalyst 4.0 (256) available on the web (http://www.metaboanalyst.ca/) were used to generate scores/loading plots and Heatmaps.

Methylation array analysis

We analyzed the raw data from the Illumina Infinium MethylationEPIC array using the minfi (265, 266) package in R, with annotations from Illumina Human Methylation EPICmanifest v0.3.0 (267) and Illumina Human Methylation EPICanno.ilm10b2.hg19 v0.6.0 (268). Briefly, we loaded raw probe level data and removed those with detection $p < 0.01$. From these, we normalized the data using the preprocessQuantile() function with mergeManifest=T, which resulted in an object with 864,307 CpGs. To remove CpGs with SNPs, we ran dropLociWithSnps() with snps=c("SBE", "CpG", "Probe") and maf=0 parameters. We then filtered to keep only autosomal CpGs and only those not on cross-reactive probes (269). Each remaining CpG had a beta value (calculated using getBeta()), which is the fraction of methylated / methylated + unmethylated signal, bounded between 0 and 1. We performed Wilcoxon rank-sum tests on each CpG ($n = 8$ for each group) to determine significance of any differences. We also determined the average beta level in NASH and Non-NASH patients and then retained the CpGs whose average Δ beta > 0.05 and whose $p < 0.05$.

We annotated subsets of CpGs across features of the genome using the genomation package in R (270), with hg19 knownGene and CpG island .bed files downloaded from the UCSC Table Browser (271) (autosomal data only) as inputs. To generate a heatmap visualization, we arcsine transformed the beta values for significantly differentially methylated CpGs and clustered the rows and columns using the heatmap.2() function from the gplots package (https://cran.r-project.org/web/packages/gplots/index.html) in R.

Microarray analysis of mRNA transcripts

Microarray analysis pipeline were done in the proprietary Agilent Gene Spring GX v14.8 software. At the gene level, spot signals were normalized by 75% percentile, control probes removed, and 46,308 genes kept for statistical analysis. These were then filtered to keep only autosomal genes in TxDb.Hsapiens.UCSC.hg19.knownGene (272) (20,214 genes kept) for further analysis in R. Using the t.test() function, we determined significance of expression difference between NASH and Non-NASH patients (n = 8 each). We determined 345 genes to have $p < 0.05$ and $\log2(\text{NASH/Non-NASH}) > 1$, which are shown in magenta in Figure S4A. All RNA expression data (20,214 genes) were used for the integration of DNA methylation and gene expression data (see below).

Integration of DNA methylation and gene expression data

For a more integrative analysis of DNA methylation and gene expression, we merged the CpG data from gene promoters with corresponding gene expression data. To determine significantly differentially methylated CpGs in gene promoters, we filtered for those annotated as TSS1500 or TSS200 (426 CpGs). We then merged these CpGs with the RNA microarray data by gene name, resulting in 367 promoter CpG-gene pairs. To understand the relationship between CpG methylation and gene expression, we used cor.test() in R, with individual beta values, expression values, and method="spearman" as inputs. CpGs whose correlation p-values < 0.05 (11 CpGs in total) were kept for further analysis. The Circos visualization was generated using the circlize package (273) in R. Kyoto Encyclopedia of Genes and Genome (KEGG) pathway analyses on selected subsets of genes were performed as described in (274). The $-\log_{10}$(p-value) is shown for each pathway in the figures, as calculated by hypergeometric test in R.

Table 3. List of antibodies and dilutions used in immunoblot analyses

Antigen	Primary Antibody	Dilution	Secondary Antibody	Dilution
AMPK-pT172	pAMPK Antibody, #2531 (Cell signalling, Danvers, MA, USA)	1:1000	Goat α-rabbit HRP, P0448 (Dako Agilent)	1:5000
AMPK	AMPK Antibody #2532S (Cell signalling, Danvers, MA, USA)	1:1000	Goat α-rabbit HRP, P0448 (Dako Agilent)	1:5000
AKT-pT308	p-Akt Antibody, #4056 (Cell signalling Danvers, MA, USA)	1:1000	Goat α-rabbit HRP, P0448 (Dako Agilent)	1:5000
AKT-pT473	p-Akt Antibody, #4060 (Cell signalling, Danvers, MA, USA)	1:1000	Goat α-rabbit HRP, P0448 (Dako Agilent)	1:5000
AKT	AKT Antibody, #4685 (Cell signalling, Danvers, MA, USA)	1:1000	Goat α-rabbit HRP, P0448 (Dako Agilent)	1:5000
ATG7	ATG7 Antibody, #8558 (Cell signalling, Danvers, MA, USA)	1:1000	Goat α-rabbit HRP, P0448 (Dako Agilent)	1:5000
mTOR-pS2448	p-mTOR Antibody, #2971 (Cell signalling, Danvers, MA, USA)	1:1000	Goat α-rabbit HRP, P0448 (Dako Agilent)	1:2000
mTOR	mTOR Antibody, #2972 (Cell signalling, Danvers, MA, USA)	1:200	Goat α-rabbit HRP, P0448 (Dako Agilent)	1:2000
S6-pS235/236	p-S6 Antibody, #4856 (Cell signalling, Danvers, MA, USA)	1:1000	Goat α-rabbit HRP, P0448 (Dako Agilent)	1:5000
4EBP1-pT37/46	p-4E-BP1 Antibody, #2855 (Cell signalling, Danvers, MA, USA)	1:1000	Goat α-rabbit HRP, P0448 (Dako Agilent)	1:5000
p62/SQSTM1	SQSTM1 / p62 Antibody, #5114 (Cell signalling, Danvers, MA, USA)	1:1000	Goat α-rabbit HRP, P0448 (Dako Agilent)	1:5000
Caspase 3	Cleaved Caspase-3 Antibody, #9664 (Cell signalling, Danvers, MA, USA)	1:1000	Goat α-rabbit HRP, P0448 (Dako Agilent)	1:5000
Caspase 8	Caspase-8 Antibody, #9746 (Cell signalling, Danvers, MA, USA)	1:1000	Goat α-rabbit HRP, P0448 (Dako Agilent)	1:5000
Caspase 9	Caspase-9 Antibody, C7729 (Sigma, Saint Louis, MO, USA	1:1000	Goat α-rabbit HRP, P0448 (Dako Agilent)	1:5000
IL10	IL10 antibody, ab34843 (Abcam, Cambridge, UK)	1:1000	Goat α-rabbit HRP, P0448 (Dako Agilent)	1:5000
OXPHOS	OXPHOS Antibody, ab110411 (Abcam, Cambridge, UK)	1:1000	Goat α-mouse, HRP, 1D3 (Dako Agilent)	1:5000
STAT3-pT705	p-STAT3 Antibody, #9145 (Cell signalling, Danvers, MA, USA)	1:1000	Goat α-rabbit HRP, P0448 (Dako Agilent)	1:5000
STAT3	STAT3 Antibody, #9139 (Cell signalling, Danvers, MA, USA)	1:1000	Goat α-mouse HRP, P0447 (Dako, Agilent)	1:5000
LC3B	LC3B Antibody, #2775S (Cell signalling, Danvers, MA, USA)	1:1000	Goat α-rabbit HRP, P0448 (Dako Agilent)	1:5000
LAMP2A	LAMP2A Antibody, ab125068 (Abcam, Cambridge, UK)	1:1000	Goat α-rabbit HRP, P0448 (Dako Agilent)	1:5000
FASN	FASN Antibody, #3180 (Cell signalling, Danvers, MA, USA)	1:1000	Goat α-rabbit HRP, P0448 (Dako Agilent)	1:5000
TOM20	Tom20 Antibody, #42406 (Cell signalling, Danvers, MA, USA)	1:1000	Goat α-rabbit HRP, P0448 (Dako Agilent)	1:5000
MFN2	MFN2 Antibody, ab127773 (Abcam, Cambridge, UK)	1:1000	Goat α-rabbit HRP, P0448 (Dako Agilent)	1:5000
FAH	FAH Antibody, #ABN526 (Millipore, Massachusetts, USA)	1:1000	Goat α-rabbit HRP, P0448 (Dako Agilent)	1:5000

Table 4. List of genes from gene expression analysis. Results were calculated using the comparative Ct method and expressed relative to the expression of the housekeeping genes 18S (Hs03928985_g1).

Detector	Gene name
αKGDH Hs01081865_m1	Alpha---Ketoglutarate Dehydrogenase
ACACA Hs01046047_m1	Acetyl-CoA Carboxylase Alpha
ACLY Hs00153764_m1	ATP citrate lyase
IDH1 Hs00271858_m1	Isocitrate Dehydrogenase 1
IDH2 Hs00953881_m1	Isocitrate Dehydrogenase 2
IDH3A Hs00194253_m1	Isocitrate Dehydrogenase 3A
GSL1 Hs00248163_m1	Glutaminase
GLUD1 Hs03989560_s1	Glutamate Dehydrogenase 1
PC Hs00559398_m1	Pyruvate Carboxylase
SDHB Hs01042482_m1	Succinate Dehydrogenase B
ACP5 Hs00356261_m1	Acid Phosphatase 5, Tartrate Resistant
ARL8A Hs00373395_m1	ADP Ribosylation Factor Like GTPase 8A
C1orf54 Hs04398113_m1	Chromosome 1 Open Reading Frame 54
DISP2 Hs00394338_m1	Dispatched RND Transporter Family Member 2
HDAC9 Hs00206843_m1	Histone Deacetylase 9
MARK3 Hs01058270_m1	Microtubule Affinity Regulating Kinase 3
RAB31 Hs00199313_m1	RAB31, Member RAS Oncogene Family
TDRD6 Hs01597145_m1	Tudor Domain Containing 6
TRIP10 Hs01012747_m1	Thyroid Hormone Receptor Interactor 10
UGT3A2 Hs04177793_m1	UDP Glycosyltransferase Family 3 Member A2
ZNF197 Hs01560359_m1	Zinc Finger Protein 197

Results

UNIVERSITAT ROVIRA I VIRGILI
ASSESSING DIAGNOSTIC AND THERAPEUTIC TARGETS IN OBESITY-ASSOCIATED LIVER DISEASES
Noemí Cabré Casares

STUDY I

Bariatric surgery reverses non-alcoholic fatty liver disease in morbid obesity and while reducing oxidative stress and inflammation

UNIVERSITAT ROVIRA I VIRGILI
ASSESSING DIAGNOSTIC AND THERAPEUTIC TARGETS IN OBESITY-ASSOCIATED LIVER DISEASES
Noemí Cabré Casares

Metabolic outcomes and remission of hepatic alterations post-BS

Pre-BS, patients with severe obesity had decreased insulin sensitivity, increased chronic low-grade inflammation, higher prevalence of T2DM, dyslipidemia and hypertension, compared to the healthy population. We observed a high ratio of women to men in the obese cohort. Data presented here are without sex segregation because of the longitudinal nature of the study and, as well, because logistic regression analyses discarded sex as a determinant factor in diagnosis and/or disease outcomes. According to the NAS score, non-NASH, uncertain NASH and definite NASH were recorded in 43.8%, 34.6% and 21.6% of patients, respectively (Table 5).

One-year post-BS, most clinical and biological metabolic outcomes significantly improved, together with a general amelioration of histological features of NAFLD; improvement was more evident in the most severe cases. Mild steatosis was observed in 4 patients (3%), mild lobular inflammation (<2 foci) in 22 patients (18.4%) and hepatocyte ballooning in 21 patients (17.5%). Fibrosis also improved, especially in the few patients with bridging fibrosis (Table 6 and Figure 15). Of note, one patient with pre-surgery liver cirrhosis presented only periportal/perisinusoidal fibrosis one-year post-surgery (Figure 16).

Oxidation and inflammation and their association with NASH

We found a significantly higher proportion of PON1, 4-hydroxy-2-nonenal and CD68 stained cells in liver biopsies of patients with NASH (n=94), compared to non-NASH patients (n=191). Sirius red positive areas were also significantly higher (Figure 17a). CD68 stained cells were more frequent in areas with inflammation and PON1 staining was stronger in hepatocytes with ballooning degeneration. Fat accumulation and 4-hydroxy-2-nonenal staining were more intense in fibrous areas (Figure 18).

Table 5. Selected characteristics in patients with severe obesity and in the control group

	Control group (n=404)	Obese patients (n=436)		
		Non-NASH (n=191)	Uncertain NASH (n=151)	NASH (n=94)
Male, n (%)	175 (43.1)	41 (21.5) [a]	41 (27.2) [b]	25 (26.6) [c]
Age, years	46 (35 - 59)	46 (39 - 56)	49 (42 - 57)	48 (42.25 - 56.75)
BMI, kg/m^2	26.78 (23.34 – 28.12)	44.6 (41.3 - 49.2) [a]	46.6 (43.0 - 51.4) [b,d]	46.3 (42.3 - 51.5) [c]
T2DM, n (%)	26 (6.3)	60 (31.6) [a]	66 (44.0) [b,d]	48 (51.1) [c,e]
Hypertension, n (%)	62 (15)	104 (54.5) [a]	83 (55.0) [b]	62 (66.0) [c,e]
Dyslipidemia, n (%)	36 (8.7)	55 (28.8) [a]	58 (38.4) [b,d]	40 (42.6) [c,e]
Medication, n (%)				
Metformin	6 (1.4)	33 (17.3) [a]	45 (30.0) [b,d]	36 (38.3) [c,e]
Insulin	-	10 (5.2)	16 (10.6) [d]	10 (10.6)
Sulfonylureas	6 (1.4)	8 (4.2) [a]	11 (7.3) [b]	9 (9.6) [c]
ACEIs+ARA II	15 (3.6)	55 (28.8) [a]	51 (33.8) [b]	41 (43.6) [c,e]
Diuretics	20 (4.8)	15 (7.9)	14 (9.3) [b]	12 (12.8) [c]
Statins	8 (1.9)	31 (16.3) [a]	34 (22.5) [b]	19 (20.4) [c]
Biochemical variables				
Total cholesterol, mmol/L	5.2 (4.6 - 5.9)	4.1 (3.5 - 4.8) [a]	4.4 (3.6 - 5.1) [b]	4.4 (3.8 - 5.0) [c]
HDL-cholesterol, mmol/L	1.4 (1.2 - 1.7)	1.2 (0.9 - 1.5) [a]	1.1 (0.85 - 1.4) [b]	1.1 (0.88 - 1.3) [c]
LDL-cholesterol, mmol/L	3.1 (2.6 - 3.8)	2.7 (2.1 - 3.2) [a]	2.7 (2.1 - 3.3) [b]	2.8 (2.4 - 3.4) [c]
Triglycerides, mmol/L	1.1 (0.7 - 1.5)	1.5 (1.1 - 2.0) [a]	1.7 (1.3 - 2.4) [b,d]	1.8 (1.2 - 2.4) [c,e]
Glucose, mmol/L	4.7 (4.3 - 5.2)	6.7 (5.6 - 8.3) [a]	7.4 (5.9 - 9.4) [b,d]	7.6 (6.2 - 10.9) [c,e]
Insulin, pmol/L	49.4 (31.9 - 70.0)	78.8 (39.2 - 131.1) [a]	82.6 (49.1 - 135.0) [b]	82.6 (53.4 - 145.1) [c]
HOMA-IR	1.5 (0.9 - 2.3)	3.6 (1.7 - 5.6) [a]	4.3 (2.1 - 7.1) [b,d]	5.0 (2.4 - 7.6) [c,e]
AST, µKat/L	0.35 (0.30 - 0.41)	0.45 (0.3 - 0.6) [a]	0.50 (0.39 - 0.81) [b]	0.87 (0.56 - 1.3) [c,e,f]
ALT, µKat/L	0.32 (0.23 - 0.44)	0.4 (0.3 - 0.6) [a]	0.53 (0.38 - 0.86) [b,d]	0.88 (0.56 - 1.3) [c,e,f]
CRP, mg/L	1.2 (0.5 - 2.7)	1.3 (0.5 - 4.3)	2.5 (0.70 - 9.4) [b,d]	1.83 (0.80 - 10.90)[c,e]
Steatosis grade				
≤5%	-	132 (69.1)	27 (17.9)	-
5-33%	-	54 (28.3)	74 (49.0)	9 (9.6)
33-66%	-	5 (2.6)	47 (31.1)	50 (53.2)
>66%	-	-	3 (2.0) [d]	35 (37.2) [e,f]
Lobular inflammation				
No foci	-	65 (34.2)	8 (5.3)	-
<2 foci	-	100 (52.6)	54 (36.0)	18 (19.1)
2-4 foci	-	26 (13.2)	64 (42.0)	52 (55.3)
> 4 foci	-	-	25 (16.7) [d]	24 (25.5) [e,f]
Hepatocellular ballooning				
No	-	163 (85.3)	75 (49.6)	7 (7.4)
Few cells		24 (12.7)	67 (44.4) [d]	60 (63.8) [e,f]
Many cells	-	4 (2.0)	9 (6.0)	27 (28.7) [e,f]
Fibrosis				
None (F0)	-	74 (38.7)	28 (18.5)	23 (24.4)
Perisinusoidal or periportal (F1)	-	78 (40.8)	67 (44.3)	21 (22.3)
Perisinusoidal and portal (F2)	-	32 (16.7)	41 (27.1)	29 (30.8)
Bridging fibrosis (F3)	-	7 (3.6)	15 (9.9)	20 (21.3) [e,f]
Cirrhosis (F4)	-	-	-	1(1.0)

Values are shown as number of cases and percentages or medians and interquartile ranges. ACEIs: Angiotensin-converting-enzyme inhibitor; ALT: Alanine aminotransferase; AST: Aspartate aminotransferase; ARA-II: Angiotensin II receptor antagonists; BMI: Body mass index; CRP: C-reactive protein; HDL: High-density lipoprotein; HOMA-IR: Homeostatic model assessment of insulin resistance; HTG: Hypertriglyceridemia; LDL: Low-density lipoprotein; NASH: Non-alcoholic steatohepatitis; T2DM: Type 2 diabetes mellitus. Significant differences ($p < 0.05$ or lower) in comparisons are indicated by a Control vs non-NASH. b Control vs Uncertain NASH. c Control vs NASH. d Non-NASH vs Uncertain NASH. e Non-NASH vs NASH. f Uncertain NASH vs NASH.

Table 6. Selected variables in patients with severe obesity and paired liver biopsies at baseline and 12 months after laparoscopic sleeve gastrectomy.

	Baseline (n=120)	**12 months after surgery** (n=120)	***p*-value**
BMI, kg/m2	46.4 (42.8)	31.2 (29.1-34.7)3	<0.001
Total cholesterol, mmol/L	4.3 (3.7-5.3)	4.7 (4.2-5.4)	<0.001
HDL-cholesterol, mmol/L	1.0 (0.8-1.4)	1.4 (1.2-1.7)	<0.001
LDL-cholesterol, mmol/L	3.1 (2.5-3.9)	3.0 (2.5-3.3)	0.127
Triglycerides, mmol/L	1.5 (1.1-2.3)	0.9 (0.8-1.3)	<0.001
Glucose, mmol/L	7.0 (6.0-9.1)	4.7 (4.5-5.)	<0.001
Insulin, pmol/L	100.8 (54.3-162.2)	39.6 (24.0-60.1)	<0.001
HOMA-IR	4.4 (2.8-7.5)	1.3 (0.4-2.5)	<0.001
AST, µKat/L	0.6 (0.4-0.8)	0.3 (0.2-0.3)	<0.001
ALT, µKat/L	0.5 (0.4-0.8)	0.2 (0.2-0.3)	<0.001
CRP, mg/L	3.0 (0.82-8.6)	1.5 (0.5-4.2)	<0.001
Steatosis grade			
<5%	25 (20.8)	116 (96.6)	
5-33%	46 (38.3)	4 (3.3)	
>33-66%	37 (30.8)	-	
>66%	12 (10)	-	<0.001
Lobular inflammation			
No foci	25 (20.8)	98 (81.6)	
<2 foci	38 (31.6)	22 (18.4)	
2-4 foci	41 (34.2)	-	
> 4 foci	16 (13.3)	-	<0.001
Hepatocellular ballooning			
No	49 (40.8)	98 (81.6)	
Few cells	65 (54.1)	19 (15.8)	
Many cells	6 (5.0)	3 (2.5)	<0.001
Fibrosis			
None (F0)	20 (16.6)	55 (45.8)	
Perisinusoidal or periportal (F1)	51 (42.8)	60 (50.0)	
Perisinusoidal and portal (F2)	39 (32.5)	5 (4.1)	
Bridging fibrosis (F3)	9 (7.5)	-	
Cirrhosis (F4)	1 (0.8)	-	<0.001

Values are shown as number of cases and percentages or medians and interquartile ranges. ALT, alanine aminotransferase; AST, aspartate aminotransferase; BMI, body mass index; CRP, C-reactive protein; HDL, high-density lipoprotein; HOMA-IR, homeostatic model assessment of insulin resistance; LDL, low-density lipoprotein

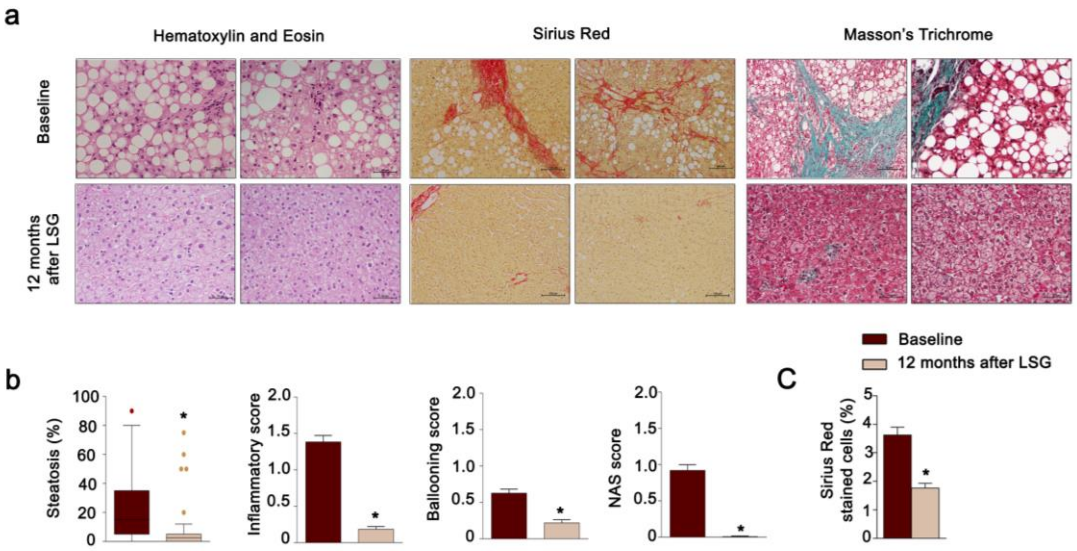

Figure 15. Post-laparoscopic sleeve gastrectomy (LSG) improvement in liver histological features of patients with non-alcoholic fatty liver disease. (a) Representative microphotographs (bars indicate 100x magnification) of baseline and 12 months post-surgery hepatic biopsies stained with Hematoxylin and Eosin, Sirius Red and Masson's Trichrome. (b) Steatosis, inflammation ballooning and NAS score were quantified according to the non-alcoholic fatty liver activity score (NAS) system. (C) Sirius Red was quantified as percentage of positively-stained areas. *p < 0.001 by Mann-Whitney U test.

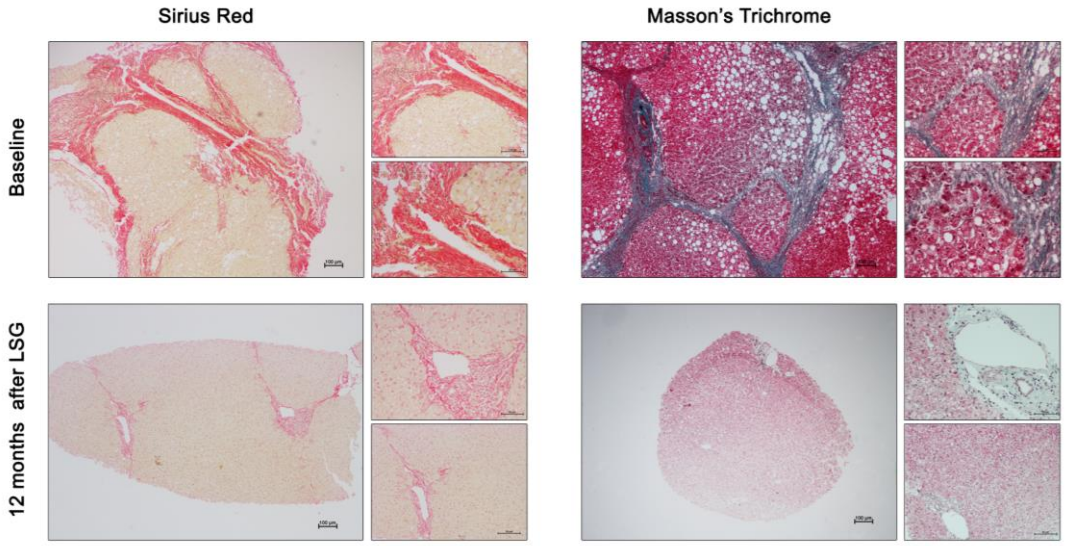

Figure 16. Post-laparoscopic sleeve gastrectomy resolution of bridging fibrosis and cirrhosis. Histological evaluation (bars indicate 40x magnification) from different cuts in a single patient with liver cirrhosis indicates fibrosis reduction after surgery.

We observed significant alterations in the pre-surgery circulating levels of molecules that tracked with oxidation and inflammation. Serum paraoxonase and lactonase activities were significantly decreased in obese patients, but serum PON-1 concentration remained unaltered. Low PON-1 activities were associated with high plasma CCL2, but these measurements did not track with patients through the different stages of NAFLD (Figure 17b). Circulating levels of TNF-α and IL-10 were also significantly different from those found in control subjects, but differences between non-NASH and NASH patients were either minor or negligible. Plasma galectin-3 levels were significantly higher in patients with NASH when compared with non-NASH patients (Figure 17b).

BS outcomes promote remission of hepatic alterations through multiple cellular responses

Using selected key markers, we compared oxidation, inflammation and fibrosis in liver tissues at baseline and 12 months post-BS. There were significant reductions in the hepatic immunochemical expressions of PON-1, 4-hydroxy-2-nonenal, CD68, CCL2, CCR2, TNF-α, and galectin-3; but IL-10 staining remained unaltered (Figure 19). For cross validation we used western blot analysis. We observed a significant reduction in the expression of TNF-α and galectin-3, with minor changes in IL-10. Variations in the expression of CD163 did not reach statistical significance. We also assessed the effect of BS in relation to the hepatic expression of STAT-3 and phosphorylated STAT-3. Both had 4-fold increase in expression post-surgery, which would indicate increased production and activation following NAFLD remission. The extent of hepatic glycated PON-1 (the 45 kD band), which is less effective in providing protection against oxidative response, was not significantly reduced. However, the unmodified, more active enzyme (the 40 kD band) that had been practically absent pre-surgery, was prominent post-surgery. Finally, we observed a significant decrease in the expression of α-smooth muscle actin (α-SMA) and sonic hedgehog (Shh) protein, indicating regression of liver fibrosis-activating pathways (Figure 20a).

Significant variations were observed in circulating paraoxonase activity and galectin-3 levels post-surgery. Circulating PON-1 and CCL2 concentrations remained high in patients with biopsy-proven NAFLD remission. Mean plasma TNF-α concentrations were normalized, and circulating IL-10 levels were even higher following remission (Figure 20b).

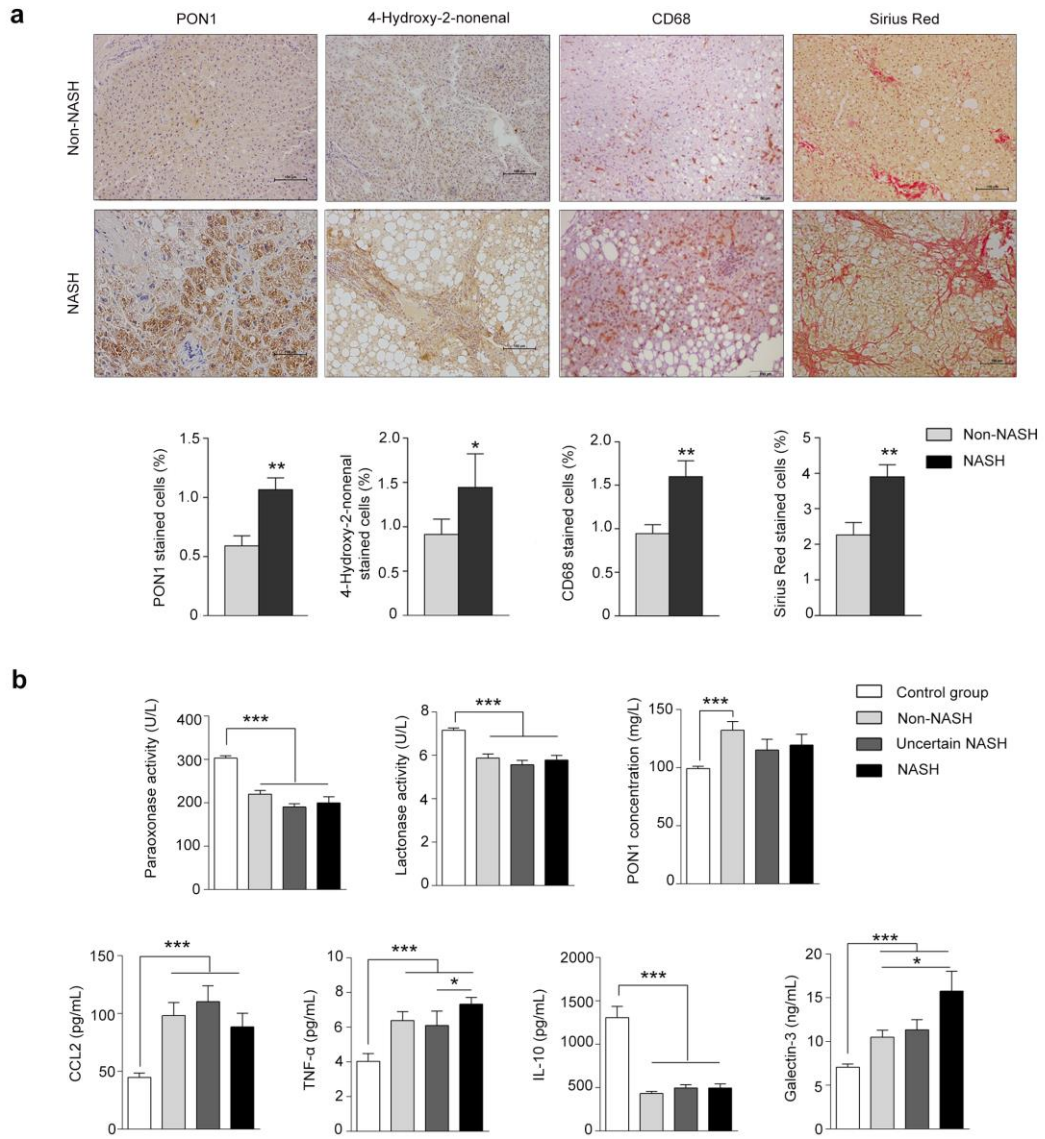

Figure 17. Hepatic oxidation and inflammation discriminate patients with NASH from those without. (a) NASH patients had higher hepatic paraoxonase-1 (PON1), 4-hydroxy-2-nonenal, and cluster of differentiation 68 (CD68) expressions and Sirius Red staining compared to non-NASH individuals (bars indicate 100 x magnifications). (b) Circulating levels of paraoxonase and lactonase activities, and paraoxonase-1 (PON1), chemokine (C-C motif) ligand 2 (CCL2), tumor necrosis factor-α (TNF-α), interleukin-10 (IL-10) and galectin-3 concentrations. *p < 0.05, **p < 0.01, ***p < 0.001 by the Mann-Whitney U test.

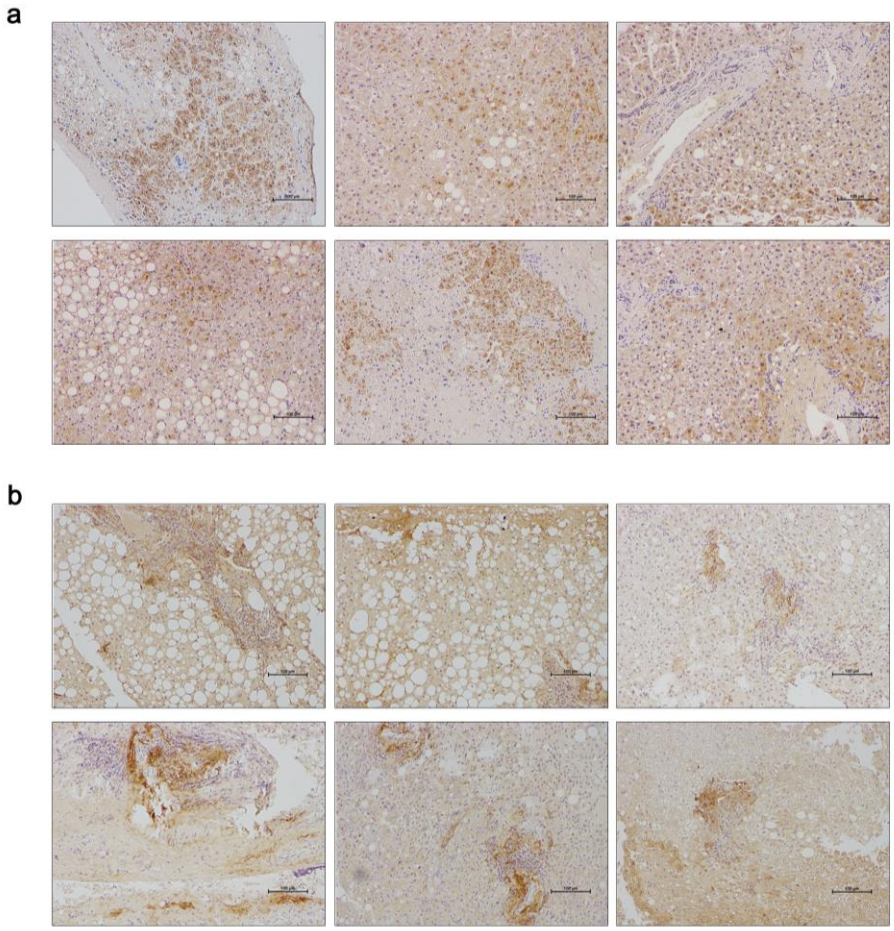

Figure 18. Oxidative markers distribution in NASH liver patients.. Representative microphotographs (bars indicate 100x magnification) indicating paraoxonase-1 (a) and 4-hydroxy-2-nonenal (b) staining. Paraoxonase-1 staining was predominantly observed in cells with fat accumulation and 4-hydroxy-2-nonenal in association with areas in which fibrosis was predominant.

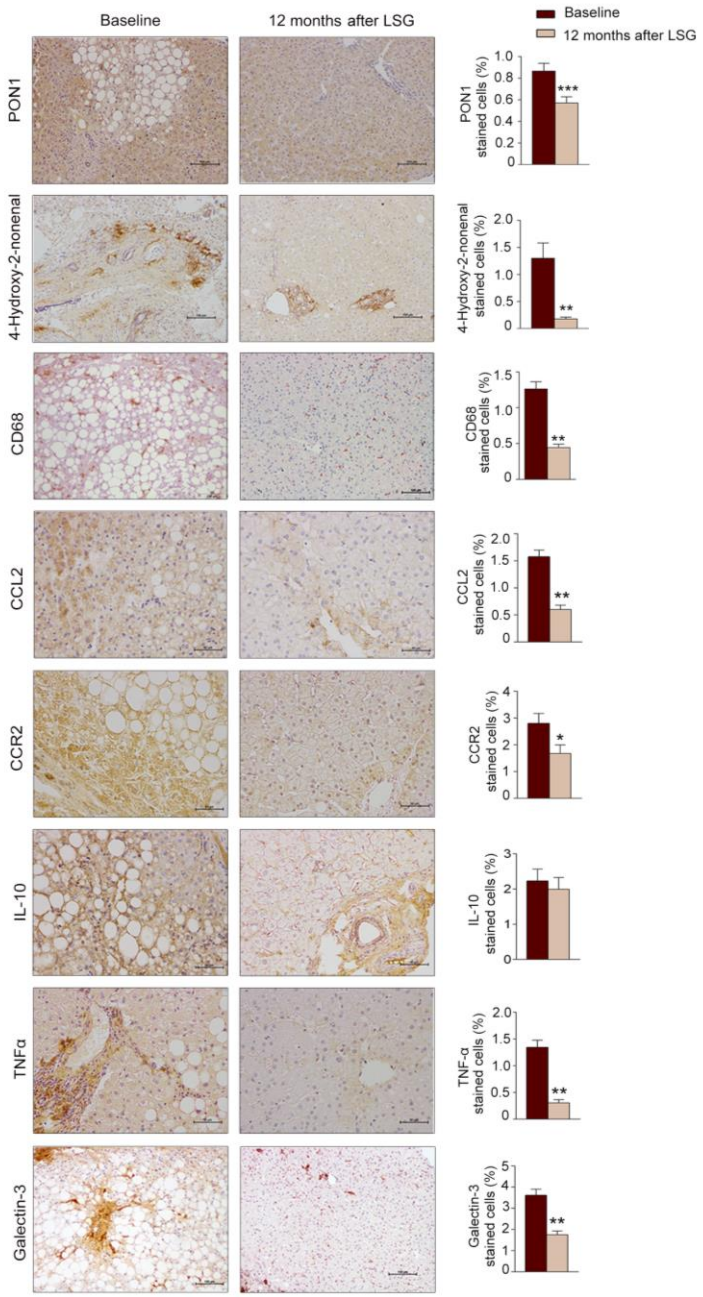

Figure 19. Effect of laparoscopic sleeve gastrectomy in oxidation and low-grade systemic inflammatory balance. Differences in the hepatic immunochemical staining of paraoxonase-1 (PON1), 4-hydroxy-2-nonenal, cluster of differentiation 68 (CD68), chemokine (C-C motif) ligand 2 (CCL2), C-C motif chemokine receptor 2 (CCR2), tumor necrosis factor-α (TNF-α), interleukin-10 (IL-10) and galectin-3 in patients pre- and 12 months post-surgery (bars indicate 100x magnification). *p < 0.01, **p < 0.001 by the Mann-Whitney U test.

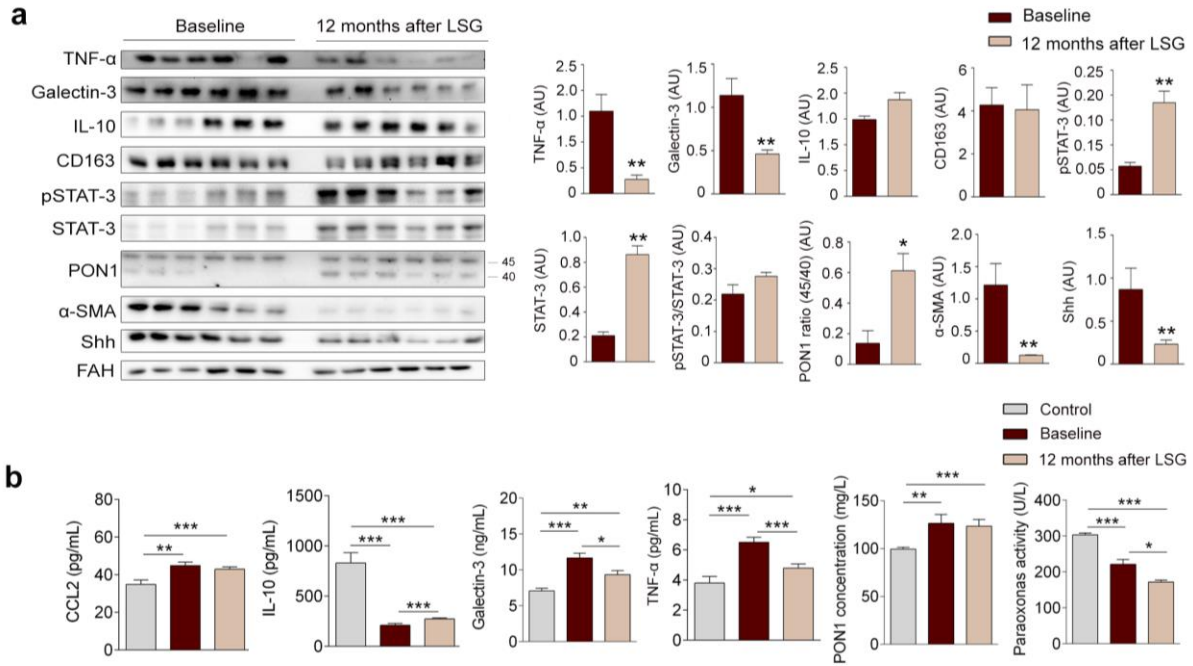

Figure 20. Laparoscopic sleeve gastrectomy (LSG) improves the hepatic levels of oxidative stress and inflammation markers. (a) Western Blot analysis of tumor necrosis factor-α (TNF-α), galectin-3, interleukin-10 (IL-10), cluster of differentiation 163 (CD163), phosphorylated signal transducer and activator of transcription-3 (pSTAT3), signal transducer and activator of transcription-3 (STAT3), paraoxonase-1 (PON1), α-smooth muscle actin (α-SMA), and sonic hedgehog protein (Shh). Pooled liver extracts were used for cross validation (left) and mean values of variations in the expression of selected markers are shown on the right. The graph of paraoxonase-1 shows the ratio between the 40 kD and the 45 kD isoforms. (b) Circulating levels of CCL2, IL-10, galectin-3, TNF-α, PON1 and paraoxonase activity in patients (before- and after-surgery) and in the control group. *p < 0.05, **p < 0.01, ***p < 0.001 by the Mann-Whitney U test.

STUDY II

NASH modulates circulating metabolites from energy and one-carbon metabolism in obesity: implication in NASH remission

UNIVERSITAT ROVIRA I VIRGILI
ASSESSING DIAGNOSTIC AND THERAPEUTIC TARGETS IN OBESITY-ASSOCIATED LIVER DISEASES
Noemí Cabré Casares

Targeted quantitative plasma metabolomic profile identifies the significant influence of obesity on energy and one-carbon metabolism

Morbid obesity was associated with metabolic alterations, as compared with nonobese controls (Table 7). To enlarge the scope of metabolic signals, we used a targeted metabolomic approach to selectively examine plasma metabolites to explore pathways of energy adaptation. Obesity appears to increase the oxidative changes through the citric acid cycle (CAC), and the significant plasma accumulation of most intermediates might reflect compensatory responses in mitochondrial energetics. We also found a significant increase in plasma glutamine, pyruvate and ß-hydroxybutyrate (ß- HB) levels in obese patients with respect to nonobese controls, with alterations in amino acids and metabolites derived from 1-C metabolism. Specifically, serine, cysteine, methionine, SAM and SAH levels were decreased in morbid obesity with a significant accumulation of cystathionine and choline, major carbon or methyl donors and critical components for signaling functions (Table 8, Figure 21 a, b).

Changes in circulating metabolites segregated nonobese controls from patients with morbid obesity and glutamine, ß-HB, citrate and cystathionine were the metabolites with the highest impacts on class distribution (Figure 21 c-e). The plasma levels of each of these metabolites predicted obesity, suggesting the contribution of body weight, but other metabolites, exemplified by plasma α-ketoglutarate (α-KG), were independent of body weight (Figure 22).

Values in plasma may suggest impaired energy homeostasis, metabolic inflexibility and likely induction of anaplerosis and pyruvate cycling (275). Plasma essentially reports the sum of changes from multiple organs. Hence, we investigated whether circulating metabolites could identify the effect of liver disease in regulating energy homeostasis by assessing differences between patients with and without NASH.

Table 7. Clinical and laboratory assessment in nonobese controls and obese patients

	Nonobese controls (n=50)	Obese patients (n=270)	p-*value*
Clinical characteristics			
Male, n (%)	10 (20.4)	69 (25.7)	0.279
Age, years	47 (32-62)	49 (41-58)	0.652
BMI, kg/m2	25.2 (22.3-28.0)	46.4 (42.4-51.6)	**<0.001**
T2DM, n (%)	2 (4.1)	105 (39.0)	**<0.001**
Hypertension, n (%)	4 (8.2)	169 (62.8)	**<0.001**
Dyslipidemia, n (%)	2 (4.1)	98 (36.4)	**<0.001**
Medication, %			
Metformin	1 (2.0)	76 (28.4)	**<0.001**
Insulin	-	22 (8.2)	-
Sulfonylureas	-	16 (5.9)	-
ACEIs + ARA II	1 (2.0)	22 (8.2)	**<0.001**
Diuretics	1 (2.0)	33 (12.3)	**<0.05**
Statins	-	52 (19.3)	-
Laboratory assessment			
Hemoglobin, g/dL	14.0 (13.1-14.8)	13.3 (12.5-14.4)	**0.041**
Leukocytes, x109/L	6.5 (5.9-7.5)	7.9 (6.6-9.3)	**<0.001**
Platelets, x109/L	245 (210-272)	212 (182-252)	**<0.001**
Total cholesterol, mmol/L	5.1 (4.5-5.7)	4.3 (3.7-5.1)	**<0.001**
HDL-cholesterol, mmol/L	1.6 (1.3-1.8)	1.2 (1.0-1.5)	**<0.001**
LDL-cholesterol, mmol/L	3.0 (2.5-3.6)	3.3 (2.8-3.9)	**0.01**
Triglycerides, mmol/L	0.9 (0.7-1.4)	1.0 (1.1-2.2)	**0.01**
Glucose, mmol/L	4.7 (4.3-5.3)	7.3 (6.2-9.1)	**<0.001**
Insulin, pmol/L	48.8 (32.9-59.5)	91.3 (46.5-149.2)	**<0.001**
HOMA-IR	1.4 (0.9-2.0)	4.3 (2.2-7.5)	**<0.001**
Albumin, g/L	43.5 (41.9-45.0)	40.4 (36.4-44.0)	**<0.001**
AST, µKat/L	0.3 (0.2-0.4)	0.5 (0.4-0.8)	**<0.001**
ALT, µKat/L	0.3 (0.2-0.4)	0.6 (0.4-0.9)	**<0.001**
GGT, µKat/L	0.2 (0.1-0.4)	0.4 (0.2-0.6)	**<0.001**
CRP, mg/L	1.3 (0.5-3.0)	5.0 (0.8-12.2)	**<0.001**

Values are expressed as number (percentage) or median (interquartile range) in the indicated units. ACEIs: angiotensin-converting-enzyme inhibitor; ALT: alanine aminotransferase; AST: aspartate aminotransferase; ARA-II: angiotensin II receptor antagonists; BMI: body mass index; CRP: C-reactive protein; GGT: γ-glutamyl transferase; HDL: high-density lipoprotein; HOMA-IR: homeostatic model assessment of insulin resistance; LDL: low-density lipoprotein; T2DM: type 2 diabetes mellitus.

Table 8. Targeted plasma metabolome in nonobese (control) and severely obese patients.

	Metabolite	Non-obese controls (n=50)	Obese patients (n=270)	Fold change	*p*-value
Energy Metabolism	**α-ketoglutarate**	11.0 (8.2-14.5)	17.2 (12.5-23.4)	1.6	**<0.001**
	β-hydroxybutyrate	32.9 (24.7-42.0)	252.4 (118.8 - 429.3)	7.7	**<0.001**
	Aconitate	0.4 (0.3-0.5)	0.8 (0.5 - 1.0)	2.0	**<0.001**
	Alanine	271.4 (204.8-282.9)	171.8 (131.0-218.2)	-1.6	**<0.001**
	Aspartate	6.4 (4.6-8.0)	2.2 (1.5-3.2)	-2.9	**<0.001**
	(Iso)Citrate	26.3 (18.3-30.9)	59.5 (48.6-71.2)	2.3	**<0.001**
	Fumarate	0.4 (0.3-0.6)	0.97 (0.2-2.7)	2.4	**<0.001**
	Glucose*	4.7 (4.3-5.3)	7.3 (6.2-9.1)	1.6	**<0.001**
	Glutamate	102.6 (87.6-135.0)	62.8 (48.3-79.3)	-1.6	**<0.001**
	Glutamine	25.8 (17.8-31.2)	66.6 (51.5-81.9)	2.6	**<0.001**
	Isoleucine	60.0 (51.6-65.2)	34.2 (22.6-47.6)	-1.8	**<0.001**
	Lactate*	2.3 (2.0-2.4)	1.5 (1.2-3.0)	-1.5	**<0.001**
	Leucine	99.5 (84.4-112.0)	56.9 (37.6-80.3)	-1.7	**<0.001**
	Malate	2.1 (1.7-2.7)	3.3 (2.2-15.2)	1.6	**<0.001**
	Malonyl-CoA	2.9 (2.5-3.5)	1.3 (1.0-1.6)	-2.2	**<0.001**
	Oxaloacetate	1.1 (0.8-1.4)	1.6 (0.9-2.6)	1.5	**<0.001**
	Pyruvate	228.7 (118.2-326.2)	501.3 (317.5-674.7)	2.2	**<0.001**
	Serine	95.1 (79.2-111.4)	39.4 (24.3-50.0)	-2.4	**<0.001**
	Succinate	8.1 (6.7-9.2)	8.4 (6.6-10.8)	1.0	0.262
	Succinyl-CoA	8.6 (7.0-10.9)	3.4 (2.1-4.4)	-2.5	**<0.001**
	Valine	167.9 (149.3-191.2)	121.3 (88.4-154.4)	-1.4	**<0.001**
1-C Metabolism	**Betaine**	14.1 (10.5-20.7)	10.5 (8.7 - 13.5)	-1.3	**0.014**
	Choline	95.4 (82.4-109.4)	137.8 (98.0 - 166.3)	1.4	**0.002**
	Cystathionine	0.6 (0.5-0.7)	1.0 (0.9 - 1.1)	1.7	**<0.001**
	Cysteine	3.6 (3.2-4.7)	2.5 (2.1 - 2.9)	-1.4	**<0.001**
	Dimethylglycine	87.7 (80.9-96.3)	115.3 (90.2 - 135.1)	1.3	**0.001**
	Folic acid	0.21 (0.20-0.24)	0.16 (0.13 - 0.20)	-1.3	**0.001**
	Formyl-THF	0.10 (0.004-0.16)	0.13 (0.08 - 0.15)	1.3	0.456
	Glycine	138.5 (113.9-184.2)	175.1 (149.6 - 201.1)	1.3	**<0.001**
	Homocysteine	5.3 (4.4-6.1)	5.3 (4.7 - 5.9)	1.0	0.845
	Methionine	258.3 (227.9-312.8)	179.9 (163.4 - 211.6)	-1.4	**<0.001**
	Methylcobalamine	3.4 (2.3-5.8)	4.0 (1.9 - 5.3)	1.2	0.301
	Riboflavin (B2)	26.3 (21.9-46.5)	57.6 (39.4 - 78.2)	2.2	**<0.001**
	SAH	0.008 (0.007-0.011)	0.006 (0.005 - 0.008)	-1.3	**0.032**
	SAM	3.8 (3.4-4.0)	2.9 (1.8 - 4.3)	-1.3	**0.033**

Data are expressed as median (interquartile range) in µmol/L except those marked with an asterisk denoting mmol/L. SAH, S-adenosylhomocysteine; SAM, S-adenosylmethionine; THF, Tetrahydrofolate.

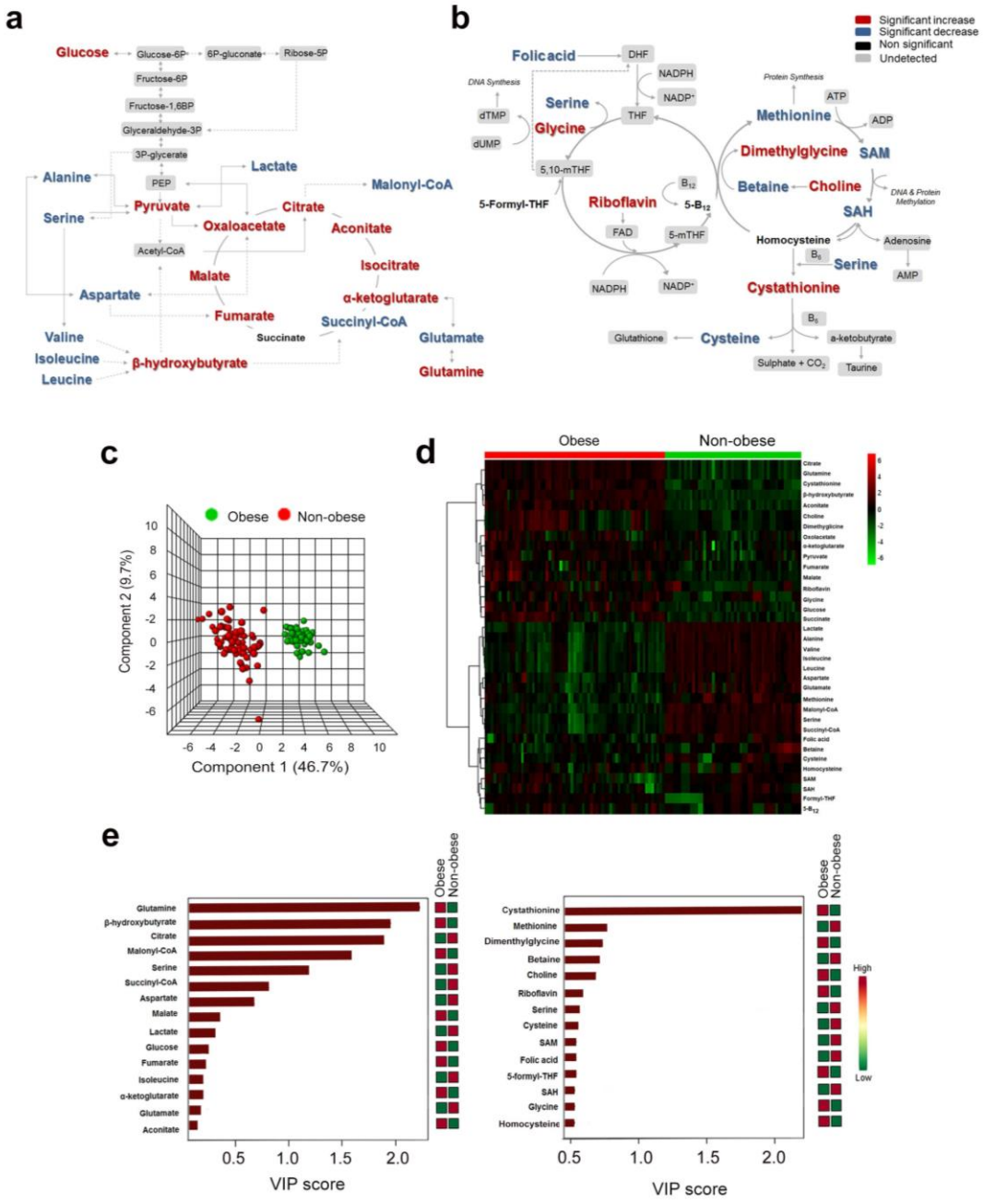

Figure 21. Morbid obesity perturbs plasma metabolome. Variations in the levels of plasma metabolites from energy (a) and one-carbon metabolism (b) between obese patients and nonobese controls are schematized, with colors indicating the statistical assessment according to the legend. Partial least square discriminant (PLS-DA) (c) and heat map (d) analyses were used to visualize the segregation between both groups. Variable importance in projection (VIP) scores (e) that provide the relative impact of each metabolite in the PLS-DA.

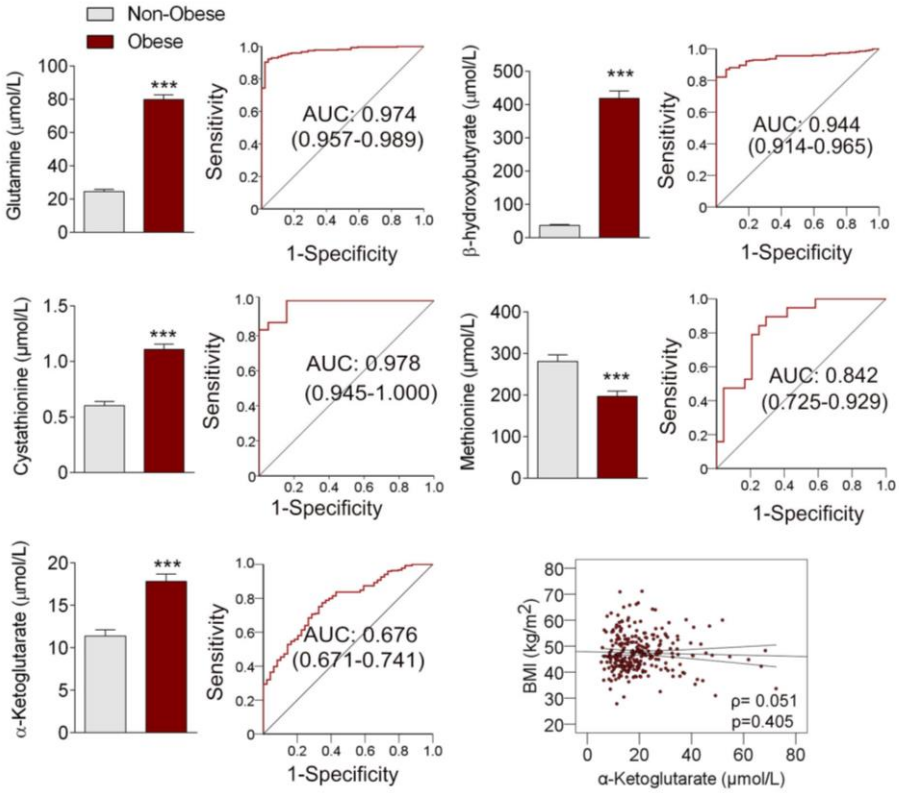

Figure 22. Obesity may influence the interpretation of plasma metabolite levels. Plasma glutamine, cystathionine, β-hydroxybutyrate and methionine levels correlated (Spearman test, $p < 0.05$) almost perfectly with body mass index, and ROC curve-based model evaluation indicated their ability to distinguish obese and nonobese participants. In contrast, other metabolites, exemplified by α-ketoglutarate, were apparently independent of body weight and adiposity. Asterisks denote statistical significance (***$p<0.001$) by the Wilcoxon rank-sum test.

NASH impacts metabolic adaptation pathways

Histologic features and clinical and laboratory variables identified progressive metabolic disturbances closely related to liver disease (Figure 23 a, Table 9). Liver alterations were heterogeneous, and we compared the plasma metabolome between patients with minor changes (non-NASH) and those with unambiguous NASH. The number of metabolites with the ability to segregate patients with and without NASH was lower than those distinguishing patients with and without obesity (Table 10), and plasma α-KG, oxaloacetate and isoleucine levels had the highest impacts on the class distribution (Figure 23 b-d).

The histopathological features in patients with NASH were associated with a significant accumulation of plasma glucose, lactate and pyruvate, indicating reprogrammed glucose metabolism. These findings were accompanied by increased plasma concentrations of alanine, aspartate and branched chain amino acids (BCAAs) in NASH patients. Among metabolites from the CAC, only plasma oxaloacetate and α-KG levels were significantly increased in NASH patients, which in the presence of higher plasma glutamate likely indicated CAC replenishment via glutaminolysis.

As glutamine is metabolized via glutaminolysis to be converted into α-KG and lactate, high plasma concentrations of these metabolites might indicate the role of NASH in the organismal metabolic responses (276). Plasma metabolites from 1-C metabolism also revealed significant alterations in the form of serine-to-glycine and SAM-to- SAH conversions in NASH patients (Figure 24 a). We then explored whether these metabolic alterations persisted or reversed after BC.

Table 9. Clinical and laboratory assessment in obese patients segregated by liver histologic features and NASH patients 12 months after surgery.

	Non-NASH (n=130)	NASH (n=53)	NASH after surgery (n=53)
Clinical characteristics			
Male, n (%)	29 (22.3)	18 (33.9)	-
Age, years	47 (41 - 57)	50 (42 - 58)	-
BMI, Kg/m^2	45.7 (42.3 - 51.6)	46.6 (42.5 - 51.9) [a]	34.3 (31.3-37.5) [b, c]
T2DM, n (%)	45 (34.6)	29 (54.7) [a]	9 (16.7) [b, c]
Hypertension, n (%)	76 (58.4)	41 (77.3) [a]	23 (43.4) [b, c]
Dyslipidaemia, n (%)	40 (30.7)	23 (43.3) [a]	5 (9.4) [b, c]
Medication (%)			
Metformin	31 (23.8)	20 (37.7) [a]	8 (15.1) [b, c]
Insulin	7 (5.3)	7 (13.2)	2 (3.3) [b, c]
Sulfonylureas	7 (5.3)	7 (13.2)	-
ACEIs + ARABS	48 (36.9)	26 (49)	9 (16.7) [b, c]
Diuretics	12.7 (9.7)	8 (15.1)	-
Statins	21 (15.9)	12 (22.6)	5 (9.4) [b, c]
Laboratory assessment			
Hemoglobin, g/dL	13.0 (12.4 - 14.1)	13.4 (12.1 - 14.4) [a]	13.3 (12.2-14.7)
Leukocytes, x10^9/L	7.6 (6.2 - 9.6)	7.8 (6.6 - 8.7)	6.6 (5.3-7.5) [b, c]
Platelets, x10^9/L	207.5 (184 - 254)	225.0 (179.0 - 249.5)	231.0 (184.8-287.5)
Ferritin, µg/L	55.0 (24.8 - 87.0)	97.4 (24.5 - 202.45) [a]	57.2 (23.6-110.8) [b, c]
Total-cholesterol, mmol/L	4.9 (4.5 - 5.4)	4.9 (4.3 - 5.5)	5.0 (4.5-5.9) [b, c]
HDL-cholesterol, mmol/L	1.4 (1.1 - 1.7)	1.1 (0.9 - 1.4) [a]	3.0 (2.6-3.5) [b, c]
LDL-cholesterol, mmol/L	2.8 (2.4 - 3.5)	2.8 (2.4 - 3.9)	1.6 (1.3-1.9) [b, c]
Triglycerides, mmol/L	1.5 (1.1 - 2.0)	1.7 (1.2 - 2.3) [a]	1.0 (0.8-1.2) [b, c]
Glucose, mmol/L	6.8 (6.0 - 8.4)	7.8 (6.2 - 11.4) [a]	4.7 (4.3-5.4) [b, c]
Insulin, pmol/L	97.9 (41.8 - 152.4)	109.2 (65.1 - 193.7) [a]	39.6 (24.0-60.1) [b, c]
HOMA-IR	4.1 (1.8 - 6.7)	6.1 (3.4 - 8.7) [a]	1.2 (0.7-1.9) [b, c]
Albumin, g/L	43.0 (40.0 - 44.0)	41.0 (36.6 - 44.0)	43.0 (41.0-45.0) [c]
AST, µkat/L	0.5 (0.4 - 0.7)	0.7 (0.5 - 1.2) [a]	0.3 (0.2-0.3) [b, c]
ALT, µkat/L	0.5 (0.3 - 0.8)	0.7 (0.5 - 1.2) [a]	0.2 (0.2-0.3) [b, c]
GGT, µkat/L	0.3 (0.2 - 0.4)	0.5 (0.3 - 0.7) [a]	0.2 (0.2-0.4) [b, c]
CRP, mg/L	5.1 (4.3 - 7.0)	5.8 (4.8 - 7.1)	0.3 (0.2-0.5) [b, c]
Liver histologic features			
Steatosis			
<5%	81 (62.0)	-	51 (96.7)
5-33%	45 (34.8)	5 (7.9)	2 (3.3) [b, c]
34-66%	4 (3.3)	33 (57.9)	-
>66%		20 (34.2) [a]	-
Lobular inflammation			
No foci	40 (30.4)	-	43 (81.6)
<2 foci	69 (53.3)	8 (13.2)	10 (18.4) [b, c]
2-4 foci	20 (15.2)	26 (44.7)	-
>4 foci	-	24 (42.1) [a]	-
Hepatocellular ballooning			
None	124 (95.7)	9 (15.8)	43 (81.6)
Few cells	3 (2.2)	44 (76.3)	10 (18.4)
Many cells	-	5 (7.9) [a]	
Fibrosis			
None (F0)	52 (40.2)	20 (34.2)	24 (45.8)
Perisinusoidal or periportal(F1)	57 (43.5)	14 (23.7)	27 (50.0)
Perisinusoidal and portal (F2)	17 (13.0)	9 (15.8)	2 (4.2) [b, c]
Bridging fibrosis (F3)	1 (1.1)	12 (21.1)	-

Values were expressed as number (percentage) or median (interquartile range) in the indicated units. ACEIs: angiotensin-converting-enzyme inhibitor; ALT: alanine aminotransferase; AST: aspartate aminotransferase; ARA-II: angiotensin II receptor antagonists; BMI: body mass index; CRP: C-reactive protein; GGT: γ-glutamyl transferase; HDL: high-density lipoprotein; HOMA-IR: homeostatic model assessment of insulin resistance; LDL: low-density lipoprotein; T2DM: type 2 diabetes mellitus. The letters denote significant (at least $p<0.05$) differences comparing a non-NASH vs NASH, b non-NASH vs NASH after surgery and c NASH vs NASH after surgery.

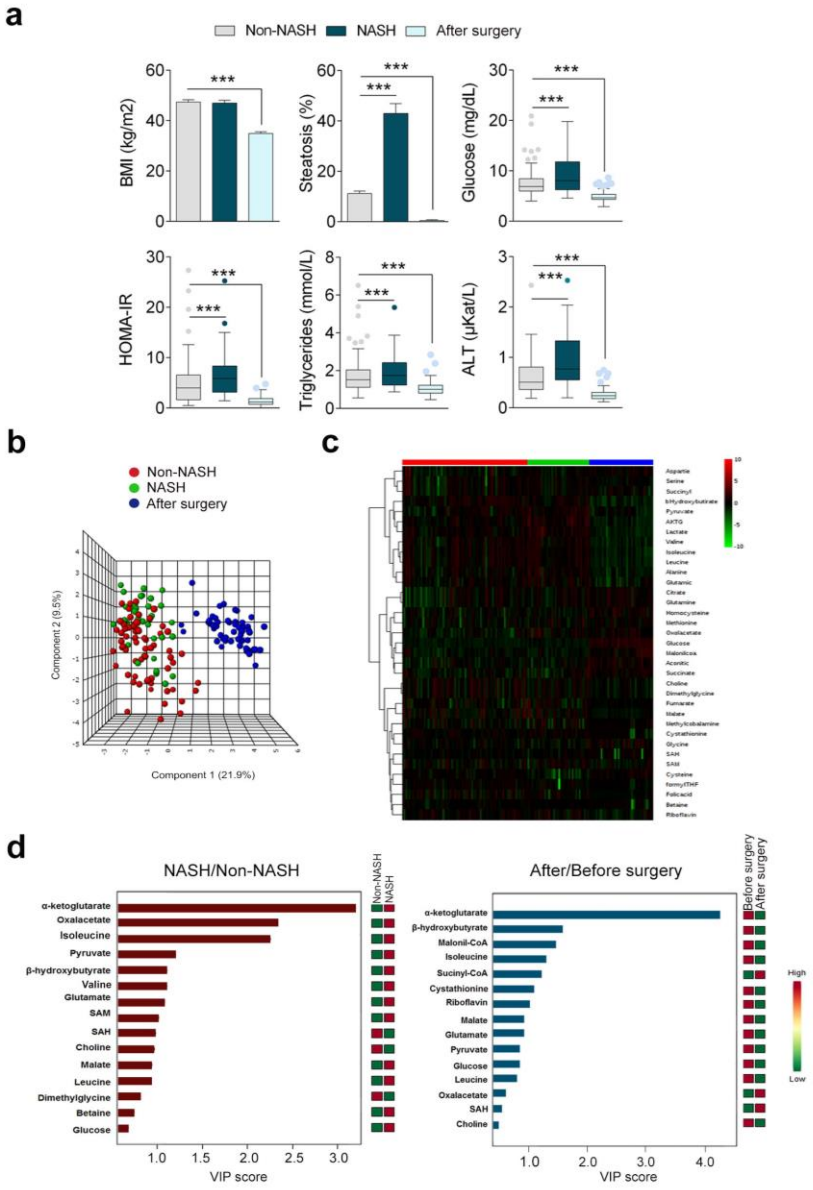

Figure 23. The metabolic adaptive responses in obesity are closely related to liver alterations. Routine clinical and laboratory assessment disclosed the metabolic consequences of different liver histologic features (a). Partial least square discriminant (PLS-DA) (b) and heatmap (c) analyses visualized differences in the plasma metabolome after surgery and the challenging task that represents distinguishing patients with and without NASH. Plasma α-ketoglutarate was the metabolite with the largest impact in projecting metabolic changes between patients with and without NASH and between NASH patients before vs. after surgery attending to the VIP scores (d). Asterisks denote statistical significance (*p < 0.05, **p < 0.01, ***p < 0.001) by the Wilcoxon rank-sum test.

Table 10. Plasma metabolome in obese patients with and without NASH.

	Metabolite	Non-NASH (n=130)	NASH (n=53)	Fold change	*p*-value
Energy Metabolism	**α-ketoglutarate**	13.05 (10.7-17.5)	19.7 (13.9-27.6)	1.5	**<0.001**
	β-hydroxybutyrate	286.8 (163.4-490.3)	247.9 (105.5-419.7)	-1.2	0.110
	Aconitate	0.74 (0.5-1.0)	0.7 (0.6-1.0)	1.1	0.369
	Alanine	149.8 (114.5-192.3)	183.5 (140.1-220.7)	1.2	**<0.001**
	Aspartate	1.7 (1.2-2.9)	2.3 (1.5-3.2)	1.4	**0.013**
	(Iso)Citrate	58.8 (47.7-69.2)	61.7 (48.8-71.9)	1.0	0.379
	Fumarate	1.0 (0.2-3.8)	0.6 (0.2.2.5)	-1.7	0.447
	Glucose*	6.6 (5.9-8.1)	7.6 (6.3-9.6)	1.2	**<0.001**
	Glutamate	54.5 (42.3-67.7)	65.9 (52.8-83.7)	1.2	**<0.001**
	Glutamine	64.6 (51.3-78.8)	68.6 (51.8-82.7)	1.1	0.317
	Isoleucine	28.2 (18.4-46.6)	34.8 (25.6-48.1)	1.2	**<0.001**
	Lactate*	1.4 (1.1-1.6)	1.7 (1.3-2.1)	1.2	**<0.001**
	Leucine	50.3 (31.7-75.9)	61.6 (42.4-81.9)	1.2	**0.015**
	Malate	2.8 (1.9-15.6)	3.6 (2.5-14.7)	1.3	0.142
	Malonyl-CoA	1.3 (1.1-1.7)	1.3 (1.0-1.6)	1.0	0.216
	Oxaloacetate	1.1 (0.9-1.9)	1.7 (1.0-2.8)	1.5	**<0.001**
	Pyruvate	409.2 (285.7-613.2)	537.0 (386.9-714.9)	1.3	**<0.001**
	Serine	39.6 (21.2-58.0)	38.2 (24.8-48.1)	1.0	0.645
	Succinate	8.2 (6.5-10.0)	8.4 (6.8-11.1)	1.0	0.222
	Succinyl-CoA	3.4 (2.0-5.2)	3.4 (2.2-4.2)	1.0	0.631
	Valine	113.3 (81.0-147.8)	127.3 (94.0-158.1)	1.1	**0.008**
1-C Metabolism	**Betaine**	9.9 (7.0-13.3)	10.7 (9.6-13.7)	1.1	0.119
	Choline	137.8 (97.2-198.7)	110.8 (93.4-148.3)	-1.2	0.937
	Cystathionine	1.1 (0.9-1.2)	1.0 (0.9-1.2)	-1.1	0.371
	Cysteine	2.4 (2.0-2.7)	2.8 (2.2-3.1)	-1.2	**0.041**
	Dimethylglycine	111.4 (89.9-161.9)	97.2 (86.9-121.2)	-1.1	0.965
	Folic acid	0.16 (0.13-0.23)	0.16 (0.14-0.21)	1.0	0.788
	Formyl-THF	0.14 (0.09-0.16)	0.09 (0.06-0.13)	-1.6	0.766
	Glycine	177.4 (162.2-202.6)	177.6 (139.1-204.9)	1.0	0.232
	Homocysteine	5.3 (4.7-5.8)	5.1 (4.4-5.9)	1.0	0.468
	Methylcobalamine (B12)	4.0 (1.6-5.1)	4.2 (2.1-9.5)	1.1	0.502
	Methionine	176.7 (156.8-211.9)	184.7 (170.2-215.5)	1.0	0.222
	Riboflavin (B2)	58.0 (43.1-78.3)	54.9 (33.3-82.5)	-1.1	0.866
	SAH	0.007 (0.006-0.009)	0.006 (0.005-0.008)	-1.2	**0.030**
	SAM	2.4 (1.7-4.1)	3.8 (1.8-5.0)	1.6	**0.020**

Data are expressed as median (interquartile range) in µmol/L except those marked with an asterisk denoting mmol/L. SAH, S-adenosylhomocysteine; SAM, S-adenosylmethionine; THF, Tetrahydrofolate

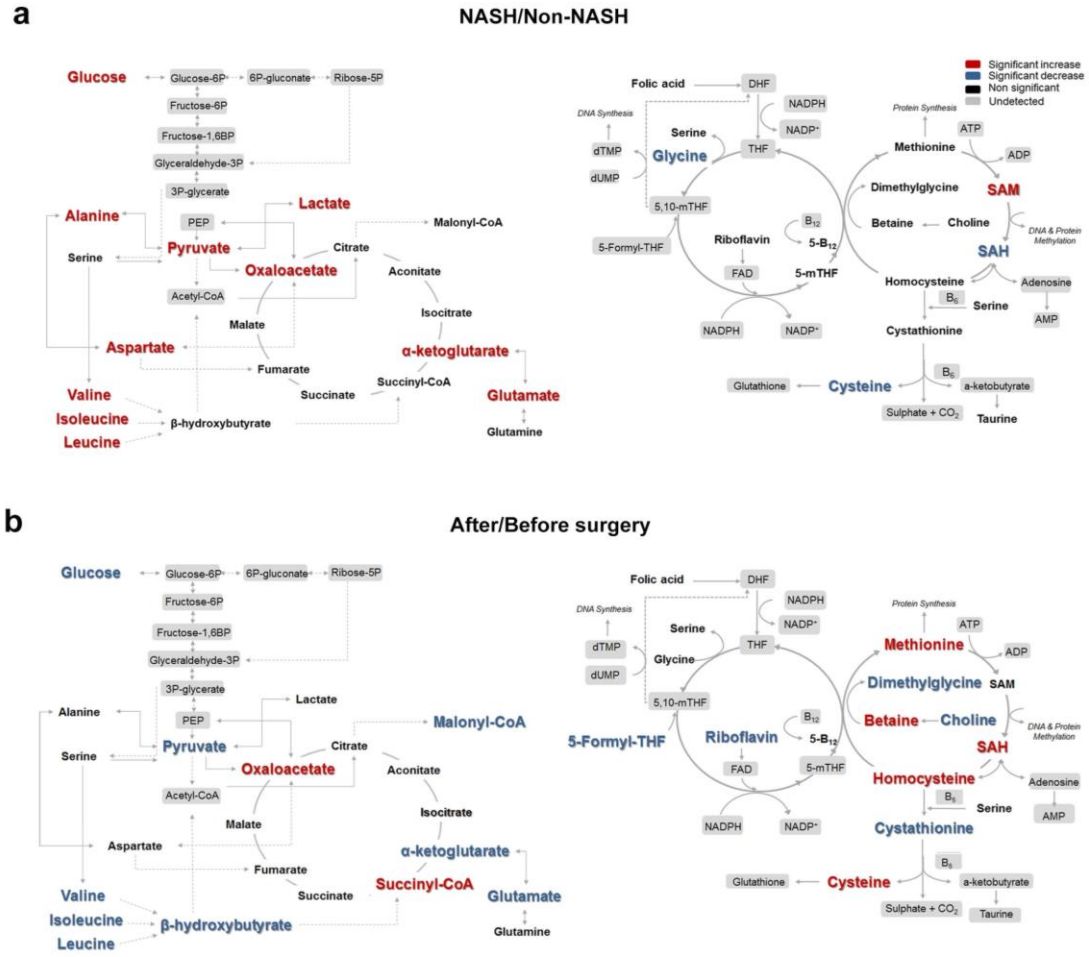

Figure 24. Bariatric surgery reverses NASH-associated disturbances in the plasma metabolome. Schematized view of differences in plasma metabolites related to energy and one-carbon metabolism in comparing patients with vs. without NASH (a) and NASH patients before vs. after surgery (b). Colors denoted statistical comparisons as indicated in the legend.

Bariatric surgery restores the perturbed metabolic responses

One year after bariatric surgery, NASH patients were reexamined and paired liver biopsies demonstrated NASH remission. Body weight decreased significantly, but patients remained obese (BMI > 30 kg/m2), though there were significant improvements in the severity and prevalence of diabetes, hypertension, and dyslipidaemia (Table 9). Variations in plasma metabolites segregated NASH patients before vs. after surgery (Figure 23 b, c, e) and plasma α-KG levels provided the largest impact on class distribution. Most plasma levels of CAC intermediates returned to values close to normal in nonobese controls. The significant reduction in plasma glutamate and α-KG after surgery and the simultaneous higher level of succinate indicated that glutaminolysis was no longer preponderant in the follow-up.

Bariatric surgery also normalized plasma levels of circulating amino acids and metabolites from 1-C metabolism (Figure 24 b, Table 11). We also found that surgery restored the increased 5-mC levels in circulating leukocytes of patients with NASH (Figure 25 a) indicating differential and reversible DNA methylation in leukocytes. Variations in metabolites with influence in DNA methylation (Figure 24 b) suggest the potential role of metaboloepigenetic processes in NASH progression. However, the plasma α-KG to succinate ratio, which represents the relative proportions of the substrates and products of enzymes involved in methylation, was significantly altered only after surgery and did not differentiate patients with and without NASH (Figure 25 a). Of note, correlations between most metabolite levels and the leukocyte 5-mC level did not reach statistical significance between patients with and without NASH but the SAM-to-SAH ratio and plasma α-KG level were significantly associated with steatosis (Figure 25 c). After surgery, the DNA 5mC level was negatively correlated with the changes in SAM-to-SAH ratio and positively correlated with plasma α-KG levels (Figure 25 d). However, the diagnostic and predictive value of the 5-mC levels in DNA from leukocytes did not result into clinical benefit (data not shown) and we explored, without this input, the putative role of circulating metabolites as noninvasive biomarkers.

Table 11. Plasma metabolome in NASH patients before and 12 months after surgery

	Metabolite	Before surgery (n=53)	12 months after surgery (n=53)	Fold change	*p*-value
Energy Metabolism	**α-ketoglutarate**	16.6 (13.4-20.9)	7.2 (6.1-9.0)	-2.3	**<0.001**
	β-hydroxybutyrate	431.1 (316.1-549.8)	39.1 (21.8 - 78.3)	-11	**<0.001**
	Aconitate	1.3 (1.0-1.8)	1.2 (0.9 - 1.5)	-1.1	0.766
	Alanine	129.0 (107.0-165.0)	117.8 (103.5-136.0)	-1.1	0.054
	Aspartate	2.9 (2.2-3.7)	3.0 (2.8-4.0)	1	0.138
	(Iso)Citrate	68.0 (56.0-78.8)	65.5 (55.1-76.6)	1	0.502
	Fumarate	0.8 (0.6-2.0)	0.7 (0.6-0.9)	-1.1	0.441
	Glucose*	6.8 (5.8-9.0)	4.7 (4.3-5.4)	-1.4	**<0.001**
	Glutamate	67.0 (55.2-85.9)	44.8 (31.9-58.3)	-1.5	**<0.001**
	Glutamine	79.8 (61.9-96.7)	84.2 (72.5-92.7)	1.1	0.109
	Isoleucine	25.0 (16.6-35.1)	12.8 (8.6-16.0)	-2	**<0.001**
	Lactate*	1.7 (1.4-2.0)	1.5 (1.3-2.0)	-1.1	0.172
	Leucine	63.1 (45.3-83.0)	46.8 (29.7-61.7)	-1.3	**<0.001**
	Malate	3.4 (2.5-9.8)	3.2 (2.5-3.8)	-1.1	0.061
	Malonyl-CoA	4.0 (2.3-4.9)	1.5 (1.2-1.7)	-2.7	**<0.001**
	Oxaloacetate	1.6 (1.1-2.2)	2.3 (1.8-3.2)	1.4	**<0.001**
	Pyruvate	513.6 (285.3-562.4)	223.7 (187.9-356.5)	-2.3	**<0.001**
	Serine	29.9 (23.1-39.4)	29.1 (22.9-34.4)	1	0.414
	Succinate	12.6 (10.4-14.9)	11.5 (10.4-12.8)	-1.1	0.065
	Succinyl-CoA	3.4 (2.4-4.2)	5.6 (3.8-8.1)	1.6	**<0.001**
	Valine	135.2 (93.4-169.0)	115.0 (83.7-147.3)	-1.2	0.038
1-C Metabolism	**Betaine**	10.5 (8.7 - 13.5)	13.2 (10.7 - 15.4)	1.3	**0.003**
	Choline	137.8 (98.0 - 166.3)	106.7 (85.7 - 118.0)	-1.3	**<0.001**
	Cystathionine	1.0 (0.9 - 1.1)	0.5 (0.4 - 0.6)	-2	**<0.001**
	Cysteine	2.5 (2.1 - 2.9)	3.0 (2.4 - 3.5)	1.2	**<0.001**
	Dimethylglycine	95.3 (80.2 - 115.1)	82.5 (72.9 - 103.9)	-1.2	**<0.001**
	Folic acid	0.16 (0.13 - 0.20)	0.19 (0.16 - 0.25)	1.2	0.056
	Formyl-THF	0.13 (0.08 - 0.15)	0.05 (0.04 - 0.08)	-2.6	**<0.001**
	Glycine	175.1 (149.6 - 201.1)	191.3 (146.9 - 232.4)	1.1	0.068
	Homocysteine	5.3 (4.7 - 5.9)	6.0 (5.5 - 7.0)	1.1	**<0.001**
	Methionine	179.9 (163.4 - 211.6)	215.8 (190.8 - 233.4)	1.2	**<0.001**
	Methylcobalamine	4.0 (1.9 - 5.3)	3.3 (1.8 - 4.7)	-1.2	0.536
	Riboflavin (B2)	57.6 (39.4 - 78.2)	34.0 (24.1 - 50.5)	-1.7	**<0.001**
	SAH	0.006 (0.005 - 0.008)	0.007 (0.006 - 0.008)	1.2	**0.003**
	SAM	2.9 (1.8 - 4.3)	2.2 (1.8 - 3.5)	-1.3	0.176

Data were expressed as median (interquartile range) in µmol/L except those marked with an asterisk denoting mmol/L. SAH, S-adenosylhomocysteine; SAM, S-adenosylmethionine; THF, Tetrahydrofolate.

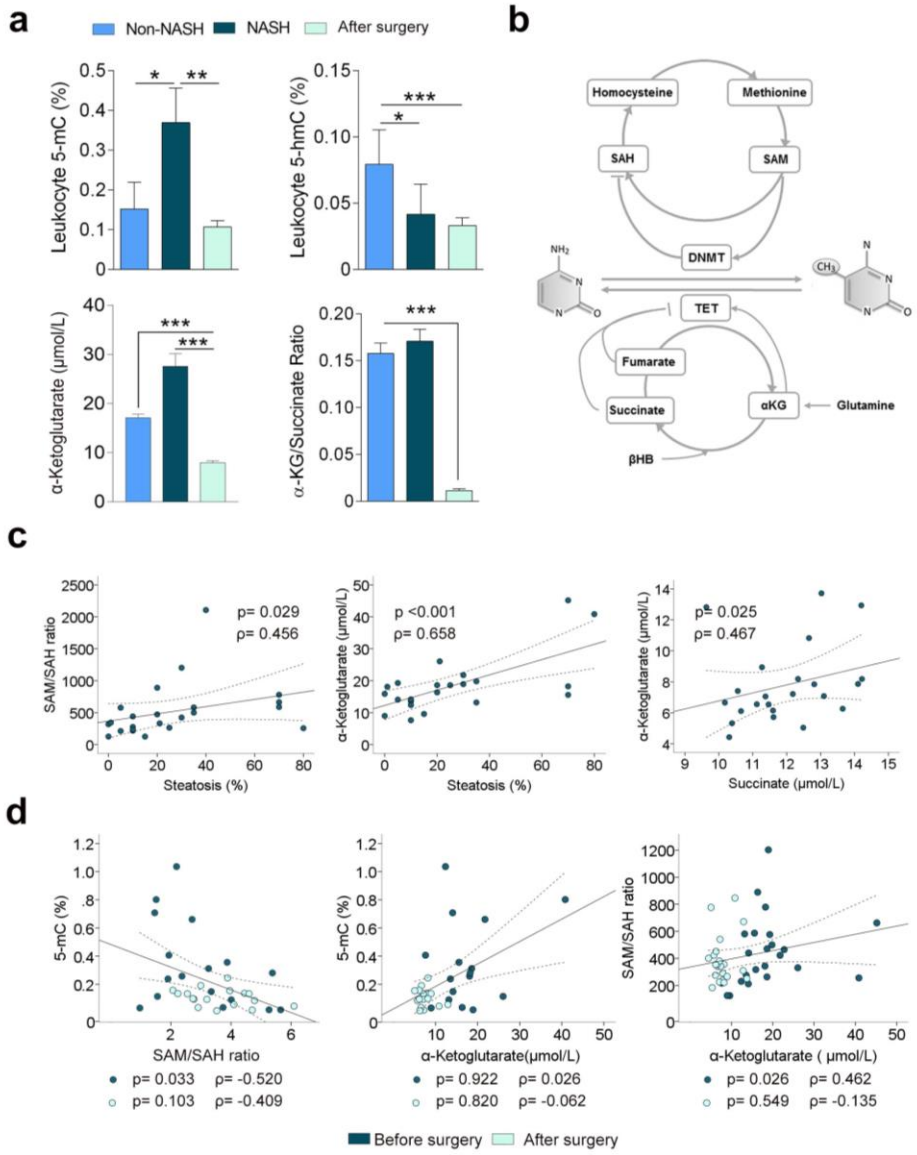

Figure 25. NASH affects plasma DNA methylation. The differential global DNA methylation was assessed as 5-methylcytosine (5-mC) and 5-hydroxymethylcytosine (5-hmC) levels in circulating leukocytes (n=24 for each group), indicating associations with liver histologic features and plasma α-ketoglutarate and succinate levels (a). Metabolites from the citric acid cycle and methionine cycles (b) correlated with steatosis when comparing patients with and without NASH (c) but not with global DNA methylation. In contrast, 5-mC level was restored in NASH patients after surgery and paralleled changes in circulating metabolites, suggesting the potential role of metaboloepigenetic processes (d). Asterisks denote statistical significance (*p < 0.05, **p < 0.01, ***p < 0.001) by the Wilcoxon rank-sum test, β-HB, β-hydroxybutyrate; DNMT, DNA methyltransferase; TET, ten-eleven translocation.

Plasma metabolome identifies biomarkers to distinguish patients with and without NASH and predict NASH remission

The drawbacks associated with liver biopsy represent a considerable constraint to clinically detect the severity and progression of liver disease and to assess NASH remission after treatment. The current markers of liver injury, plasma aminotransferases, did not discriminate patients with and without NASH with AUC values between 0.511 and 0.837 and 45% of misinterpretations (Figure 26 a). In contrast, reduction after surgery in plasma aminotransferases provided an assessment of NASH remission with 10% of uncertainties (Figure 26 b).

Logistic regression models and ROC analyses using the concentration of energy-balance metabolites in plasma revealed that the combination of plasma α-KG, pyruvate and oxaloacetate levels improved the diagnostic accuracy of NASH, with AUC values between 0.680 and 0.938 and reduced misinterpretations (Figure 27 a). Similarly, the combined decrease in plasma α-KG and ß-HB levels was also a good predictive biomarker of NASH remission with an AUC between 0.938 and 1 (Figure 27 b). More importantly, the combination of reductions in plasma α-KG, ß-HB and AST levels predicted NASH remission without ambiguity (Figure 27 c).

These results need to be validated in the routine clinical assessment, i.e., without controlled and batched laboratory assessment, but strongly suggest that the explorative second biopsy should be limited to NASH patients without changes in these measurements over time. Eventually, these simple measurements might be used to evaluate the effectiveness of therapies in NASH patients.

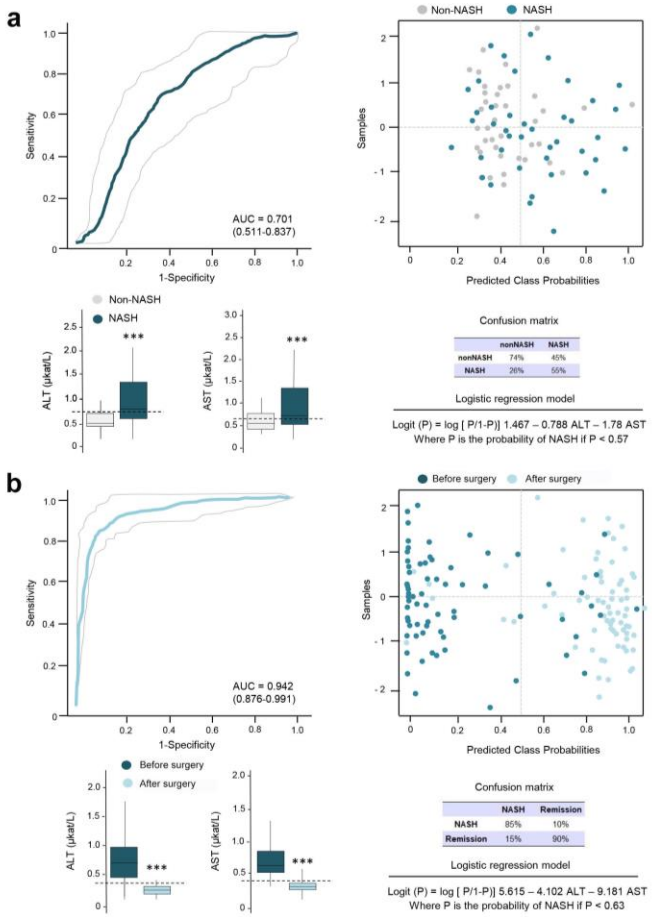

Figure 26. The diagnostic and predictive value of plasma aminotransferase levels. Logistic regression models and ROC curve-based model evaluation indicated that measurements of aminotransferases (ALT and AST) were practically useless to distinguish between patients with and without NASH (a). However, paired measurements before and after surgery may contribute to the assessment of NASH remission (b). Asterisks denote statistical significance (***p < 0.001) by the Wilcoxon rank-sum test.

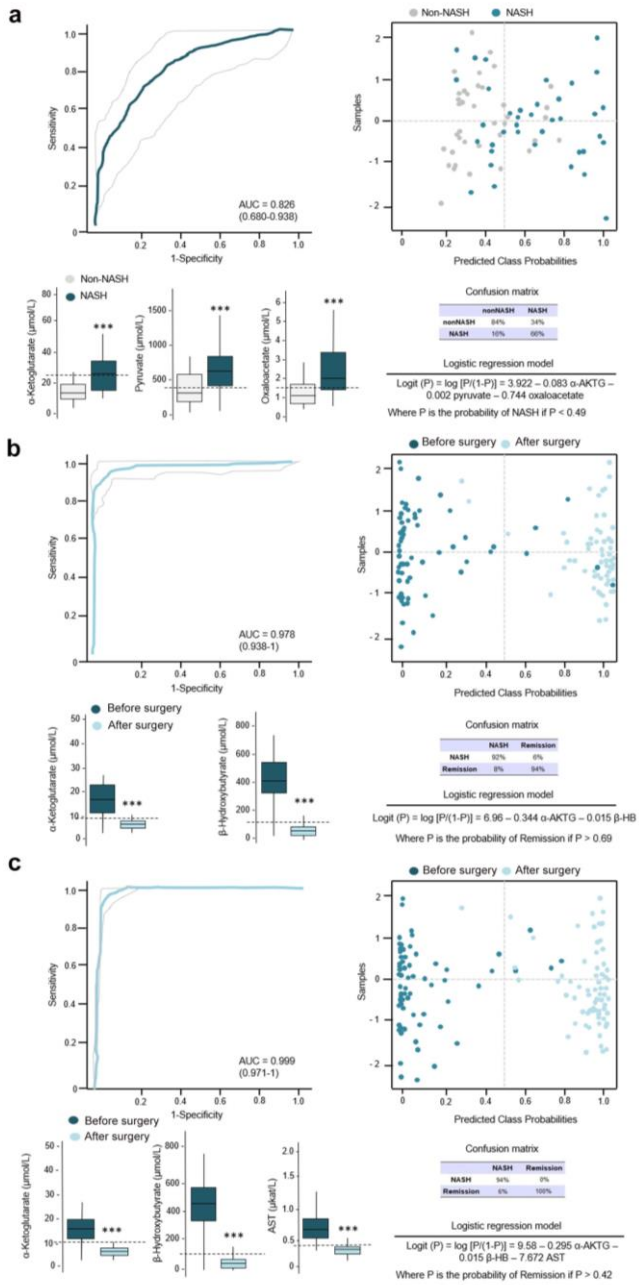

Figure 27. Paired measurements of selected metabolites predict NASH remission. ROC curve-based model evaluation indicated that selected circulating metabolites provide tools to distinguish patients with and without NASH, but the number of misinterpretations remains relatively high (a). Paired measurements of plasma α-ketoglutarate and β-hydroxybutyrate levels before and after surgery might be useful to predict NASH remission (b). Remarkably, the addition of variations in AST level to the model predicted bariatric surgery induced NASH remission without ambiguity. Asterisks denote statistical significance (***p < 0.001) by the Wilcoxon rank-sum test.

STUDY III

α-Ketoglutarate regulates AMPK/mTOR-driven pathways in NASH remission: therapeutic perspectives through rewiring metabolism and epigenetics

UNIVERSITAT ROVIRA I VIRGILI
ASSESSING DIAGNOSTIC AND THERAPEUTIC TARGETS IN OBESITY-ASSOCIATED LIVER DISEASES
Noemí Cabré Casares

Liver metabolic responses in NASH and the association with cell survival related to chronic oxidative stress and mitochondrial dysfunction.

Clinical and laboratory variables identified progressive metabolic disturbances closely related to liver disease (Table 12). Patients with NASH provided paired liver biopsies one year after bariatric surgery demonstrating NASH remission, weight loss (although remained obese), and improvement in diabetes, hypertension and dyslipidemia.

The mechanisms responsible for steatosis continuing benign (at least temporarily) in some patients but not in others remain speculative but appear associated with the differential resilience towards oxidative stress. The accumulation of lipoperoxides and the activation of antioxidant enzymes defined NASH livers and segregated non-NASH livers without confusions. Moreover, these alterations completely reverted after NASH remission (Figure 28 a). Mechanisms are likely multifactorial and related to pathways with potential to control immune responses and modulate proliferation and cell death, as indicated by correlating changes in the expression of IL-10 and signal pSTAT-3 (Figure 28 b). In the same scenario, we found in NASH livers a reduction in the expression of succinate dehydrogenase (complex II), which governs in the overall flux of mitochondrial ROS and as general sensor for apoptosis (Figure 28 c, d). Mitochondrial dynamics and mitochondria-endoplasmic reticulum interactions regulate systemic energy balance coordinating the correct function of the CAC, and oxidative phosphorylation via the electron transport chain (ETC) (Figure 28 e). In NASH livers fragmented mitochondrial network and higher number of mitochondria with lower size and heterogeneous shape, and lower number of autophagosomes were consistent observations with transmission electronic microscopy and discriminated livers with or without NASH (Figure 29 a). We also found in NASH with respect to non-NASH livers a significant under expression of the translocase of the outer mitochondrial membrane (TOM20) and MFN2, likely molecular effectors during mitochondrial biogenesis (Figure 29 b).

In NASH livers, compared with non-NASH livers, mTORC1 was activated with increased phosphorylation of the ribosomal S6 and 4EBP1 substrates (Figure 29 b). Metabolic and oxidative stress appear to be the triggers of mTORC1 hyperactivation with alternative feedback loops signaled by increased fatty acid oxidation indicated by higher expression of fatty acid synthase (FASN), increased AKT phosphorylation and decreased AMPK phosphorylation. Autophagy was also compromised in NASH livers with altered LC3 II to LC3 I ratio, accumulation of p62 and reduced LAMP2A expression. Apoptosis, mitochondrial dysfunction and the autophagic flux were improved in livers with confirmed NASH remission after surgery (Figure 29 c). The decreased phosphorylation of S6, 4EBP1 and AKT with increased AMPK phosphorylation suggested mTORC1 inhibition accompanied by the higher expression of TOM20 and MFN2 and the significant decrease in FASN and apoptotic markers. The increased LC3II to LC3I ratio, the lack of p62 accumulation and the increased expression of LAMP2A also suggested the recovery in liver autophagy after surgery (Figure 29 c, d).

Table 12. Clinical laboratory assessment and liver histologic features in patients with NASH and 12 months after surgery.

	Non-NASH (NAS ≤ 2) (n=31)	NASH (NAS ≥ 5) (n=31)	NASH, one-year afte surgery (n=31)
Clinical characteristics			
Male, n (%)	10 (32.3)	10 (32.3)	-
Age, years	46.0 (39.0-56.0)	49.0 (44.0-56.0)	-
BMI, Kg/m^2	44.0 (41.4-46.4)	46.5 (42.6-53.6)	31.4 (28.7-33.4) [b, c]
T2DM, n (%)	11 (35.5)	17 (54.8)	4 (12.9)
Hypertension, n (%)	17 (54.8)	21 (67.7)	10 (32.3) [b, c]
Dyslipidaemia, n (%)	9 (29.0)	12 (38.7)	2 (6.5) [b, c]
Medication (%)			
Metformin	4 (12.9)	12 (38.7) [a]	4 (12.9) [b, c]
Insulin	2 (6.5)	5 (16.1)	1 (3.2) [b, c]
Sulfonylureas	1 (3.2)	2 (6.5)	-
ACEIs + ARA-II	11 (35.5)	14 (45.2)	4 (12.9) [b, c]
Diuretics	4 (12.9)	5 (16.1)	-
Statins	5 (16.1)	5 (16.1)	2 (6.5) [b, c]
Laboratory assessment			
Hemoglobin, g/dL	13.2 (12.7-14.7)	13.4 (12.7-14.8)	13.1 (12.3-14.0)
Leukocytes, x10^9/L	7.5 (6.3-9.4)	7.6 (6.5-10.7)	6.0 (5.0-7.5) [c]
Platelets, x10^9/L	197 (187-266)	243 (181-314)	227 (209-251)
Ferritin, µg/L	44.4 (25.0-143.7)	112.4 (31.2-203.3)	32.2 (12.2-85.5) [b, c]
Total-cholesterol, mmol/L	4.3 (3.4-5.2)	4.3 (3.8-5.0)	4.8 (4.1-5.4)
HDL-cholesterol, mmol/L	1.2-0.9-1.6)	1.2 (0.9-1.4)	1.5 (1.3-1.7) [c]
LDL-cholesterol, mmol/L	2.4 (1.9-2.8)	2.6 (2.4-3.7) [a]	2.8 (2.3-3.3)
Triglycerides, mmol/L	1.5 (1.0-2.3)	1.7 (1.3-2.5) [a]	0.9 (0.6-1.4) [b, c]
Glucose, mmol/L	6.5 (6.1-8.9)	7.6 (6.2-8.7) [a]	4.5 (4.3-5.1) [b, c]
Insulin, pmol/L	90.9 (28.3-140.3)	108.0 (48.7-143.7) [a]	40.9 (20.9-58.6) [b, c]
HOMA-IR	4.1 (1.3-6.3)	6.7 (2.7-8.1) [a]	1.2 (0.6-1.9) [b, c]
Albumin, g/L	44.0 (41.0-45.0)	43.0 (41.0-46.0)	42.0 (41.0-44.0)
AST, µkat/L	0.5 (0.4-0.7)	0.7 (0.5-1.3) [a]	0.3 (0.2-0.3) [b, c]
ALT, µkat/L	0.5 (0.3-0.7)	0.7 (0.5-1.4) [a]	0.2 (0.2-0.3) [b, c]
GGT, µkat/L	0.3 (0.2-0.5)	0.5 (0.3-0.8) [a]	0.2 (0.1-0.5) [c]
CRP, mg/L	0.9 (0.5-1.5)	1.9 (0.6-1.5) [a]	0.4 (0.2-0.4) [b, c]
Liver histologic features			
Steatosis			
<5%	27 (87.1)	-	31 (100) [c]
5-33%	3 (9.7)	3 (9.7) [a]	-
34-66%	1 (3.2)	15 (48.4)	-
>66%	-	13 (41.9)	-
Lobular inflammation			
No foci	12 (38.7)	-	24 (77.4) [b, c]
<2 foci	16 (51.6)	5 (16.1) [a]	7 (22.6)
2-4 foci	3 (9.7)	21 (67.7)	-
>4 foci	-	5 (16.1)	-
Hepatocellular Ballooning			
None	26 (83.8)	2 (6.5) [a]	31 (100) [b, c]
Few cells	5 (16.1)	20 (64.5)	-
Many cells	-	9 (29.0)	-
Fibrosis			
None (F0)	8 (25.8)	4 (12.9)	17 (54.8) [b, c]
Perisinusoidal or periportal (F1)	18 (58.1)	8 (25.8)	13 (41.9)
Perisinusoidal and portal (F2)	5 (16.1)	15 (48.4)	1 (3.3) [b, c]
Bridging fibrosis (F3)	-	4 (12.9)	-

Values are shown as number of cases and percentages or medians and interquartile range. ACEIs: Angiotensin-converting-enzyme inhibitor; ALT: Alanine transaminase; AST: Aspartate transaminase; ARA-II: Angiotensin II receptor antagonists; BMI: Body mass index; CRP: C-reactive protein; HDL: High-density lipoprotein; HOMA-IR: Homeostatic model assessment of insulin resistance; HTG: Hypertriglyceridemia; LDL: Low-density lipoprotein; T2DM: Type 2 diabetes mellitus. Significant differences in comparisons are indicated by a non-NASH vs NASH. b Non-NASH vs 12 months after surgery. c NASH vs 12 months after surgery (at least $p<0.05$).

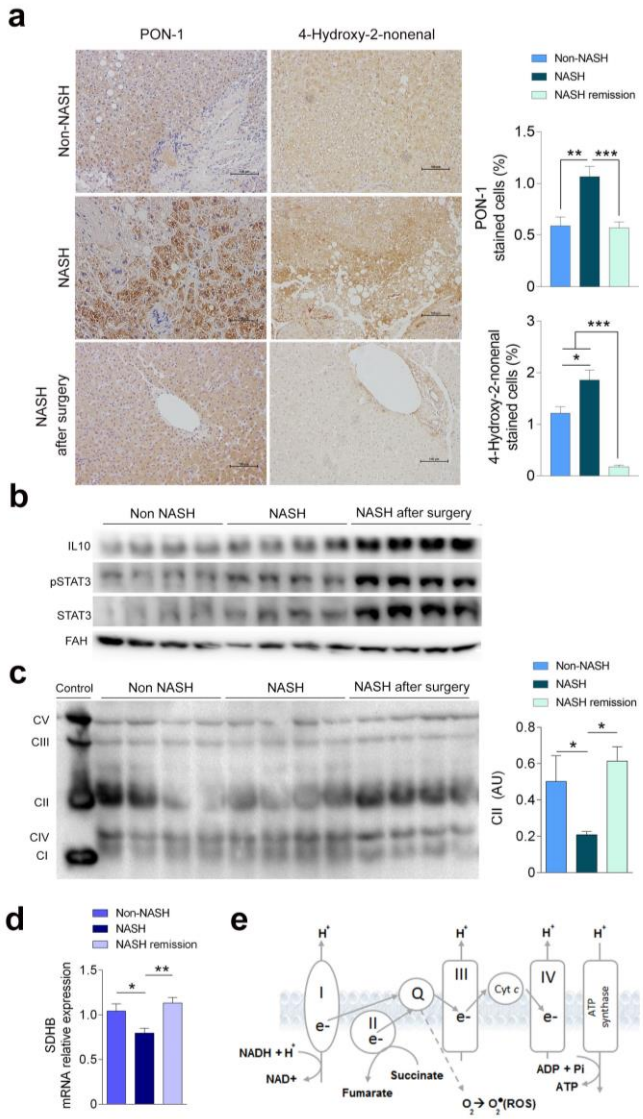

Figure 28. Hepatic oxidative stress and mitochondrial dysfunction were associated with NASH.
(a) Histological evaluation of Non-NASH and NASH patients indicates oxidative stress by immunochemical staining of paraoxonase-1 (PON1) and 4-hydroxy-2-nonenal. Representative microphotographs (bars indicate 100 x magnifications) are shown on right, with a quantification of positively-stained area in the right. (b) The level of the inflammatory response interleukin 10 (IL-10), and activator of transcription 3 (STAT-3) were determined by western blot for liver patients as indicated. (c) Oxidative phosphorylation (OXPHOS) mitochondrial complexes representing the five mitochondrial oxidative phosphorylation complexes were used to examine the expression of mitochondrial proteins in liver patients with (n=12) or without NASH (n=12) and NASH remission (n=12). (d) Gene expression of succinate dehydrogenase B (SDHB). (e) Representative shema of OXPHOS. Asterisks denote significance (* $p < 0.05$, ** $p < 0.01$, ***$p < 0.001$ by Wilcoxon rank-sum test).

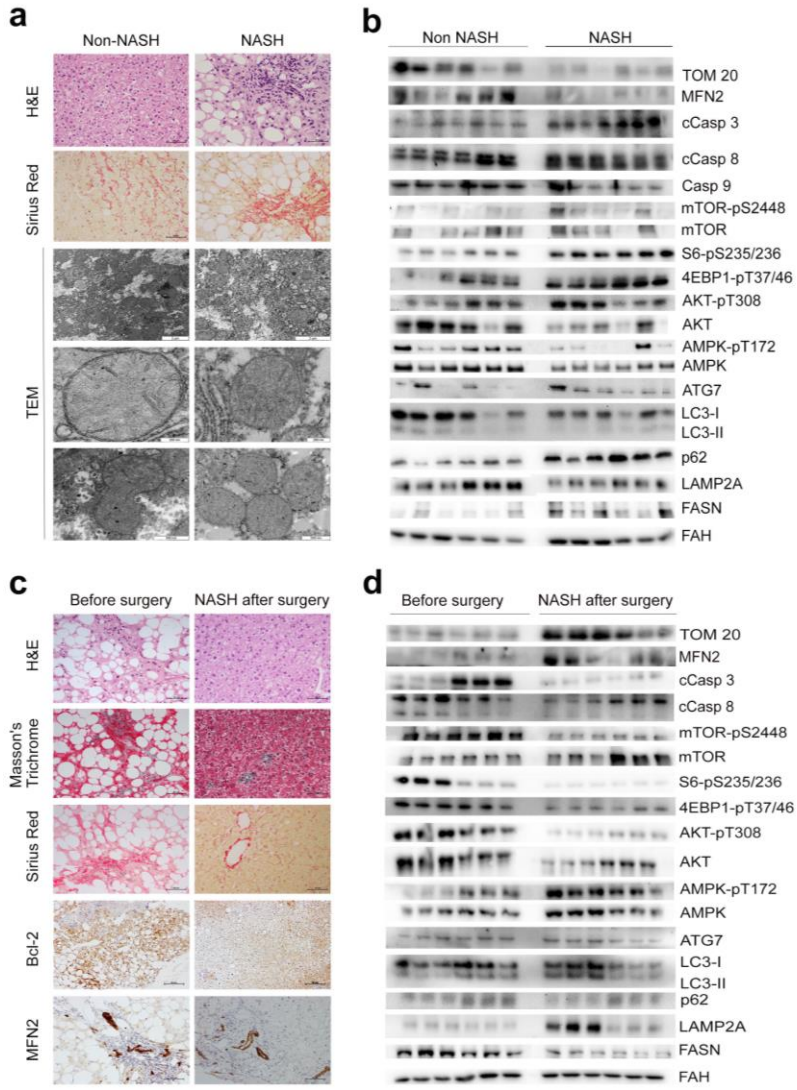

Figure 29. Mitochondrial integrity shapes the mechanisms AMPK/mTORC1 of hepatocyte death in livers with NASH after bariatric surgery. (a) Representative microphotographs (bars indicate 100x magnification) of liver sections stained with hematoxylin and eosin (H&E) and Sirius Red. Representative TEM liver images and immunoblot analysis (n=24) of mitochondria in NASH patients indicates lower degree of mitochondrial dysfunction. (b) Western blot analysis of apoptotic markers and mTORC1 downstream targets from Non-NASH (n=12) and NASH (n=12) patients. (c) Representative microphotographs (bars indicate 100x magnification) of before and 12 months after surgery in patients with paired liver biopsies indicates changes post-surgery by Hematoxylin an Eosin (H&E), Sirius Red and Masson's Trichrome staining. Histological evaluation after surgery indicates apoptosis and mitochondrial dysfunction by immunochemical staining of B-cell lymphoma 2 (Bcl-2) and mitofusin 2 (MFN2). (d) Western blot analysis of apoptotic markers involved in energy generation and autophagy signaling markers before (n=12) and after surgery (n=12) in liver samples.

NASH drives distinct metabolic rearrangements in the livers and suggests the role of α-KG in energy homeostasis.

We found that a relatively low number of metabolites distinctly segregated patients with or without NASH (Table 12). The more prominent difference in NASH livers with respect to non-NASH livers was the major alteration in the α-KG to succinate conversion revealed by the accumulation of hepatic glutamine, α-KG, citrate and pyruvate. These findings also denoted the potential role of glutaminolysis and reduced metabolic flexibility in NASH development (Figure 30 a). Of note, reductive carboxylation apparently induced the conversion of α-KG into citrate and the accumulation of both key lipogenic molecules might explain the higher steatosis in NASH livers. Changes in the expression of involved enzymes were consistent (Figure 30 b). Specifically, the upregulation of both glutamate dehydrogenase and glutaminase combined with the downregulation of α-KG dehydrogenase and pyruvate carboxylase. At the same time, the accumulation of fructose-6-phosphate and the decrease in 6-phospho-gluconate may indicate a suppressor effect in glycolysis (Table 13), and we also observed significant changes among metabolites from 1-C metabolism. Glycine, SAH and methionine were significantly decreased but taurine concentration increased significantly in NASH livers. These alterations and the positive correlation between steatosis and the SAM-to-SAH ratio, substrate and product of essential methyltransferase reactions, may likely result in lower glutathione levels and increased ROS burden (Figure 30 c, Table 12). These findings had a significant impact in the segregation between NASH and non-NASH livers (Figure 31 a).

Table 13. Liver metabolome in obese patients with or without NASH.

	Metabolite	Non-NASH (n=31)	NASH (n=31)	Fold change	*p*-value
Energy Metabolism	**α-ketoglutarate**	35.5 (29.7 - 41.3)	44.1 (34.0 - 50.1)	1.2	**<0.001**
	β-hydroxybutyrate	1983.8 (1505.2 - 2479.0)	1702.4 (1297.4 - 2088.8)	-1.2	0.156
	Aconitate	59.8 (42.3 - 75.5)	59.4 (45.3 - 65.5)	1.0	0.875
	Alanine	6317.9 (5450.0 - 6920.4)	6755.4 (5793.2- 7278.3)	1.0	0.156
	Aspartate	1108.1 (732.8 - 1282.0)	1190.3 (849.5 - 1547.5)	1.1	0.198
	(Iso)Citrate	1.2 (0.7 - 1.6)	1.7 (1.1 - 3.1)	1.4	**0.008**
	Fructose-1,6BP	90.0 (75.04 - 102.2)	101.1 (85.4 - 108.7)	1.1	0.064
	Fructose-6P	158.6 (133.37 - 166.6)	181.8 (154.6 - 197.6)	1.1	**0.006**
	Fumarate	208.2 (163.4 - 285.7)	210.8 (163.9 - 261.6)	1.0	0.803
	Glucose	1184.6 (756.3 - 1448.8)	1037.4 (815.0 - 1037.4)	-1.1	0.118
	6P-Gluconate	98.7 (70.5 - 124.6)	73.6 (51.9 - 92.3)	-1.3	**0.027**
	Glucose-6P	137.7 (114.3 - 157.8)	153.8 (129.5 - 165.6)	1.1	0.121
	Glutamate	3618.1 (2422.5 - 4818.9)	4937.1 (3517.6 - 5867.2)	1.4	0.172
	Glutamine	22121.1 (18181.2-26284.2)	25245.6 (17964.8-32496.9)	1.2	**0.033**
	Glyceraldehyde-3P	82.7 (55.3 - 105.1)	71.5 (59.5 - 86.8)	-1.2	0.643
	Glycerate-3P	334.8 (302.4 - 473.4)	383.6 (315.7 - 543.2)	1.1	0.643
	Isoleucine	2091.6 (1230.6 - 2658.0)	2084.2 (1790.4 - 2420.0)	1.0	0.916
	Lactate	10570.4 (9565.5 - 13807.5)	10859.0 (9835.8 - 12126.4)	1.0	0.875
	Leucine	3833.8 (2459.6 - 5032.7)	3727.5 (3011.5 - 4416.4)	1.0	0.655
	Malate	425.3 (351.4 - 512.6)	446.3 (341.0 - 585.4)	1.0	0.872
	Oxolacetate	22.7 (14.8-38.8)	28.1 (13.8-46.2)	1.2	0.553
	Phosphoenolpyruvate (PEP)	100.5 (75.3 - 157.8)	109.6 (87.3 - 136.5)	1.1	0.478
	Pyruvate	75.1 (59.9 - 89.3)	108.4 (64.8 - 164.7)	1.4	**<0.001**
	Ribose-5P	126.8 (98.0 - 163.4)	123.1 (115.8 - 123.9)	1.0	0.703
	Serine	5561.7 (3382.7 - 7489.2)	6252.8 (5384.2 - 8002.2)	1.1	0.312
	Succinate	251.7 (198.5 - 322.5)	253.7 (206.52- 312.4)	1.0	0.813
	Valine	2743.2 (1572.0 - 3641.0)	2541.4 (1829.0 - 3136.1)	-1.1	0.665
1-C Metabolism	**5-mTHF**	68.6 (53.2 - 128.6)	59.6 (31.3 - 89.7)	-1.2	0.198
	AMP	199.5 (98.9 - 350.7)	187.3 (109.1 - 275.4)	-1.1	0.723
	Betaine	267.8 (171.1 - 356.6)	310.8 (179.4 - 323.9)	1.2	0.813
	Choline	1175.3 (927.6 - 1486.8)	1227.3 (1052.6 - 1327.6)	1.0	0.415
	Cystathionine	8.1 (5.9 - 11.2)	9.4 (7.2 - 11.7)	1.2	0.438
	Cysteine	27806.3 (16442.9 - 47769.9)	25289.8 (4208.4 - 37467.6)	-1.1	0.160
	Dimethylglycine	1208.5 (889.1 - 1467.6)	1387.0 (1126.9 - 1715.8)	1.1	0.131
	dUMP	1.5 (1.1 - 2.1)	1.3 (1.0 - 1.8)	-1.1	0.276
	Folic acid	0.12 (0.07 - 0.17)	0.10 (0.05 - 0.14)	-1.2	0.185
	Formyl-THF	0.19 (0.12 - 0.27)	0.15 (0.11 - 0.17)	-1.3	0.198
	Glycine	4810.2 (833.0-8174.1)	1544.9 (797.3-2512.9)	-3.1	**0.025**
	Homocysteine	1007.4 (663.1 - 1808.2)	1366.0 (689.9 - 3074.2)	1.4	0.180
	Methionine	361.5 (245.8 - 671.3)	287.1 (199.5 - 333.4)	-1.3	**0.009**
	NADPH	258.3 (178.9 - 328.1)	213.2 (140.5 - 263.2)	-1.2	**0.040**
	Pyridoxal-5-P (B6)	2.1 (1.4 - 2.8)	2.5 (1.5 - 3.8)	1.2	0.386
	Riboflavin (B2)	3.4 (2.2 - 5.3)	3.3 (2.5 - 4.1)	1.0	0.478
	SAH	126.9 (106.5 - 149.6)	90.3 (75.8 - 104.5)	-1.4	**<0.001**
	SAM	45.5 (29.6 - 54.9)	50.0 (37.7 - 69.2)	1.1	0.149
	Taurine	92.9 (71.2 - 119.0)	128.1 (96.2 - 136.1)	1.4	**0.016**

Data were expressed as median (interquartile range) in µmol/100 mg of tissue. SAH, S-adenosylhomocysteine; SAM, S-adenosylmethionine; THF, Tetrahydrofolate. Significant differences (at least p<0.05).

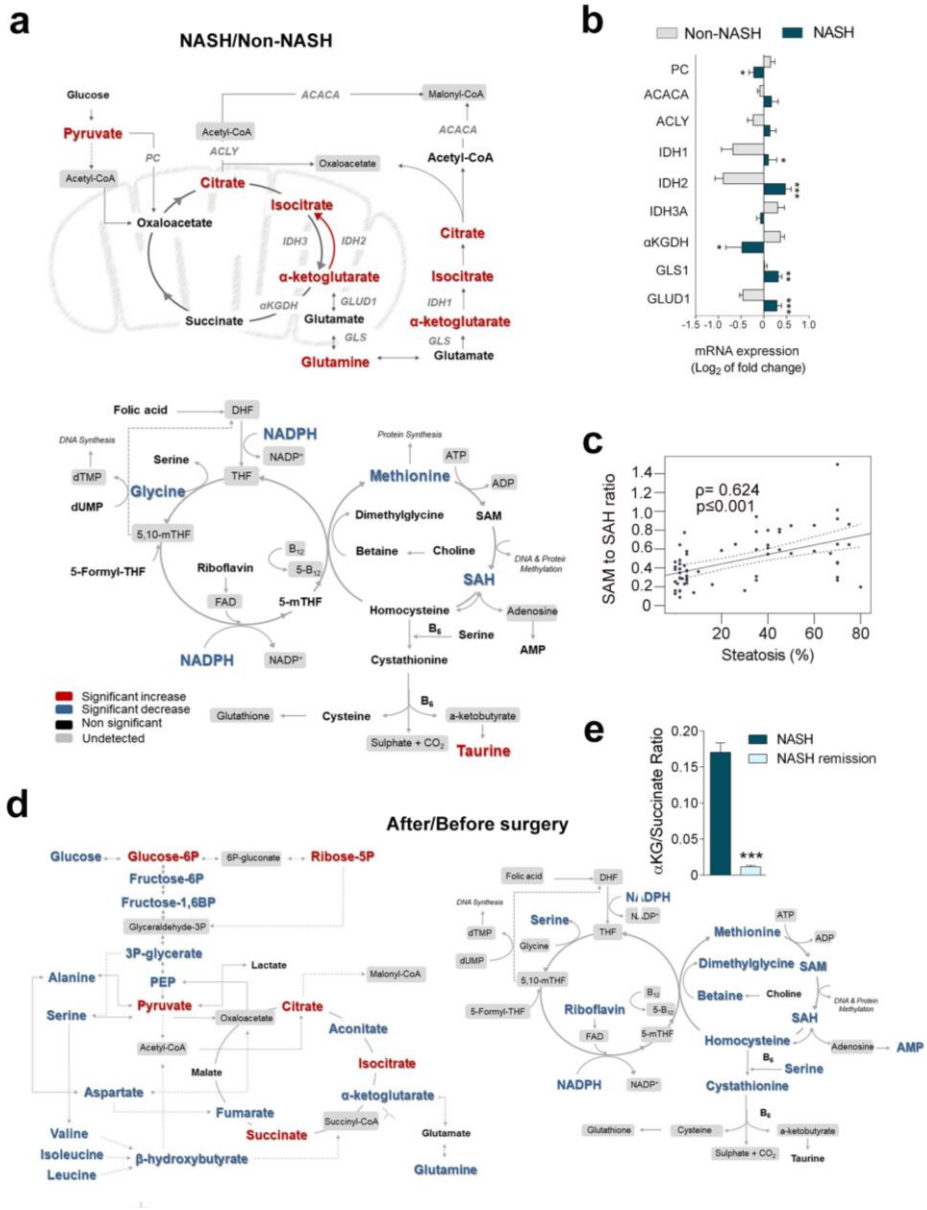

Figure 30. Reversion of liver metabolic perturbation in NASH patients after bariatric surgery.
(a) Representation of the energy metabolism and 1-C intermediates in liver between NASH (n=31) and Non-NASH (n=31) patients measured by mass spectrometry. (b) Gene expression fold-changes (Log_2 based) in enzymatic genes related to glutaminolysis process. (c) Liver correlation (Spearman test $p < 0.05$) between SAM/SAH ratio levels and steatosis grade. (d) Liver metabolites from CAC and 1-C metabolism revealed distinct segregation between patients before and after bariatric surgery. (e) αKG-to-succinate ratio in liver before and after surgery. Metabolites are marked in blue (significant decrease), red (significant increase), grey (non-significant) and black (undetected). Statistical significance was estimated when $p < 0.05$, ** $p < 0.01$, ***$p < 0.001$ by Wilcoxon rank-sum test.

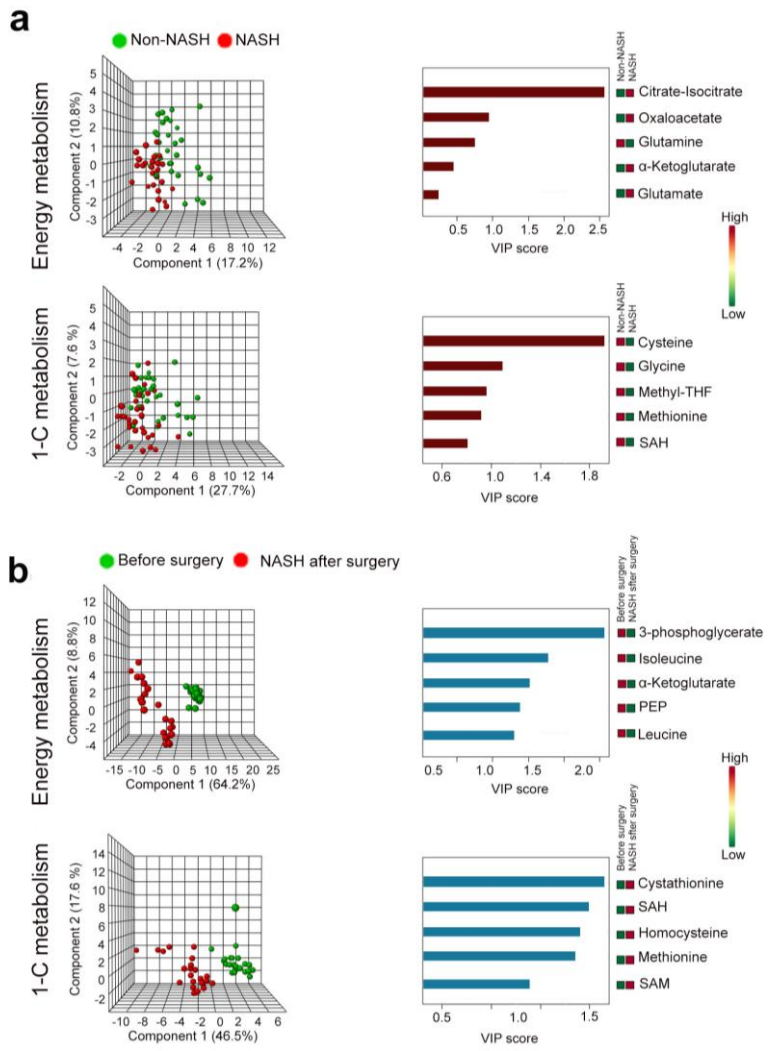

Figure 31. (a) PLS-DA and VIP scores analysis denote that metabolites related to reductive carboxylation and methionine cycle discriminate among with or without NASH livers. (b) PLS-DA and VIP score non-supervised analysis shown an important segregation of patients before and after surgery attending metabolites involved in energy and 1-C metabolism. Asterisks denote significance (***$p < 0.001$ by Wilcoxon rank-sum test).

Reliably, liver metabolome in NASH patients after BC revealed reduction in hepatic levels of glucose and glycolytic intermediates distal to glucose-6-phospate suggested an increased entry of glucose-derived intermediates into mitochondrial biosynthetic metabolism after NASH remission (Figure 30 d and Table 14). The accumulation of glucose-6-phosphate and ribose-5-phosphate also indicated a shift towards the pentose-phosphate pathway. The reduction in the liver concentration of ß-HB and amino acids, including glutamine and BCAAs, also supported the restoration of glycolysis and the reversal in glutamine dependency. Decreased hepatic serine levels after remission might increase the flux through pyruvate formation in cytosol and decrease the flux to anaplerotic reactions that drive glutamine-derived carbon into the CAC in NASH livers. The change from the reductive to an oxidative metabolism after NASH remission was further confirmed by the associated decrease of hepatic α-KG and the increase in succinate levels. Liver citrate levels remained high after surgery. In contrast, all metabolites involved in 1-C metabolism remained unaltered or significantly decreased and the SAM to SAH ratio was restored (Figure 30 d, Figure 31 b). Moreover, we observed that the elevated α-KG-to-succinate ratio found in NASH livers was reverted after surgery (Figure 30 e). The challenge remains in ascertaining the relationship between these findings and potential pathogenic events. Taken together, our data suggest the previously unrecognized role of mTORC1 activation promoting a NASH phenotype in livers of obese patients. For this purpose, we then explored in a cell model whether increased α-KG is sufficient to facilitate mTORC1 activation.

The accumulation of α-KG in hepatocytes modulates cell survival and the mTORC1-mediated metabolic response.

Amino acid-starved HepG2 cells treated with cumulative amounts of the cell-permeable αKG analog (DMKG) increased αKG levels in cells and intensified cell death in a dose-dependent manner (Figure 32 a). The likely mechanism was apoptosis as indicated by the rising expression of cleaved caspases and higher detection of late apoptotic (Annexin V / PI positive) cells (Figure 32 b,c). The activation of mTORC1 in DMKG-treated cells was indicated by the α-KG-dose-dependent increase in S6 (S235/236) phosphorylation and correlated with an increase of AKT (T308) phosphorylation and with a decrease in AMPK (T172) phosphorylation. Apoptosis was combined with autophagy inhibition as indicated by the rising accumulation of p62 and the progressive decrease in the formation of LC3II. The lack of AKT phosphorylation at S473 and the non-significant changes in the expression of LAMP2A and FASN were also suggestive (Figure 33 a).

Table 14. Liver metabolome before and after surgery (12months).

	Metabolite	Before surgery (n=31)	12 months after surgery (n=31)	Fold change	p-value
Energy Metabolism	**α-ketoglutarate**	37.6 (30.4 - 46.8)	3.7 (2.9 - 5.7)	-10.2	**<0.001**
	β-hydroxybutyrate	1901.2 (1388.7 - 2364.2)	224.9 (202.0 - 277.6)	-8.5	**<0.001**
	Aconitate	59.4 (44.5 - 69.2)	14.3 (10.2-22.2)	-4.1	**<0.001**
	Alanine	6557.5 (5652.4 - 7109.1)	3128.0 (1798.0 - 5530.9)	-2.1	**<0.001**
	Aspartate	1109.6 (828.9 - 1368.2)	292.3 (230.0 - 364.2)	-3.8	**<0.001**
	(Iso)Citrate	1.4 (0.8 - 2.0)	8.4 (6.0 - 12.1)	6.0	**<0.001**
	Fructose-1,6BP	90.5 (79.8 - 107.4)	57.1 (35.6 - 75.7)	-1.6	**<0.001**
	Fructose-6P	159.9 (140.1 - 182.3)	88.6 (57.5-143.2)	-1.8	**<0.001**
	Fumarate	209.5 (163.0 - 283.5)	83.7 (47.2 - 107.1)	-2.5	**<0.001**
	Glucose	1037.4 (809.1 - 1281.7)	735.7 (370.0 - 909.8)	-1.4	**<0.001**
	Glucose-6P	139.3 (118.3 - 165.0)	253.6 (148.6 - 304.2)	1.8	**<0.001**
	Glutamate	4443.1 (2488.4 - 5496.7)	5281.1 (3598.3 - 7617.7)	1.2	0.094
	Glutamine	25503.4 (18015.5-33831.5)	21106.9 (14789.9-52127.8)	-1.2	**<0.001**
	Glycerate-3P	357.5 (308.1 - 496.4)	211.1 (184.7 - 217.9)	-1.7	**<0.001**
	Isoleucine	2089.7 (1636.6 - 2527.7)	121.1 (88.7 - 267.6)	-17.3	**<0.001**
	Lactate	10744.9 (9678.2 - 12824.5)	11212.1 (4996.0 - 18339.0)	1.0	0.956
	Leucine	3727.5 (2876.9 - 4720.9)	376.0 (302.9 - 686.7)	-9.9	**<0.001**
	Malate	440.4 (346.0 - 525.4)	430.8 (270.0 - 559.8)	1.0	0.800
	Phosphoenolpyruvate (PEP)	103.2 (81.4 - 147.7)	21.9 (5.8 - 27.6)	-4.7	**<0.001**
	Pyruvate	75.1 (61.9 - 123.6)	150.3 (65.7 - 209.6)	2.0	**0.025**
	Ribose-5P	123.1 (109.4 - 146.1)	341.7 (231.9 - 464.4)	2.8	**<0.001**
	Serine	5818.5 (3939.3 - 7716.9)	2672.3 (1558.9 - 3790.0)	-2.2	**<0.001**
	Succinate	251.7 (199.9 - 322.0)	622.1 (345.2 - 950.0)	2.5	**<0.001**
	Valine	2552.8 (1813.8 - 3290.3)	339.6 (204.4 - 610.7)	-7.5	**<0.001**
1-C Metabolism	**AMP**	187.31 (100.8 - 332.7)	112.2 (49.4 - 137.5)	-1.7	**0.003**
	Betaine	275.3 (171.1 - 341.8)	212.7 (126.0 - 258.7)	-1.3	**0.016**
	Choline	1185.4 (999.6 - 1337.3)	1163.4 (543.0 - 1713.1)	1.0	0.644
	Cystathionine	8.1 (6.0 - 11.3)	1.4 (0.8 - 1.9)	-5.8	**<0.001**
	Dimethylglycine	1224.1 (957.7 - 1654.7)	872.6 (436.3 - 1220.3)	-1.4	**0.001**
	Homocysteine	1189.1 (667.4 - 2173.5)	242.2 (121.9 - 455.6)	-4.9	**<0.001**
	Methionine	292.9 (219.5 - 501.3)	72.3 (49.4 - 107.4)	-4.1	**<0.001**
	NADPH	228.7 (150.8 - 293.0)	71.8 (48.6 - 81.5)	-3.2	**<0.001**
	Pyridoxal-5-P (B6)	2.2 (1.4 - 3.5)	1.8 (1.4 - 2.8)	-1.2	0.400
	Riboflavin (B2)	3.3 (2.3 - 4.3)	2.2 (1.3 - 3.4)	-1.5	**0.003**
	SAH	106.3 (83.1 - 130.0)	29.1 (15.7 - 37.4)	-3.7	**<0.001**
	SAM	47.0 (33.0 - 61.2)	14.5 (8.5 - 26.6)	-3.2	**<0.001**
	Taurine	103.6 (78.4 - 129.8)	96.6 (50.9 - 162.6)	-1.1	0.651

Data were expressed as median (interquartile range) in µmol/100 mg of tissue. SAH, S-adenosylhomocysteine; SAM, S-adenosylmethionine; THF, Tetrahydrofolate. Significant differences (at least p<0.05).

Even moderate increases in cellular α-KG levels induced a significant metabolic reprogramming in this cell model (Figure 34 a). Treatment with 2mM of DMKG, compared with untreated cells mimicked glutaminolysis activation and increased most energy-balance metabolites especially those from the CAC. Conversely, metabolites from 1-C metabolism were either unaffected or significantly decreased by increased cellular α-KG levels with the exception of serine levels (Figure 33 b and Table 15).

Most observations resembled those found in livers with NASH, a condition in which there is an apparent maladaptive response of cellular processes to energy status. It seems apparent that therapies focused on AMPK/mTOR-driven pathways that can regulate and coordinate cellular and whole-body energy homeostasis might have beneficial effects in NASH development.

Metformin is a potential candidate acting directly by reducing energy charge through inhibition of the respiratory-chain complex I. The data from randomized clinical trials with metformin are not encouraging but low quality in design, dose, duration and histologic features do not exclude beneficial effects. The addition of metformin, an energy disruptor and AMPK activator regulated the α-KG-induced effects of metformin. The effects on apoptosis were unclear because metformin decreased the levels of cleaved caspases but simultaneously induced a consistent rise in late apoptotic cells (Figure 32 b, c) indicating additional toxic effects, which were likely responsible for inconsistent effects on autophagy with significant p62 degradation and lower expression in LAMP2A but without statistically significant changes in LC3II levels. However, metformin prevented the DMKG-mediated upregulation of mTORC1 signaling restoring S6, AKT and AMPK phosphorylation and decreasing FASN expression (Figure 33 c). Metformin also abrogated the α-KG-induced metabolic effects restoring the levels of energy-balance metabolites with further reduction in metabolites from 1-C metabolism with the exception of homocysteine and SAH (Figure 33 d, Figure 34 b and Table 16). These results suggest a link with our previous findings suggesting the effect of metformin on DNA methylation and histone modifications regulating the expression of genes.

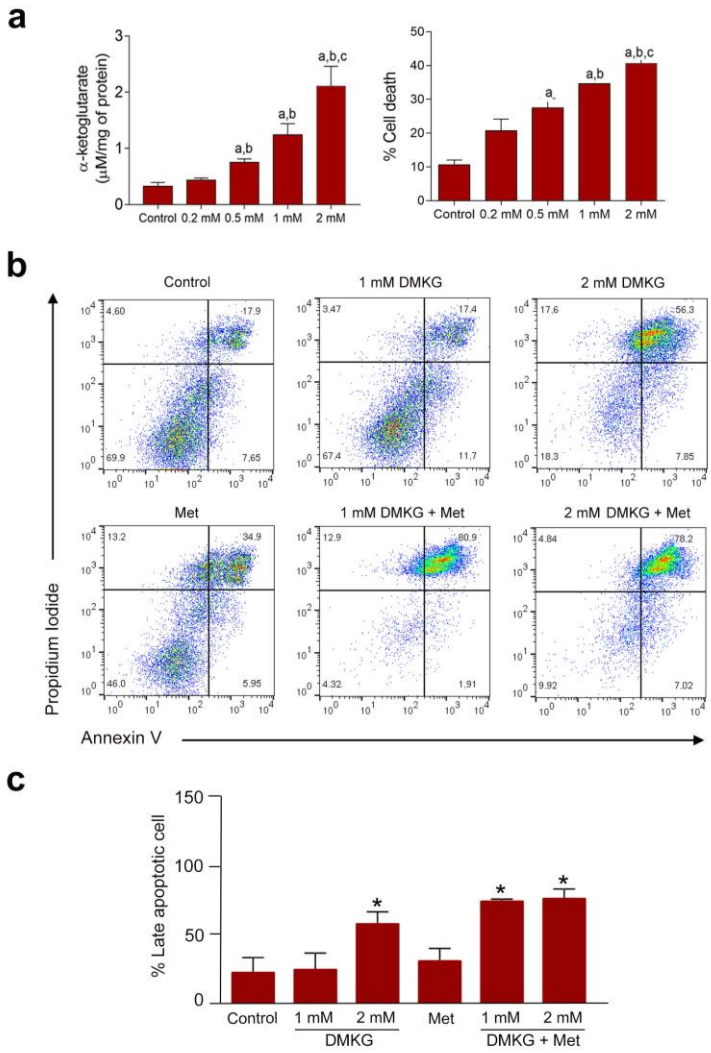

Figure 32. DMKG and metformin treatment in HepG2 cells induce apoptosis. (A) Intracellular α-KG concentrations of each studied group incubated with increasing concentrations of DMKG. Data were normalized by concentration of total protein and HepG2 cell viability in relation to an increasing DMKG concentration. Statistical significance was estimated by Wilcoxon rank-sum test. [a]Significant difference compared with control group; [b]significant differences compared with 0.2 mM group; [c]significant differences compared with 0.5 mM group. (b) Apoptosis induction was determined by annexin V / propidium iodide (PI) staining by flow cytometry. (c) Late apoptotic cells percentage was determined as the percentage of cells positive for both annexin V and PI. Graphs show mean values ± SEM (n=3). Statistical significance was estimated when $p<0.05$ by Anova post hoc Bonferroni).

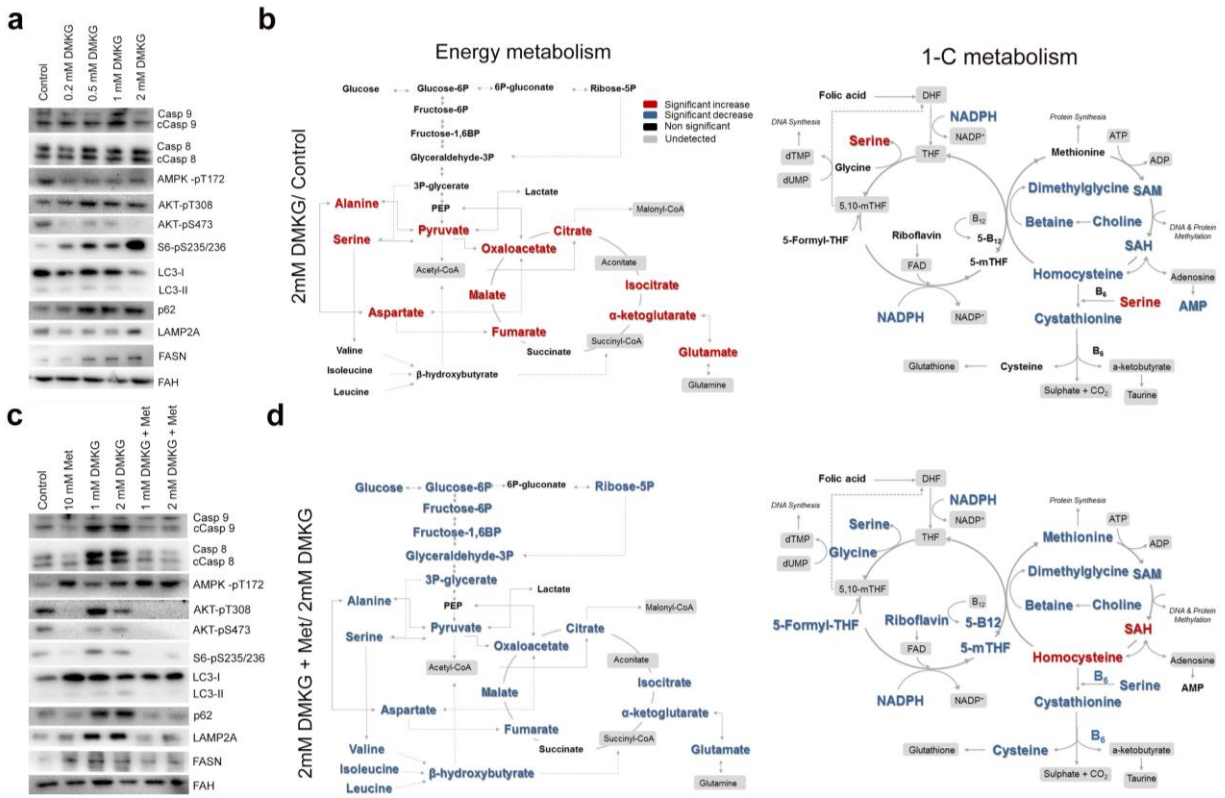

Figure 33. α-Ketoglutarate activates mTORC1 in hepatocytes and imitates metabolic perturbations observed in NASH: a potential role for metformin. (a) Western blot analysis of proteins related to energy metabolism, autophagy and apoptosis in HepG2 cells with DMKG treatment at the indicated concentrations for 72 hours. (b) Representation of energy and 1-C metabolism intermediates in HepG2 cells treated with 2mM DMKG. (c) Western Blot analysis of proteins related to energy metabolism, autophagy and apoptosis in HepG2 cells incubated with DMKG and metformin for 72 hours. (d) Energy and 1-C metabolism intermediates in HepG2 cells after corresponding treatment. Metabolites are marked in blue (significant decrease), red (significant increase), grey (non-significant) and black (undetected). Statistical significance was estimated when $p<0.05$.

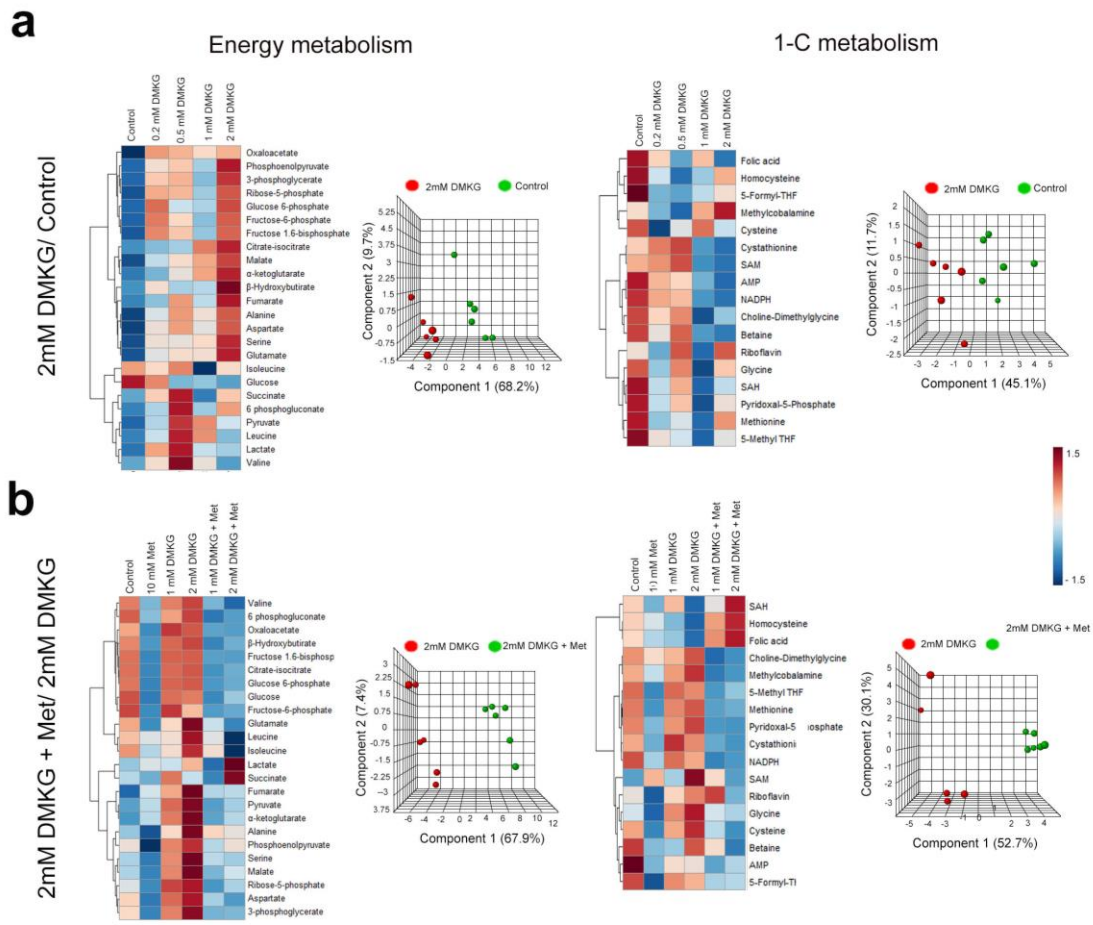

Figure 34. Heatmap and PLSDA analysis obtained from metabolomics data of relevant energy and 1-C metabolism intermediates in cells incubated with increasing concentrations of 2 mM DMKG (a) and 2mM DMKG plus 10mM metformin (b). Rows: metabolites; columns: samples; color key indicates metabolite expression value (blue: lowest; red: highest).

Table 15. Targeted metabolome of HEPG2 cells with or without 2 mM DMKG

Metabolite	Untreated (n=6)	2 mM DMKG (n=6)	Fold change	*p*-value
α-ketoglutarate	0.2 (0.2-0.4)	2.0 (1.3-3.1)	10.0	**0.002**
β-hydroxybutyrate	2.7 (1.9-3.6)	3.3 (2.7-5.2)	1.2	0.240
Alanine	11.0 (8.9-15.0)	44.4 (33.6-76.6)	4.0	**0.002**
Aspartate	17.8 (12.7-51.4)	86.3 (57.3-144.5)	4.8	**0.026**
(Iso)Citrate	1.6 (1.4-2.3)	2.9 (2.4-4.4)	1.8	**0.041**
Fructose-1,6BP	9.1 (6.7-14.5)	15.1 (8.5-25.2)	1.7	0.240
Fructose-6P	57 (35.8-75.1)	82.6 (50.0-119.2)	1.4	0.240
Fumarate	1.3 (1-1.9)	6.5 (3.9-8.9)	5.0	**0.002**
Glucose	102.9 (76.6-166.7)	85.8 (62.4-105.9)	-1.2	0.310
6P-Gluconate	2.3 (2.1-3.6)	3.4 (2.4-4.1)	1.5	0.485
Glucose-6P	16.9 (10.8-26.1)	26.4 (14.3-42.5)	1.6	0.240
Glutamate	29.8 (8.2-63.9)	238.6 (168.8-385.8)	8.0	**0.002**
Glycerate-3P	19.0 (11.5-29.9)	40.1 (22.4-66.9)	2.1	0.065
Isoleucine	15.2 (13.0-26.1)	16.1 (15.8-16.4)	1.1	0.485
Lactate	295.4 (241.5-361.6)	326.0 (241.6-408.3)	1.1	0.818
Leucine	37.0 (31.5-49.3)	45.3 (32.8-52.4)	1.2	0.699
Malate	2.8 (2.51-3.8)	11.5 (8.6-19.7)	4.1	**0.002**
Oxaloacetate	8.1 (6.5-11.9)	17.5 (10.4-22.6)	2.2	**0.041**
Phosphoenolpyruvate (PEP)	1.9 (0.8-4.2)	3.6 (2.4-8.1)	1.9	0.240
Pyruvate	1.4 (1.1-2.2)	2.8 (2.2-3.4)	2.0	**0.041**
Ribose-5P	2.6 (1.4-3.9)	4.0 (3.3-4.9)	1.5	0.132
Serine	20.4 (10.8-31.8)	81.2 (53.3-117.6)	4.0	**0.004**
Succinate	46.3 (45.1-56.6)	54.6 (42.6-75.4)	1.2	0.485
Valine	45.8 (38.0-53.1)	48.8 (36.4-60.4)	1.1	0.818
AMP	5.4 (1.1-6.7)	0.7 (0.5-1.2)	-7.7	**0.045**
Betaine*	0.08 (0.05-0.10)	0.03 (0.02-0.05)	-2.7	**0.026**
Choline-Dimethylglycine	0.5 (0.3-0.8)	0.2 (0.08-0.3)	-2.5	**0.015**
Cystathionine*	19.3 (18.1-35.1)	17.8 (15.0-18.2)	-1.1	**0.015**
Cysteine	7833.3 (5791.2-11418.9)	6516.2 (6356.8-7043.1)	-1.2	0.485
Folic acid*	4.2 (2.9-5.4)	2.4 (2.0-4.0)	-1.8	0.180
Formyl-THF*	2.8 (2.4-6.4)	2.6 (1.1-6.3)	-1.1	0.589
Glycine	70.9 (53.6-75.0)	57.5 (48.5-79.3)	-1.2	0.699
Homocysteine	0.11 (0.08-0.14)	0.07 (0.04-0.09)	-1.6	**0.041**
Methyl-THF*	5.0 (3.0-9.6)	3.3 (2.2-3.5)	-1.5	0.093
Methylcobalamine (B12)*	1.1 (0.6-2.3)	1.7 (1.5-2.0)	1.5	0.485
Methionine	0.36 (0.25-0.76)	0.38 (0.26-0.68)	1.1	0.485
NADPH	1.1 (0.8-1.2)	0.5 (0.3-0.6)	-2.2	**0.015**
Pyridoxal 5-P (B6)*	35.0 (31.8-48.9)	28.7 (22.5-46.1)	-1.2	0.240
Riboflavin (B2)*	3.5 (3.4-7.5)	5.9 (3.8-6.0)	1.7	0.589
SAH*	0.10 (0.06-0.23)	0.08 (0.04-0.09)	-1.3	**0.009**
SAM	0.71 (0.65-0.80)	0.58 (0.48-0.65)	-1.2	**0.041**

Data were expressed as median (interquartile range) in µmol / mg of protein except those marked with an asterisk denoting nmol / mg of protein. SAH, S-adenosylhomocysteine; SAM, S-adenosylmethionine; THF, Tetrahydrofolate. Significant differences (at least $p<0.05$).

Table 16. Targeted metabolome of HEPG2 cells treated with 2 mM DMKG with or without metformin (10mM).

	Metabolite	Without metformin (n=6)	With metformin (n=6)	Fold change	*p*-value
Energy Metabolism	**α-ketoglutarate**	1.7 (1.1-1.8)	0.8 (0.7-0.9)	-2.1	**0.002**
	β-hydroxybutyrate	6.6 (4.4-8.2)	1.8 (1.4-2.3)	-3.7	**0.002**
	Alanine	17.3 (7.8-24.9)	15.9 (7.2-40.7)	-1.1	**0.041**
	Aspartate	73.3 (59.3-96.1)	25.7 (19.2-33.0)	-2.9	**0.002**
	(Iso)Citrate	2.4 (2.8-5.9)	0.9 (0.8-1.1)	-2.7	**0.002**
	Fructose-1,6BP	9.9 (3.8-14.4)	0.7 (0.6-0.8)	-14.1	**0.002**
	Fructose-6P	69.9 (47.0-94.1)	2.7 (2.4-3.8)	-25.9	**0.004**
	Fumarate	7.2 (4.2-8.2)	3.3 (22.9-4.3)	-2.2	**0.002**
	Glucose	90.9 (77.2-98.2)	48.8 (45.9-62.2)	-1.9	**0.004**
	6P-Gluconate	4.6 (2.4-5.1)	0.5 (0.3-0.8)	-9.2	0.051
	Glucose-6P	16.5 (5.8-24.3)	1.0 (0.7-1.2)	-16.5	**0.002**
	Glutamate	244.1 (11.8-300.0)	3.0 (1.6-6.6)	-81.4	**<0.001**
	Glycerate-3P	37.1 (7.6-45.6)	13 (4.2-12.1)	-2.9	**0.002**
	Isoleucine	30.3 (20.3-52.5)	17.8 (16.1-22.9)	-1.7	**0.009**
	Lactate	391.9 (369.8-447.5)	505.1 (395.8-677.0)	1.3	0.240
	Leucine	66.2 (39.9-117.0)	42.1 (38.8-44.8)	-1.6	**0.002**
	Malate	20.9 (14.0-26.1)	8.9 (7.4-12.3)	-2.3	**0.002**
	Oxaloacetate	29.6 (25.6-32.1)	2.9 (2.2-3.1)	-10.2	**0.002**
	Phosphoenolpyruvate (PEP)	14.8 (6.0-16.1)	2.3 (0.9-3.0)	-6.4	0.240
	Pyruvate	3.5 (2.5-6.4)	1.8 (1.3-2.7)	-1.9	**0.004**
	Ribose-5P	4.5 (2.6-4.9)	2.2 (1.8-3.4)	-2.0	**0.041**
	Serine	107.1 (73.4-231.3)	43.2 (26.6-91.6)	-2.5	**0.009**
	Succinate	66.3 (62.2-71.2)	73.8 (61.1 9.3)	1.1	0.065
	Valine	67.1 (58.5-55.2)	53.9 (47.7-77.5)	-1.2	**0.041**
1-C Metabolism	**AMP**	1.5 (1.1-1.6)	1.0 (0.6-1.2)	-1.5	0.589
	Betaine*	0.03 (0.02-0.04)	0.02 (0.02-0.04)	-1.5	**0.003**
	Choline-Dimethylglycine	0.10 (0.03-0.10)	0.02 (0.01-0.03)	-5.0	**0.002**
	Cystathionine*	19.5 (17.9-21.0)	8.5 (8.3-8.8)	-2.3	**0.002**
	Cysteine	6169.5 (5000.6-7957.9)	4306.1 (3873.7-6194.6)	-1.4	**0.009**
	Folic acid*	3.1 (1.5-5.2)	3.3 (1.5-5.8)	1.1	0.062
	Formyl-THF*	1.5 (0.8-2.7)	0.8 (0.5-0.9)	-1.9	**0.041**
	Glycine	67.7 (54.1-75.5)	47.1 (38.7-62.6)	-1.4	**0.041**
	Homocysteine	0.7 (0.6-0.9)	1.2 (0.8-1.5)	1.7	**0.004**
	Methyl-THF*	3.6 (2.3-3.7)	0.4 (0.3-0.7)	-9.0	**0.002**
	Methylcobalamine (B12)*	1.1 (0.6-1.6)	0.3 (0.2-0.5)	-3.7	**0.004**
	Methionine	0.5 (0.3-0.6)	0.2 (0.1-0.3)	-2.5	**0.002**
	NADPH	1.3 (1.0-1.3)	0.2 (0.1-0.4)	-6.5	**0.002**
	Pyridoxal 5-P (B6)*	36.8 (33.6-51.6)	27.3 (22.4-31.5)	-1.3	**0.009**
	Riboflavin (B2)*	6.7 (4.4-7.3)	4.7 (4.0-6.1)	-1.4	**0.004**
	SAH*	0.09 (0.07-0.13)	0.12 (0.08-0.24)	1.3	**0.041**
	SAM	0.7 (0.6-0.9)	0.2 (0.1-0.4)	-3.5	**0.008**

Data were expressed as median (interquartile range) in µmol / mg of protein except those marked with an asterisk denoting nmol / mg of protein. SAH, S-adenosylhomocysteine; SAM, S-adenosylmethionine; THF, Tetrahydrofolate. Significant differences (at least p<0.05).

The integrative analysis of DNA methylation and gene expression data discriminates NASH from non-NASH livers.

The changes caused by NASH in the relative abundance of metabolites with the ability to function as epigenetic modifiers suggested that differences in liver DNA methylation might correlate with differences in liver gene expression with a potential prominent role in NASH development. We found a significant effect on DNA methylation during NASH, specifically in the context of 5-mC conversion to 5-hmC (Figure 35 a). To conclusively determine how these metabolic differences can influence NASH pathology requires further investigation, but the relationships revealed by our analyses between the relative abundance of metabolites in the livers of patients with or without NASH implicate crosstalk between metabolism and DNA methylation in NASH progression (Figure 36). To gain a comprehensive insight into the variation in genomic DNA methylation between Non-NASH and NASH livers, we explored the methylation levels of cytosine 5 prime to guanine (CpG) sites in commercially available single-stranded linear sequences. The average β values between NASH and non-NASH livers of 637,380 CpG sites correlated significantly indicating a largely stable CpG methylation (Figure 35 b). We identified 2,508 differentially methylated CpG sites, which segregated livers with or without NASH (Figure 35 b-d). Hypo- and hyper-methylation was equally distributed between groups and were notably located in CpG islands from gene promoters (≈ 25%), gene body (≈ 44%) or intergenic regions (≈ 31%) (Figure 35 e, f). We focused our analysis to transcripts corresponding to promoters and covering functional regions both from transcriptional start site to 200 nucleotides upstream and from 200 to 1500 nucleotides upstream according to KEEG pathway analysis (Figure 35 g, i).

To better understand the effects of NASH on gene expression, we performed transcriptional analysis using microarrays (see methods). Transcriptional analysis identified the significantly different expression of 345 genes that segregated livers with or without NASH (Figure 37 a, b). A comprehensive list of differentially expressed genes in NASH livers included 144 upregulated and 201 downregulated genes (Table 17). According to KEEG analysis genes with lower expression in NASH livers were involved in pathways related to metabolism and those upregulated were associated with functions such as cell adhesion and migration, chemokine and cytokine signaling, and metabolic signaling pathways (Figure 37 c).

The resulting 367 differentially methylated CpG sites in CpG islands from promoters likely associated with transcriptional activity were compared testing for significant inverse correlation between promoter methylation and gene expression and we identified genes that segregated NASH from non-NASH livers. After testing for significant inverse correlation between promoter methylation and gene expression, our analysis showed that 11 CpGs (corresponding to 11 genes) displayed an increase or decrease in promoter methylation corresponding to a decrease or increase of gene expression, respectively (inverse Spearman correlation $p < 0.05$). Of these, 5 CpGs (corresponding to: DISP2, MARK3, TDRD6, TRIP10 and ZNF197) were significantly hypermethylated in NASH, and 6 CpGs (corresponding to: ACP5, ARL8A, C1orf54, HDAC9, RAB31 and UGT3A2) were significantly hypomethylated (Figure 38 a). Figure 39 shows individual patient methylation and expression data for the genes with negative correlation between DNA methylation and mRNA expression in NASH vs. Non-NASH. The genomic locations of these 11 genes across autosomes are visualized using a Circos plot (Figure 38b) to explore the relationship between chromosome localization, DNA methylation, and gene expression. To determine the biological relevance that these 11 genes have with respect to NASH pathogenesis, we curated a comprehensive list of molecular functions or biological processes associated with them. This analysis revealed functions in the regulation of riboflavin metabolism, insulin signaling pathway, pathways in cancer, lysosome modulation, RET signaling pathway and chemokine signaling pathway, to name a few (see Table 16 for comprehensive list).

Finally, our 11 gene candidates were validated by gene expression (Figure 38 c). Our data indicated the plausible importance of altered DNA methylation in the pathogenesis of NASH and we propose the significant hypermethylation of TDRD6 promoter in NASH livers and the significant hypomethylation of ACP5, C1orf54, HDAC9 promoters as potential candidates. Taken together, these studies demonstrate locus specific regulation of DNA methylation that differs between obese patients with or without NASH. Mechanistically, our findings indicate that some of these methylation changes correlate with gene expression, providing novel insights into molecular pathogenesis of this disease.

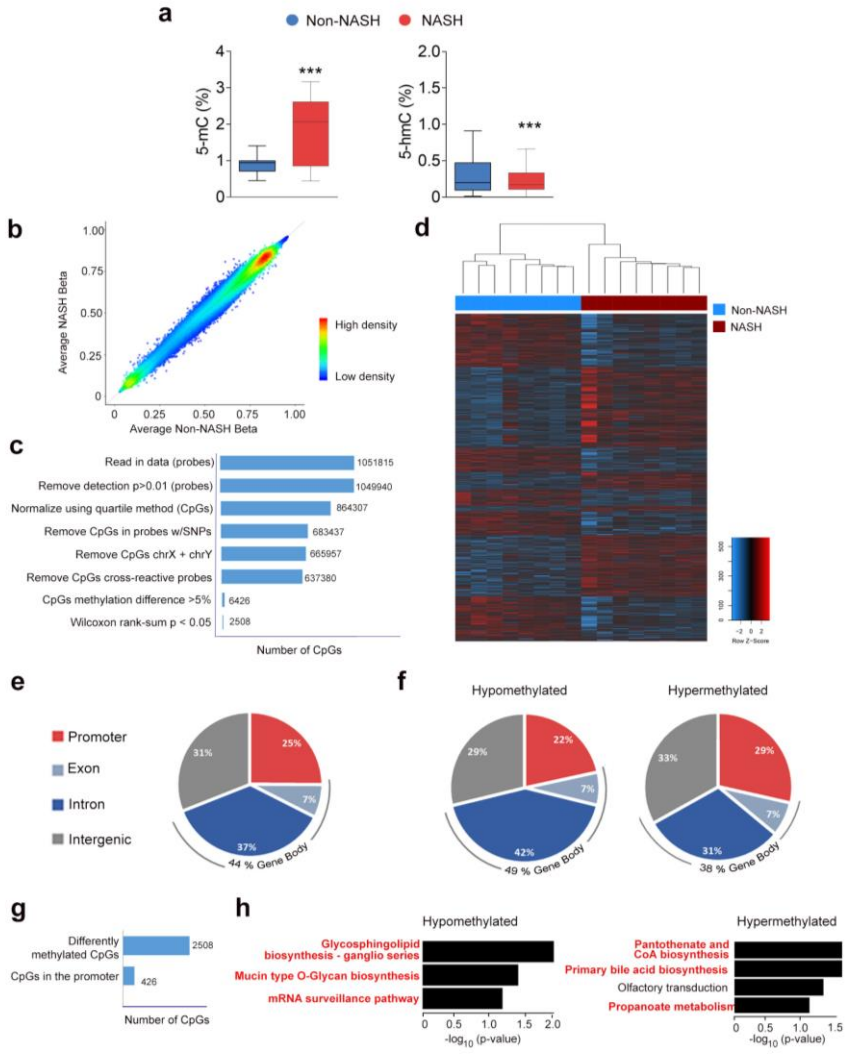

Figure 35. Global DNA methylation arrays reveal differences in CpG methylation between non-NASH and NASH patients. (a) 5-mC and 5-hmC levels measured by mass spectrometry in liver. (b) Density plot showing average Beta values at 637,380 filtered CpG sites in Non-NASH and NASH patients. (c) Graphical representation of the filtering process used to determine significantly differentially methylated CpGs. To investigate methylation differences, we kept only CpGs with average methylation difference > 5% between NASH and Non-NASH, and determined those with $p < 0.05$ (Wilcoxon rank-sum test). (d) Heatmap showing methylation levels for 2508 significantly differentially methylated CpGs (Wilcoxon rank-sum test $p < 0.05$ and average methylation difference > 5%). (e) Genomic distribution of all differently methylated CpGs across promoters (red), exons (light blue), introns (dark blue), and intergenic regions (grey). (f) Genomic localization of hypo- or hypermethylated CpGs, demonstrating no preferential change at these regions (color scale same as e). (g) Distribution of differentially methylated CpGs between promoters and non-promoter regions. (i) KEGG pathway analysis of genes whose promoters contain significantly hypo- (left) or hypermethylated (right) CpGs. The most clinically relevant pathways are highlighted in red.

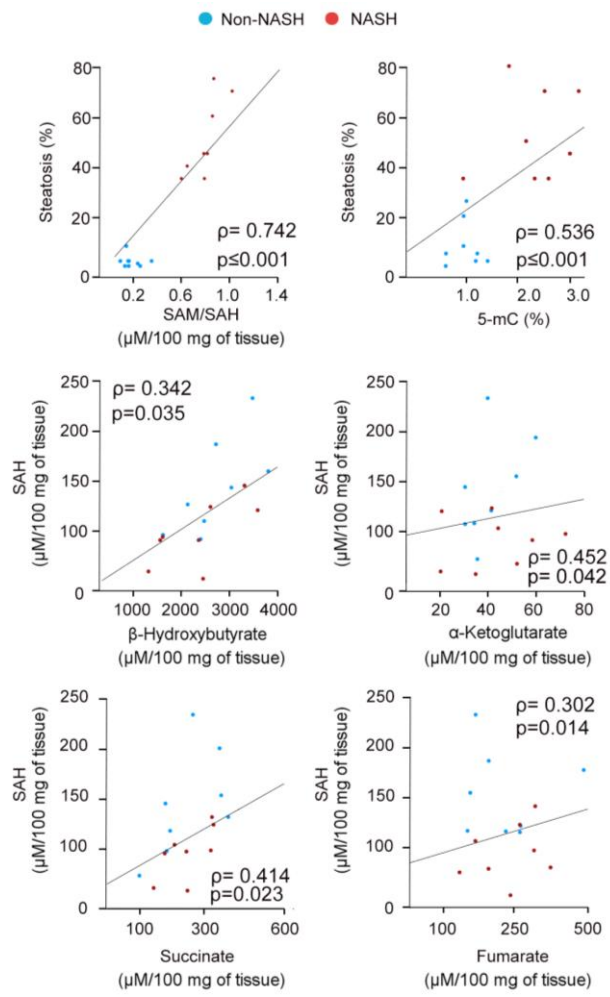

Figure 36. Relationships between methionine, TCA cycle and DNA methylation. Significant correlations (Spearman cor.test() $p < 0.05$) denote the connection between metabolism and DNA methylation in the progression of NASH.

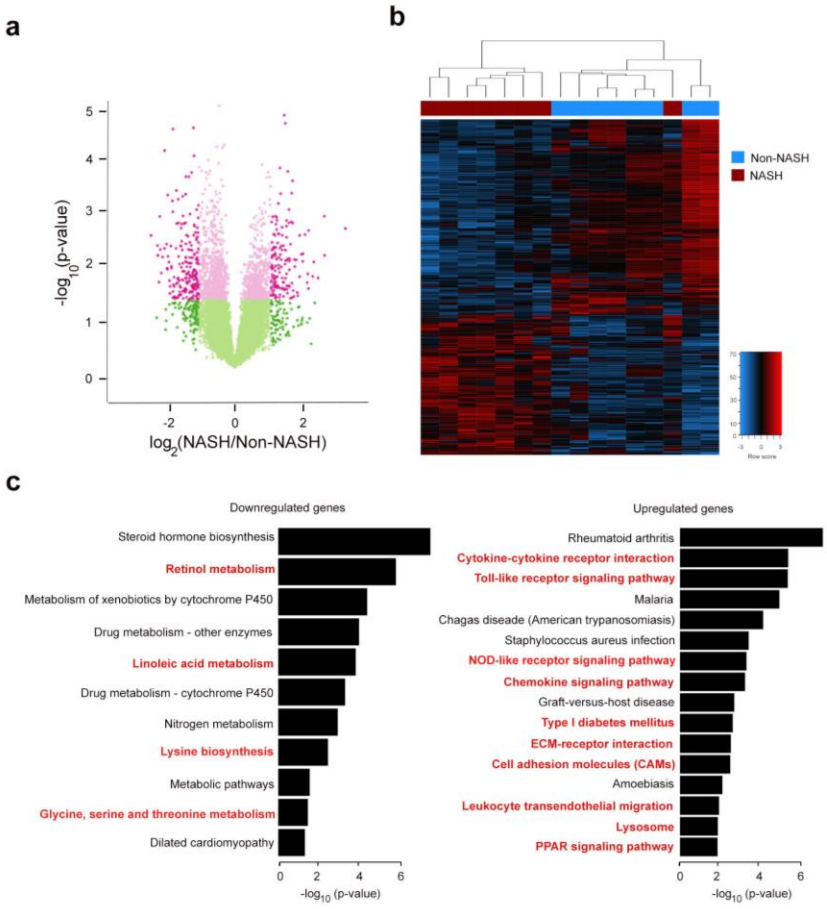

Figure 37. Global mRNA microarray analysis identifies significant expression differences between non-NASH and NASH patients.

(a) Volcano plot of mRNA expression differences between NASH and Non-NASH patients plotted against the p-value of the expression difference. The x-axis indicates log2(NASH/Non-NASH), while the y-axis shows -log10(p-value) of the t-test. Pink coloring indicates p-values < 0.05, while darker shading indicates absolute value of log2(fold-change) in expression greater than 1. (b) Unsupervised hierarchical clustering of 345 significantly differentially expressed genes ($p < 0.05$ and absolute value of log2(fold-change) > 1) reveals a clear separation between NASH and Non-NASH (shown as red and blue bars across the top of the heatmap, respectively). The heatmap was generated using row scaling, and color range indicates low (blue) to high (red) gene expression. (c) Of the 345 significantly differentially expressed genes from the microarray, 201 are downregulated (left) and 144 upregulated (right). KEGG pathway analysis is shown, with the most clinically relevant pathways distinguished in red.

Table 17. Up- and down-regulated genes in NASH.

Cell adhesion molecules (CAMs)
Chemokine signaling pathway
Leukocyte transendothelial migration
Lysosome
Metabolism regulation
Solute Carrier Family
Small Nucleolar RNA

Up regulated

ACP5, ADCYAP1R1, AJUBA, APOL3, B3GNT5, BBC3, BHLHA15, BTG2, C12orf5, C15orf48, C2orf82, C5AR1, CAPG, CCDC109B, CCL2, CCL20, CCL3, CCNB2, CD209, CD3G, CD52, CD83, CDCA2, CDH15, CDHR2, CFTR, CH25H, CLDN11, CLDN5, CLECL1, COL1A1, COL1A2, COL4A2-AS1, CPXM2, CPZ, CRTAM, CTSV, CXCL10, CXCL3, CXCL8, CXCL9, DOK5, DOK6, EDN2, EEF1A2, EGR2, EGR3, EZR-AS1, FABP4, FABP5, FAM151A, FAM90A7P, FAR2, FCAMR, FFAR3, FMO1, FNDC5, FOXL2, FPR2, GATA3, GEM, GLIPR1, GPNMB, GPR182, GPR183, HIST1H1B, HIST1H3B, HLA-DQA1, HLA-DRB5, HMGCS1, HSPB8, HULC, IGSF22, IL10RB-AS1, IL1B, IL4I1, INHBE, ISM1, KCNJ3, LAMP3, LINC00884, LINC00885, LOC154872, LPL, LYPD1, MB, MB21D2, MCM2, MMP9, MNDA, NANOS3, NFKBIE, NR4A3, NTN3, OSM, PADI1, PCDH9-AS2, PEG10, PLA2G7, PLAUR, PLCXD2, PLXNC1, PODN, PRAMEF10, PROK2, PSRC1, QPCT, RASSF9, RFTN1, RGS16, RGS2, RNF186, RRAD, SEC14L3, SIX1, SLC22A13, SMIM24, SORT1, SPP1, SQLE, STMN2, TACC3, TBXAS1, THBS2 ,THEMIS, THY1, TIFAB, TLR9, TM4SF19, TMEM200A, TNFAIP3, TNFSF9, TREM2, TRHDE-AS1, TRIM59, TRIM63, TYMS, UGT3A2, UHRF1, UNC93A, WNT2 ,WNT5A, ZNF620, ZNF683

Down regulated

AASS, ABCA10, ACKR2, ACOT6, ADAM1A, ADCY1, ADCY10, ADHFE1, ADTRP, AFF3, AFG3L1P, AGR2, AKR1C6P, ALPK2, ANKRD23, ANO8, ARHGEF26, ARHGEF4, C1orf228, C1QTNF3, CA3, CA9, CAPN3, CATSPER3, CCDC158, CCDC162P, CCDC180, CCDC38, CCDC84, CELSR3, CENPJ, CFAP70, CHAD, CHKB, CHRD, CIART, CIT, CLASRP, CLCN2, CMYA5, COLCA2, CPT1B, CRYGS, CSPP1, CXCL2, CYP1A1, CYP3A4, CYP3A43, CYP3A5, CYP3A7, CYP4Z1, DCDC5, DCPS, DDX43, DFNB59, DGCR14, DKFZp434J0226, EFCAB1, ENO1-AS1, ERN1, FAM132A, FAM193B, FAM76B, FAM83A-AS1, FKBP5, FLJ21408, FLJ31104, FOXO1, FUT3, GADD45G, GNMT, GNRH1, GOLGA7B, GPR128, GPT2, GSTA7P, HAL, HERC2P2, HERC2P7, HERC5, HIGD1B, HORMAD2, HSD17B3, HSD3B1, ICA1, IFRD1, IGF1,IGFBP2, INS-IGF2, IRX3, ITGA10, KCNMB3, KGFLP1, KIAA0895L, KPNA7, KRT42P, KRT71, L3MBTL1, LCE2D, LGI4, LGSN, LHX4-AS1, LINC00238, LINC00659, LINC00939, LINC01125, LOC100270804, LOC100289230, LOC100505918, LOC285626, LOC644656, LOC729603, LRRC73, LYG1, MAST2, MEGF6, MREG, MT1IP, MTHFD2L, MTUS2, MYO15A, MYOM1, NBPF14, NEAT1, NEIL1, NINJ2, NNMT, NOXO1, NRBP2, OAT, P4HA1, PAPD7, PAQR6, PARP6, PATL2, PDZD3, PILRA, PILRB, POFUT2, POU6F1, PPARGC1A, PRR26, PRSS50, PSPH, PTPRH, PYROXD2, PZP, RAD51AP2, RDH12, REC8, RFPL4AL1, RHBG, RIC3, S100A1, SEC16B, SH2B1, SH2D6, SLC10A5, SLC16A1, SLC23A2, SLC25A18, SLC29A2, SLC34A1, SMIM5, SNORA33, SNORA41, SNORA6, SNORA70B, SNORA70C, SNORA70E, SNORA72, SNORD18C, SNORD85, SNORD98, SOCS2, SYBU, TAS1R3, TAS2R19, TBC1D3B, TBC1D3C, TCAF2, TCERG1, TDRD6, TFRC, TG, TMCO6, TPTE2P5, TRPV1, TSKU, TSNAXIP1, UBE2Q2L, UCN, UGT2A1, VCPKMT, WDR60, ZDHHC11, ZNF211, ZNF266, ZNF276, ZNF507, ZNF833P

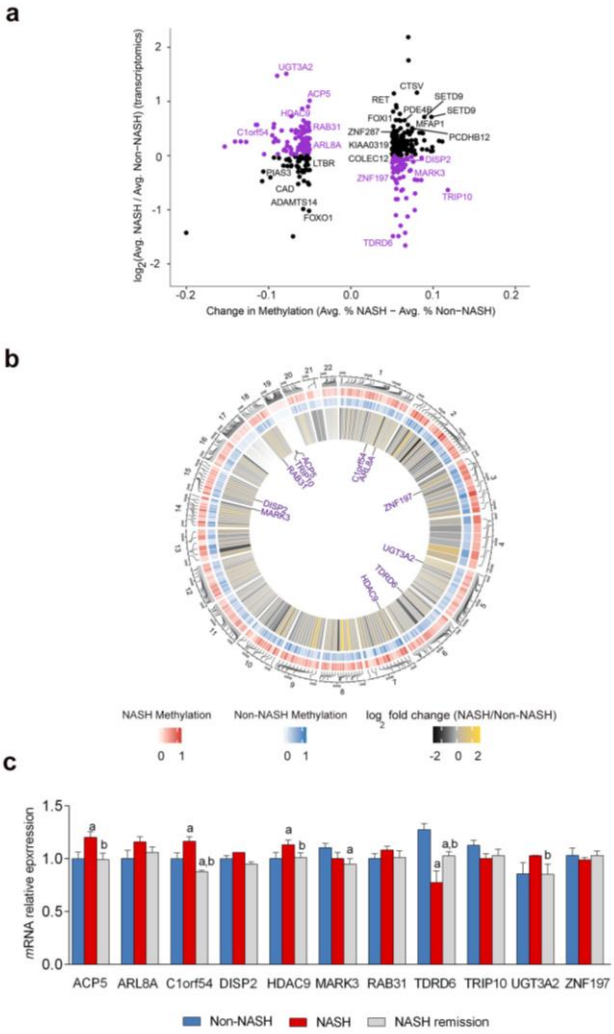

Figure 38. Relationship between DNA methylation and mRNA expression.
(a) Relationship between average change in methylation (NASH – Non-NASH; on the x-axis) is plotted against the log2(fold-change) of gene expression (NASH/Non-NASH; y-axis) for 367 differentially methylated CpGs within promoters of genes with microarray expression data. Purple coloring indicates CpGs in promoters of genes whose expression goes up or down with promoter hypo- or hypermethylation, respectively. Text labels indicate genes corresponding to promoter CpGs with significant correlation between methylation and gene expression ($p < 0.05$ using cor.test() in R), and purple text highlights those with an increase or decrease in expression with promoter hypo- or hypermethylation, respectively. (b) Circos plot showing the 367 CpGs from (a), with red and blue layers indicating localization and methylation levels respectively in NASH and Non-NASH patients. The interior layer shows log2(fold-change) in mRNA levels between NASH and Non-NASH patients and text labels indicate CpGs highlighted in purple in (a). (c) Gene expression validation of 11 candidate gens. [a]Significant difference compared with Non-NASH vs NASH; [b]significant differences compared with NASH vs NASH-remission. Statistical significance was estimated when $p<0.05$ by Wilcoxon rank-sum test.

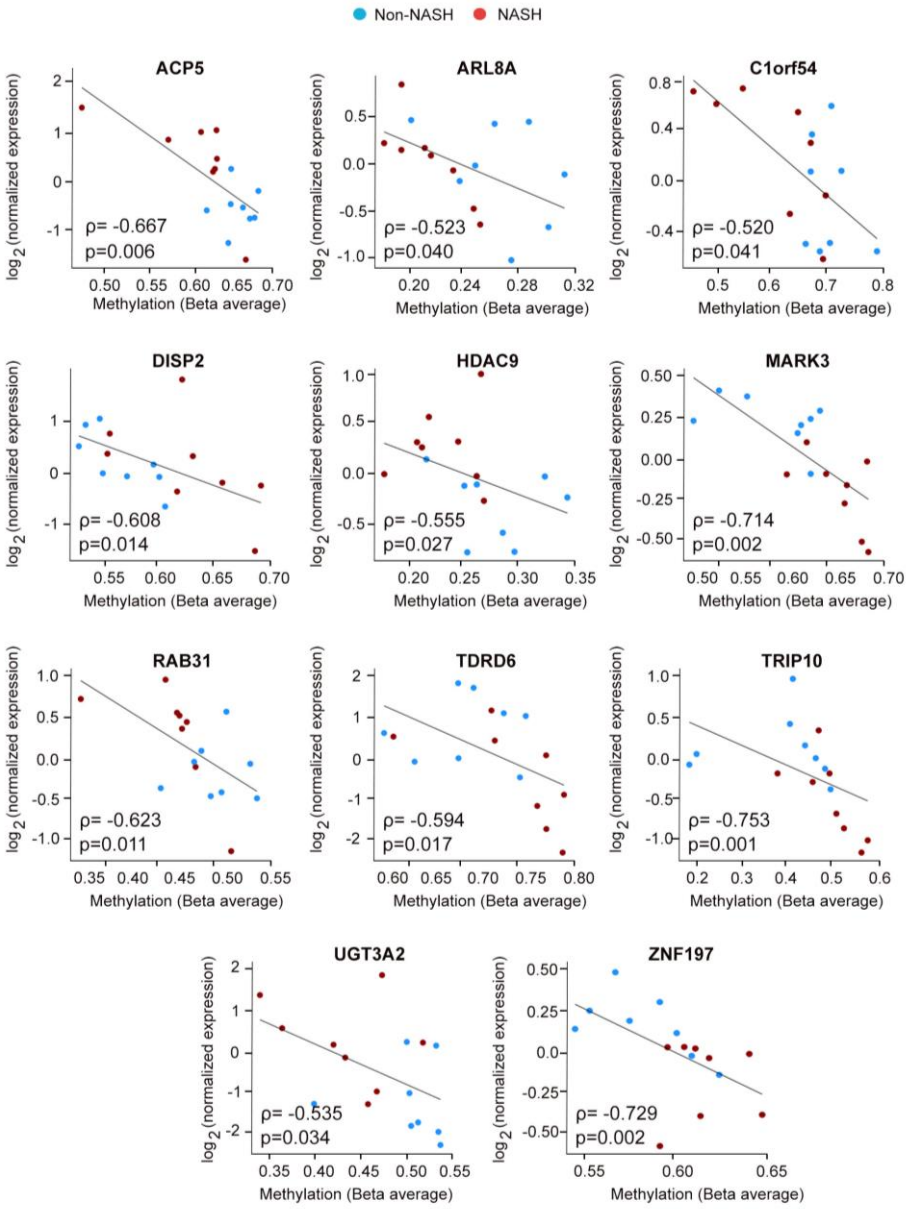

Figure 39. Genes with the highest significant changes in DNA methylation and gene expression. Correlation plots of DNA methylation (Beta average) versus gene expression (log2 expression) in NASH vs. Non-NASH patients (Spearman cor.test() $p < 0.05$) for the 11 genes with negative correlation between DNA methylation and mRNA expression.

Table 18. Genes with the negative correlation of DNA methylation and mRNA expression between Non-NASH and NASH patients

Gene	Gene Name	CpG name	Region	Super pathway	Entrez gene	p-value	Log_2 Fold change (NASH/Non-NASH)
ACP5	Acid Phosphatase 5, Tartrate Resistant	cg01524690	TSS200	-Metabolism of vitamins and cofactors -Lysosome	54	0.006	1.01
ARL8A	ADP Ribosylation Factor Like GTPase 8A	cg08649954	TSS1500	- Innate Immune System lysosomes motility	127829	0.040	0.12
C1orf54	Chromosome 1 Open Reading Frame 54	cg06334965	TSS200	-Unknown	79630	0.041	0.37
DISP2	Dispatched RND Transporter Family Member 2	cg17063840	TSS1500	-Signaling by Hedgehog -Signaling by GPCR	85455	0.014	-0.10
HDAC9	Histone Deacetylase 9	cg19585556	TSS200 TSS1500	Signaling by NOTCH1, macrophage differentiation and intracellular calcium signaling	9734	0.028	0.61
MARK3	Microtubule Affinity Regulating Kinase 3	cg26623547	TSS1500	-RET signaling. -Signaling MAPKS kinase activity BRAF	4140	0.003	-0.44
RAB31	RAB31, Member RAS Oncogene Family	cg18456459	TSS1500	-Member RAS Oncogene Family	11031	0.012	0.53
TDRD6	Tudor Domain Containing 6	cg11931223	TSS200	-Gene expression	221400	0.017	-1.49
TRIP10	Thyroid Hormone Receptor Interactor 10	cg18732869	TSS200	-Regulation of lipid metabolism Insulin signaling-generic cascades	9322	0.001	-0.64
UGT3A2	UDP Glycosyltransferase Family 3 Member A2	cg10402936	TSS1500	-Cytochrome P450 - arranged by substrate type	167127	0.035	1.51
ZNF197	Zinc Finger Protein 197	cg11557071	TSS1500	- Chemokine signaling pathway	10168	0.002	-0.31

Discussion

UNIVERSITAT ROVIRA I VIRGILI
ASSESSING DIAGNOSTIC AND THERAPEUTIC TARGETS IN OBESITY-ASSOCIATED LIVER DISEASES
Noemí Cabré Casares

The high prevalence of obesity is a global public health problem, declared it as "*global epidemic*" (5, 15). Type III obesity (BMI>40 kg/m^2) is a pathologic condition that fails in adaptation to metabolic changes caused by increase food intake and metabolic disturbances, which are associated with severely NCDs, including diabetes and liver disorders (17, 22, 51).

In the context of obesity, up to 70% of patients have liver steatosis and/or inflammation (22, 277). NAFLD is an important comorbidity of obesity and is recognized worldwide as the most common cause of chronic liver disease in adults and children. Its incidence and prevalence are constantly increasing (277, 278). Furthermore, NAFLD is not a simple disease; it includes a spectrum of hepatic abnormalities which extends from simple steatosis or NAFL to NASH, a pathological entity associated with an increased risk for developing more serious diseases such as cirrhosis, liver failure and hepatocellular carcinoma (25).

BS is the most radical therapy for the severe obesity accompanied with metabolic syndrome and NASH, leading typically to massive weight loss and, improvement of liver histology. However, the clinical use of this procedure remains low even in patients meeting all criteria for eligibility (279). Here in we provide evidence that all comorbidities, including NAFLD, significantly improved within one-year post-surgery, following weight loss and metabolic improvement. Our findings of the impact of BS in NAFLD regression are consistent with previous studies (236-239, 280). The glycemic control improvement in all diabetic patients and the likely beneficial effects on diabetes-associated end-organ complications is particularly important (281). To consider surgery in patients with lower weight excess and suboptimal control of T2DM has been widely endorsed by Diabetes Organizations (282). The lack of clinical influence of these recommendations might result in denying diabetic patients an effective therapy. Here we add another indication to be evaluated because BS resolves NAFLD including NASH and fibrosis in most cases. This major impact on the liver was concordant with results from other prospectively designed studies and planned biopsy programs (237).

The transition from NAFL to NASH remains uncertain. However, it is unlikely related to body weight, and provably associated with increased insulin resistance, hyperglycemia, hyperlipidemia and other metabolic disturbances. Understanding the transition from non-NASH to NASH requires investigating the relationship between oxidative stress, mitochondrial dysfunction and hepatocellular death (35, 58, 64).

It is important to recognize and target the hepatic consequences of nutrient overload. Dietary restraint improves liver function and histologic features in mice (283), but in the clinical setting, dietary advice is clearly insufficient to stop the growing incidence and prevalence of obesity-associated diseases (284). Unbalanced nutritional status may lead to the accumulation of fat in hepatocytes, which sequentially induces mitochondrial dysfunction, oxidative stress, inflammation, and cell death. Remission through dietary interventions is uncommon, and our findings might have therapeutic and pathogenic implications in searching effective treatment procedures to reverse NAFLD and/or avoiding progression from simple steatosis to NASH.

Recent evidence suggests that continuous adaptation of "*remodeling*" of hepatic mitochondrial metabolism or mitochondrial dysfunction play a key role in the pathogenesis of simple steatosis/NASH (285). Mechanisms promoting NAFLD progression involve multiple cellular adaptations to the oxidative stress occurring when fatty acid metabolism is impaired by MRC stress (119). This adaptation is increased in obese humans with NASH, who also exhibit greater hepatic insulin resistance, hepatic oxidative stress, and systemic inflammation. The decreased activities of MRCs increase pro-inflammatory status, influences the proliferation and, activate macrophage polarization. For example, the release of certain molecules that promotes tissue damage such as TNF-α levels, leading to additional lipid peroxidation which, in turn induces the production of CCL2, and fibrogenic factors such as, transforming growth factor β (TGF-β). TGF-β stimulates hepatic stellate cells in injured livers to become myofibroblast (MFs), which activate collagen synthesis that finally drives fibrosis progression (101, 103, 286).

In the first study we show that oxidation, inflammation and fibrosis were clearly altered in patients with NASH compared to those without NASH. Moreover, oxidation, inflammation and fibrosis in the liver substantially improved after surgery. The measurement of PON1 and CCL2 that have been previously shown good indicators of these phenomena assessed the improvement. In particular, we had previously observed the close relationship between PON1 and CCL2 in the regulation of hepatic oxidative stress and inflammation (76, 287). In mice, *pon1* gene deficiency promotes fatty liver disease and *ccl2* gene deficiency abrogates it (115, 287, 288). In humans, polyphenols attenuate liver damage modulating gene expression pathways that regulate the roles of PON1 and CCL2 in oxidative stress and the inflammatory response respectively (289, 290). Both processes are important in macrophage polarization, with potential impact on promoting the resolution of liver

disease (99). Increasingly, galectin-3 has been recognized as a modulator of oxidative stress, inflammation, fibrosis and angiogenesis (291). The decrease in liver galectin-3 expression and the simultaneous decrease in the liver expression of α-SMA post-surgery appears to modify the hedgehog-signaling pathway, indicating that transition from the quiescent stellate cells to myofibroblast stellate cells may be reversible (292-294).

Our results suggest a sequential involvement of multiple cellular responses, and support the concept of using a combination of different therapies to achieve non-invasive regulation of several molecular networks. Assaying a single, expensive and potentially toxic new compound does not seem a desirable strategy, considering the multi-factorial nature of NAFLD development (103, 286, 295). Protection of the liver requires considerable weight loss and deep changes in lifestyle. Some well-tried and safe drugs may help improve insulin sensitivity but are fairly ineffective without dietary restraint (283). Our histology evidence confirmed that reducing oxidative stress and suppressing activation of liver inflammatory cells are mandatory targets. Dietary antioxidants, insulin sensitizers, and lipid-lowering agents can, when used in combination, boost intracellular protection against lipoperoxides, suppress key inflammatory signaling systems, and induce reparative stress signaling (296, 297); all of which warrant further randomized controlled trials with a multi-targeting approach to determine dosage, length of treatment and combinatory modes of action (298).

Mitochondria plays an important role in hepatocyte metabolism, being the primary site for the oxidation of fatty acids and oxidative phosphorylation. NAFLD affects mitochondrial metabolism and metabolic pathways which can lead to perturbations in metaboloepigenetic processes (184). The choice of potential therapeutic targets needs to consider that NASH is a multisystem disease with an important mitochondrial contribution to the defective metabolic responses (49). Mitochondrial dysfunction eventually perturb energy and 1-C metabolism and the involved metabolites may be measured in the circulation (263).

The second study focused on plasma target metabolomics, which includes energy and 1-C metabolism. Metabolomics is arising attention as powerful tool to provide identification and quantification of systemic biological changes. To date, a few studies have explored the detailed metabolic profile in severe obesity using target metabolomics strategies. Thus, we developed mass

spectrometry–based methods for robust and accurate quantitation of a defined set of closely related metabolites (252-254). Our observations suggest that the critical links between obesity and liver disease are closely related to the mitochondrial integrity of energy and 1-C metabolism. Fluctuations in the plasma metabolome assessed complex effects associated with the severity of liver disease, as were almost completely reversed after NASH remission. In human obesity, the liver may efficiently respond to nutrient overload during a period of time but the onset and development of NASH represents a critical event leading to metabolic inflexibility (299). The clinical relevance in obesity of increased CAC activity, whole-body protein catabolism and pyruvate-driven gluconeogenesis remains to be established, although the increased anaplerotic flux and glutaminolysis-derived accumulation of plasma α-KG in NASH patients may supply pathogenic clues (300, 301). Our data suggest that obese patients, especially those with metabolic syndrome, might benefit from bariatric surgery at an earlier stage. Plasma α-KG identifies obese patients with hepatic steatosis (263). Our findings suggest that circulating metabolites provide signals of the impaired metabolic state that might lead to NASH development when there is an insufficient adaptive hepatic response. NASH was associated with perturbed pathways in glucose and fatty acid oxidation with convergence in the metabolism of amino acids and lipids (302). These perturbed pathways were restored after surgery following NASH remission.

Targeted quantitation of plasma α-KG, pyruvate and oxaloacetate levels revealed differences between patients with and without NASH that may be used a interesting noninvasive diagnostic biomarkers. A major finding of this study was that paired measurements of these metabolites, before and after surgery, provided excellent results to predict NASH remission without ambiguity, indicating a reliable alternative to liver biopsy in assessing the effectiveness of clinical management in NASH patients. Similarly, metabolites from the methionine cycle, succinate and α-KG have been reported as mediators in the dynamic process of methylation linked to altered cellular metabolism in disease states (303, 304). Circulating metabolites from energy and 1-C metabolism provide a global picture of metabolic interorgan crosstalk with potential importance in liver metabolic research associated with the growing obesity epidemics.

Plasma α-KG levels may distinguish lean controls from obese patients with a high predictive accuracy and predict obese patients with or without NASH better than commonly used biomarkers (263). This result supports the potential clinical utility of plasma α-KG levels. However, additional

validation is required. In the third study, our data strongly support the notion that α-KG in NASH patients is mainly incorporated into the TCA cycle though increased glutaminolysis. α-KG is produced from isocitrate by oxidative decarboxylation catalysed by isocitrate dehydrogenase (IDH). α-KG can also be produced anaplerotically via process termed glutaminolysis (145, 149). Incorporation of α-KG into the CAC cycle is the major anaplerotic step in proliferating cells and is critical for the production of oxolacetate which reacts with acetyl-CoA to produce citrate (151, 305) . Moreover, in the liver of NASH patients, the reductive glutamine carboxylation of the α-ketoglutarate to citrate is favoured. That is, metabolic changes promote glutamine and the primary carbon source for citrate and fatty acid synthesis (305).

One year after BS we showed an important metabolic shift of profile in the liver. Our results determine that glycolytic intermediates were decreased, although CAC intermediates were significantly increased after BS. Conversely, livers after bariatric surgery apparently exhibited a decreased dependency in reductive glutamine metabolism capable of replenishing the high levels of lipogenic acetyl-CoA/malonyl-CoA, as shown in low levels of α-KG. Besides, we observed a significative reduction of ketogenesis, because of low levels of BCAAs and β-hydroxybutyrate. A similar picture emerged when assessing plasma samples (207, 263). The significant reduction of BCAAs improves ketogenesis and patients restore glutamine dependency with decreasing glutaminolysis.

Glutaminolysis-induced mTORC1 activation stimulates protein synthesis and cell growth (an elevated concentration of amino acids (alanine, serine, and glutamate) indicates protein synthesis induced by the over activation of mTORC1). mTORC1 activation by amino acids controls insulin signalling, a key aspect of body metabolism, that, in pathophysiological process, can lead to metabolic diseases (150). Our results suggest that mTORC1 signalling pathway is over-activated in liver patients with NASH and promotes anabolism (306, 307). The activation of the mTORC1 pathway causes the downregulation of the AMPK pathway. The AKT/mTORC1 complex inhibits autophagy and promotes an imbalance of pAMPK/AMPK ratio. Our in vitro study, showed that mTORC1 signalling pathway is over activated in groups treated with DMKG, and this over activation is greater as the concentration of DMKG increases, suggesting that the presence of α-KG caused cell death in a dose-dependent manner. However, 12 months after BS our results suggest significative inactivation of Akt/mTORC1 axis. This inhibition, restores phosphorylation/activation of AMPK,

reduces the production of malonyl-CoA and FASN are reduced. These results indicate that NASH remission requires inhibition of mTORC1 to restore autophagy flux (308). This fact was due to an over activation of mTORC1 by glutaminolysis (141, 145). Overall, these results supported the idea that the capacity of glutaminolysis to sustain mTORC1 activation could be an important factor in the severity of NASH.

Manipulating metabolites that work as epigenetic modifiers offers novel therapeutic possibilities and the relevance of DNA methylation in NASH management is highlighted (309-312). Variations in methionine concentration lead to changes in the SAM/SAH ratio, which impact many methylation reactions including cytosine methylation to from 5-mC methylation. Hence, our analysis confirmed that energy and 1-C metabolism contribute to DNA methylation/demethylation. Metabolites involved in intracellular energy balance (α-KG, glutamine and β- hydroxybutyrate) can modulate the enzymatic function of DNA methylation. Hence, our analysis supports that there was a significant relationship between energy and one-carbon metabolism, and NASH progression. Significative correlations between SAH and citric acid cycle metabolism were also found in liver and plasma, suggesting an important interconnection with the metabolism and the regulation of global DNA methylation. These results allude that multiple mechanisms, including and energy and one-carbon metabolism, play an important role modulating DNA methylation, especially in patients with NASH.

.

Conclusions

UNIVERSITAT ROVIRA I VIRGILI
ASSESSING DIAGNOSTIC AND THERAPEUTIC TARGETS IN OBESITY-ASSOCIATED LIVER DISEASES
Noemí Cabré Casares

Conclusions

- ✓ Resolution of mitochondrial dysfunction promotes the beneficial effect of bariatric surgery in obesity-associates liver disease.
- ✓ Measurement of circulating metabolites from energy and one-carbon metabolism provides non-invasive and effective disease biomarkers for NASH diagnosis.
- ✓ Liver metabolome reveals the contribution of α-Ketoglutarate in mTORC1-driven metabolic perturbations.
- ✓ mTORC1 coordinates autophagy and apoptosis in NASH development through glutaminolysis preponderance.
- ✓ Metabolic-epigenetic effects distinguish patients with and without NASH and these effects may be restored by bariatric surgery.

UNIVERSITAT ROVIRA I VIRGILI
ASSESSING DIAGNOSTIC AND THERAPEUTIC TARGETS IN OBESITY-ASSOCIATED LIVER DISEASES
Noemí Cabré Casares

References

UNIVERSITAT ROVIRA I VIRGILI
ASSESSING DIAGNOSTIC AND THERAPEUTIC TARGETS IN OBESITY-ASSOCIATED LIVER DISEASES
Noemí Cabré Casares

1. Collaboration NCDRF. Trends in adult body-mass index in 200 countries from 1975 to 2014: a pooled analysis of 1698 population-based measurement studies with 19.2 million participants. Lancet. 2016;387(10026):1377-96.

2. Organization WH. Obesity and overweight. Fact sheet N°311 Updated 16 feb. 2018

3. Despres JP. Body fat distribution and risk of cardiovascular disease: an update. Circulation. 2012;126(10):1301-13.

4. Javed A, Jumean M, Murad MH, Okorodudu D, Kumar S, Somers VK, et al. Diagnostic performance of body mass index to identify obesity as defined by body adiposity in children and adolescents: a systematic review and meta-analysis. Pediatr Obes. 2015;10(3):234-44.

5. Corey KE, Kaplan LM. Obesity and liver disease: the epidemic of the twenty-first century. Clin Liver Dis. 2014;18(1):1-18.

6. Organization WH. Obesity and overweight. Fact sheet N°311 Updated June 2016.

7. Flegal KM, Carroll MD, Ogden CL, Curtin LR. Prevalence and trends in obesity among US adults, 1999-2008. JAMA. 2010;303(3):235-41.

8. Ogden CL, Carroll MD, Kit BK, Flegal KM. Prevalence of childhood and adult obesity in the United States, 2011-2012. JAMA. 2014;311(8):806-14.

9. Popkin BM. Global nutrition dynamics: the world is shifting rapidly toward a diet linked with noncommunicable diseases. Am J Clin Nutr. 2006;84(2):289-98.

10. Townshend T, Lake AA. Obesogenic urban form: theory, policy and practice. Health Place. 2009;15(4):909-16.

11. Martin AA, Davidson TL. Human cognitive function and the obesogenic environment. Physiol Behav. 2014;136:185-93.

12. van der Klaauw AA, Farooqi IS. The hunger genes: pathways to obesity. Cell. 2015;161(1):119-32.

13. Puhl R, Brownell KD. Bias, discrimination, and obesity. Obes Res. 2001;9(12):788-805.

14. Castro AV, Kolka CM, Kim SP, Bergman RN. Obesity, insulin resistance and comorbidities? Mechanisms of association. Arq Bras Endocrinol Metabol. 2014;58(6):600-9.

15. Gonzalez-Muniesa P, Martinez-Gonzalez MA, Hu FB, Despres JP, Matsuzawa Y, Loos RJF, et al. Obesity. Nat Rev Dis Primers. 2017;3:17034.

16. Font-Burgada J, Sun B, Karin M. Obesity and Cancer: The Oil that Feeds the Flame. Cell Metab. 2016;23(1):48-62.

17. Gallagher EJ, LeRoith D. Epidemiology and molecular mechanisms tying obesity, diabetes, and the metabolic syndrome with cancer. Diabetes Care. 2013;36 Suppl 2:S233-9.

18. Iacobini C, Pugliese G, Blasetti Fantauzzi C, Federici M, Menini S. Metabolically healthy versus metabolically unhealthy obesity. Metabolism. 2019;92:51-60.

19. Kahn SE, Hull RL, Utzschneider KM. Mechanisms linking obesity to insulin resistance and type 2 diabetes. Nature. 2006;444(7121):840-6.

20. Tron'ko ND, Zak KP. [Obesity and diabetes mellitus]. Lik Sprava. 2013(8):3-21.

21. Adler M, Schaffner F. Fatty liver hepatitis and cirrhosis in obese patients. Am J Med. 1979;67(5):811-6.

22. Woo Baidal JA, Lavine JE. The intersection of nonalcoholic fatty liver disease and obesity. Sci Transl Med. 2016;8(323):323rv1.

23. Rui L. Energy metabolism in the liver. Compr Physiol. 2014;4(1):177-97.

24. Erickson SK. Nonalcoholic fatty liver disease. J Lipid Res. 2009;50 Suppl:S412-6.

25. Brunt EM, Wong VW, Nobili V, Day CP, Sookoian S, Maher JJ, et al. Nonalcoholic fatty liver disease. Nat Rev Dis Primers. 2015;1:15080.

26. Smith BW, Adams LA. Nonalcoholic fatty liver disease and diabetes mellitus: pathogenesis and treatment. Nat Rev Endocrinol. 2011;7(8):456-65.

27. Loomba R, Sanyal AJ. The global NAFLD epidemic. Nat Rev Gastroenterol Hepatol. 2013;10(11):686-90.

28. Anstee QM, Targher G, Day CP. Progression of NAFLD to diabetes mellitus, cardiovascular disease or cirrhosis. Nat Rev Gastroenterol Hepatol. 2013;10(6):330-44.

29. Younossi ZM, Koenig AB, Abdelatif D, Fazel Y, Henry L, Wymer M. Global epidemiology of nonalcoholic fatty liver disease-Meta-analytic assessment of prevalence, incidence, and outcomes. Hepatology. 2016;64(1):73-84.

30. Younossi Z, Anstee QM, Marietti M, Hardy T, Henry L, Eslam M, et al. Global burden of NAFLD and NASH: trends, predictions, risk factors and prevention. Nat Rev Gastroenterol Hepatol. 2018;15(1):11-20.

31. Caballeria L, Pera G, Auladell MA, Toran P, Munoz L, Miranda D, et al. Prevalence and factors associated with the presence of nonalcoholic fatty liver disease in an adult population in Spain. Eur J Gastroenterol Hepatol. 2010;22(1):24-32.

32. Wong RJ, Aguilar M, Cheung R, Perumpail RB, Harrison SA, Younossi ZM, et al. Nonalcoholic steatohepatitis is the second leading etiology of liver disease among adults awaiting liver transplantation in the United States. Gastroenterology. 2015;148(3):547-55.

33. Sanyal AJ, Brunt EM, Kleiner DE, Kowdley KV, Chalasani N, Lavine JE, et al. Endpoints and clinical trial design for nonalcoholic steatohepatitis. Hepatology. 2011;54(1):344-53.

34. Cohen JC, Horton JD, Hobbs HH. Human fatty liver disease: old questions and new insights. Science. 2011;332(6037):1519-23.

35. Michelotti GA, Machado MV, Diehl AM. NAFLD, NASH and liver cancer. Nat Rev Gastroenterol Hepatol. 2013;10(11):656-65.

36. Nassir F, Ibdah JA. Role of mitochondria in nonalcoholic fatty liver disease. Int J Mol Sci. 2014;15(5):8713-42.

37. Kotronen A, Westerbacka J, Bergholm R, Pietilainen KH, Yki-Jarvinen H. Liver fat in the metabolic syndrome. J Clin Endocrinol Metab. 2007;92(9):3490-7.

38. Buzzetti E, Pinzani M, Tsochatzis EA. The multiple-hit pathogenesis of non-alcoholic fatty liver disease (NAFLD). Metabolism. 2016;65(8):1038-48.

39. Romeo S, Kozlitina J, Xing C, Pertsemlidis A, Cox D, Pennacchio LA, et al. Genetic variation in PNPLA3 confers susceptibility to nonalcoholic fatty liver disease. Nat Genet. 2008;40(12):1461-5.

40. Chalasani N, Guo X, Loomba R, Goodarzi MO, Haritunians T, Kwon S, et al. Genome-wide association study identifies variants associated with histologic features of nonalcoholic Fatty liver disease. Gastroenterology. 2010;139(5):1567-76, 76 e1-6.

41. Kozlitina J, Smagris E, Stender S, Nordestgaard BG, Zhou HH, Tybjaerg-Hansen A, et al. Exome-wide association study identifies a TM6SF2 variant that confers susceptibility to nonalcoholic fatty liver disease. Nat Genet. 2014;46(4):352-6.

42. DiStefano JK, Kingsley C, Craig Wood G, Chu X, Argyropoulos G, Still CD, et al. Genome-wide analysis of hepatic lipid content in extreme obesity. Acta Diabetol. 2015;52(2):373-82.

43. Valenti L, Al-Serri A, Daly AK, Galmozzi E, Rametta R, Dongiovanni P, et al. Homozygosity for the patatin-like phospholipase-3/adiponutrin I148M polymorphism influences liver fibrosis in patients with nonalcoholic fatty liver disease. Hepatology. 2010;51(4):1209-17.

44. Liu YL, Reeves HL, Burt AD, Tiniakos D, McPherson S, Leathart JB, et al. TM6SF2 rs58542926 influences hepatic fibrosis progression in patients with non-alcoholic fatty liver disease. Nat Commun. 2014;5:4309.

45. Zarrinpar A, Gupta S, Maurya MR, Subramaniam S, Loomba R. Serum microRNAs explain discordance of non-alcoholic fatty liver disease in monozygotic and dizygotic twins: a prospective study. Gut. 2016;65(9):1546-54.

46. Zeybel M, Hardy T, Wong YK, Mathers JC, Fox CR, Gackowska A, et al. Multigenerational epigenetic adaptation of the hepatic wound-healing response. Nat Med. 2012;18(9):1369-77.

47. Tilg H, Moschen AR, Roden M. NAFLD and diabetes mellitus. Nat Rev Gastroenterol Hepatol. 2017;14(1):32-42.

48. Samuel VT, Shulman GI. Nonalcoholic Fatty Liver Disease as a Nexus of Metabolic and Hepatic Diseases. Cell Metab. 2018;27(1):22-41.

49. Byrne CD, Targher G. NAFLD: a multisystem disease. J Hepatol. 2015;62(1 Suppl):S47-64.

50. Tan CY, Vidal-Puig A. Adipose tissue expandability: the metabolic problems of obesity may arise from the inability to become more obese. Biochem Soc Trans. 2008;36(Pt 5):935-40.

51. de Ferranti S, Mozaffarian D. The perfect storm: obesity, adipocyte dysfunction, and metabolic consequences. Clin Chem. 2008;54(6):945-55.

52. Tilg H, Moschen AR. Insulin resistance, inflammation, and non-alcoholic fatty liver disease. Trends Endocrinol Metab. 2008;19(10):371-9.

53. Jung UJ, Choi MS. Obesity and its metabolic complications: the role of adipokines and the relationship between obesity, inflammation, insulin resistance, dyslipidemia and nonalcoholic fatty liver disease. Int J Mol Sci. 2014;15(4):6184-223.

54. McArdle MA, Finucane OM, Connaughton RM, McMorrow AM, Roche HM. Mechanisms of obesity-induced inflammation and insulin resistance: insights into the emerging role of nutritional strategies. Front Endocrinol (Lausanne). 2013;4:52.

55. Fuchs CD, Claudel T, Trauner M. Role of metabolic lipases and lipolytic metabolites in the pathogenesis of NAFLD. Trends Endocrinol Metab. 2014;25(11):576-85.

56. Perry RJ, Samuel VT, Petersen KF, Shulman GI. The role of hepatic lipids in hepatic insulin resistance and type 2 diabetes. Nature. 2014;510(7503):84-91.

57. Samuel VT, Shulman GI. The pathogenesis of insulin resistance: integrating signaling pathways and substrate flux. J Clin Invest. 2016;126(1):12-22.

58. Friedman SL, Neuschwander-Tetri BA, Rinella M, Sanyal AJ. Mechanisms of NAFLD development and therapeutic strategies. Nat Med. 2018;24(7):908-22.

59. Anderson N, Borlak J. Molecular mechanisms and therapeutic targets in steatosis and steatohepatitis. Pharmacol Rev. 2008;60(3):311-57.

60. Lambert JE, Ramos-Roman MA, Browning JD, Parks EJ. Increased de novo lipogenesis is a distinct characteristic of individuals with nonalcoholic fatty liver disease. Gastroenterology. 2014;146(3):726-35.

61. Donnelly KL, Smith CI, Schwarzenberg SJ, Jessurun J, Boldt MD, Parks EJ. Sources of fatty acids stored in liver and secreted via lipoproteins in patients with nonalcoholic fatty liver disease. J Clin Invest. 2005;115(5):1343-51.

62. Browning JD, Horton JD. Molecular mediators of hepatic steatosis and liver injury. J Clin Invest. 2004;114(2):147-52.

63. Tamura S, Shimomura I. Contribution of adipose tissue and de novo lipogenesis to nonalcoholic fatty liver disease. J Clin Invest. 2005;115(5):1139-42.

64. Sumida Y, Niki E, Naito Y, Yoshikawa T. Involvement of free radicals and oxidative stress in NAFLD/NASH. Free Radic Res. 2013;47(11):869-80.

65. Cichoz-Lach H, Michalak A. Oxidative stress as a crucial factor in liver diseases. World J Gastroenterol. 2014;20(25):8082-91.

66. Manti S, Romano C, Chirico V, Filippelli M, Cuppari C, Loddo I, et al. Nonalcoholic Fatty liver disease/non-alcoholic steatohepatitis in childhood: endocrine-metabolic "mal-programming". Hepat Mon. 2014;14(5):e17641.

67. Fridovich I. The biology of oxygen radicals. Science. 1978;201(4359):875-80.

68. Weseler AR, Bast A. Oxidative stress and vascular function: implications for pharmacologic treatments. Curr Hypertens Rep. 2010;12(3):154-61.

69. Schieber M, Chandel NS. ROS function in redox signaling and oxidative stress. Curr Biol. 2014;24(10):R453-62.

70. Yu BP. Cellular defenses against damage from reactive oxygen species. Physiol Rev. 1994;74(1):139-62.

71. Balaban RS, Nemoto S, Finkel T. Mitochondria, oxidants, and aging. Cell. 2005;120(4):483-95.

72. Garcia-Ruiz C, Fernandez-Checa JC. Mitochondrial Oxidative Stress and Antioxidants Balance in Fatty Liver Disease. Hepatol Commun. 2018;2(12):1425-39.

73. Arauz J, Ramos-Tovar E, Muriel P. Redox state and methods to evaluate oxidative stress in liver damage: From bench to bedside. Ann Hepatol. 2016;15(2):160-73.

74. Margis R, Dunand C, Teixeira FK, Margis-Pinheiro M. Glutathione peroxidase family - an evolutionary overview. FEBS J. 2008;275(15):3959-70.

75. Camps J, Garcia-Heredia A, Hernandez-Aguilera A, Joven J. Paraoxonases, mitochondrial dysfunction and non-communicable diseases. Chem Biol Interact. 2016;259(Pt B):382-7.

76. Camps J, Rodriguez-Gallego E, Garcia-Heredia A, Triguero I, Riera-Borrull M, Hernandez-Aguilera A, et al. Paraoxonases and chemokine (C-C motif) ligand-2 in noncommunicable diseases. Adv Clin Chem. 2014;63:247-308.

77. Aubert J, Begriche K, Knockaert L, Robin MA, Fromenty B. Increased expression of cytochrome P450 2E1 in nonalcoholic fatty liver disease: mechanisms and pathophysiological role. Clin Res Hepatol Gastroenterol. 2011;35(10):630-7.

78. Jou J, Choi SS, Diehl AM. Mechanisms of disease progression in nonalcoholic fatty liver disease. Semin Liver Dis. 2008;28(4):370-9.

79. Videla LA, Rodrigo R, Araya J, Poniachik J. Insulin resistance and oxidative stress interdependency in non-alcoholic fatty liver disease. Trends Mol Med. 2006;12(12):555-8.

80. Wellen KE, Hotamisligil GS. Inflammation, stress, and diabetes. J Clin Invest. 2005;115(5):1111-9.

81. Camps J, Joven J. Chemokine ligand 2 and paraoxonase-1 in non-alcoholic fatty liver disease: The search for alternative causative factors. World J Gastroenterol. 2015;21(10):2875-82.

82. Cai J, Zhang XJ, Li H. Role of Innate Immune Signaling in Non-Alcoholic Fatty Liver Disease. Trends Endocrinol Metab. 2018;29(10):712-22.

83. Hui JM, Hodge A, Farrell GC, Kench JG, Kriketos A, George J. Beyond insulin resistance in NASH: TNF-alpha or adiponectin? Hepatology. 2004;40(1):46-54.

84. Reuter S, Gupta SC, Chaturvedi MM, Aggarwal BB. Oxidative stress, inflammation, and cancer: how are they linked? Free Radic Biol Med. 2010;49(11):1603-16.

85. Marra F, Bertolani C. Adipokines in liver diseases. Hepatology. 2009;50(3):957-69.

86. Gerner RR, Wieser V, Moschen AR, Tilg H. Metabolic inflammation: role of cytokines in the crosstalk between adipose tissue and liver. Can J Physiol Pharmacol. 2013;91(11):867-72.

87. Cha JY, Kim DH, Chun KH. The role of hepatic macrophages in nonalcoholic fatty liver disease and nonalcoholic steatohepatitis. Lab Anim Res. 2018;34(4):133-9.

88. Krenkel O, Tacke F. Liver macrophages in tissue homeostasis and disease. Nat Rev Immunol. 2017;17(5):306-21.

89. Freitas-Lopes MA, Mafra K, David BA, Carvalho-Gontijo R, Menezes GB. Differential Location and Distribution of Hepatic Immune Cells. Cells. 2017;6(4).

90. Dixon LJ, Barnes M, Tang H, Pritchard MT, Nagy LE. Kupffer cells in the liver. Compr Physiol. 2013;3(2):785-97.

91. Shaul ME, Bennett G, Strissel KJ, Greenberg AS, Obin MS. Dynamic, M2-like remodeling phenotypes of CD11c+ adipose tissue macrophages during high-fat diet--induced obesity in mice. Diabetes. 2010;59(5):1171-81.

92. Sica A, Mantovani A. Macrophage plasticity and polarization: in vivo veritas. J Clin Invest. 2012;122(3):787-95.

93. Wentworth JM, Naselli G, Brown WA, Doyle L, Phipson B, Smyth GK, et al. Pro-inflammatory CD11c+CD206+ adipose tissue macrophages are associated with insulin resistance in human obesity. Diabetes. 2010;59(7):1648-56.

94. Mantovani A, Sica A, Sozzani S, Allavena P, Vecchi A, Locati M. The chemokine system in diverse forms of macrophage activation and polarization. Trends Immunol. 2004;25(12):677-86.

95. Beljaars L, Schippers M, Reker-Smit C, Martinez FO, Helming L, Poelstra K, et al. Hepatic Localization of Macrophage Phenotypes during Fibrogenesis and Resolution of Fibrosis in Mice and Humans. Front Immunol. 2014;5:430.

96. Sica A, Invernizzi P, Mantovani A. Macrophage plasticity and polarization in liver homeostasis and pathology. Hepatology. 2014;59(5):2034-42.

97. Wan J, Benkdane M, Teixeira-Clerc F, Bonnafous S, Louvet A, Lafdil F, et al. M2 Kupffer cells promote M1 Kupffer cell apoptosis: a protective mechanism against alcoholic and nonalcoholic fatty liver disease. Hepatology. 2014;59(1):130-42.

98. Duarte N, Coelho IC, Patarrao RS, Almeida JI, Penha-Goncalves C, Macedo MP. How Inflammation Impinges on NAFLD: A Role for Kupffer Cells. Biomed Res Int. 2015;2015:984578.

99. Alisi A, Carpino G, Oliveira FL, Panera N, Nobili V, Gaudio E. The Role of Tissue Macrophage-Mediated Inflammation on NAFLD Pathogenesis and Its Clinical Implications. Mediators Inflamm. 2017;2017:8162421.

100. Pradere JP, Kluwe J, De Minicis S, Jiao JJ, Gwak GY, Dapito DH, et al. Hepatic macrophages but not dendritic cells contribute to liver fibrosis by promoting the survival of activated hepatic stellate cells in mice. Hepatology. 2013;58(4):1461-73.

101. Angulo P, Machado MV, Diehl AM. Fibrosis in nonalcoholic Fatty liver disease: mechanisms and clinical implications. Semin Liver Dis. 2015;35(2):132-45.

102. Ju C, Tacke F. Hepatic macrophages in homeostasis and liver diseases: from pathogenesis to novel therapeutic strategies. Cell Mol Immunol. 2016;13(3):316-27.

103. Schuster S, Cabrera D, Arrese M, Feldstein AE. Triggering and resolution of inflammation in NASH. Nat Rev Gastroenterol Hepatol. 2018;15(6):349-64.

104. O'Neill LA, Pearce EJ. Immunometabolism governs dendritic cell and macrophage function. J Exp Med. 2016;213(1):15-23.

105. Lunt SY, Vander Heiden MG. Aerobic glycolysis: meeting the metabolic requirements of cell proliferation. Annu Rev Cell Dev Biol. 2011;27:441-64.

106. Russell DG, Huang L, VanderVen BC. Immunometabolism at the interface between macrophages and pathogens. Nat Rev Immunol. 2019;19(5):291-304.

107. Mishra P, Chan DC. Metabolic regulation of mitochondrial dynamics. J Cell Biol. 2016;212(4):379-87.

108. Wang C, Youle RJ. The role of mitochondria in apoptosis*. Annu Rev Genet. 2009;43:95-118.

109. Chow J, Rahman J, Achermann JC, Dattani MT, Rahman S. Mitochondrial disease and endocrine dysfunction. Nat Rev Endocrinol. 2017;13(2):92-104.

110. Westermann B. Mitochondrial fusion and fission in cell life and death. Nat Rev Mol Cell Biol. 2010;11(12):872-84.

111. Berman SB, Pineda FJ, Hardwick JM. Mitochondrial fission and fusion dynamics: the long and short of it. Cell Death Differ. 2008;15(7):1147-52.

112. Chan DC. Fusion and fission: interlinked processes critical for mitochondrial health. Annu Rev Genet. 2012;46:265-87.

113. Chan DC. Mitochondria: dynamic organelles in disease, aging, and development. Cell. 2006;125(7):1241-52.

114. Labbe K, Murley A, Nunnari J. Determinants and functions of mitochondrial behavior. Annu Rev Cell Dev Biol. 2014;30:357-91.

115. Camps J R-GE, García-Heredia A, Triguero I, Riera-Borrull M, Hernández-Aguilera A, Luciano-Mateo F, Fernández-Arroyo S, Joven J. Paraoxonases and chemokine (C-C motif) ligand-2 in noncommunicable diseases. Adv Clin Chem 2014;63:247-308.

116. Bonora M, Patergnani S, Rimessi A, De Marchi E, Suski JM, Bononi A, et al. ATP synthesis and storage. Purinergic Signal. 2012;8(3):343-57.

117. Nsiah-Sefaa A, McKenzie M. Combined defects in oxidative phosphorylation and fatty acid beta-oxidation in mitochondrial disease. Biosci Rep. 2016;36(2).

118. Foroughi M, Maghsoudi Z, Khayyatzadeh S, Ghiasvand R, Askari G, Iraj B. Relationship between non-alcoholic fatty liver disease and inflammation in patients with non-alcoholic fatty liver. Adv Biomed Res. 2016;5:28.

119. Sunny NE, Bril F, Cusi K. Mitochondrial Adaptation in Nonalcoholic Fatty Liver Disease: Novel Mechanisms and Treatment Strategies. Trends Endocrinol Metab. 2017;28(4):250-60.

120. Fujii H, Kawada N. Inflammation and fibrogenesis in steatohepatitis. J Gastroenterol. 2012;47(3):215-25.

121. Perez-Carreras M, Del Hoyo P, Martin MA, Rubio JC, Martin A, Castellano G, et al. Defective hepatic mitochondrial respiratory chain in patients with nonalcoholic steatohepatitis. Hepatology. 2003;38(4):999-1007.

122. Rolo AP, Teodoro JS, Palmeira CM. Role of oxidative stress in the pathogenesis of nonalcoholic steatohepatitis. Free Radic Biol Med. 2012;52(1):59-69.

123. Hirota K, Fukamizu A. Transcriptional regulation of energy metabolism in the liver. J Recept Signal Transduct Res. 2010;30(6):403-9.

124. Soboll S. Regulation of energy metabolism in liver. J Bioenerg Biomembr. 1995;27(6):571-82.

125. Yuan HX, Xiong Y, Guan KL. Nutrient sensing, metabolism, and cell growth control. Mol Cell. 2013;49(3):379-87.

126. Herzig S, Shaw RJ. AMPK: guardian of metabolism and mitochondrial homeostasis. Nat Rev Mol Cell Biol. 2018;19(2):121-35.

127. Hardie DG, Schaffer BE, Brunet A. AMPK: An Energy-Sensing Pathway with Multiple Inputs and Outputs. Trends Cell Biol. 2016;26(3):190-201.

128. Combs TP, Marliss EB. Adiponectin signaling in the liver. Rev Endocr Metab Disord. 2014;15(2):137-47.

129. Ruderman NB, Carling D, Prentki M, Cacicedo JM. AMPK, insulin resistance, and the metabolic syndrome. J Clin Invest. 2013;123(7):2764-72.

130. Burkewitz K, Zhang Y, Mair WB. AMPK at the nexus of energetics and aging. Cell Metab. 2014;20(1):10-25.

131. Sinha-Hikim I, Sinha-Hikim AP, Shen R, Kim HJ, French SW, Vaziri ND, et al. A novel cystine based antioxidant attenuates oxidative stress and hepatic steatosis in diet-induced obese mice. Exp Mol Pathol. 2011;91(1):419-28.

132. Saxton RA, Sabatini DM. mTOR Signaling in Growth, Metabolism, and Disease. Cell. 2017;169(2):361-71.

133. Shimobayashi M, Hall MN. Making new contacts: the mTOR network in metabolism and signalling crosstalk. Nat Rev Mol Cell Biol. 2014;15(3):155-62.

134. Ma XM, Blenis J. Molecular mechanisms of mTOR-mediated translational control. Nat Rev Mol Cell Biol. 2009;10(5):307-18.

135. Cybulski N, Hall MN. TOR complex 2: a signaling pathway of its own. Trends Biochem Sci. 2009;34(12):620-7.

136. Lamming DW, Ye L, Katajisto P, Goncalves MD, Saitoh M, Stevens DM, et al. Rapamycin-induced insulin resistance is mediated by mTORC2 loss and uncoupled from longevity. Science. 2012;335(6076):1638-43.

137. Lamming DW, Sabatini DM. A Central role for mTOR in lipid homeostasis. Cell Metab. 2013;18(4):465-9.

138. Ricoult SJ, Manning BD. The multifaceted role of mTORC1 in the control of lipid metabolism. EMBO Rep. 2013;14(3):242-51.

139. Kenerson HL, Yeh MM, Yeung RS. Tuberous sclerosis complex-1 deficiency attenuates diet-induced hepatic lipid accumulation. PLoS One. 2011;6(3):e18075.

140. Peterson TR, Sengupta SS, Harris TE, Carmack AE, Kang SA, Balderas E, et al. mTOR complex 1 regulates lipin 1 localization to control the SREBP pathway. Cell. 2011;146(3):408-20.

141. Csibi A, Fendt SM, Li C, Poulogiannis G, Choo AY, Chapski DJ, et al. The mTORC1 pathway stimulates glutamine metabolism and cell proliferation by repressing SIRT4. Cell. 2013;153(4):840-54.

142. Blenis J. TOR, the Gateway to Cellular Metabolism, Cell Growth, and Disease. Cell. 2017;171(1):10-3.

143. Saxton RA, Sabatini DM. mTOR Signaling in Growth, Metabolism, and Disease. Cell. 2017;168(6):960-76.

144. Gonzalez A, Hall MN. Nutrient sensing and TOR signaling in yeast and mammals. EMBO J. 2017;36(4):397-408.

145. Duran RV, Hall MN. Regulation of TOR by small GTPases. EMBO Rep. 2012;13(2):121-8.

146. Sancak Y, Peterson TR, Shaul YD, Lindquist RA, Thoreen CC, Bar-Peled L, et al. The Rag GTPases bind raptor and mediate amino acid signaling to mTORC1. Science. 2008;320(5882):1496-501.

147. Sengupta S, Peterson TR, Sabatini DM. Regulation of the mTOR complex 1 pathway by nutrients, growth factors, and stress. Mol Cell. 2010;40(2):310-22.

148. Taylor PM. Role of amino acid transporters in amino acid sensing. Am J Clin Nutr. 2014;99(1):223S-30S.

149. Duran RV, Oppliger W, Robitaille AM, Heiserich L, Skendaj R, Gottlieb E, et al. Glutaminolysis activates Rag-mTORC1 signaling. Mol Cell. 2012;47(3):349-58.

150. Duran RV, MacKenzie ED, Boulahbel H, Frezza C, Heiserich L, Tardito S, et al. HIF-independent role of prolyl hydroxylases in the cellular response to amino acids. Oncogene. 2013;32(38):4549-56.

151. Altman BJ, Stine ZE, Dang CV. From Krebs to clinic: glutamine metabolism to cancer therapy. Nat Rev Cancer. 2016;16(11):749.

152. Mizushima N, Levine B, Cuervo AM, Klionsky DJ. Autophagy fights disease through cellular self-digestion. Nature. 2008;451(7182):1069-75.

153. Schneider JL, Cuervo AM. Liver autophagy: much more than just taking out the trash. Nat Rev Gastroenterol Hepatol. 2014;11(3):187-200.

154. Ueno T, Komatsu M. Autophagy in the liver: functions in health and disease. Nat Rev Gastroenterol Hepatol. 2017;14(3):170-84.

155. Kaushik S, Singh R, Cuervo AM. Autophagic pathways and metabolic stress. Diabetes Obes Metab. 2010;12 Suppl 2:4-14.

156. Klionsky DJ, Cregg JM, Dunn WA, Jr., Emr SD, Sakai Y, Sandoval IV, et al. A unified nomenclature for yeast autophagy-related genes. Dev Cell. 2003;5(4):539-45.

157. Zhang Y, Sowers JR, Ren J. Targeting autophagy in obesity: from pathophysiology to management. Nat Rev Endocrinol. 2018;14(6):356-76.

158. Levine B, Kroemer G. Biological Functions of Autophagy Genes: A Disease Perspective. Cell. 2019;176(1-2):11-42.

159. Kaur J, Debnath J. Autophagy at the crossroads of catabolism and anabolism. Nat Rev Mol Cell Biol. 2015;16(8):461-72.

160. Singh R, Cuervo AM. Autophagy in the cellular energetic balance. Cell Metab. 2011;13(5):495-504.

161. Czaja MJ. Function of Autophagy in Nonalcoholic Fatty Liver Disease. Dig Dis Sci. 2016;61(5):1304-13.

162. Kaushik S, Cuervo AM. The coming of age of chaperone-mediated autophagy. Nat Rev Mol Cell Biol. 2018;19(6):365-81.

163. Tasset I, Cuervo AM. Role of chaperone-mediated autophagy in metabolism. FEBS J. 2016;283(13):2403-13.

164. Tekirdag K, Cuervo AM. Chaperone-mediated autophagy and endosomal microautophagy: Joint by a chaperone. J Biol Chem. 2018;293(15):5414-24.

165. Rodriguez-Navarro JA, Kaushik S, Koga H, Dall'Armi C, Shui G, Wenk MR, et al. Inhibitory effect of dietary lipids on chaperone-mediated autophagy. Proc Natl Acad Sci U S A. 2012;109(12):E705-14.

166. Kaushik S, Cuervo AM. Chaperones in autophagy. Pharmacol Res. 2012;66(6):484-93.

167. Czaja MJ. Functions of autophagy in hepatic and pancreatic physiology and disease. Gastroenterology. 2011;140(7):1895-908.

168. Koga H, Kaushik S, Cuervo AM. Altered lipid content inhibits autophagic vesicular fusion. FASEB J. 2010;24(8):3052-65.

169. Yan S, Huda N, Khambu B, Yin XM. Relevance of autophagy to fatty liver diseases and potential therapeutic applications. Amino Acids. 2017;49(12):1965-79.

170. Liu K, Czaja MJ. Regulation of lipid stores and metabolism by lipophagy. Cell Death Differ. 2013;20(1):3-11.

171. Singh R, Cuervo AM. Lipophagy: connecting autophagy and lipid metabolism. Int J Cell Biol. 2012;2012:282041.

172. Schulze RJ, Sathyanarayan A, Mashek DG. Breaking fat: The regulation and mechanisms of lipophagy. Biochim Biophys Acta Mol Cell Biol Lipids. 2017;1862(10 Pt B):1178-87.

173. Zhou K, Yao P, He J, Zhao H. Lipophagy in nonliver tissues and some related diseases: Pathogenic and therapeutic implications. J Cell Physiol. 2019;234(6):7938-47.

174. Menendez JA, Joven J. One-carbon metabolism: an aging-cancer crossroad for the gerosuppressant metformin. Aging (Albany NY). 2012;4(12):894-8.

175. Ordovas JM, Smith CE. Epigenetics and cardiovascular disease. Nat Rev Cardiol. 2010;7(9):510-9.

176. Sales VM, Ferguson-Smith AC, Patti ME. Epigenetic Mechanisms of Transmission of Metabolic Disease across Generations. Cell Metab. 2017;25(3):559-71.

177. da Silva RP, Kelly KB, Al Rajabi A, Jacobs RL. Novel insights on interactions between folate and lipid metabolism. Biofactors. 2014;40(3):277-83.

178. Lu SC, Huang ZZ, Yang H, Mato JM, Avila MA, Tsukamoto H. Changes in methionine adenosyltransferase and S-adenosylmethionine homeostasis in alcoholic rat liver. Am J Physiol Gastrointest Liver Physiol. 2000;279(1):G178-85.

179. Locasale JW. Serine, glycine and one-carbon units: cancer metabolism in full circle. Nat Rev Cancer. 2013;13(8):572-83.

180. Mentch SJ, Locasale JW. One-carbon metabolism and epigenetics: understanding the specificity. Ann N Y Acad Sci. 2016;1363:91-8.

181. Ducker GS, Rabinowitz JD. One-Carbon Metabolism in Health and Disease. Cell Metab. 2017;25(1):27-42.

182. Zhang N. Role of methionine on epigenetic modification of DNA methylation and gene expression in animals. Anim Nutr. 2018;4(1):11-6.

183. Lu SC, Mato JM. S-adenosylmethionine in liver health, injury, and cancer. Physiol Rev. 2012;92(4):1515-42.

184. Hernandez-Aguilera A, Fernandez-Arroyo S, Cuyas E, Luciano-Mateo F, Cabre N, Camps J, et al. Epigenetics and nutrition-related epidemics of metabolic diseases: Current perspectives and challenges. Food Chem Toxicol. 2016;96:191-204.

185. Luciano-Mateo F, Hernandez-Aguilera A, Cabre N, Camps J, Fernandez-Arroyo S, Lopez-Miranda J, et al. Nutrients in Energy and One-Carbon Metabolism: Learning from Metformin Users. Nutrients. 2017;9(2).

186. Murphy SK, Yang H, Moylan CA, Pang H, Dellinger A, Abdelmalek MF, et al. Relationship between methylome and transcriptome in patients with nonalcoholic fatty liver disease. Gastroenterology. 2013;145(5):1076-87.

187. Lee J, Kim Y, Friso S, Choi SW. Epigenetics in non-alcoholic fatty liver disease. Mol Aspects Med. 2017;54:78-88.

188. Hardy T, Mann DA. Epigenetics in liver disease: from biology to therapeutics. Gut. 2016;65(11):1895-905.

189. Page A, Mann DA. Epigenetic regulation of liver fibrosis. Clin Res Hepatol Gastroenterol. 2015;39 Suppl 1:S64-8.

190. Arendt BM, Comelli EM, Ma DW, Lou W, Teterina A, Kim T, et al. Altered hepatic gene expression in nonalcoholic fatty liver disease is associated with lower hepatic n-3 and n-6 polyunsaturated fatty acids. Hepatology. 2015;61(5):1565-78.

191. Ahrens M, Ammerpohl O, von Schonfels W, Kolarova J, Bens S, Itzel T, et al. DNA methylation analysis in nonalcoholic fatty liver disease suggests distinct disease-specific and remodeling signatures after bariatric surgery. Cell Metab. 2013;18(2):296-302.

192. Gerhard GS, Malenica I, Llaci L, Chu X, Petrick AT, Still CD, et al. Differentially methylated loci in NAFLD cirrhosis are associated with key signaling pathways. Clin Epigenetics. 2018;10(1):93.

193. Huang Z, Cai L, Tu BP. Dietary control of chromatin. Curr Opin Cell Biol. 2015;34:69-74.

194. Katada S, Imhof A, Sassone-Corsi P. Connecting threads: epigenetics and metabolism. Cell. 2012;148(1-2):24-8.

195. Reid MA, Dai Z, Locasale JW. The impact of cellular metabolism on chromatin dynamics and epigenetics. Nat Cell Biol. 2017;19(11):1298-306.

196. Lu C, Thompson CB. Metabolic regulation of epigenetics. Cell Metab. 2012;16(1):9-17.

197. Lempradl A, Pospisilik JA, Penninger JM. Exploring the emerging complexity in transcriptional regulation of energy homeostasis. Nat Rev Genet. 2015;16(11):665-81.

198. Su X, Wellen KE, Rabinowitz JD. Metabolic control of methylation and acetylation. Curr Opin Chem Biol. 2016;30:52-60.

199. TeSlaa T, Chaikovsky AC, Lipchina I, Escobar SL, Hochedlinger K, Huang J, et al. alpha-Ketoglutarate Accelerates the Initial Differentiation of Primed Human Pluripotent Stem Cells. Cell Metab. 2016;24(3):485-93.

200. (EASO). EAftSotLEEAftSoDEEAftSoO. EASL-EASD-EASO Clinical Practice Guidelines for the management of non-alcoholic fatty liver disease. Journal of Hepatoly. 2016;64(6):1388-402.

201. Wong VW, Adams LA, de Ledinghen V, Wong GL, Sookoian S. Noninvasive biomarkers in NAFLD and NASH - current progress and future promise. Nat Rev Gastroenterol Hepatol. 2018;15(8):461-78.

202. Browning JD. Statins and hepatic steatosis: perspectives from the Dallas Heart Study. Hepatology. 2006;44(2):466-71.

203. Bugianesi E, Manzini P, D'Antico S, Vanni E, Longo F, Leone N, et al. Relative contribution of iron burden, HFE mutations, and insulin resistance to fibrosis in nonalcoholic fatty liver. Hepatology. 2004;39(1):179-87.

204. Chalasani N, Younossi Z, Lavine JE, Charlton M, Cusi K, Rinella M, et al. The diagnosis and management of nonalcoholic fatty liver disease: Practice guidance from the American Association for the Study of Liver Diseases. Hepatology. 2018;67(1):328-57.

205. Cengiz M, Senturk S, Cetin B, Bayrak AH, Bilek SU. Sonographic assessment of fatty liver: intraobserver and interobserver variability. Int J Clin Exp Med. 2014;7(12):5453-60.

206. Reeder SB, Hu HH, Sirlin CB. Proton density fat-fraction: a standardized MR-based biomarker of tissue fat concentration. J Magn Reson Imaging. 2012;36(5):1011-4.

207. Calvo N, Beltran-Debon R, Rodriguez-Gallego E, Hernandez-Aguilera A, Guirro M, Marine-Casado R, et al. Liver fat deposition and mitochondrial dysfunction in morbid obesity: An approach combining metabolomics with liver imaging and histology. World J Gastroenterol. 2015;21(24):7529-44.

208. Sahebkar A, Sancho E, Abello D, Camps J, Joven J. Novel circulating biomarkers for non-alcoholic fatty liver disease: A systematic review. J Cell Physiol. 2018;233(2):849-55.

209. Rhee EP, Gerszten RE. Metabolomics and cardiovascular biomarker discovery. Clin Chem. 2012;58(1):139-47.

210. Kalhan SC, Guo L, Edmison J, Dasarathy S, McCullough AJ, Hanson RW, et al. Plasma metabolomic profile in nonalcoholic fatty liver disease. Metabolism. 2011;60(3):404-13.

211. Griffiths WJ, Koal T, Wang Y, Kohl M, Enot DP, Deigner HP. Targeted metabolomics for biomarker discovery. Angew Chem Int Ed Engl. 2010;49(32):5426-45.

212. Cox DG, Oh J, Keasling A, Colson KL, Hamann MT. The utility of metabolomics in natural product and biomarker characterization. Biochim Biophys Acta. 2014;1840(12):3460-74.

213. Thoma C, Day CP, Trenell MI. Lifestyle interventions for the treatment of non-alcoholic fatty liver disease in adults: a systematic review. J Hepatol. 2012;56(1):255-66.

214. Sanyal AJ, Chalasani N, Kowdley KV, McCullough A, Diehl AM, Bass NM, et al. Pioglitazone, vitamin E, or placebo for nonalcoholic steatohepatitis. N Engl J Med. 2010;362(18):1675-85.

215. Alkhouri N, Carter-Kent C, Feldstein AE. Apoptosis in nonalcoholic fatty liver disease: diagnostic and therapeutic implications. Expert Rev Gastroenterol Hepatol. 2011;5(2):201-12.

216. Barreyro FJ, Holod S, Finocchietto PV, Camino AM, Aquino JB, Avagnina A, et al. The pan-caspase inhibitor Emricasan (IDN-6556) decreases liver injury and fibrosis in a murine model of non-alcoholic steatohepatitis. Liver Int. 2015;35(3):953-66.

217. Mazza A, Fruci B, Garinis GA, Giuliano S, Malaguarnera R, Belfiore A. The role of metformin in the management of NAFLD. Exp Diabetes Res. 2012;2012:716404.

218. Phielix E, Szendroedi J, Roden M. The role of metformin and thiazolidinediones in the regulation of hepatic glucose metabolism and its clinical impact. Trends Pharmacol Sci. 2011;32(10):607-16.

219. Marchesini G, Brizi M, Bianchi G, Tomassetti S, Zoli M, Melchionda N. Metformin in non-alcoholic steatohepatitis. Lancet. 2001;358(9285):893-4.

220. Nair S, Diehl AM, Wiseman M, Farr GH, Jr., Perrillo RP. Metformin in the treatment of non-alcoholic steatohepatitis: a pilot open label trial. Aliment Pharmacol Ther. 2004;20(1):23-8.

221. Uygun A, Kadayifci A, Isik AT, Ozgurtas T, Deveci S, Tuzun A, et al. Metformin in the treatment of patients with non-alcoholic steatohepatitis. Aliment Pharmacol Ther. 2004;19(5):537-44.

222. Jinnouchi H, Sugiyama S, Yoshida A, Hieshima K, Kurinami N, Suzuki T, et al. Liraglutide, a glucagon-like peptide-1 analog, increased insulin sensitivity assessed by hyperinsulinemic-euglycemic clamp examination in patients with uncontrolled type 2 diabetes mellitus. J Diabetes Res. 2015;2015:706416.

223. Barb D, Portillo-Sanchez P, Cusi K. Pharmacological management of nonalcoholic fatty liver disease. Metabolism. 2016;65(8):1183-95.

224. Krenkel O, Puengel T, Govaere O, Abdallah AT, Mossanen JC, Kohlhepp M, et al. Therapeutic inhibition of inflammatory monocyte recruitment reduces steatohepatitis and liver fibrosis. Hepatology. 2018;67(4):1270-83.

225. Friedman S, Sanyal A, Goodman Z, Lefebvre E, Gottwald M, Fischer L, et al. Efficacy and safety study of cenicriviroc for the treatment of non-alcoholic steatohepatitis in adult subjects with liver fibrosis: CENTAUR Phase 2b study design. Contemp Clin Trials. 2016;47:356-65.

226. Friedman SL, Ratziu V, Harrison SA, Abdelmalek MF, Aithal GP, Caballeria J, et al. A randomized, placebo-controlled trial of cenicriviroc for treatment of nonalcoholic steatohepatitis with fibrosis. Hepatology. 2018;67(5):1754-67.

227. Singh S, Osna NA, Kharbanda KK. Treatment options for alcoholic and non-alcoholic fatty liver disease: A review. World J Gastroenterol. 2017;23(36):6549-70.

228. Federico A, Dallio M, Loguercio C. Silymarin/Silybin and Chronic Liver Disease: A Marriage of Many Years. Molecules. 2017;22(2).

229. Solhi H, Ghahremani R, Kazemifar AM, Hoseini Yazdi Z. Silymarin in treatment of non-alcoholic steatohepatitis: A randomized clinical trial. Caspian J Intern Med. 2014;5(1):9-12.

230. Loguercio C, Andreone P, Brisc C, Brisc MC, Bugianesi E, Chiaramonte M, et al. Silybin combined with phosphatidylcholine and vitamin E in patients with nonalcoholic fatty liver disease: a randomized controlled trial. Free Radic Biol Med. 2012;52(9):1658-65.

231. Hahl T, Peromaa-Haavisto P, Tarkiainen P, Knutar O, Victorzon M. [Fast track bariatric surgery]. Duodecim. 2016;132(1):63-70.

232. Elder KA, Wolfe BM. Bariatric surgery: a review of procedures and outcomes. Gastroenterology. 2007;132(6):2253-71.

233. Angrisani L, Santonicola A, Iovino P, Formisano G, Buchwald H, Scopinaro N. Bariatric Surgery Worldwide 2013. Obes Surg. 2015;25(10):1822-32.

234. Bachler T, le Roux CW, Bueter M. How do patients' clinical phenotype and the physiological mechanisms of the operations impact the choice of bariatric procedure? Clin Exp Gastroenterol. 2016;9:181-9.

235. Manco M, Mosca A, De Peppo F, Caccamo R, Cutrera R, Giordano U, et al. The Benefit of Sleeve Gastrectomy in Obese Adolescents on Nonalcoholic Steatohepatitis and Hepatic Fibrosis. J Pediatr. 2017;180:31-7 e2.

236. Aldoheyan T, Hassanain M, Al-Mulhim A, Al-Sabhan A, Al-Amro S, Bamehriz F, et al. The effects of bariatric surgeries on nonalcoholic fatty liver disease. Surg Endosc. 2017;31(3):1142-7.

237. Lassailly G, Caiazzo R, Buob D, Pigeyre M, Verkindt H, Labreuche J, et al. Bariatric Surgery Reduces Features of Nonalcoholic Steatohepatitis in Morbidly Obese Patients. Gastroenterology. 2015;149(2):379-88; quiz e15-6.

238. de Freitas AC, Campos AC, Coelho JC. The impact of bariatric surgery on nonalcoholic fatty liver disease. Curr Opin Clin Nutr Metab Care. 2008;11(3):267-74.

239. Taitano AA, Markow M, Finan JE, Wheeler DE, Gonzalvo JP, Murr MM. Bariatric surgery improves histological features of nonalcoholic fatty liver disease and liver fibrosis. J Gastrointest Surg. 2015;19(3):429-36; discussion 36-7.

240. Kleiner DE, Brunt EM, Van Natta M, Behling C, Contos MJ, Cummings OW, et al. Design and validation of a histological scoring system for nonalcoholic fatty liver disease. Hepatology. 2005;41(6):1313-21.

241. Aranda N, Viteri FE, Montserrat C, Arija V. Effects of C282Y, H63D, and S65C HFE gene mutations, diet, and life-style factors on iron status in a general Mediterranean population from Tarragona, Spain. Ann Hematol. 2010;89(8):767-73.

242. Camps J, Marsillach J, Joven J. The paraoxonases: role in human diseases and methodological difficulties in measurement. Crit Rev Clin Lab Sci. 2009;46(2):83-106.

243. Hernandez-Aguilera A, Sepulveda J, Rodriguez-Gallego E, Guirro M, Garcia-Heredia A, Cabre N, et al. Immunohistochemical analysis of paraoxonases and chemokines in arteries of patients with peripheral artery disease. Int J Mol Sci. 2015;16(5):11323-38.

244. Andersen MN, Etzerodt A, Graversen JH, Holthof LC, Moestrup SK, Hokland M, et al. STAT3 inhibition specifically in human monocytes and macrophages by CD163-targeted corosolic acid-containing liposomes. Cancer Immunol Immunother. 2019;68(3):489-502.

245. Salminen P, Helmio M, Ovaska J, Juuti A, Leivonen M, Peromaa-Haavisto P, et al. Effect of Laparoscopic Sleeve Gastrectomy vs Laparoscopic Roux-en-Y Gastric Bypass on Weight Loss at 5 Years Among Patients With Morbid Obesity: The SLEEVEPASS Randomized Clinical Trial. JAMA. 2018;319(3):241-54.

246. Brunt EM. Nonalcoholic fatty liver disease and the ongoing role of liver biopsy evaluation. Hepatol Commun. 2017;1(5):370-8.

247. Bertran N, Camps J, Fernandez-Ballart J, Arija V, Ferre N, Tous M, et al. Diet and lifestyle are associated with serum C-reactive protein concentrations in a population-based study. J Lab Clin Med. 2005;145(1):41-6.

248. Matthews DR, Hosker JP, Rudenski AS, Naylor BA, Treacher DF, Turner RC. Homeostasis model assessment: insulin resistance and beta-cell function from fasting plasma glucose and insulin concentrations in man. Diabetologia. 1985;28(7):412-9.

249. Chalasani N, Younossi Z, Lavine JE, Diehl AM, Brunt EM, Cusi K, et al. The diagnosis and management of non-alcoholic fatty liver disease: practice Guideline by the American Association for the Study of Liver Diseases, American College of Gastroenterology, and the American Gastroenterological Association. Hepatology. 2012;55(6):2005-23.

250. Rockey DC, Caldwell SH, Goodman ZD, Nelson RC, Smith AD, American Association for the Study of Liver D. Liver biopsy. Hepatology. 2009;49(3):1017-44.

251. Brunt EM, Kleiner DE, Wilson LA, Belt P, Neuschwander-Tetri BA, Network NCR. Nonalcoholic fatty liver disease (NAFLD) activity score and the histopathologic diagnosis in NAFLD: distinct clinicopathologic meanings. Hepatology. 2011;53(3):810-20.

252. Riera-Borrull M, Rodriguez-Gallego E, Hernandez-Aguilera A, Luciano F, Ras R, Cuyas E, et al. Exploring the Process of Energy Generation in Pathophysiology by Targeted Metabolomics: Performance of a Simple and Quantitative Method. J Am Soc Mass Spectrom. 2016;27(1):168-77.

253. Cuyas E, Fernandez-Arroyo S, Verdura S, Garcia RA, Stursa J, Werner L, et al. Metformin regulates global DNA methylation via mitochondrial one-carbon metabolism. Oncogene. 2018;37(7):963-70.

254. Fernandez-Arroyo S, Cuyas E, Bosch-Barrera J, Alarcon T, Joven J, Menendez JA. Activation of the methylation cycle in cells reprogrammed into a stem cell-like state. Oncoscience. 2015;2(12):958-67.

255. Rossella F, Polledri E, Bollati V, Baccarelli A, Fustinoni S. Development and validation of a gas chromatography/mass spectrometry method for the assessment of genomic DNA methylation. Rapid Commun Mass Spectrom. 2009;23(17):2637-46.

256. Chong J, Soufan O, Li C, Caraus I, Li S, Bourque G, et al. MetaboAnalyst 4.0: towards more transparent and integrative metabolomics analysis. Nucleic Acids Res. 2018;46(W1):W486-W94.

257. Storey JD, Tibshirani R. Statistical significance for genomewide studies. Proc Natl Acad Sci U S A. 2003;100(16):9440-5.

258. Dietrich S, Floegel A, Troll M, Kuhn T, Rathmann W, Peters A, et al. Random Survival Forest in practice: a method for modelling complex metabolomics data in time to event analysis. Int J Epidemiol. 2016;45(5):1406-20.

259. Xia J, Wishart DS. Using MetaboAnalyst 3.0 for Comprehensive Metabolomics Data Analysis. Curr Protoc Bioinformatics. 2016;55:14 0 1- 0 91.

260. Ciangura C, Nocca D, Lindecker V. [Guidelines for clinical practice for bariatric surgery]. Presse Med. 2010;39(9):953-9.

261. Friedewald WT, Levy RI, Fredrickson DS. Estimation of the concentration of low-density lipoprotein cholesterol in plasma, without use of the preparative ultracentrifuge. Clin Chem. 1972;18(6):499-502.

262. Bedossa P, Poitou C, Veyrie N, Bouillot JL, Basdevant A, Paradis V, et al. Histopathological algorithm and scoring system for evaluation of liver lesions in morbidly obese patients. Hepatology. 2012;56(5):1751-9.

263. Rodriguez-Gallego E, Guirro M, Riera-Borrull M, Hernandez-Aguilera A, Marine-Casado R, Fernandez-Arroyo S, et al. Mapping of the circulating metabolome reveals alpha-ketoglutarate as a predictor of morbid obesity-associated non-alcoholic fatty liver disease. Int J Obes (Lond). 2015;39(2):279-87.

264. Folch J, Lees M, Sloane Stanley GH. A simple method for the isolation and purification of total lipides from animal tissues. J Biol Chem. 1957;226(1):497-509.

265. Aryee MJ, Jaffe AE, Corrada-Bravo H, Ladd-Acosta C, Feinberg AP, Hansen KD, et al. Minfi: a flexible and comprehensive Bioconductor package for the analysis of Infinium DNA methylation microarrays. Bioinformatics. 2014;30(10):1363-9.

266. Fortin JP, Triche TJ, Jr., Hansen KD. Preprocessing, normalization and integration of the Illumina HumanMethylationEPIC array with minfi. Bioinformatics. 2017;33(4):558-60.

267. KD H. IlluminaHumanMethylationEPICmanifest: Manifest for Illumina's EPIC methylation arrays. R package version 0.3.0, 2016
http://bioconductor.org/packages/release/data/annotation/html/IlluminaHumanMethylationEPICmanifest.html.

268. KD H. IlluminaHumanMethylationEPICanno.ilm10b2.hg19: Annotation for Illumina's EPIC methylation arrays. R package version 0.6.0, 2016 http://bioconductor.org/packages/release/data/annotation/html/IlluminaHumanMethylationEPICanno.ilm10b2.hg19.html 2016.

269. Pidsley R, Zotenko E, Peters TJ, Lawrence MG, Risbridger GP, Molloy P, et al. Critical evaluation of the Illumina MethylationEPIC BeadChip microarray for whole-genome DNA methylation profiling. Genome Biol. 2016;17(1):208.

270. Akalin A, Franke V, Vlahovicek K, Mason CE, Schubeler D. Genomation: a toolkit to summarize, annotate and visualize genomic intervals. Bioinformatics. 2015;31(7):1127-9.

271. Karolchik D, Hinrichs AS, Furey TS, Roskin KM, Sugnet CW, Haussler D, et al. The UCSC Table Browser data retrieval tool. Nucleic Acids Res. 2004;32(Database issue):D493-6.

272. Carlson M MB. TxDb.Hsapiens.UCSC.hg19.knownGene: Annotation package for TxDb object(s). R package version 3.2.2. 2015.

273. Gu Z, Gu L, Eils R, Schlesner M, Brors B. circlize Implements and enhances circular visualization in R. Bioinformatics. 2014;30(19):2811-2.

274. Rosa-Garrido M, Chapski DJ, Schmitt AD, Kimball TH, Karbassi E, Monte E, et al. High-Resolution Mapping of Chromatin Conformation in Cardiac Myocytes Reveals Structural Remodeling of the Epigenome in Heart Failure. Circulation. 2017;136(17):1613-25.

275. Kelley DE, Goodpaster B, Wing RR, Simoneau JA. Skeletal muscle fatty acid metabolism in association with insulin resistance, obesity, and weight loss. Am J Physiol. 1999;277(6):E1130-41.

276. DeWaal D, Nogueira V, Terry AR, Patra KC, Jeon SM, Guzman G, et al. Hexokinase-2 depletion inhibits glycolysis and induces oxidative phosphorylation in hepatocellular carcinoma and sensitizes to metformin. Nat Commun. 2018;9(1):446.

277. Dietrich P, Hellerbrand C. Non-alcoholic fatty liver disease, obesity and the metabolic syndrome. Best Pract Res Clin Gastroenterol. 2014;28(4):637-53.

278. Fabbrini E, Sullivan S, Klein S. Obesity and nonalcoholic fatty liver disease: biochemical, metabolic, and clinical implications. Hepatology. 2010;51(2):679-89.

279. Panagiotou OA, Markozannes G, Adam GP, Kowalski R, Gazula A, Di M, et al. Comparative Effectiveness and Safety of Bariatric Procedures in Medicare-Eligible Patients: A Systematic Review. JAMA Surg. 2018;153(11):e183326.

280. de Abreu MR, Ramos AP, Vendramini RC, Brunetti IL, Pepato MT. Steatosis and hepatic markers before and shortly after bariatric surgery. Ann Clin Biochem. 2007;44(Pt 1):63-9.

281. Martin WP, Docherty NG, Le Roux CW. Impact of bariatric surgery on cardiovascular and renal complications of diabetes: a focus on clinical outcomes and putative mechanisms. Expert Rev Endocrinol Metab. 2018;13(5):251-62.

282. Rubino F, Nathan DM, Eckel RH, Schauer PR, Alberti KG, Zimmet PZ, et al. Metabolic Surgery in the Treatment Algorithm for Type 2 Diabetes: a Joint Statement by International Diabetes Organizations. Obes Surg. 2017;27(1):2-21.

283. Riera-Borrull M, Garcia-Heredia A, Fernandez-Arroyo S, Hernandez-Aguilera A, Cabre N, Cuyas E, et al. Metformin Potentiates the Benefits of Dietary Restraint: A Metabolomic Study. Int J Mol Sci. 2017;18(11).

284. Collaboration NCDRF. Worldwide trends in body-mass index, underweight, overweight, and obesity from 1975 to 2016: a pooled analysis of 2416 population-based measurement studies in 128.9 million children, adolescents, and adults. Lancet. 2017;390(10113):2627-42.

285. Patterson RE, Kalavalapalli S, Williams CM, Nautiyal M, Mathew JT, Martinez J, et al. Lipotoxicity in steatohepatitis occurs despite an increase in tricarboxylic acid cycle activity. Am J Physiol Endocrinol Metab. 2016;310(7):E484-94.

286. Schuppan D, Surabattula R, Wang XY. Determinants of fibrosis progression and regression in NASH. J Hepatol. 2018;68(2):238-50.

287. Rull A, Geeraert B, Aragones G, Beltran-Debon R, Rodriguez-Gallego E, Garcia-Heredia A, et al. Rosiglitazone and fenofibrate exacerbate liver steatosis in a mouse model of obesity and hyperlipidemia. A transcriptomic and metabolomic study. J Proteome Res. 2014;13(3):1731-43.

288. Rull A, Vinaixa M, Angel Rodriguez M, Beltran R, Brezmes J, Canellas N, et al. Metabolic phenotyping of genetically modified mice: An NMR metabonomic approach. Biochimie. 2009;91(8):1053-7.

289. Beltran-Debon R, Alonso-Villaverde C, Aragones G, Rodriguez-Medina I, Rull A, Micol V, et al. The aqueous extract of Hibiscus sabdariffa calices modulates the production of monocyte chemoattractant protein-1 in humans. Phytomedicine. 2010;17(3-4):186-91.

290. Joven J, Micol V, Segura-Carretero A, Alonso-Villaverde C, Menendez JA, Bioactive Food Components P. Polyphenols and the modulation of gene expression pathways: can we eat our way out of the danger of chronic disease? Crit Rev Food Sci Nutr. 2014;54(8):985-1001.

291. Rubinstein N, Ilarregui JM, Toscano MA, Rabinovich GA. The role of galectins in the initiation, amplification and resolution of the inflammatory response. Tissue Antigens. 2004;64(1):1-12.

292. Henderson NC, Mackinnon AC, Farnworth SL, Poirier F, Russo FP, Iredale JP, et al. Galectin-3 regulates myofibroblast activation and hepatic fibrosis. Proc Natl Acad Sci U S A. 2006;103(13):5060-5.

293. Verdelho Machado M, Diehl AM. The hedgehog pathway in nonalcoholic fatty liver disease. Crit Rev Biochem Mol Biol. 2018;53(3):264-78.

294. Machado MV, Diehl AM. Hedgehog signalling in liver pathophysiology. J Hepatol. 2018;68(3):550-62.

295. Bangru S, Arif W, Seimetz J, Bhate A, Chen J, Rashan EH, et al. Alternative splicing rewires Hippo signaling pathway in hepatocytes to promote liver regeneration. Nat Struct Mol Biol. 2018;25(10):928-39.

296. Herranz-Lopez M, Fernandez-Arroyo S, Perez-Sanchez A, Barrajon-Catalan E, Beltran-Debon R, Menendez JA, et al. Synergism of plant-derived polyphenols in adipogenesis: perspectives and implications. Phytomedicine. 2012;19(3-4):253-61.

297. Zhong S, Fan Y, Yan Q, Fan X, Wu B, Han Y, et al. The therapeutic effect of silymarin in the treatment of nonalcoholic fatty disease: A meta-analysis (PRISMA) of randomized control trials. Medicine (Baltimore). 2017;96(49):e9061.

298. Tang JT, Mao YM. Pharmacotherapy of nonalcoholic steatohepatitis: Reflections on the existing evidence. J Dig Dis. 2017;18(11):607-17.

299. Koliaki C, Szendroedi J, Kaul K, Jelenik T, Nowotny P, Jankowiak F, et al. Adaptation of hepatic mitochondrial function in humans with non-alcoholic fatty liver is lost in steatohepatitis. Cell Metab. 2015;21(5):739-46.

300. Sunny NE, Parks EJ, Browning JD, Burgess SC. Excessive hepatic mitochondrial TCA cycle and gluconeogenesis in humans with nonalcoholic fatty liver disease. Cell Metab. 2011;14(6):804-10.

301. Petersen KF, Befroy DE, Dufour S, Rothman DL, Shulman GI. Assessment of Hepatic Mitochondrial Oxidation and Pyruvate Cycling in NAFLD by (13)C Magnetic Resonance Spectroscopy. Cell Metab. 2016;24(1):167-71.

302. Gancheva S, Jelenik T, Alvarez-Hernandez E, Roden M. Interorgan Metabolic Crosstalk in Human Insulin Resistance. Physiol Rev. 2018;98(3):1371-415.

303. Wu SC, Zhang Y. Active DNA demethylation: many roads lead to Rome. Nat Rev Mol Cell Biol. 2010;11(9):607-20.

304. Fedeles BI, Singh V, Delaney JC, Li D, Essigmann JM. The AlkB Family of Fe(II)/alpha-Ketoglutarate-dependent Dioxygenases: Repairing Nucleic Acid Alkylation Damage and Beyond. J Biol Chem. 2015;290(34):20734-42.

305. Fendt SM, Bell EL, Keibler MA, Olenchock BA, Mayers JR, Wasylenko TM, et al. Reductive glutamine metabolism is a function of the alpha-ketoglutarate to citrate ratio in cells. Nat Commun. 2013;4:2236.

306. Laplante M, Sabatini DM. mTOR signaling at a glance. J Cell Sci. 2009;122(Pt 20):3589-94.

307. Laplante M, Sabatini DM. Regulation of mTORC1 and its impact on gene expression at a glance. J Cell Sci. 2013;126(Pt 8):1713-9.

308. Puri P, Chandra A. Autophagy modulation as a potential therapeutic target for liver diseases. J Clin Exp Hepatol. 2014;4(1):51-9.

309. Nano J, Ghanbari M, Wang W, de Vries PS, Dhana K, Muka T, et al. Epigenome-Wide Association Study Identifies Methylation Sites Associated With Liver Enzymes and Hepatic Steatosis. Gastroenterology. 2017;153(4):1096-106 e2.

310. Hardy T, Zeybel M, Day CP, Dipper C, Masson S, McPherson S, et al. Plasma DNA methylation: a potential biomarker for stratification of liver fibrosis in non-alcoholic fatty liver disease. Gut. 2017;66(7):1321-8.

311. Wu J, Zhang R, Shen F, Yang R, Zhou D, Cao H, et al. Altered DNA Methylation Sites in Peripheral Blood Leukocytes from Patients with Simple Steatosis and Nonalcoholic Steatohepatitis (NASH). Med Sci Monit. 2018;24:6946-67.

312. Ferrari A, Longo R, Silva R, Mitro N, Caruso D, De Fabiani E, et al. Epigenome modifiers and metabolic rewiring: New frontiers in therapeutics. Pharmacol Ther. 2019;193:178-93.

Annex

UNIVERSITAT ROVIRA I VIRGILI
ASSESSING DIAGNOSTIC AND THERAPEUTIC TARGETS IN OBESITY-ASSOCIATED LIVER DISEASES
Noemí Cabré Casares

Elsevier Editorial System(tm) for Metabolism
Manuscript Draft

Manuscript Number:

Title: Bariatric surgery reverses non-alcoholic fatty liver disease in morbid obesity and while reducing oxidative stress and inflammation

Article Type: Original Research Article

Corresponding Author: Dr. Jordi Camps, PhD

Corresponding Author's Institution: Hospital Universitari de Sant Joan

First Author: Noemí Cabré

Order of Authors: Noemí Cabré; Fedra Luciano-Mateo; Salvador Fernández-Arroyo; Gerard Baiges-Gayà; Anna Hernández-Aguilera; Montserrat Fibla; Raul Fernández-Julià; Marta París; Fàtima Sabench; Daniel Del Castillo; Javier A Menéndez; Jordi Camps, PhD; Jorge Joven

Suggested Reviewers: Thomas M Vondriska
David Geffen School of Medicine, University of California, Los Angeles,, University of California in Los Angeles
tvondriska@mednet.ucla.edu
Dr. Vondriska is an expert in metabolism, including proteomics, epigenetics, and the relatioships between metabolic alterations and obesity and cardiovascular disease.

Alejandro Gugliucci
Laboratory of Oxidation and Glycation, Touro University-California
alejandro.gugliucci@tu.edu
Dr. Gugliucci is an expert in oxidative stress and its relationship with inflammation, and antioxidant defence systems, in diabetes, obesity and cardiovascular diseases.

Tiziana Bacchetti
Dipartimento di Scienze della Vita e dell'Ambiente, Università Politecnica delle Marche, Italy
tizianaba@gmail.com
Dr. Bacchetti is an expert in oxidative stress and its relationship with inflammation, and antioxidant defence systems, in diabetes, obesity and cancer.

Opposed Reviewers:

Hospital Universitari Sant Joan
REUS

Dr. Christos S. Mantzoros, MD, DSc, PhD h.c.
Editor-in-Chief
METABOLISM

Reus, April 16, 2019

Dear Dr. Mantzoros,

Please find enclosed our manuscript entitled *"Bariatric surgery reverses non-alcoholic fatty liver disease in morbid obesity and while reducing oxidative stress and inflammation"* to be considered for publication in METABOLISM.

Our study shows that the histology and liver function of patients with morbid obesity are significantly improved after bariatric surgery via mechanisms that involve the reduction of oxidative stress and inflammatory processes.

The present manuscript has not been published previously, and will not be sent to another journal until an editorial decision has been taken by METABOLISM.

All contributing authors have seen and approved this final version of the manuscript submitted for publication.

We look forward to your opinion as to whether our manuscript reaches a suitable standard for inclusion in your Journal.

Yours sincerely,

Dr. Jordi Camps
Unitat de Recerca Biomèdica
Hospital Universitari de Sant Joan
43201 Reus, Catalonia, Spain.

Highlights

- NAFLD was frequent and heterogeneous in patients with severe obesity
- Bariatric surgery was associated with remission of NAFLD and NASH
- Oxidative stress and inflammation markers improved following bariatric surgery
- Oxidation and inflammation are key elements in NAFLD progression and remission

Type of article: Original Research Article

Bariatric surgery reverses non-alcoholic fatty liver disease in morbid obesity and while reducing oxidative stress and inflammation

Noemí Cabré[1,2], Fedra Luciano-Mateo[1,2], Salvador Fernández-Arroyo[1,2], Gerard Baiges-Gayà[2], Anna Hernández-Aguilera[1,2], Montserrat Fibla[2], Raul Fernández-Julià[3], Marta París[4], Fàtima Sabench[1,4], Daniel Del Castillo[1,4], Javier A. Menéndez[5,6] Jordi Camps[1,2,*], Jorge Joven[1,2,7]

[1]*Department of Medicine and Surgery, Universitat Rovira i Virgili, Reus, Spain*

[2]*Unitat de Recerca Biomèdica, Hospital Universitari Sant Joan, Institut d'Investigació Sanitària Pere Virgili, Universitat Rovira i Virgili, Reus, Spain*

[3]*Àrea Bàsica de Salut La Selva del Camp, Tarragona*

[4]*Department of Surgery, Hospital Universitari Sant Joan, Institut d'Investigació Sanitària Pere Virgili, Universitat Rovira i Virgili, Reus, Spain*

[5]*Program Against Cancer Therapeutic Resistance (ProCURE), Metabolism and Cancer Group, Catalan Institute of Oncology, Girona, Spain*

[6]*Girona Biomedical Research Institute (IDIBGI), Girona, Spain*

[7]*The Southern Catalonia Campus of International Excellence, Tarragona, Spain*

***Corresponding author at:** Unitat de Recerca Biomèdica, Hospital Universitari de Sant Joan, C. Sant Joan s/n, 43201-Reus, Spain.

E-mail address: jcamps@grupsagessa.com (J. Camps)

Short title

Bariatric surgery and hepatic oxidation and inflammation

ABSTRACT

Background & Aims: Hepatic alterations, such as in non-alcoholic fatty liver disease (NAFLD) and non-alcoholic steatohepatitis (NASH) are frequently associated with obesity. To investigate the molecular mechanisms of these alterations and to identify molecules that could be used as potential therapeutic targets, we investigated the modulation of hepatic indices of oxidative stress and inflammation in obese patients undergoing bariatric surgery (BS).

Methods: Patients (n=436) attending our obesity clinic underwent BS for weight loss. We obtained a diagnostic intraoperative liver biopsy, and a sub-cohort (n=120) agreed to a 1-year follow-up that included donation of blood samples and additional liver biopsies. Selected key molecules in blood and liver tissue were used to investigate the hepatic alterations in obesity, and their response to BS.

Results: One year post-surgery, the prevalence of diabetes, dyslipidemia and hypertension decreased significantly. BS improved liver histology features in all patients. Improvement was greater in severe cases of NAFLD including those with steatohepatitis, bridging fibrosis or cirrhosis. Significant pre-surgery differences in plasma, and liver markers of oxidative stress and inflammation (including chemokine C-C motif ligand 2, paraoxonase-1, galectin-3, and sonic hedgehog) were observed between patients with, and those without, NASH; post-surgery indicated consistent improvements in these parameters.

Conclusion: Our study shows that the histology and liver function of patients with morbid obesity are significantly improved after BS via mechanisms that involve the reduction of oxidative stress and inflammatory processes. These data encourage the use of BS as a therapeutic option to improve, or resolve, NAFLD.

Keywords: Cytokines; fibrosis; galectin-3; metabolic surgery; oxidation

Abbreviations: BMI, body mass index; CD, cluster of differentiation; CCL2, chemokine (C-C motif) ligand 2; CCR2, C-C chemokine receptor type 2; DAB, 3,3'-diaminobenzidine; FAA, fumarylacetoacetase; HOMA-IR, homeostasis model assessment-insulin resistance; HDL, high-density lipoproteins; IL-10, interleukin-10; NAFLD, non-alcoholic fatty liver disease; NAS, non-alcoholic fatty liver activity score; NASH, non-alcoholic steatohepatitis; PON1, paraoxonase-1; pSTAT3, phospho signal transducer and activator of transcription 3; Shh, sonic hedgehog; α-SMA, α-smooth muscle actin; STAT3, signal transducer and activator of transcription 3; T2DM, type 2 diabetes mellitus; TBBL, 5-thiobutyl butyrolactone; TNF-α, tumor necrosis factor-α.

1. Introduction

Risks of hepatic disease and metabolic abnormalities increase with higher body mass index (BMI) [1]. In the liver, accumulation of fat causes multiple alterations, such as non-alcoholic fatty liver disease (NAFLD) and non-alcoholic steatohepatitis (NASH) which, if untreated or undetected, may subsequently result in life-threatening diseases such as cirrhosis or hepatocellular carcinoma [2]. Management of liver impairment associated with severe obesity presents unique challenges. Intensive changes in lifestyle remain the primary treatment options but which, over the long term, are frequently unsuccessful. Bariatric surgery (BS) appears to be a safe and efficient procedure to reduce weight, but data are sparse regarding its effectiveness in treating the hepatic alterations [1].

Oxidative stress and inflammation are related to the onset and development of liver diseases [3]. Excessive nutrient intake impairs the redox status in the liver which stimulates inflammation [3]. The molecular mechanisms accounting for these alterations involve modifications of enzyme activity, post-translational modifications of proteins, and activation of nuclear receptors; the consequence is a global modification of metabolic networks [4]. Several biomarkers of oxidative stress and inflammation have been associated with liver diseases. Paraoxonase-1 (PON1) is a lipolactonase and esterase with antioxidant activity present in the hepatocytes, as well as bound to high-density lipoproteins (HDL) in the circulation [5]. Serum PON1 activity is decreased in liver diseases and in several other non-communicable diseases in which there is an increase in free radical production [6]. Oxidative stress and decreased PON1 activity result in an increase in the production of pro-inflammatory cytokines such as chemokine (C-C motif) ligand 2 (CCL2) and tumor necrosis factor-α (TNF-α) [6]. In patients with liver impairment, the circulating levels of these cytokines correlate with the severity of the hepatic inflammation [7,8], while the pharmacological inhibition of CCL2 results in improved liver function [9]. In addition, oxidative stress and inflammation increase the synthesis of galectin-3, and activate the sonic hedgehog (Shh) pathway, both of which stimulate fibrogenesis [10,11]. The inflammatory processes are counteracted by anti-inflammatory cytokines such as interleukin-10 (IL-10), Conversely, some studies have found increase in liver disease during attempts to attenuate hepatic injury [12].

The aim of the present study was to investigate molecular mechanisms underlying hepatic alterations in patients with morbid obesity. Analyses included changes in the circulating levels and hepatic expression of markers of oxidative stress and inflammation pre- and post-BS.

2. Materials and Methods

2.1. Study design and participants

This was a prospective, 12 month follow-up, longitudinal study including 436 patients with severe obesity who underwent laparoscopic sleeve gastrectomy at the *Hospital Universitari de Sant Joan de Reus*. Patients provided 12-hours fasting blood samples immediately before surgery together with an intraoperative wedge-liver biopsy. Written informed consent was obtained according to the procedures approved by our Institutional Review Board (OBESPAD/14-07-31proj3 project) and the ethical guidelines of the 1975 Declaration of Helsinki. Exclusion criteria were age <25 years, alcohol abuse, infectious diseases, primary sclerosing cholangitis, autoimmune diseases, and cancer. One hundred and twenty patients agreed to have a second blood extraction and a liver biopsy at 12 months post-surgery, and signed fully informed consent (OM-NAFLD, ESO3/18012013 project). Biopsies were performed by ultrasound-guided, percutaneous needle puncture. Patients were classified according to the non-alcoholic fatty liver score (NAS) system. The scales included the unweighted sum of steatosis (0-3), lobular inflammation (0-3) and ballooning (0-2) scores. Values assigned were ≤ 2 for non-NASH, >2 and ≤4 for uncertain NASH, and ≥5 for definite NASH. Information for fibrosis included the absence of fibrosis (F0), mild to moderate fibrosis (F1 and F2), bridging fibrosis (F3) and cirrhosis (F4) [13]. Liver biopsies were assessed by a single experienced pathologist who was blinded with respect to the provenance of the samples.

For comparisons, we used sera of healthy non-obese controls (n=404) in which NAFLD diagnosis was discarded using imaging procedures (INFLAMET/15-04/4proj7 project). These subjects were participants in a population-based study conducted in our geographical area. They had no clinical or analytical evidence of renal insufficiency, hepatic damage, or neoplasia. The samples (stored at –80ºC) were obtained from the

Biological Samples Bank of our Institution. A detailed description of this population has been published [14].

2.2. Measurement of circulating levels of selected biochemical parameters

Serum and EDTA-plasma samples were collected after centrifugation and stored at −80ºC for batched analyses. Serum PON1 concentrations were determined using an in-house ELISA with antibodies specific of PON1 [5]. Serum PON1 lactonase and esterase activities were determined using synthetic substrates. Lactonase activity was measured as the hydrolysis of 5-thiobutyl butyrolactone (TBBL), and paraoxonase (esterase) activity was determined as the rate of hydrolysis of paraoxon [5]. Plasma concentrations of CCL2, IL-10, TNF-α and galectin-3 were measured by ELISA (PeproTech, London, UK; and R&D Systems, Minneapolis, MN, USA). Serum alanine aminotransferase (ALT) and aspartate aminotransferase (AST) activities, and cholesterol, HDL-cholesterol, LDL-cholesterol, triglycerides, glucose, C-reactive protein (CRP), and insulin concentrations were analyzed using standard tests in a Roche Modular Analytics P800 system (Roche Diagnostics, Basel, Switzerland).

2.3. Immunohistochemical analyses in hepatic biopsies

Procedures were performed essentially as previously reported [15]. To assess differences in oxidation and inflammation, we analyzed the hepatic immunohistochemical expression of 4-hydroxy-2-nonenal (a marker of lipid peroxidation), cluster of differentiation 68 (CD68, a marker of macrophages), PON1, CCL2, C-C chemokine receptor type 2 (CCR2), IL-10, TNF-α, and galectin-3. The appropriate primary and secondary antibodies and other reagents are described in Supplementary Table S1. Positive staining was quantified using the Image J software (National Institutes of Health, Bethesda, MD, USA).

2.4. Western blotting of liver tissue

Protein lysates (50 µg) from frozen liver tissues were subjected to 8%−14% sodium dodecyl sulfate polyacrylamide gel electrophoresis. The resolved proteins were transferred to polyvinylidene difluoride membranes (Thermo Fisher, Barcelona, Spain) using bovine serum albumin at 5% in Tris-buffered saline, 0.1% Tween-20 (pH = 7.4) as

blocking agent. Membranes were incubated with the corresponding primary and secondary antibodies for PON1, galectin-3, TNF-α, IL-10, CD163 (a marker of anti-inflammatory macrophages) [16], signal transducer and activator of transcription 3 (STAT-3) and its phosphorylated form (pSTAT-3), which regulate multiple metabolic processes [16], α-smooth muscle actin (α-SMA), and sonic hedgehog (Shh); these last two proteins being associated with liver fibrosis. Technical details and reagents are reported in Supplementary Table S1. Fumarylacetoacetate hydrolase (FAH) was used as a reference (control) protein. Protein bands were visualized using SuperSignal West Femto chemiluminescent substrate (Pierce, Rockford, IL, USA) and analyzed with a ChemiDoc system using Image Lab 2.0 software (Bio-Rad Laboratories, Hercules, CA, USA).

2.5. Statistical analyses

Kolmogorov-Smirnov test was used to assess the distribution characteristics of variables. Student's *t*-test (parametric) or Mann-Whitney *U*- test (non-parametric) were used to assess differences between any two groups of variables. Analyses were performed with the SPSS 22.0 package (IBM Corp., Armonk, NY, USA). Statistical significance was set at $p \leq 0.05$.

3. Results

3.1. Metabolic outcomes and remission of hepatic alterations post-BS

Pre-BS, patients with severe obesity had decreased insulin sensitivity, increased chronic low-grade inflammation, higher prevalence of type 2 diabetes mellitus (T2DM), dyslipemia and hypertension, compared to the healthy population. We observed a high ratio of women to men in the obese cohort. Data presented here are without sex segregation because of the longitudinal nature of the study and, as well, because logistic regression analyses discarded sex as a determinant factor in diagnosis and/or disease outcomes. According to the NAS score, non-NASH, uncertain NASH and definite NASH were recorded in 43.8%, 34.6% and 21.6% of patients, respectively (Table 1).

One year post-BS, most clinical and biological metabolic outcomes significantly improved, together with a general amelioration of histological features of NAFLD; improvement was more evident in the most severe cases. Mild steatosis was observed in 4 patients (3%), mild lobular inflammation (<2 foci) in 22 patients (18.4%) and hepatocyte ballooning in 21 patients (17.5%). Fibrosis also improved, especially in the few patients with bridging fibrosis (Table 2 and Fig. 1). Of note, one patient with pre-surgery liver cirrhosis presented only periportal/perisinusoidal fibrosis one year post-surgery (Supplementary Fig. 1).

3.2. Oxidation and inflammation and their association with NASH

We found a significantly higher proportion of PON1, 4-hydroxy-2-nonenal and CD68 stained cells in liver biopsies of patients with NASH (n=94), compared to non-NASH patients (n=191). Sirius-red-positive areas were also significantly higher (Fig. 2A). CD68 stained cells were more frequent in areas with inflammation and PON1 staining was stronger in hepatocytes with ballooning degeneration. Fat accumulation and 4-hydroxy-2-nonenal staining were more intense in fibrous areas (Supplementary Fig. 2).

We observed significant alterations in the pre-surgery circulating levels of molecules that tracked with oxidation and inflammation. Serum paraoxonase and lactonase activities were significantly decreased in obese patients, but serum PON-1 concentration remained unaltered. Low PON-1 activities were associated with high plasma CCL2, but these measurements did not track with patients through the different stages of NAFLD (Fig. 2B). Circulating levels of TNF-α and IL-10 were also significantly different from those found in control subjects, but differences between non-NASH and NASH patients were either minor or negligible. Plasma galectin-3 levels were significantly higher in patients with NASH when compared with non-NASH patients (Fig. 2B).

3.3. BS outcomes promote remission of hepatic alterations through multiple cellular responses

Using selected key markers we compared oxidation, inflammation and fibrosis in liver tissues at baseline and 12 months post-BS. There were significant reductions in the hepatic immunochemical expressions of PON-1, 4-hydroxy-2-nonenal, CD68, CCL2,

CCR2, TNF-α, and galectin-3; but IL-10 staining remained unaltered (Fig. 3). For cross validation we used western blot analysis. We observed a significant reduction in the expression of TNF-α and galectin-3, with minor changes in IL-10. Variations in the expression of CD163 did not reach statistical significance. We also assessed the effect of BS in relation to the hepatic expression of STAT-3 and phosphorylated STAT-3. Both had 4-fold increase in expression post-surgery, which would indicate increased production and activation following NAFLD remission. The extent of hepatic glycated PON-1 (the 45 kD band), which is less effective in providing protection against oxidative response, was not significantly reduced. However, the unmodified, more active enzyme (the 40 kD band) that had been practically absent pre-surgery, was prominent post-surgery. Finally, we observed a significant decrease in the expression of α-smooth muscle actin (α-SMA) and sonic hedgehog (Shh) protein, indicating regression of liver fibrosis-activating pathways (Fig. 4).

Significant variations were observed in circulating paraoxonase activity and galectin-3 levels post-surgery. Circulating PON-1 and CCL2 concentrations remained high in patients with biopsy-proven NAFLD remission. Mean plasma TNF-α concentrations were normalized, and circulating IL-10 levels were even higher following remission (Supplementary Fig. 3).

4. Discussion

BS is a safe and effective procedure for weight loss in persons with severe obesity refractory to lifestyle modifications [17]. However, the clinical take-up of this procedure remains low even in patients meeting all criteria for eligibility. Here we provide evidence that all comorbidities, including NAFLD, significantly improved within one year post-surgery, following weight loss and metabolic improvement. Our findings of the impact of BS on NAFLD regression are consistent with previous studies [1].

Indices of oxidation, inflammation and fibrosis were clearly altered in patients with NASH compared to those without NASH. Moreover, oxidation, inflammation and fibrosis in the liver substantially improved post-surgery. The measurement of molecules that have been shown to be good indicators of these phenomena confirmed the improvement. In particular, we had previously observed the close relationship between PON1 and CCL2 in the regulation of hepatic oxidative stress and inflammation

[18,19]. In mice, *pon1* gene deficiency promotes fatty liver disease and *ccl2* gene deficiency abrogates it [18]. In humans, polyphenols attenuate liver damage by modulating gene expression pathways that regulate the roles of PON1 and CCL2 in oxidative stress and the inflammatory response [20]. Both processes are important in macrophage polarization, with potential impact on promoting the resolution of liver disease [21]. Increasingly, galectin-3 has been recognized as a modulator of oxidative stress, inflammation, fibrosis and angiogenesis [22]. The decrease in liver galectin-3 expression and the simultaneous decrease in the liver expression of α-SMA post-surgery appears to modify the hedgehog-signaling pathway; indicating that transition from the quiescent stellate cells to myofibroblastic stellate cells may be reversible [23]. In the current study we observed that BS resulted in a significant increase in hepatic STAT-3, a cytoplasmic protein that, when phosphorylated, induces transcription of genes promoting cellular protective and proliferative effects [24].

Limitations of this study are inherent in the design; in particular, the lack of randomized control subjects, a relatively short-term follow-up, and enrolment of referral patients at a single hospital. Further, criteria for entry into the study were strict and carefully characterized; aspects that are not feasible in routine clinical practice. As such, surveillance bias cannot be ruled out. Future research should investigate long-term outcomes post-surgery. However, the sparse data available indicate a clear association with sustained weight loss, reduced comorbidities, and higher effectiveness compared to intensive lifestyle interventions [25]. Moreover, our study was restricted to a limited set of biomarkers associated with oxidative stress and inflammation. We do not rule out the possibility that other factors such as changes in lipogenesis, endoplasmic reticulum stress, insulin resistance or fibrogenesis could be related to the remission of hepatic alterations [26,27].

Our results suggest a sequential involvement of multiple cellular responses, and support the concept of applying a combination of different therapies to achieve non-invasive regulation of several molecular networks. Assaying a single, expensive and potentially toxic new compound does not seem a desirable strategy, considering the multi-factorial nature of NAFLD development. Positive modulation of liver function requires considerable weight loss and profound changes in lifestyle. Some well-tried and safe drugs may help improve insulin sensitivity but are fairly ineffective without

dietary restraint [28]. Our histology evidence confirmed that reducing oxidative stress and suppressing activation of liver inflammatory cells are valuable therapeutic targets. Dietary antioxidants, insulin sensitizers, and lipid-lowering agents can, when used in combination, boost intracellular protection against lipoperoxides, suppress key inflammatory signaling systems, and induce reparative stress signaling [29,30]; all of which warrant further randomized controlled trials with a multi-targeting approach to determine dosage, duration of treatment, and modes of action when used in combinations.

In conclusion, our study suggests that BS improves the histology and liver function of patients with morbid obesity. The mechanism involves the reduction of oxidative stress and inflammatory processes. These data encourage the use of BS as a therapeutic option to improve, or resolve, obesity-associated liver disease.

Acknowledgements

This study was supported by grant PI15/00285 from the *Instituto de Salud Carlos III* (Madrid, Spain), co-funded by the *Fondo Europeo de Desarrollo Regional* (FEDER), and by grant 60/U/2016 from the *Fundació La Marató de TV3* (Barcelona, Spain).

Conflict of Interest

No potential conflicts of interest declared.

Author Contribution

Study concept and design: Noemí Cabré, Jordi Camps, Jorge Joven. Acquisition of data: Noemí Cabré, Fedra Luciano-Mateo, Salvador Fernández-Arroyo, Gerard Baiges-Gayà, Anna Hernández-Aguilera, Montserrat Fibla, Raül Fernandez-Julià, Marta París, Fàtima Sabench, Daniel del Castillo, Javier A. Menéndez. Analysis and interpretation of data: Noemí Cabré, Fedra Luciano-Mateo, Javier A. Menéndez, Jordi Camps, Jorge Joven. Drafting the manuscript: Noemí Cabré, Jordi Camps. Critical revision of the manuscript: Javier A. Menéndez, Jordi Camps, Jorge Joven. Funding acquisition: Jordi Camps, Jorge Joven. Study supervision: Jordi Camps, Jorge Joven

References

[1] Fakhry TK, Mhaskar R, Schwitalla T, Muradova E, Gonzalvo JP, Murr MM. Bariatric surgery improves nonalcoholic fatty liver disease: a contemporary systematic review and meta-analysis. Surg Obes Relat Dis 2018; pii: S1550-7289(18)30403–9. doi:10.1016/j.soard.2018.12.002. [Epub ahead of print].

[2] Friedman SL, Neuschwander-Tetri BA, Rinella M, Sanyal AJ. Mechanisms of NAFLD development and therapeutic strategies. Nat Med 2018;24:908–922.

[3] Mansouri A, Gattolliat CH, Asselah T. Mitochondrial dysfunction and signaling in chronic liver diseases. Gastroenterology 2018;155:629–647.

[4] Masarone M, Rosato V, Dallio M, Gravina AG, Aglitti A, Loguercio C, et al. Role of oxidative stress in pathophysiology of nonalcoholic fatty liver disease. Oxid Med Cell Longev 2018;2018:9547613.

[5] Camps J, Marsillach J, Joven J. The paraoxonases: role in human diseases and methodological difficulties in measurement. Crit Rev Clin Lab Sci 2009;46:83–106.

[6] Camps J, Rodríguez-Gallego E, García-Heredia A, Triguero I, Riera-Borrull M, Hernández-Aguilera A, et al. Paraoxonases and chemokine (C-C motif) ligand-2 in noncommunicable diseases. Adv Clin Chem 2014;63:247–308.

[7] Camps J, Hernandez-Aguilera A, Garcia-Heredia A, Cabre N, Luciano-Mateo F, Arenas M, et al. Relationships between metformin, paraoxonase-1 and the chemokine (C-C Motif) ligand 2. Curr Clin Pharmacol 2016;11:250–258.

[8] Marsillach J, Bertran N, Camps J, Ferré N, Riu F, Tous M, et al. The role of circulating monocyte chemoattractant protein-1 as a marker of hepatic inflammation in patients with chronic liver disease. Clin Biochem 2005;38:1138–1140.

[9] Lopetuso LR, Mocci G, Marzo M, D'Aversa F, Rapaccini GL, Guidi L, et al. Harmful effects and potential benefits of anti-tumor necrosis factor (TNF)-α on the liver. Int J Mol Sci 2018;19:pii: E2199. doi: 10.3390/ijms19082199.

[10] Li LC, Li J, Gao J. Functions of galectin-3 and its role in fibrotic diseases. J Pharmacol Exp Ther 2014;351:336–343.

[11] Castellone MD, Laukkanen MO. TGF-beta1, WNT, and SHH signaling in tumor progression and in fibrotic diseases. Front Biosci (Schol Ed) 2017;9:31–45.

[12] Kawaratani H, Tsujimoto T, Douhara A, Takaya H, Moriya K, Namisaki T, et al. The effect of inflammatory cytokines in alcoholic liver disease. Mediators Inflamm 2013;2013:495156.

[13] Kleiner DE, Brunt EM, Van Natta M, Behling C, Contos MJ, Cummings OW, et al. Design and validation of a histological scoring system for nonalcoholic fatty liver disease. Hepatology 2005;41:1313–1321.

[14] Aranda N, Viteri FE, Montserrat C, Arija V. Effects of C282Y, H63D, and S65C HFE gene mutations, diet, and life-style factors on iron status in a general Mediterranean population from Tarragona, Spain. Ann Hematol 2010;89:767–1773.

[15] Hernández-Aguilera A, Sepúlveda J, Rodríguez-Gallego E, Guirro M, García-Heredia A, Cabré N, et al. Immunohistochemical analysis of paraoxonases and chemokines in arteries of patients with peripheral artery disease. Int J Mol Sci 2015;16:11323–11338.

[16] Andersen MN, Etzerodt A, Graversen JH, Holthof LC, Moestrup SK, Hokland M, et al. STAT3 inhibition specifically in human monocytes and macrophages by CD163-targeted corosolic acid-containing liposomes. Cancer Immunol Immunother 2019. doi: 10.1007/s00262-019-02301-3. [Epub ahead of print].

[17] Surve A, Cottam D, Zaveri H, Cottam A, Belnap L, Richards C, et al. Does the future of laparoscopic sleeve gastrectomy lie in the outpatient surgery center? A retrospective study of the safety of 3162 outpatient sleeve gastrectomies. Surg Obes Relat Dis 2018; doi: 10.1016/j.soard.2018.05.027 [Epub ahead of print].

[18] García-Heredia A, Kensicki E, Mohney RP, Rull A, Triguero I, Marsillach J, et al. Paraoxonase-1 deficiency is associated with severe liver steatosis in mice fed a high-fat high-cholesterol diet: a metabolomic approach. J Proteome Res 2013;12:1946–1955.

[19] Rull A, Geeraert B, Aragonès G, Beltrán-Debón R, Rodríguez-Gallego E, García-Heredia A, et al. Rosiglitazone and fenofibrate exacerbate liver steatosis in a mouse model of obesity and hyperlipidemia. A transcriptomic and metabolomic study. J Proteome Res 2014;13:1731–1743.

[20] Beltrán-Debón R, Alonso-Villaverde C, Aragonès G, Rodríguez-Medina I, Rull A, Micol V, et al. The aqueous extract of Hibiscus sabdariffa calices modulates the production of monocyte chemoattractant protein-1 in humans. Phytomedicine 2010;17:186–191.

[21] Alisi A, Carpino G, Oliveira FL, Panera N, Nobili V, Gaudio E. The role of tissue macrophage-mediated inflammation on NAFLD pathogenesis and its clinical implications. Mediators Inflamm 2017;2017:8162421.

[22] Henderson NC, Mackinnon AC, Farnworth SL, Poirier F, Russo FP, Iredale JP, et al. Galectin-3 regulates myofibroblast activation and hepatic fibrosis. Proc Natl Acad Sci USA 2006;103:5060–5065.

[23] Verdelho Machado M, Diehl AM. The hedgehog pathway in nonalcoholic fatty liver disease. Crit Rev Biochem Mol Biol 2018;53:264–278.

[24] Wang H, Lafdil F, Kong X, Gao B. Signal transducer and activator of transcription 3 in liver diseases: a novel therapeutic target. Int J Biol Sci 2011;7:536–550.

[25] Gregor MF, Yang L, Fabbrini E, Mohammed BS, Eagon JC, Hotamisligil GS, et al. Endoplasmic reticulum stress is reduced in tissues of obese subjects after weight loss. Diabetes. 2009;58:693–700.

[26] Latorre J, Moreno-Navarrete JM, Mercader JM, Sabater M, Rovira Ò, Gironès J, et al. Decreased lipid metabolism but increased FA biosynthesis are coupled with changes in liver microRNAs in obese subjects with NAFLD. Int J Obes (Lond) 2017;41:620–630.

[27] Kunešová M, Sedláčková B, Bradnová O, Tvrzická E, Staňková B, Šrámková P, et al. Fatty acid composition of adipose tissue triglycerides in obese diabetic women after bariatric surgery: a 2-year follow up. Physiol Res 2015;64 (Suppl 2):S155–S166.

[28] Riera-Borrull M, García-Heredia A, Fernández-Arroyo S, Hernández-Aguilera A, Cabré N, Cuyàs E, et al. Metformin potentiates the benefits of dietary restraint: A metabolomic study. Int J Mol Sci 2017;18.pii: E2263.

[29] Herranz-López M, Fernández-Arroyo S, Pérez-Sanchez A, Barrajón-Catalán E, Beltrán-Debón R, Menéndez JA, et al. Synergism of plant-derived polyphenols in adipogenesis: perspectives and implications. Phytomedicine 2012;19:253–261.

[30] Zhong S, Fan Y, Yan Q, Fan X, Wu B, Han Y, et al. The therapeutic effect of silymarin in the treatment of nonalcoholic fatty disease: A meta-analysis (PRISMA) of randomized control trials. Medicine (Baltimore) 2017;96:e9061.

Figure legends

Fig. 1. Post-laparoscopic sleeve gastrectomy (LSG) improvement in liver histological features of patients with non-alcoholic fatty liver disease.

(A) Representative microphotographs (bars indicate 100x magnification) of baseline and 12 months post-surgery hepatic biopsies stained with Hematoxylin and Eosin, Sirius Red and Masson's Trichrome. (B) Steatosis, inflammation ballooning and NAS score were quantified according to the non-alcoholic fatty liver activity score (NAS) system. (C) Sirius Red was quantified as percentage of positively-stained areas. $*p <$ 0.001 by the Mann-Whitney *U* test.

Fig. 2. Hepatic oxidation and inflammation discriminate patients with NASH from those without.

(A) NASH patients had higher hepatic paraoxonase-1 (PON1), 4-hydroxy-2-nonenal, and cluster of differentiation 68 (CD68) expressions and Sirius Red staining compared to non-NASH individuals (bars indicate 100x magnification). (B) Circulating levels of paraoxonase and lactonase activities, and paraoxonase-1 (PON1), chemokine (C-C motif) ligand 2 (CCL2), tumor necrosis factor-α (TNF-α), interleukin-10 (IL-10) and galectin-3 concentrations. $*p < 0.05$, $**p < 0.01$, $*** p < 0.001$ by the Mann-Whitney *U* test.

Fig. 3. Effect of laparoscopic sleeve gastrectomy in oxidation and low-grade systemic inflammatory balance.

Differences in the hepatic immunochemical staining of paraoxonase-1 (PON1), 4-hydroxy-2-nonenal, cluster of differentiation 68 (CD68), chemokine (C-C motif) ligand 2 (CCL2), C-C motif chemokine receptor 2 (CCR2), tumor necrosis factor-α (TNF-α), interleukin-10 (IL-10) and galectin-3 in patients pre- and 12 months post-surgery (bars indicate 100x magnification). $*p < 0.01$, $**p < 0.001$ by the Mann-Whitney *U* test.

Fig. 4. laparoscopic sleeve gastrectomy (LSG) improves the hepatic levels of oxidative stress and inflammation markers.

Western Blot analysis of tumor necrosis factor-α (TNF-α), galectin-3, interleukin-10 (IL-10), cluster of differentiation 163 (CD163), phosphorylated signal transducer and activator of transcription-3 (pSTAT3), signal transducer and activator of transcription-3 (STAT3), paraoxonase-1 (PON1), α-smooth muscle actin (α-SMA), and sonic hedgehog protein (Shh). Pooled liver extracts were used for cross validation (left) and mean values of variations in the expression of selected markers are shown on the right. The graph of paraoxonase-1 shows the ratio between the 40 kD and the 45 kD isoforms. *$p < 0.05$, **$p < 0.01$, ***$p < 0.001$ by the Mann-Whitney *U* test.

Table 1. Selected characteristics in patients with severe obesity and in the control group

	Control group (n=404)	Obese patients (n=436)		
		Non-NASH (n=191)	Uncertain NASH (n=151)	NASH (n=94)
Male, n (%)	175 (43.1)	41 (21.5) [a]	41 (27.2) [b]	25 (26.6) [c]
Age, years	46 (35 - 59)	46 (39 - 56)	49 (42 - 57)	48 (42.25 - 56.75)
BMI, kg/m2	26.78 (23.34 – 28.12)	44.6 (41.3 - 49.2) [a]	46.6 (43.0 - 51.4) [b,d]	46.3 (42.3 - 51.5) [c]
T2DM, n (%)	26 (6.3)	60 (31.6) [a]	66 (44.0) [b,d]	48 (51.1) [c,e]
Hypertension, n (%)	62 (15)	104 (54.5) [a]	83 (55.0) [b]	62 (66.0) [c,e]
Dyslipidemia, n (%)	36 (8.7)	55 (28.8) [a]	58 (38.4) [b,d]	40 (42.6) [c,e]
Medication, n (%)				
Metformin	6 (1.4)	33 (17.3) [a]	45 (30.0) [b,d]	36 (38.3) [c,e]
Insulin	-	10 (5.2)	16 (10.6) [d]	10 (10.6)
Sulfonylureas	6 (1.4)	8 (4.2) [a]	11 (7.3) [b]	9 (9.6) [c]
ACEIs+ARA II	15 (3.6)	55 (28.8) [a]	51 (33.8) [b]	41 (43.6) [c,e]
Diuretics	20 (4.8)	15 (7.9)	14 (9.3) [b]	12 (12.8) [c]
Statins	8 (1.9)	31 (16.3) [a]	34 (22.5) [b]	19 (20.4) [c]
Biochemical variables				
Total cholesterol, mmol/L	5.2 (4.6 - 5.9)	4.1 (3.5 - 4.8) [a]	4.4 (3.6 - 5.1) [b]	4.4 (3.8 - 5.0) [c]
HDL-cholesterol, mmol/L	1.4 (1.2 - 1.7)	1.2 (0.9 - 1.5) [a]	1.1 (0.85 - 1.4) [b]	1.1 (0.88 - 1.3) [c]
LDL-cholesterol, mmol/L	3.1 (2.6 - 3.8)	2.7 (2.1 - 3.2) [a]	2.7 (2.1 - 3.3) [b]	2.8 (2.4 - 3.4) [c]
Triglycerides, mmol/L	1.1 (0.7 - 1.5)	1.5 (1.1 - 2.0) [a]	1.7 (1.3 - 2.4) [b,d]	1.8 (1.2 - 2.4) [c,e]
Glucose, mmol/L	4.7 (4.3 - 5.2)	6.7 (5.6 - 8.3) [a]	7.4 (5.9 - 9.4) [b,d]	7.6 (6.2 - 10.9) [c,e]
Insulin, pmol/L	49.4 (31.9 - 70.0)	78.8 (39.2 - 131.1) [a]	82.6 (49.1 - 135.0) [b]	82.6 (53.4 - 145.1) [c]
HOMA-IR	1.5 (0.9 - 2.3)	3.6 (1.7 - 5.6) [a]	4.3 (2.1 - 7.1) [b,d]	5.0 (2.4 - 7.6) [c,e]
AST, µKat/L	0.35 (0.30 - 0.41)	0.45 (0.3 - 0.6) [a]	0.50 (0.39 - 0.81) [b]	0.87 (0.56 - 1.3) [c,e,f]
ALT, µKat/L	0.32 (0.23 - 0.44)	0.4 (0.3 - 0.6) [a]	0.53 (0.38 - 0.86) [b,d]	0.88 (0.56 - 1.3) [c,e,f]
CRP, mg/L	1.2 (0.5 - 2.7)	1.3 (0.5 - 4.3)	2.5 (0.70 - 9.4) [b,d]	1.83 (0.80 - 10.90) [c,e]
Steatosis grade				
≤5%	-	132 (69.1)	27 (17.9)	-
5-33%	-	54 (28.3)	74 (49.0)	9 (9.6)
33-66%	-	5 (2.6)	47 (31.1)	50 (53.2)
>66%	-	-	3 (2.0) [d]	35 (37.2) [e,f]
Lobular inflammation				
No foci	-	65 (34.2)	8 (5.3)	-
<2 foci	-	100 (52.6)	54 (36.0)	18 (19.1)
2-4 foci	-	26 (13.2)	64 (42.0)	52 (55.3)
> 4 foci	-	-	25 (16.7) [d]	24 (25.5) [e,f]
Hepatocellular ballooning				
No	-	163 (85.3)	75 (85.4)	7 (7.4)
Few cells		24 (12.7)	67 (44.4) [d]	60 (63.8) [e,f]
Many cells	-	4 (2.0)	9 (6.0)	27 (28.7) [e,f]
Fibrosis				
None (F0)	-	74 (38.7)	28 (18.5)	23 (24.4)
Perisinusoidal or periportal (F1)	-	78 (40.8)	67 (44.3)	21 (22.3)
Perisinusoidal and portal (F2)	-	32 (16.7)	41 (27.1)	29 (30.8)
Bridging fibrosis (F3)	-	7 (3.6)	15 (9.9)	20 (21.3) [e,f]
Cirrhosis (F4)	-	-	-	1(1.0)

Values are shown as number of cases and percentages or medians and interquartile ranges. ACEIs: Angiotensin-converting-enzyme inhibitor; ALT: Alanine aminotransferase; AST: Aspartate aminotransferase; ARA-II: Angiotensin II receptor antagonists; BMI: Body mass index; CRP: C-reactive protein; HDL: High-density lipoprotein; HOMA-IR: Homeostatic model assessment of insulin resistance; HTG: Hypertriglyceridemia; LDL: Low-density lipoprotein; NASH: Non-alcoholic steatohepatitis; T2DM: Type 2 diabetes mellitus. Significant differences ($p \leq 0.05$ or lower) in comparisons are indicated by [a] Control vs non-NASH. [b] Control vs Uncertain NASH. [c] Control vs NASH. [d] Non-NASH vs Uncertain NASH. [e] Non-NASH vs NASH. [f] Uncertain NASH vs NASH.

Table 2. Selected variables in patients with severe obesity and paired liver biopsies at baseline and 12 months after laparoscopic sleeve gastrectomy.

	Baseline (n=120)	**12 months after surgery** (n=120)	***p*-value**
BMI, kg/m2	46.4 (42.8)	31.2 (29.1-34.7)3	<0.001
Total cholesterol, mmol/L	4.3 (3.7-5.3)	4.7 (4.2-5.4)	<0.001
HDL-cholesterol, mmol/L	1.0 (0.8-1.4)	1.4 (1.2-1.7)	<0.001
LDL-cholesterol, mmol/L	3.1 (2.5-3.9)	3.0 (2.5-3.3)	0.127
Triglycerides, mmol/L	1.5 (.1-2.3)	0.9 (0.8-1.3)	<0.001
Glucose, mmol/L	7.0 (6.0-9.1)	4.7 (4.5-5.)	<0.001
Insulin, pmol/L	100.8 (54.3-162.2)	39.6 (24.0-60.1)	<0.001
HOMA-IR	4.4 (2.8-7.5)	1.3 (0.4-2.5)	<0.001
AST, µKat/L	0.6 (0.4-0.8)	0.3 (0.2-0.3)	<0.001
ALT, µKat/L	0.5 (0.4-0.8)	0.2 (0.2-0.3)	<0.001
CRP, mg/L	3.0 (0.82-8.6)	1.5 (0.5-4.2)	<0.001
Steatosis grade			
<5%	25 (20.8)	116 (96.6)	
5-33%	46 (38.3)	4 (3.3)	
>33-66%	37 (30.8)	-	
>66%	12 (10)	-	<0.001
Lobular inflammation			
No foci	25 (20.8)	98 (81.6)	
<2 foci	38 (31.6)	22 (18.4)	
2-4 foci	41 (34.2)	-	
> 4 foci	16 (13.3)	-	<0.001
Hepatocellular ballooning			
No	49 (40.8)	98 (81.6)	
Few cells	65 (54.1)	19 (15.8)	
Many cells	6 (5.0)	3 (2.5)	<0.001
Fibrosis			
None (F0)	20 (16.6)	55 (45.8)	
Perisinusoidal or periportal (F1)	51 (42.8)	60 (50.0)	
Perisinusoidal and portal (F2)	39 (32.5)	5 (4.1)	
Bridging fibrosis (F3)	9 (7.5)	-	
Cirrhosis (F4)	1 (0.8)	-	<0.001

Values are shown as number of cases and percentages or medians and interquartile ranges. ALT, alanine aminotransferase; AST, aspartate aminotransferase; BMI, body mass index; CRP, C-reactive protein; HDL, high-density lipoprotein; HOMA-IR, homeostatic model assessment of insulin resistance; LDL, low-density lipoprotein.

Figure 1

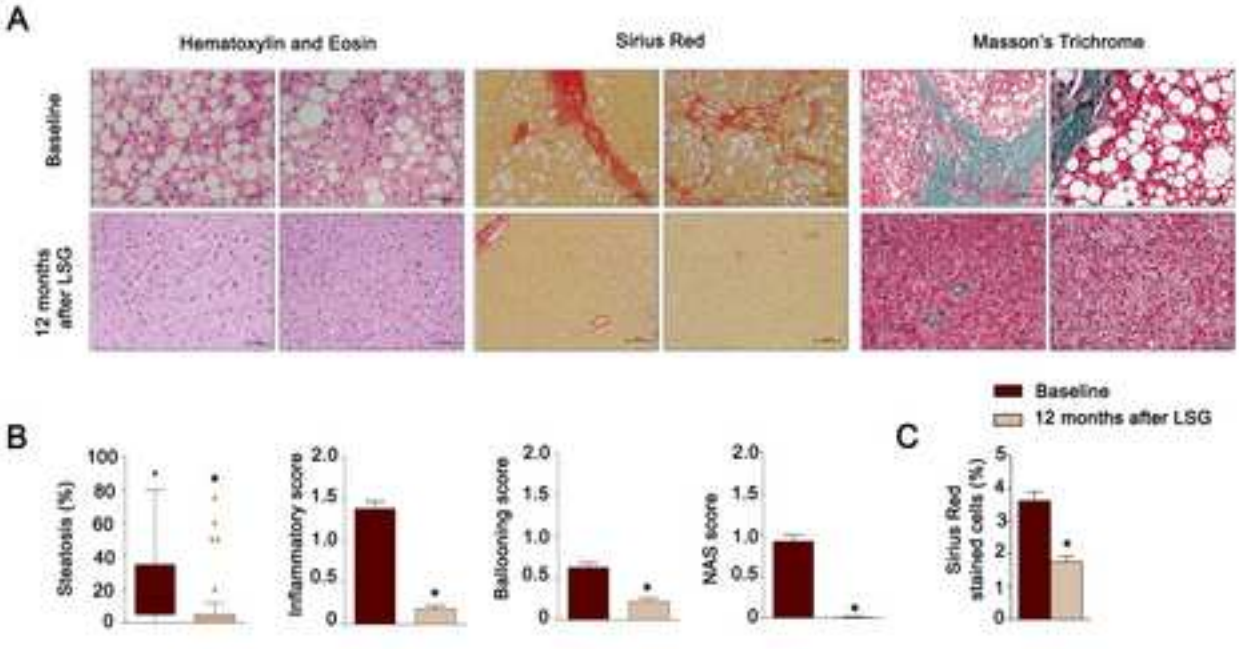

Figure 2

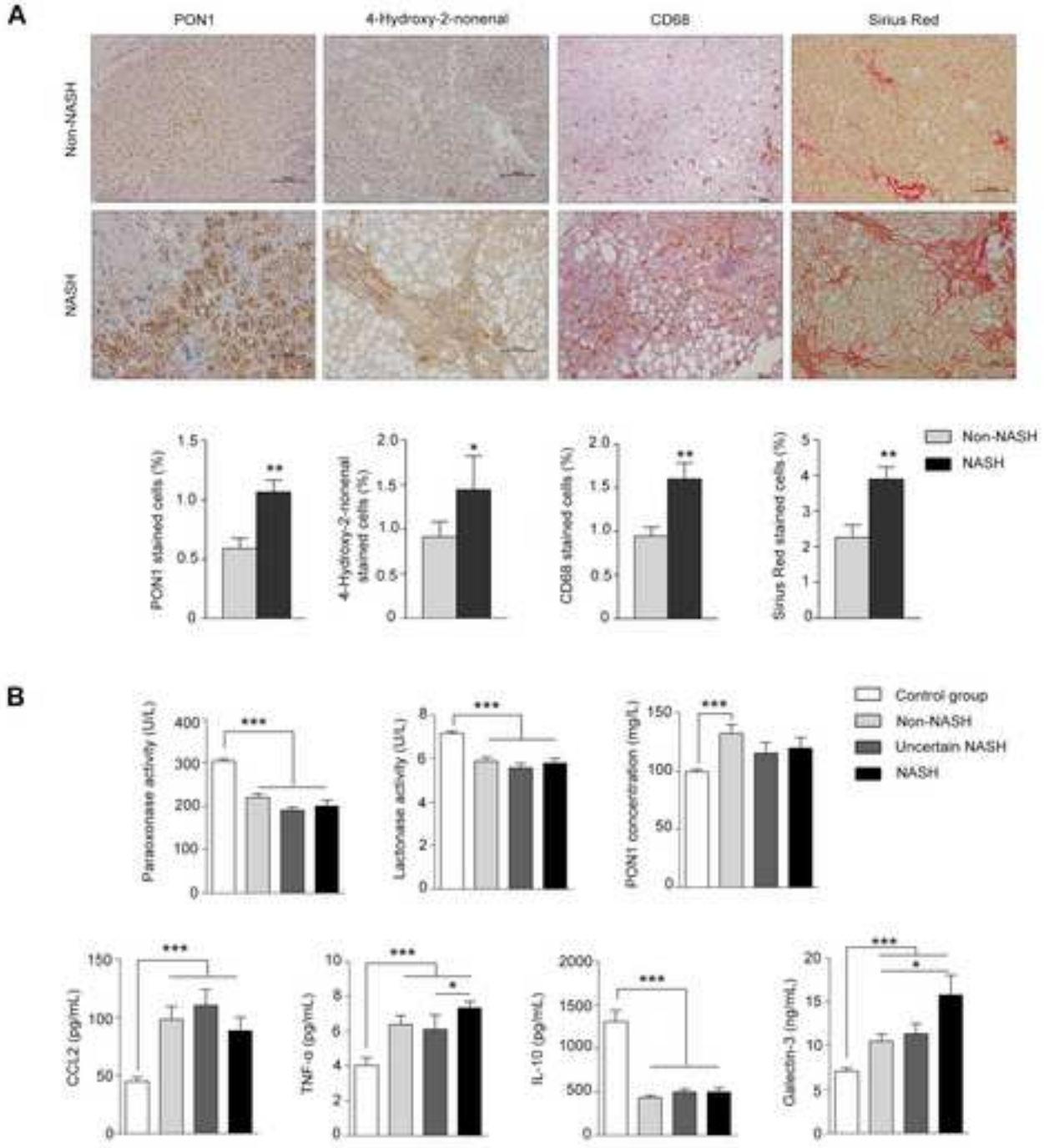

Figure 3
Click here to download high resolution image

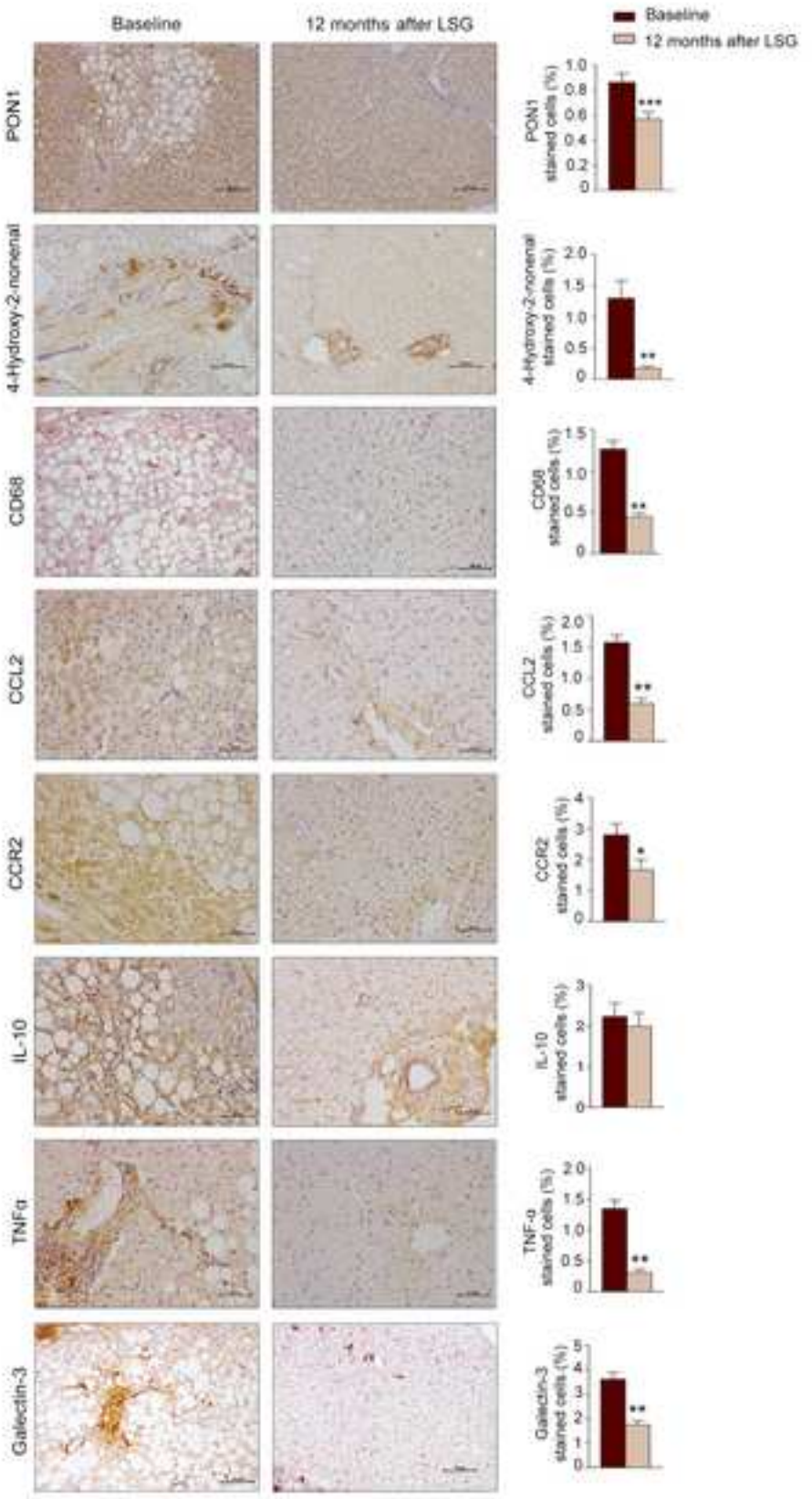

Figure 4

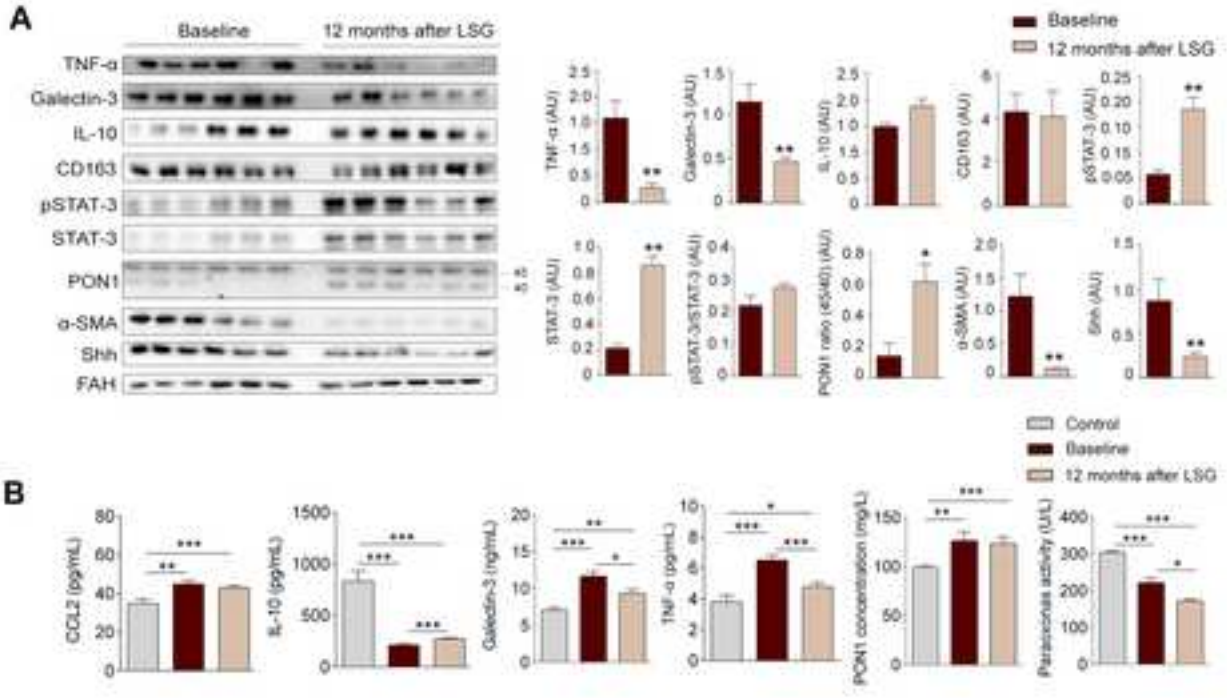

STROBE Statement—checklist of items that should be included in reports of observational studies

	Item No	Recommendation	Page No
Title and abstract	1	(*a*) Indicate the study's design with a commonly used term in the title or the abstract	1,2
		(*b*) Provide in the abstract an informative and balanced summary of what was done and what was found	2
Introduction			
Background/rationale	2	Explain the scientific background and rationale for the investigation being reported	4
Objectives	3	State specific objectives, including any prespecified hypotheses	5
Methods			
Study design	4	Present key elements of study design early in the paper	5
Setting	5	Describe the setting, locations, and relevant dates, including periods of recruitment, exposure, follow-up, and data collection	5
Participants	6	(*a*) *Cohort study*—Give the eligibility criteria, and the sources and methods of selection of participants. Describe methods of follow-up *Case-control study*—Give the eligibility criteria, and the sources and methods of case ascertainment and control selection. Give the rationale for the choice of cases and controls *Cross-sectional study*—Give the eligibility criteria, and the sources and methods of selection of participants	5
		(*b*) *Cohort study*—For matched studies, give matching criteria and number of exposed and unexposed *Case-control study*—For matched studies, give matching criteria and the number of controls per case	
Variables	7	Clearly define all outcomes, exposures, predictors, potential confounders, and effect modifiers. Give diagnostic criteria, if applicable	6,7
Data sources/ measurement	8*	For each variable of interest, give sources of data and details of methods of assessment (measurement). Describe comparability of assessment methods if there is more than one group	6,7
Bias	9	Describe any efforts to address potential sources of bias	7
Study size	10	Explain how the study size was arrived at	6
Quantitative variables	11	Explain how quantitative variables were handled in the analyses. If	6,7

		applicable, describe which groupings were chosen and why	
Statistical methods	12	(*a*) Describe all statistical methods, including those used to control for confounding	7
		(*b*) Describe any methods used to examine subgroups and interactions	6,7
		(*c*) Explain how missing data were addressed	6,7
		(*d*) *Cohort study*—If applicable, explain how loss to follow-up was addressed *Case-control study*—If applicable, explain how matching of cases and controls was addressed *Cross-sectional study*—If applicable, describe analytical methods taking account of sampling strategy	7
		(*e*) Describe any sensitivity analyses	

Continued on next page

Results

Participants	13*	(a) Report numbers of individuals at each stage of study—eg numbers potentially eligible, examined for eligibility, confirmed eligible, included in the study, completing follow-up, and analysed	7-9
		(b) Give reasons for non-participation at each stage	7-9
		(c) Consider use of a flow diagram	
Descriptive data	14*	(a) Give characteristics of study participants (eg demographic, clinical, social) and information on exposures and potential confounders	Table 1
		(b) Indicate number of participants with missing data for each variable of interest	Tables
		(c) *Cohort study*—Summarise follow-up time (eg, average and total amount)	
Outcome data	15*	*Cohort study*—Report numbers of outcome events or summary measures over time	7-9, Tables
		Case-control study—Report numbers in each exposure category, or summary measures of exposure	7-9, Tables
		Cross-sectional study—Report numbers of outcome events or summary measures	7-9, Tables
Main results	16	(*a*) Give unadjusted estimates and, if applicable, confounder-adjusted estimates and their precision (eg, 95% confidence interval). Make clear which confounders were adjusted for and why they were included	Tables and figures
		(*b*) Report category boundaries when continuous variables were categorized	Tables and figures
		(*c*) If relevant, consider translating estimates of relative risk into absolute risk for a meaningful time period	
Other analyses	17	Report other analyses done—eg analyses of subgroups and interactions, and sensitivity analyses	

Discussion

Key results	18	Summarise key results with reference to study objectives	9-11
Limitations	19	Discuss limitations of the study, taking into account sources of potential bias or imprecision. Discuss both direction and magnitude of any potential bias	9-11
Interpretation	20	Give a cautious overall interpretation of results considering objectives, limitations, multiplicity of analyses, results from similar studies, and other relevant evidence	9-11
Generalisability	21	Discuss the generalisability (external validity) of the study results	9-11

Other information

Funding	22	Give the source of funding and the role of the funders for the present study and, if applicable, for the original study on which the present article is based	11

*Give information separately for cases and controls in case-control studies and, if applicable, for exposed and unexposed groups in cohort and cross-sectional studies.

Note: An Explanation and Elaboration article discusses each checklist item and gives methodological background and published examples of transparent reporting. The STROBE checklist is best used in conjunction with this article (freely available on the Web sites of PLoS Medicine at http://www.plosmedicine.org/, Annals of Internal Medicine at http://www.annals.org/, and Epidemiology at http://www.epidem.com/). Information on the STROBE Initiative is available at www.strobe-statement.org.

UNIVERSITAT ROVIRA I VIRGILI
ASSESSING DIAGNOSTIC AND THERAPEUTIC TARGETS IN OBESITY-ASSOCIATED LIVER DISEASES
Noemí Cabré Casares

HEPATOLOGY

NASH modulates circulating metabolites from energy and one-carbon metabolism in obesity: implication in NASH remission

Journal:	*Hepatology*
Manuscript ID	Draft
Wiley - Manuscript type:	Original
Date Submitted by the Author:	n/a
Complete List of Authors:	Cabré, Noemí; Hospital Universitari Sant Joan de Reus, Unitat de Recerca Biomèdica Luciano-Mateo, Fedra; Hospital Universitari Sant Joan de Reus, Unitat de Recerca Biomèdica Baiges-Gayà, Gerard; Hospital Universitari Sant Joan de Reus, Unitat de Recerca Biomèdica Fernández-Arroyo, Salvador; Hospital Universitari Sant Joan de Reus, Unitat de Recerca Biomèdica Hernández-Aguilera, Anna; Hospital Universitari Sant Joan de Reus, Unitat de Recerca Biomèdica París, Marta; Hospital Universitari Sant Joan de Reus, Unitat de Recerca Biomèdica Sabench, Fàtima; Hospital Universitari Sant Joan de Reus, Unitat de Recerca Biomèdica del Castillo, Daniel; Hospital Universitari Sant Joan de Reus, Department of Surgery López-Miranda, José; Instituto de Salud Carlos III Menéndez, Javier; Hospital Universitari de Girona Doctor Josep Trueta Camps, Jordi; Hospital Universitari Sant Joan de Reus, Unitat de Recerca Biomèdica Joven, Jorge; Hospital Universitari Sant Joan de Reus
Keywords:	α-ketoglutarate, β-hydroxybutyrate, bariatric surgery, epigenetics, metabolomics

Type of manuscript: Original article

NASH modulates circulating metabolites from energy and one-carbon metabolism in obesity: implication in NASH remission

Noemí Cabré [1,2], Fedra Luciano-Mateo [1,2], Gerard Baiges-Gayà [1,2], Salvador Fernández-Arroyo [1,2], Anna Hernández-Aguilera [1,2], Marta París [3], Fàtima Sabench [3], Daniel Del Castillo [3], José López-Miranda [4], Javier A. Menéndez [5,6], Jordi Camps [1,2] and Jorge Joven [1,2,7].

[1] *Universitat Rovira i Virgili, Department of Medicine and Surgery, Reus, Spain*
[2] *Unitat de Recerca Biomèdica (URB-CRB), Hospital Universitari de Sant Joan, Institut d'Investigacio Sanitaria Pere Virgili, Universitat Rovira i Virgili, Reus, Spain*
[3] *Department of Surgery, Hospital Universitari de Sant Joan, Institut d'Investigació Sanitaria Pere Virgili, Universitat Rovira i Virgili, Reus, Spain*
[4] *CIBER Fisiopatología de la Obesidad y Nutrición (CIBEROBN), Instituto de Salud Carlos III, Cordoba, Spain.*
[5] *Program Against Cancer Therapeutic Resistance (ProCURE), Metabolism and Cancer Group , Catalan Institute of Oncology, Girona , Spain.*
[6] *Girona Biomedical Research Institute (IDIBGI), Girona , Spain.*
[7] *The Campus of International Excellence Southern Catalonia, Tarragona, Spain.*

Running head: Targeted plasma metabolomics in NASH

Keywords: α-ketoglutarate, β-hydroxybutyrate, bariatric surgery, DNA methylation, epigenetics, metabolomics

Word count (from abstract to figure legends): 5193
Pages: 25
Figures: 5
Tables: 2
Supplemental information: Supplemental information includes two figures and three tables

Footnote page

Address correspondence and reprint requests to:
Jordi Camps, Ph.D. or Jorge Joven, M.D., Ph.D.
Unitat de Recerca Biomèdica, Hospital Universitari de Sant Joan, C. Sant Joan s/n, 43201-Reus, Spain.
Email jcamps@grupsagessa.com, jjoven@grupsagessa.com
Tel: +34-977-310-300

Abbreviations: α-KG: α-Ketoglutarate; β-HB: β-Hydroxybutyrate; 1-C: one-carbon; 5-mC: 5-methycytosine; 5-hmC: 5-hydroximethylcytosine; ALT: alanine aminotransferase; AST: aspartate aminotransferase; BMI, body mass index; BCAA: branched chain amino acid; CAC; citric acid cycle; HOMA-IR, homeostasis model assessment-insulin resistance; HDL, high-density lipoproteins; LDL: low-density lipoprotein; NAFLD, non-alcoholic fatty liver disease; NAS, non-alcoholic fatty liver activity score; NASH, non-alcoholic steatohepatitis; SAM: S-adenosyl methionine; SAH: S-adenosylhomocysteine; T2DM, type 2 diabetes mellitus.

Funding:
This study was supported by grants 60/U/2016 from the Fundació La Marató de TV3 (Barcelona, Spain) and PI15/00285 from the Instituto de Salud Carlos III (Madrid, Spain). It has been also co-funded by the Fondo Europeo de Desarrollo Regional (FEDER) and the Agència de Gestió d'Ajuts Universitaris i de Recerca (SGR1227).

Abstract

Liver biopsy is central to identify nonalcoholic steatohepatitis (NASH) in patients and to assess their therapeutic follow-up. Noninvasive biomarkers may facilitate the clinical task and the investigation of hypothetical drugs. We investigated the potential as biomarkers of metabolites associated with mitochondrial integrity that is compromised in these patients and links nutrition and the epigenome. We developed mass spectrometry-based methods to quantitate metabolites from energy and one-carbon metabolism in plasma and DNA methyl cytosine levels in peripheral leukocytes. We performed measurements in samples from morbidly obese patients undergoing bariatric surgery to identify specific metabolic patterns and to test the diagnostic ability to distinguish between patients with and without NASH. From NASH patients, a second plasma sample and liver biopsy were obtained one year after surgery to assess the ability of metabolomics to predict remission. The targeted plasma metabolomic profiles identified connections between human liver metabolism and morbid obesity. Differential DNA methylation in leukocytes was reversible and associated with hepatic lesions. Combined models of single or paired plasma measurements of α-ketoglutarate, β-hydroxybutyrate, pyruvate and oxaloacetate reduced the uncertainty in clinical diagnosis of NASH (area under receiver-operating characteristic curve (AUC) of 0.826) and predicted NASH remission without ambiguity (AUC of 0.999). We conclude that plasma mitochondrial metabolites could mitigate the need for liver biopsy to evaluate the effectiveness of therapies in NASH patients.

The liver is particularly susceptible to the metabolic challenge caused by obesity. The incidence and prevalence of nonalcoholic steatohepatitis (NASH) are increasing to epidemic proportions, with implications for morbidity and mortality.[1-3] Mechanisms leading to NASH onset and progression remain poorly understood, available data are mostly inferred from nonclinical models, and there is no pharmacological intervention specifically approved for NASH management.[4] Investigation in humans is challenging due to a number of ethical and clinical considerations. Efforts to discover noninvasive biomarkers might fulfill an unmet clinical need with the potential for accelerating pharmacologic research. NASH is often asymptomatic and laboratory or imaging techniques may help to suspect the disease but discrimination of obese patients with and without NASH ultimately requires liver biopsy, a procedure with potential pitfalls.[5] Equally, the accurate assessment of pharmacologic approaches requires repeated liver biopsies, which is unrealistic.[6] Targeting lifestyle factors remains the cornerstone of clinical management, but its failure rate is high,[7] especially in patients with morbid obesity (body mass index (BMI) ≥40 kg/m^2) who have a higher risk of noncommunicable diseases.[8] These patients, however, might represent a unique research opportunity in searching for noninvasive biomarkers of liver alterations. In particular, these patients are likely candidates for bariatric surgery that can achieve rapid weight loss and/or resolve comorbidities, including NASH.[9]

The choice of potential therapeutic targets needs to consider that NASH is a multisystem disease with an important mitochondrial contribution to the defective metabolic responses.[10] Overfed mitochondria eventually perturb energy and one-carbon (1-C) metabolism and the involved metabolites may be

measured in the circulation.[11] We hypothesized that plasma levels of metabolites from these pathways would highlight the prominent role of liver disease in regulating metabolic changes in this clinical model, and might provide clinically useful biomarkers.[12] Interpretation might be difficult because changes in plasma result from the action of multiple transporters of metabolites into and out of cells,[13] which may represent a disadvantage for using nontargeted, nonquantitative techniques that detect numerous but small differences among metabolites.[14,15]. Thus, we developed mass spectrometry–based methods for robust and accurate quantitation of a defined set of closely related metabolites.[11,16,17] In addition, some of these metabolites are either methyl donors or rate-limiting factors for the catalytic activity of enzymes that play a role in chromatin methylation.[18] Then we investigated whether this approach bears potential translational relevance to noninvasively assess the obesity-associated liver diseases.[19-21]

Materials and Methods

PARTICIPANTS

Among patients referred to the Bariatric Surgery Unit at the *Hospital Universitari de Sant Joan de Reus* 270 patients with homogeneous ethnic origin consented to participate according to current guidelines and to the procedures[8, 22] approved by our Institutional Review Board and Ethics Committee (OBESPAD/14.07-31proj3 and INFLAMET/15-04/4proj7) and provided written informed consent to an intraoperative liver biopsy and donation of a preoperative fasting blood sample. Histologic discrimination was based on the non-alcoholic fatty liver score (NAS) system with care to avoid excluding

advanced cases with low steatosis.[5,23-25] Only patients at both sides of the clinical spectrum classified as non-NASH (n=130) i.e., with only minor liver alterations, or NASH (n = 53) were included. NASH patients also agreed to undergo blood donation, and a second biopsy was performed by ultrasound-guided, percutaneous needle puncture (OM-NAFLD, ESO3/18012013) at 12 months post-surgery. Relevant data were extracted from clinical records. Healthy age- and sex-matched nonobese controls (n=50) were recruited among participants in a previous population-based study[26] in whom liver alterations were excluded via liver imaging techniques and laboratory assessment.[8] The BMI was calculated as the weight in kilograms divided by the square of the height in meters. A similar time of fasting (at least 10 hours) was considered essential for collecting blood samples, and EDTA-plasma aliquots were immediately stored at -80 °C for batched analyses. Readily available laboratory measurements were analyzed using standard tests in a Roche Modular Analytics P800 system (Roche Diagnostics, Basel, Switzerland). Homeostatic model assessment for insulin resistance (HOMA-IR) was calculated as described.[27]

LIVER BIOPSIES

Portions of the liver were obtained with wedge resection during the surgical procedure, and paired biopsies in NASH patients were obtained with needle devices 12 months after surgery, which required cooperation from trained pathologists, radiologists and surgeons.[28,29] Histologic features in sections stained with hematoxylin and eosin, Masson's trichrome and Sirius red dyes were evaluated by the scores for steatosis (0-3), lobular inflammation (0-3), and ballooning (0-2), for a total (unweighted) score ranging from 0 to 8. Non-NASH

patients scored ≤ 2, and NASH patients scored ≥ 5. Liver fibrosis was assessed considering the scale defined as F0, normal; F1a or F1b, mild or moderate focal pericellular fibrosis in zone 3; F1c, portal fibrosis; F2, perivenular and pericellular fibrosis confined to zones 2 and 3, with or without portal or periportal fibrosis; F3, bridging or extensive fibrosis with architectural distortion; and F4, cirrhosis.[23-25]

QUANTITATIVE TARGETED METABOLOMICS PLATFORM

Chromatographic conditions and methods to optimize reproducibility and robustness for the simultaneous measurement of selected metabolites from energy and 1-C metabolism have been previously described.[16,17,30]. Briefly, surrogate deuterated standards were added to maximize technical precision during the injection and recovery during the extraction procedures (Isotec Stable Isotopes, Miamisburg, OH, USA). The calibration curves were prepared immediately before each assay using commercially available metabolites (Fluka, St Gallen, Switzerland). The samples for gas chromatography (GC-EI-QTOF-MS) were derivatized and analyzed on an Agilent Technologies (Santa Clara, CA, USA) 7890A gas chromatograph coupled with an electron impact (EI) source to a 7200 quadrupole time-of-flight mass spectrometer (QTOF-MS) equipped with a 7693 autosampler module and a J&W Scientific HP-5MS column (30 m × 0.25 mm, 0.25 μm). The liquid chromatography platform (UHPLC-ESI-QqQ-MS) was based on an Agilent 1290 Infinity Ultra High Performance Liquid Chromatograph (UHPLC) coupled with an iFunnel electrospray ionization (ESI) source and a 6490 triple quadrupole mass spectrometer (QqQ-MS). The MS analysis alternated between MS and data-dependent MS^2 scans using dynamic exclusion. Metabolites were identified and

quantified using available reference libraries and Qualitative and Quantitative Analysis B.06.00 software (Agilent Technologies).

GENOMIC DNA METHYLATION

RNA-free DNA from peripheral blood leukocytes was prepared and purified using the QIAamp DNA Blood Mini Kit (Qiagen, Barcelona, Spain). DNA quantification and purity were assessed using a Nanodrop 1000 spectrophotometer (Thermo, Madrid, Spain) and DNA was dissolved in RNase-free water to obtain 100 µL aliquots of 1 µg. The internal standard solution containing deuterated bases was added and vacuum dried for up to 48 h. The residue was dissolved in 15 µL of formic acid (98%), and the vials were sealed and heated at 150 °C for 3 h to hydrolyze DNA to the free bases, vacuum-dried overnight and dissolved in a solution containing calibration curves and quality control material. Samples were run on the UHPLC-ESI-QqQ-MS platform described above. This method ensures the ability to discriminate small differences in 5-methylcytosine (5-mC) and 5-hydroxymethylcytosine (5-hmC) levels but the low throughput limited the number of measurements in batched analyses.

STATISTICAL ANALYSIS

The employed statistical software included the program 'R' (http://cran.r-project.org), the SPSS 25.0 package (IBM, Madrid, Spain) and the MetaboAnalyst 4.0 (https://www.metaboanalyst.ca/). Significantly altered metabolites, which were corrected for multiple testing, were defined using a p-value <0.05 and a predesigned false discovery rate.[31] We used Welch's t-test and/or Wilcoxon's rank sum test for pairwise comparisons and repeated-

measurement analysis of variance for some calculations. We used multivariate statistics to improve the analysis of complex raw data and for pattern recognition. Random forests were used as a supervised classification technique to provide an unbiased estimate of prediction accuracy of classification and to select variables with the largest impacts.[32] Heat maps were used to visualize metabolomic data indicating the relative abundance of metabolites with color intensity. We also used linear discriminant analysis as a method of classification and principal component analysis as an unsupervised data analysis method to segregate the compared groups according to metabolomic data. Finally, logistic regression analysis and receiver operating characteristic (ROC) curves described and assessed binary classifications.[33] For this purpose, we also used confusion matrix and predicted class probabilities of each sample across 100 Monte-Carlo cross-validations.

Results

TARGETED QUANTITATIVE PLASMA METABOLOMIC PROFILE IDENTIFIES THE SIGNIFICANT INFLUENCE OF OBESITY ON ENERGY AND ONE-CARBON METABOLISM

Morbid obesity was associated with metabolic alterations, as compared with nonobese controls (Table 1). To enlarge the scope of metabolic signals, we used a targeted metabolomic approach to selectively examine plasma metabolites to explore pathways of energy adaptation. Obesity appears to increase the oxidative changes through the citric acid cycle (CAC), and the significant plasma accumulation of most intermediates might reflect compensatory responses in mitochondrial energetics. We also found a

significant increase in plasma glutamine, pyruvate and ß-hydroxybutyrate (ß-HB) levels in obese patients with respect to nonobese controls, with alterations in amino acids and metabolites derived from 1-C metabolism. Specifically, serine, cysteine, methionine, S-adenosyl methionine (SAM) and S-adenosylhomocysteine (SAH) levels were decreased in morbid obesity with a significant accumulation of cystathionine and choline, major carbon or methyl donors and critical components for signaling functions (Table S1, Figure 1 a, b). Changes in circulating metabolites segregated nonobese controls from patients with morbid obesity and glutamine, ß-HB, citrate and cystathionine were the metabolites with the highest impacts on class distribution (Figure 1 c-e). The plasma levels of each of these metabolites predicted obesity, suggesting the contribution of body weight, but other metabolites, exemplified by plasma α-ketoglutarate (α-KG), were independent of body weight (Figure S1). Values in plasma may suggest impaired energy homeostasis, metabolic inflexibility and likely induction of anaplerosis and pyruvate cycling.[34] Plasma essentially reports the sum of changes from multiple organs. Hence, we investigated whether circulating metabolites could identify the effect of liver disease in regulating energy homeostasis by assessing differences between patients with and without NASH.

NASH IMPACTS METABOLIC ADAPTATION PATHWAYS

Histologic features and clinical and laboratory variables identified progressive metabolic disturbances closely related to liver disease (Figure 2 a, Table 2). Liver alterations were heterogeneous, and we compared the plasma metabolome between patients with minor changes (non-NASH) and those with unambiguous NASH. The number of metabolites with the ability to segregate

patients with and without NASH was lower than those distinguishing patients with and without obesity (Table S2), and plasma α-KG, oxaloacetate and isoleucine levels had the highest impacts on the class distribution (Figure 2 b-d). The histopathological features in patients with NASH were associated with a significant accumulation of plasma glucose, lactate and pyruvate, indicating reprogrammed glucose metabolism. These findings were accompanied by increased plasma concentrations of alanine, aspartate and branched chain amino acids (BCAAs) in NASH patients. Among metabolites from the CAC, only plasma oxaloacetate and α-KG levels were significantly increased in NASH patients, which in the presence of higher plasma glutamate likely indicated CAC replenishment via glutaminolysis. As glutamine is metabolized via glutaminolysis to be converted into α-KG and lactate, high plasma concentrations of these metabolites might indicate the role of NASH in the organismal metabolic responses.[35] Plasma metabolites from 1-C metabolism also revealed significant alterations in the form of serine-to-glycine and SAM-to-SAH conversions in NASH patients (Figure 3 a). We then explored whether these metabolic alterations persisted or reversed after surgery.

BARIATRIC SURGERY RESTORES THE PERTURBED METABOLIC RESPONSES

One year after bariatric surgery, NASH patients were reexamined and paired liver biopsies demonstrated NASH remission. Body weight decreased significantly, but patients remained obese (BMI > 30 kg/m^2), though there were significant improvements in the severity and prevalence of diabetes, hypertension, and dyslipidaemia (Table 2). Variations in plasma metabolites segregated NASH patients before vs. after surgery (Figure 2 b, c, e) and

plasma α-KG levels provided the largest impact on class distribution. Most plasma levels of CAC intermediates returned to values close to normal in nonobese controls. The significant reduction in plasma glutamate and α-KG after surgery and the simultaneous higher level of succinate indicated that glutaminolysis was no longer preponderant in the follow-up. Bariatric surgery also normalized plasma levels of circulating amino acids and metabolites from 1-C metabolism (Figure 3 b, Table S3). We also found that surgery restored the increased 5-mC levels in circulating leukocytes of patients with NASH (Figure 4 a) indicating differential and reversible DNA methylation in leukocytes. Variations in metabolites with influence in DNA methylation (Figure 4 b) suggest the potential role of metaboloepigenetic processes in NASH progression. However, the plasma α-KG to succinate ratio, which represents the relative proportions of the substrates and products of enzymes involved in methylation, was significantly altered only after surgery and did not differentiate patients with and without NASH (Figure 4 a). Of note, correlations between most metabolite levels and the leukocyte 5-mC level did not reach statistical significance between patients with and without NASH but the SAM-to-SAH ratio and plasma α-KG level were significantly associated with steatosis (Figure 4 c). After surgery, the DNA 5mC level was negatively correlated with the changes in SAM-to-SAH ratio and positively correlated with plasma α-KG levels (Figure 4 d). However, the diagnostic and predictive value of the 5-mC levels in DNA from leukocytes did not result into clinical benefit (data not shown) and we explored, without this input, the putative role of circulating metabolites as noninvasive biomarkers.

PLASMA METABOLOME IDENTIFIES BIOMARKERS TO DISTINGUISH PATIENTS WITH AND WITHOUT NASH AND PREDICT NASH REMISSION

The drawbacks associated with liver biopsy represent a considerable constraint to clinically detect the severity and progression of liver disease and to assess NASH remission after treatment. The current markers of liver injury, plasma aminotransferases, did not discriminate patients with and without NASH with AUC values between 0.511 and 0.837 and 45% of misinterpretations (Figure S2 a). In contrast, reduction after surgery in plasma aminotransferases provided an assessment of NASH remission with 10% of uncertainties (Figure S2 b). Logistic regression models and ROC analyses using the concentration of energy-balance metabolites in plasma revealed that the combination of plasma α-KG, pyruvate and oxaloacetate levels improved the diagnostic accuracy of NASH, with AUC values between 0.680 and 0.938 and reduced misinterpretations (Figure 5 a). Similarly, the combined decrease in plasma α-KG and ß-HB levels was also a good predictive biomarker of NASH remission with an AUC between 0.938 and 1 (Figure 5 b). More importantly, the combination of reductions in plasma α-KG, ß-HB and AST levels predicted NASH remission without ambiguity (Figure 5 c). These results need to be validated in the routine clinical assessment, i.e., without controlled and batched laboratory assessment, but strongly suggest that the explorative second biopsy should be limited to NASH patients without changes in these measurements over time. Eventually, these simple measurements might be used to evaluate the effectiveness of therapies in NASH patients.

Discussion

It is important to recognize and target the hepatic consequences of nutrient overload. Dietary restraint improves liver function and histologic features in mice,[36] but in the clinical setting, dietary advice is clearly insufficient to halt the growing incidence and prevalence of obesity-associated diseases.[37] Our observations suggest that the critical links between obesity and liver disease are closely related to the mitochondrial integrity of energy and 1-C metabolism. Fluctuations in the plasma metabolome assessed complex effects associated with the severity of liver disease, as were almost completely reversed after NASH remission. In human obesity, the liver may efficiently respond to nutrient overload during a period of time but the onset and development of NASH represents a critical event leading to metabolic inflexibility.[38] The clinical relevance in obesity of increased CAC activity, whole-body protein catabolism and pyruvate-driven gluconeogenesis remains to be established but the increased anaplerotic flux and glutaminolysis-derived accumulation of plasma α-KG in NASH patients may supply pathogenic clues.[8,39,40] Our data suggest that obese patients, especially those with metabolic syndrome, might benefit from bariatric surgery at an earlier stage.

Plasma α-KG identifies obese patients with hepatic steatosis.[11] Our findings suggest that circulating metabolites provide signals of the impaired metabolic state and that the insufficient adaptive hepatic response might be a distinctive feature of NASH. NASH was associated with perturbed pathways in glucose and fatty acid oxidation and convergence in the metabolism of amino acids and lipids.[41] These perturbed pathways were restored after surgery following NASH

remission. Targeted quantitation of plasma α-KG, pyruvate and oxaloacetate levels revealed differences between patients with and without NASH that may be used as modest to good noninvasive diagnostic biomarkers. A major finding of this study was that paired measurements of these metabolites, before and after surgery, provided excellent results to predict NASH remission without ambiguity, indicating a reliable alternative to liver biopsy in assessing the effectiveness of clinical management in NASH patients. Similarly, metabolites from the methionine cycle, succinate and α-KG have been reported as mediators in the dynamic process of methylation linked to altered cellular metabolism in disease states.[18,42] These metabolites might provide signaling functions via the circulation with the ability to alter epigenetic cellular reprogramming. Manipulating metabolites that work as epigenetic modifiers offers novel therapeutic possibilities and the relevance of DNA methylation in NASH management is likely.[19,20,43,44] However, despite the significant effect of surgery, our data did not support the value of 5-mC and 5-hmC levels of DNA from leukocytes to segregate patients with and without NASH.

Circulating metabolites from energy and 1-C metabolism provide a global picture of metabolic interorgan crosstalk with potential importance in liver metabolic research associated with the growing obesity epidemics. Despite this encouraging insight it is important to keep several knowledge gaps and limitations in mind. First, the effect of metabolic signaling in the regulation of liver gene expression should be investigated. It is not a trivial consideration that cell types other than hepatocytes may contribute the technological and clinical challenges ahead. Second, clinical models do not provide true dynamic information and the actual value of still pictures recorded at different time points

requires cautious interpretation. In this context, we have developed versatile, simple and inexpensive electroanalytical bioplatforms.[45,46] to continuously monitor the impact of metabolic pathways and epigenetics in NASH onset and progression. These considerations represent exciting areas of future research.

Acknowledgements

NC is the recipient of a fellowship from the Universitat Rovira i Virgili (URV-PFRB-21545) and LFM is the recipient of a fellowship from the Generalitat de Catalunya (2016-FIB-00352).

Authors' contribution

JLM, JAM, JC and JJ designed the study; metabolomics studies were designed and conducted by SFA and AHA; NC, FLM, GBG and JJ conducted the experimental procedures; MP, FS, and DDC provided the human samples and were responsible of patients care; JJ wrote the manuscript with inputs from all authors; all authors have contributed to data collection and interpretation.

Conflict of interest

The authors declare no conflict of interest.

References

1. Dhanasekaran R, Felsher DW. A tale of two complications of obesity: Nonalcoholic steatohepatitis and hepatocellular carcinoma. Hepatology. 2019; doi: 10.1002/hep.30649. [Epub ahead of print].

2. World Health Organization. Obesity and overweight fact sheet. Geneva, Switzerland: World Health Organization; 2018. who.int/mediacentre/factsheets/fs311/en/.

3. Younossi ZM, Marchesini G, Pinto-Cortez H, Petta S. Epidemiology of nonalcoholic fatty liver disease and nonalcoholic steatohepatitis: Implications for liver yransplantation. Transplantation 2019; 103(1): 22-27. doi: 10.1097/TP.0000000000002484.

4. Tanaka N, Kimura T, Fujimori N, Nagaya T, Komatsu M, Tanaka E. Current status, problems, and perspectives of non-alcoholic fatty liver disease research. World J Gastroenterol 2019; 25(2): 163-177. doi: 10.3748/wjg.v25.i2.163.

5. Brunt EM. Nonalcoholic fatty liver disease and the ongoing role of liver biopsy evaluation. Hepatol Commun 2017; 1(5):370-378. doi: 10.1002/hep4.1055.

6. Neuschwander-Tetri BA. Pharmacologic management of nonalcoholic steatohepatitis. Gastroenterol Hepatol (NY) 2018; 14(10): 582-589. PMID: 30846912.

7. Vilar-Gomez E, Martinez-Perez Y, Calzadilla-Bertot L, Torres-Gonzalez A, Gra-Oramas B, Gonzalez-Fabian L, et al. Weight loss through lifestyle modification significantly reduces features of nonalcoholic steatohepatitis. Gastroenterology 2015; 149(2): 367-378. doi: 10.1053/j.gastro.2015.04.005.

8. Calvo N, Beltrán-Debón R, Rodríguez-Gallego E, Hernández-Aguilera A, Guirro M, Mariné-Casadó R, et al. Liver fat deposition and mitochondrial dysfunction in morbid obesity: An approach combining metabolomics with liver imaging and histology. World J Gastroenterol 2015;21(24):7529-7544. doi: 10.3748/wjg.v21.i24.7529.

9. Lassailly G, Caiazzo R, Buob D, Pigeyre M, Verkindt H, Labreuche J, et al. Bariatric surgery reduces features of nonalcoholic steatohepatitis in morbidly obese patients. Gastroenterology 2015; 149(2): 379-388; doi: 10.1053/j.gastro.2015.04.014.

10. Byrne CD, Targher G. NAFLD: a multisystem disease. J Hepatol 2015; 62: S47-S64. doi: 10.1016/j.jhep.2014.12.012.

11. Rodríguez-Gallego E, Guirro M, Riera-Borrull M, Hernández-Aguilera A, Mariné-Casadó R, Fernández-Arroyo S, et al. Mapping of the circulating metabolome reveals α-ketoglutarate as a predictor of morbid obesity-associated non-alcoholic fatty liver disease. Int J Obes (Lond) 2015; 39(2): 279-287. doi: 10.1038/ijo.2014.53.

12. Camps J, Joven J. Metabolite profiling can change health-care delivery to obese patients with fatty liver disease: the search for biomarkers. Clin Chem Lab Med 2017; 55(4): 501-506. doi: 10.1515/cclm-2016-0762.

13. Kory N, Wyant GA, Prakash G, Uit de Bos J, Bottanelli F, Pacold ME, et al. SFXN1 is a mitochondrial serine transporter required for one-carbon metabolism. Science. 2018; 362(6416). pii: eaat9528. doi: 10.1126/science.aat9528.

14. Kalhan SC, Guo L, Edmison J, Dasarathy S, McCullough AJ, Hanson RW, et al. Plasma metabolomic profile in nonalcoholic fatty liver disease. Metabolism 2011; 60(3): 404-413. doi: 10.1016/j.metabol.2010.03.006.

15. Barr J, Vázquez-Chantada M, Alonso C, Pérez-Cormenzana M, Mayo R, Galán A, et al. Liquid chromatography-mass spectrometry-based parallel metabolic profiling of human and mouse model serum reveals putative biomarkers

associated with the progression of nonalcoholic fatty liver disease. J Proteome Res 2010; 9(9): 4501-4512. doi: 10.1021/pr1002593.

16. Riera-Borrull M, Rodríguez-Gallego E, Hernández-Aguilera A, Luciano F, Ras R, Cuyàs E, et al. Exploring the process of energy generation in pathophysiology by targeted metabolomics: Performance of a simple and quantitative method. J Am Soc Mass Spectrom 2016; 27(1): 168-177. doi: 10.1007/s13361-015-1262-3.

17. Cuyàs E, Fernández-Arroyo S, Verdura S, García RÁ, Stursa J, Werner L, et al. Metformin regulates global DNA methylation via mitochondrial one-carbon metabolism. Oncogene 2018; 37(7): 963-970. doi: 10.1038/onc.2017.367.

18. Fedeles BI, Singh V, Delaney JC, Li D, Essigmann JM. The AlkB Family of Fe(II)/α-Ketoglutarate-dependent Dioxygenases: Repairing Nucleic Acid Alkylation Damage and Beyond. J Biol Chem 2015; 290(34): 20734-20742. doi: 10.1074/jbc.R115.656462.

19. Nano J, Ghanbari M, Wang W, de Vries PS, Dhana K, Muka T, et al. Epigenome-wide association study identifies methylation sites associated with liver enzymes and hepatic steatosis. Gastroenterology 2017; 153(4): 1096-1106.e2. doi: 10.1053/j.gastro.2017.06.003.

20. Hardy T, Zeybel M, Day CP, Dipper C, Masson S, McPherson S, et al. Plasma DNA methylation: a potential biomarker for stratification of liver fibrosis in non-alcoholic fatty liver disease. Gut 2017; 66(7): 1321-1328. doi: 10.1136/gutjnl-2016-311526.

21. Dudley E, Bond L. Mass spectrometry analysis of nucleosides and nucleotides. Mass Spectrom Rev 2014; 33(4): 302-31. doi: 10.1002/mas.21388.

22. Salminen P, Helmiö M, Ovaska J, Juuti A, Leivonen M, Peromaa-Haavisto P, et al. Effect of laparoscopic sleeve gastrectomy vs laparoscopic Roux-en-Y gastric Bypass on weight loss at 5 years among patients with morbid obesity: The SLEEVEPASS randomized clinical trial. JAMA. 2018; 319(3): 241-254. doi: 10.1001/jama.2017.20313.

23. Kleiner DE, Brunt EM, Van Natta M, Behling C, Contos MJ, Cummings OW, et al. Nonalcoholic Steatohepatitis Clinical Research Network. Design and validation of a histological scoring system for nonalcoholic fatty liver disease. Hepatology 2005; 41(6): 1313-1321. doi. 10.1002/hep.20701.

24. Brunt EM, Kleiner DE, Wilson LA, Belt P, Neuschwander-Tetri BA; NASH Clinical Research Network (CRN). Nonalcoholic fatty liver disease (NAFLD) activity score and the histopathologic diagnosis in NAFLD: distinct clinicopathologic meanings. Hepatology 2011; 53(3): 810-820. doi: 10.1002/hep.24127.

25. EASL-EASD-EASO Clinical Practice Guidelines for the management of non-alcoholic fatty liver disease. J Hepatol 2016; 64(6): 1388-1402. doi: 10.1016/j.jhep.2015.11.004.

26. Bertran N, Camps J, Fernandez-Ballart J, Arija V, Ferre N, Tous M, et al. Diet and lifestyle are associated with serum C-reactive protein concentrations in a population-based study. J Lab Clin Med 2005; 145(1): 41-46. doi. 10.1016/j.lab.2004.11.002.

27. Matthews DR, Hosker JP, Rudenski AS, Naylor BA, Treacher DF, Turner RC. Homeostasis model assessment: insulin resistance and beta-cell function from fasting plasma glucose and insulin concentrations in man. Diabetologia 1985; 28(7): 412-419. PMID: 3899825

28. Chalasani N, Younossi Z, Lavine JE, Diehl AM, Brunt EM, Cusi K, et al. The diagnosis and management of non-alcoholic fatty liver disease: Practice Guideline by the American Association for the Study of Liver Diseases, American College of Gastroenterology, and the American Gastroenterological Association. Hepatology. 2012; 55(6): 2005-2023. doi: 10.1002/hep.25762.

29. Rockey DC, Caldwell SH, Goodman ZD, Nelson RC, Smith AD. Liver biopsy. Hepatology 2009; 49: 1017-1044. doi. 10.1002/hep.22742.

30. Fernández-Arroyo S, Cuyàs E, Bosch-Barrera J, Alarcón T, Joven J, Menendez JA. Activation of the methylation cycle in cells reprogrammed into a stem cell-like state. Oncoscience 2016; 2(12): 958-967. PMID: 26909364.

31. Storey JD, Tibshirani R. Statistical significance for genomewide studies. Proc Natl Acad Sci USA 2003; 100(16): 9440-9445. PMID: 12883005

32. Dietrich S, Floegel A, Troll M, Kühn T, Rathmann W, Peters A, et al. Random survival forest in practice: a method for modelling complex metabolomics data in time to event analysis. Int J Epidemiol 2016; 45(5): 1406-1420. doi:10.1093/ije/dyw145.

33. Xia J, Wishart DS. Using metaboAnalyst 3.0 for comprehensive metabolomics data analysis. Curr Protoc Bioinformatics 2016; 55:14.10.1-14.10.91. doi: 10.1002/cpbi.11.

34. Kelley DE, Goodpaster B, Wing RR, Simoneau JA. Skeletal muscle fatty acid metabolism in association with insulin resistance, obesity, and weight loss. Am J Physiol 1999; 277(6): E1130-1141. doi: 10.1152/ajpendo.1999.277.6.E1130.

35. DeWaal D, Nogueira V, Terry AR, Patra KC, Jeon SM, Guzman G, et al. Hexokinase-2 depletion inhibits glycolysis and induces oxidative

phosphorylation in hepatocellular carcinoma and sensitizes to metformin. Nat Commun 2018; 9(1): 446. doi: 10.1038/s41467-017-02733-4.

36. Riera-Borrull M, García-Heredia A, Fernández-Arroyo S, Hernández-Aguilera A, Cabré N, Cuyàs E, et al. Metformin potentiates the benefits of dietary restraint: A metabolomic study. Int J Mol Sci 2017; 18(11). pii: E2263.doi: 10.3390/ijms18112263.

37. NCD Risk Factor Collaboration (NCD-RisC). Worldwide trends in body-mass index, underweight, overweight, and obesity from 1975 to 2016: a pooled analysis of 2416 population-based measurement studies in 128·9 million children, adolescents, and adults. Lancet 2017; 390(10113): 2627-2642. doi: 10.1016/S0140-6736(17)32129-3.

38. Koliaki C, Szendroedi J, Kaul K, Jelenik T, Nowotny P, Jankowiak F, et al. Adaptation of hepatic mitochondrial function in humans with non-alcoholic fatty liver is lost in steatohepatitis. Cell Metab 2015; 21(5): 739-746. doi: 10.1016/j.cmet.2015.04.004.

39. Sunny NE, Parks EJ, Browning JD, Burgess SC. Excessive hepatic mitochondrial TCA cycle and gluconeogenesis in humans with nonalcoholic fatty liver disease. Cell Metab 2011; 14(6):804-810. doi: 10.1016/j.cmet.2011.11.004.

40. Petersen KF, Befroy DE, Dufour S, Rothman DL, Shulman GI. Assessment of hepatic mitochondrial oxidation and pyruvate cycling in NAFLD by (13) C magnetic resonance spectroscopy. Cell Metab 2016; 24(1): 167-171. doi: 10.1016/j.cmet.2016.06.005.

41. Gancheva S, Jelenik T, Álvarez-Hernández E, Roden M. Interorgan metabolic crosstalk in human insulin resistance. Physiol Rev 2018; 98(3): 1371-1415. doi: 10.1152/physrev.00015.2017.

42. Wu SC, Zhang Y. Active DNA demethylation: many roads lead to Rome. Nat Rev Mol Cell Biol 2010; 11(9): 607-620. doi: 10.1038/nrm2950.

43. Wu J, Zhang R, Shen F, Yang R, Zhou D, Cao H, et al. Altered DNA methylation sites in peripheral blood leukocytes from patients with simple steatosis and nonalcoholic steatohepatitis (NASH). Med Sci Monit 2018; 24:6946-6967. doi: 10.12659/MSM.909747.

44. Ferrari A, Longo R, Silva R, Mitro N, Caruso D, De Fabiani E, et al. Epigenome modifiers and metabolic rewiring: New frontiers in therapeutics. Pharmacol Ther 2019; 193:178-193. doi: 10.1016/j.pharmthera.2018.08.008.

45. Martínez-García G, Pérez-Julián E, Agüí L, Cabré N, Joven J, Yáñez-Sedeño P, et al. An electrochemical enzyme biosensor for 3-hydroxybutyrate detection using screen-printed electrodes modified by reduced graphene oxide and thionine. Biosensors (Basel) 2017; 7(4). doi: 10.3390/bios7040050.

46. Povedano E, Montiel VR, Valverde A, Navarro-Villoslada F, Yáñez-Sedeño P, Pedrero M, et al. Versatile electroanalytical bioplatforms for simultaneous determination of cancer-related DNA 5-methyl- and 5-hydroxymethyl-cytosines at global and gene-specific levels in human serum and tissues. ACS Sens 2019; 4(1): 227-234. doi: 10.1021/acssensors.8b01339.

Figure legends

Fig. 1. Morbid obesity perturbs plasma metabolome. Variations in the levels of plasma metabolites from energy (a) and one-carbon metabolism (b) between obese patients and nonobese controls are schematized, with colors indicating the statistical assessment according to the legend. Partial least square discriminant (PLS-DA) (c) and heat map (d) analyses were used to visualize the segregation between both groups. Random forests analyses (e) provided the relative impact of each metabolite according to the variable influence on the projection (VIP) scores.

Fig. 2. The metabolic adaptive responses in obesity are closely related to liver alterations. Routine clinical and laboratory assessment disclosed the metabolic consequences of different liver histologic features (a). Partial least square discriminant (PLS-DA) (b) and heat map (c) analyses visualized differences in the plasma metabolome after surgery and the challenging task that represents distinguishing patients with and without NASH. Plasma α-ketoglutarate was the metabolite with the largest impact in random forests projecting metabolic changes between patients with and without NASH and between NASH patients before vs. after surgery (d). Asterisks denote statistical significance (*$p < 0.05$, **$p < 0.01$, ***$p < 0.001$) by the Wilcoxon rank-sum test.

Fig. 3. Bariatric surgery reverses NASH-associated disturbances in the plasma metabolome. Schematized view of differences in plasma metabolites related to energy and one-carbon metabolism in comparing patients with vs.

without NASH (a) and NASH patients before vs. after surgery (b). Colors denoted statistical comparisons as indicated in the legend.

Fig. 4. NASH affects plasma DNA methylation. The differential global DNA methylation was assessed as 5-methylcytosine (5-mC) and 5-hydroxymethylcytosine (5-hmC) levels in circulating leukocytes (n=24 for each group), indicating associations with liver histologic features and plasma α-ketoglutarate and succinate levels (a). Metabolites from the citric acid cycle and methionine cycles (b) correlated with steatosis when comparing patients with and without NASH (c) but not with global methylation. In contrast, 5-mC level was restored in NASH patients after surgery and paralleled changes in circulating metabolites, suggesting the potential role of metaboloepigenetic processes (d). Asterisks denote statistical significance (*p < 0.05, **p < 0.01, ***p < 0.001) by the Wilcoxon rank-sum test, β-HB, β-hydroxybutyrate; DNMT, DNA methyltransferase; TET, ten-eleven translocation.

Fig. 5. Paired measurements of selected metabolites predict NASH remission. ROC curve-based model evaluation indicated that selected circulating metabolites provide tools to distinguish patients with and without NASH but the number of misinterpretations remains relatively high (a). Paired measurements of plasma α-ketoglutarate and β-hydroxybutyrate levels before and after surgery might be useful to predict NASH remission (b). Remarkably, the addition of variations in AST level to the model predicted bariatric surgery-induced NASH remission without ambiguity. Asterisks denote statistical significance (***p < 0.001) by the Wilcoxon rank-sum test.

FIGURE 1

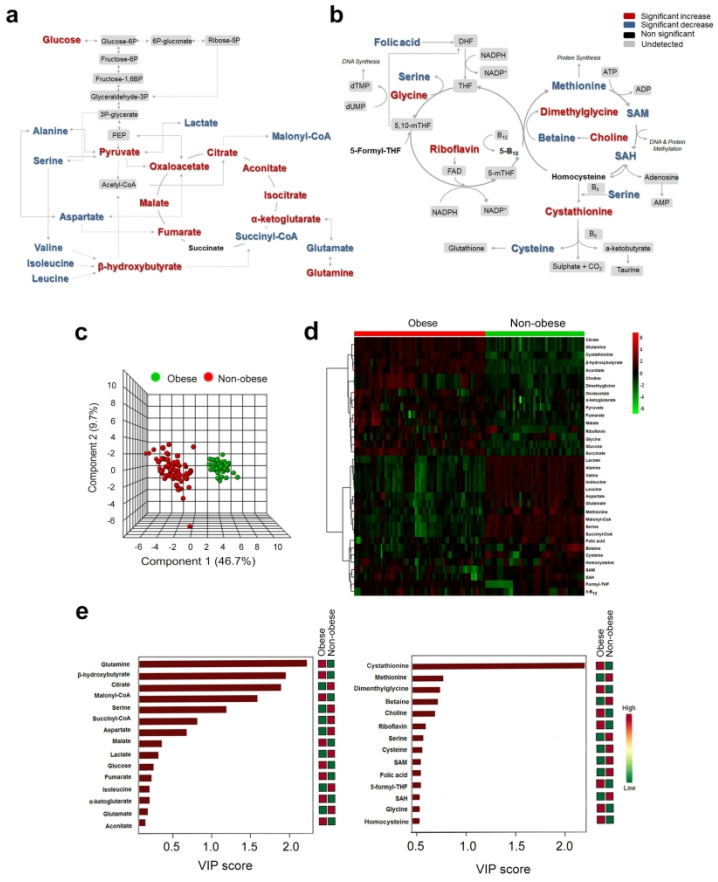

Figure 1

209x297mm (300 x 300 DPI)

FIGURE 2

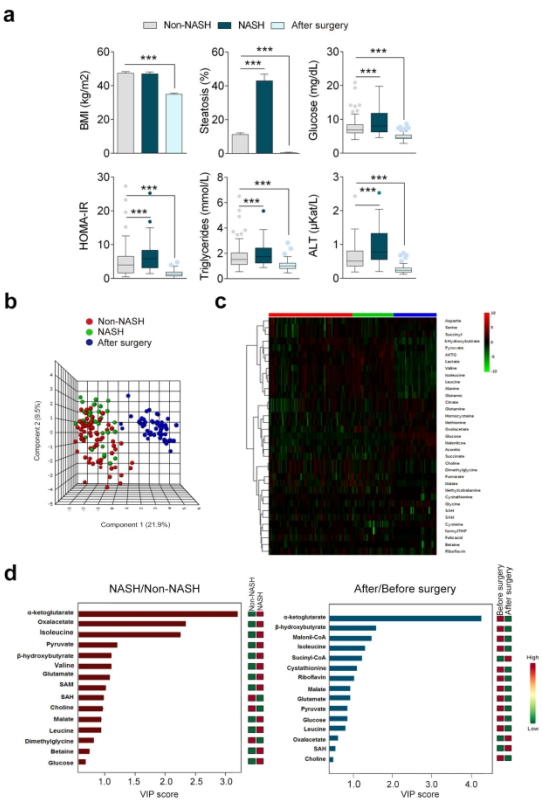

Figure 2

209x297mm (300 x 300 DPI)

FIGURE 3

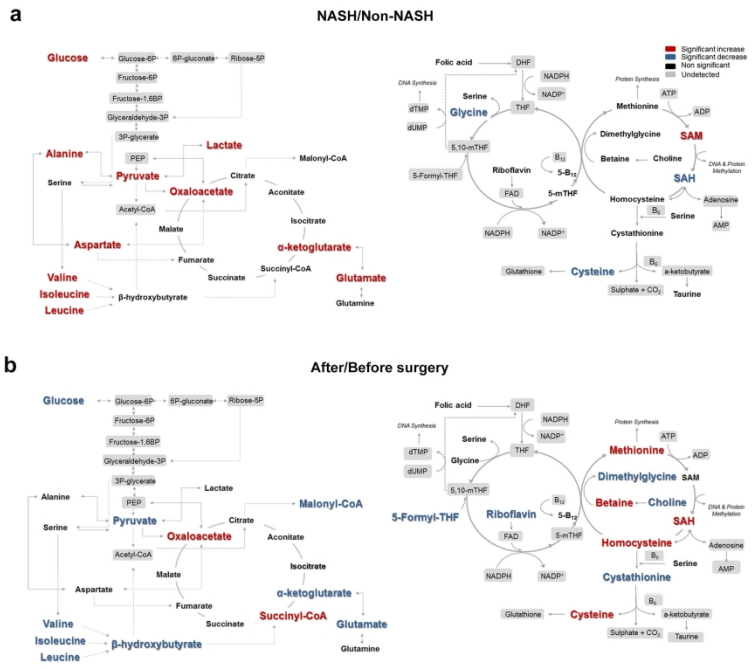

Figure 3

209x297mm (300 x 300 DPI)

FIGURE 4

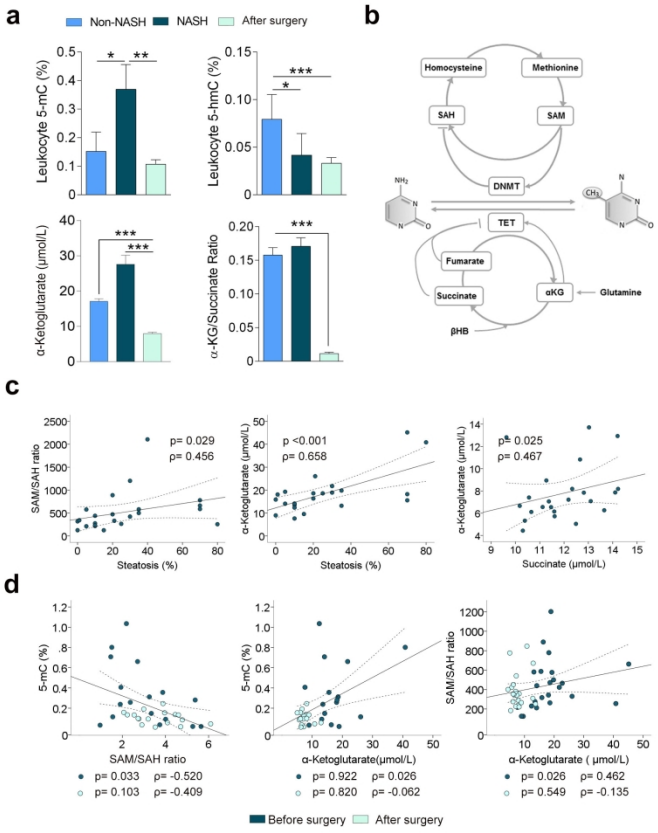

Figure 4

209x297mm (300 x 300 DPI)

FIGURE 5

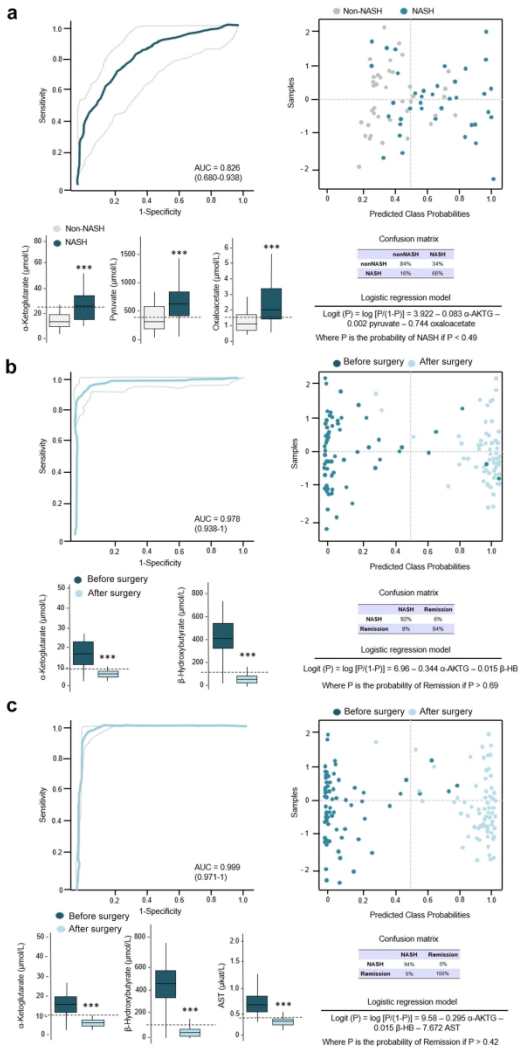

Figure 5

209x297mm (300 x 300 DPI)

Table 1. Clinical and laboratory assessment in nonobese controls and obese patients

.

	Nonobese controls (n=50)	Obese patients (n=270)	p-*value*
Clinical characteristics			
Male, n (%)	10 (20.4)	69 (25.7)	0.279
Age, years	47 (32-62)	49 (41-58)	0.652
BMI, kg/m2	25.2 (22.3-28.0)	46.4 (42.4-51.6)	**<0.001**
T2DM, n (%)	2 (4.1)	105 (39.0)	**<0.001**
Hypertension, n (%)	4 (8.2)	169 (62.8)	**<0.001**
Dyslipidemia, n (%)	2 (4.1)	98 (36.4)	**<0.001**
Medication, %			
Metformin	1 (2.0)	76 (28.4)	**<0.001**
Insulin	-	22 (8.2)	-
Sulfonylureas	-	16 (5.9)	-
ACEIs + ARA II	1 (2.0)	22 (8.2)	**<0.001**
Diuretics	1 (2.0)	33 (12.3)	**<0.05**
Statins	-	52 (19.3)	-
Laboratory assessment			
Hemoglobin, g/dL	14.0 (13.1-14.8)	13.3 (12.5-14.4)	**0.041**
Leukocytes, x109/L	6.5 (5.9-7.5)	7.9 (6.6-9.3)	**<0.001**
Platelets, x109/L	245 (210-272)	212 (182-252)	**<0.001**
Total cholesterol, mmol/L	5.1 (4.5-5.7)	4.3 (3.7-5.1)	**<0.001**
HDL-cholesterol, mmol/L	1.6 (1.3-1.8)	1.2 (1.0-1.5)	**<0.001**
LDL-cholesterol, mmol/L	3.0 (2.5-3.6)	3.3 (2.8-3.9)	**0.01**
Triglycerides, mmol/L	0.9 (0.7-1.4)	1.0 (1.1-2.2)	**0.01**
Glucose, mmol/L	4.7 (4.3-5.3)	7.3 (6.2-9.1)	**<0.001**
Insulin, pmol/L	48.8 (32.9-59.5)	91.3 (46.5-149.2)	**<0.001**
HOMA-IR	1.4 (0.9-2.0)	4.3 (2.2-7.5)	**<0.001**
Albumin, g/L	43.5 (41.9-45.0)	40.4 (36.4-44.0)	**<0.001**
AST, µKat/L	0.3 (0.2-0.4)	0.5 (0.4-0.8)	**<0.001**
ALT, µKat/L	0.3 (0.2-0.4)	0.6 (0.4-0.9)	**<0.001**
GGT, µKat/L	0.2 (0.1-0.4)	0.4 (0.2-0.6)	**<0.001**
CRP, mg/L	1.3 (0.5-3.0)	5.0 (0.8-12.2)	**<0.001**

Values are expressed as number (percentage) or median (interquartile range) in the indicated units. ACEIs: angiotensin-converting-enzyme inhibitor; ALT: alanine aminotransferase; AST: aspartate aminotransferase; ARA-II: angiotensin II receptor antagonists; BMI: body mass index; CRP: C-reactive protein; GGT: γ-glutamyl transferase; HDL: high-density lipoprotein; HOMA-IR: homeostatic model assessment of insulin resistance; LDL: low-density lipoprotein; T2DM: type 2 diabetes mellitus.

Table 2. Clinical and laboratory assessment in obese patients segregated by liver histologic features and NASH patients 12 months after surgery.

	Non-NASH (n=130)	NASH (n=53)	NASH after surgery (n=53)
Clinical characteristics			
Male, n (%)	29 (22.3)	18 (33.9)	-
Age, years	47 (41 - 57)	50 (42 - 58)	-
BMI, Kg/m^2	45.7 (42.3 - 51.6)	46.6 (42.5 - 51.9) [a]	34.3 (31.3-37.5) [b, c]
T2DM, n (%)	45 (34.6)	29 (54.7) [a]	9 (16.7) [b, c]
Hypertension, n (%)	76 (58.4)	41 (77.3) [a]	23 (43.4) [b, c]
Dyslipidaemia, n (%)	40 (30.7)	23 (43.3) [a]	5 (9.4) [b, c]
Medication (%)			
Metformin	31 (23.8)	20 (37.7) [a]	8 (15.1) [b, c]
Insulin	7 (5.3)	7 (13.2)	2 (3.3) [b, c]
Sulfonylureas	7 (5.3)	7 (13.2)	-
ACEIs + ARABS	48 (36.9)	26 (49)	9 (16.7) [b, c]
Diuretics	12.7 (9.7)	8 (15.1)	-
Statins	21 (15.9)	12 (22.6)	5 (9.4) [b, c]
Laboratory assessment			
Hemoglobin, g/dL	13.0 (12.4 - 14.1)	13.4 (12.1 - 14.4) [a]	13.3 (12.2-14.7)
Leukocytes, x10^9/L	7.6 (6.2 - 9.6)	7.8 (6.6 - 8.7)	6.6 (5.3-7.5) [b, c]
Platelets, x10^9/L	207.5 (184 - 254)	225.0 (179.0 - 249.5)	231.0 (184.8-287.5)
Ferritin, µg/L	55.0 (24.8 - 87.0)	97.4 (24.5 - 202.45) [a]	57.2 (23.6-110.8) [b, c]
Total-cholesterol, mmol/L	4.9 (4.5 - 5.4)	4.9 (4.3 - 5.5)	5.0 (4.5-5.9) [b, c]
HDL-cholesterol, mmol/L	1.4 (1.1 - 1.7)	1.1 (0.9 - 1.4) [a]	3.0 (2.6-3.5) [b, c]
LDL-cholesterol, mmol/L	2.8 (2.4 - 3.5)	2.8 (2.4 - 3.9)	1.6 (1.3-1.9) [b, c]
Triglycerides, mmol/L	1.5 (1.1 - 2.0)	1.7 (1.2 - 2.3) [a]	1.0 (0.8-1.2) [b, c]
Glucose, mmol/L	6.8 (6.0 - 8.4)	7.8 (6.2 - 11.4) [a]	4.7 (4.3-5.4) [b, c]
Insulin, pmol/L	97.9 (41.8 - 152.4)	109.2 (65.1 - 193.7) [a]	39.6 (24.0-60.1) [b, c]
HOMA-IR	4.1 (1.8 - 6.7)	6.1 (3.4 - 8.7) [a]	1.2 (0.7-1.9) [b, c]
Albumin, g/L	43.0 (40.0 - 44.0)	41.0 (36.6 - 44.0)	43.0 (41.0-45.0) [c]
AST, µkat/L	0.5 (0.4 - 0.7)	0.7 (0.5 - 1.2) [a]	0.3 (0.2-0.3) [b, c]
ALT, µkat/L	0.5 (0.3 - 0.8)	0.7 (0.5 - 1.2) [a]	0.2 (0.2-0.3) [b, c]
GGT, µkat/L	0.3 (0.2 - 0.4)	0.5 (0.3 - 0.7) [a]	0.2 (0.2-0.4) [b, c]
CRP, mg/L	5.1 (4.3 - 7.0)	5.8 (4.8 - 7.1)	0.3 (0.2-0.5) [b, c]
Liver histologic features			
Steatosis			
<5%	81 (62.0)	-	51 (96.7)
5-33%	45 (34.8)	5 (7.9)	2 (3.3) [b, c]
34-66%	4 (3.3)	33 (57.9)	-
>66%		20 (34.2) [a]	-
Lobular inflammation			
No foci	40 (30.4)	-	43 (81.6)
<2 foci	69 (53.3)	8 (13.2)	10 (18.4) [b, c]
2-4 foci	20 (15.2)	26 (44.7)	-
>4 foci	-	24 (42.1) [a]	-
Hepatocellular ballooning			
None	124 (95.7)	9 (15.8)	43 (81.6)
Few cells	3 (2.2)	44 (76.3)	10 (18.4)
Many cells	-	5 (7.9) [a]	
Fibrosis			
None (F0)	52 (40.2)	20 (34.2)	24 (45.8)
Perisinusoidal or periportal(F1)	57 (43.5)	14 (23.7)	27 (50.0)
Perisinusoidal and portal (F2)	17 (13.0)	9 (15.8)	2 (4.2) [b, c]
Bridging fibrosis (F3)	1 (1.1)	12 (21.1)	-

Values were expressed as number (percentage) or median (interquartile range) in the indicated units. ACEIs: angiotensin-converting-enzyme inhibitor; ALT: alanine aminotransferase; AST: aspartate aminotransferase; ARA-II: angiotensin II receptor antagonists; BMI: body mass index; CRP: C-reactive protein; GGT: γ-glutamyl transferase; HDL: high-density lipoprotein; HOMA-IR: homeostatic model assessment of insulin resistance; LDL: low-density lipoprotein; T2DM: type 2 diabetes mellitus. The letters denote significant (at least p<0.05) differences comparing [a] non-NASH vs NASH, [b] non-NASH vs NASH after surgery and [c] NASH vs NASH after surgery.

UNIVERSITAT ROVIRA I VIRGILI
ASSESSING DIAGNOSTIC AND THERAPEUTIC TARGETS IN OBESITY-ASSOCIATED LIVER DISEASES
Noemí Cabré Casares

Others

UNIVERSITAT ROVIRA I VIRGILI
ASSESSING DIAGNOSTIC AND THERAPEUTIC TARGETS IN OBESITY-ASSOCIATED LIVER DISEASES
Noemí Cabré Casares

LIST OF PUBLICATIONS AND COMMUNICATIONS

- Rodríguez-Tomàs E, Murcia M, Arenas M, Arguís M, Gil M, Amigó N, Torres T, Sebastià S, Baiges-Gayà G, **Cabré N**, Luciano-Mateo F, Hernández-Aguilera A, Fort-Gallifa I , Camps J*, Joven J. **Serum paraoxonase-1-related variables and lipoprotein profile in patients with lung or head and neck cancer: Effect of radiotherapy**. Antioxidants. Item status: Acepted

- **Cabré N**, Luciano-Mateo F, Baiges-Gaya G, Fernández-Arroyo S, Hernández-Aguilera A, Fibla M, Paris M, Sabench F, Daniel Del Castillo D, Menendez JA, Camps J, Jorge Joven J. **NASH modulates circulating metabolites from energy and one-carbon metabolism in obesity: implication in NASH remission.** Gastroenterology. Item status: Revision

- **Cabré N**, Luciano-Mateo F, Fernández-Arroyo S, Baiges-Gaya G, Hernández-Aguilera A, Fibla M, Fernández-Julia R, Paris M, Sabench F, Daniel Del Castillo D, Menendez JA, Camps J, Jorge Joven J. **Laparoscopic sleeve gastrectomy reverses non-alcoholic fatty liver disease modulating oxidative stress and inflammation.** Metabolism. doi.org/10.1016/j.metabol.2019.07.002. Impact factor: 6.513. Q1/D1

- Luciano-Mateo F, **Cabré N**, Fernández-Arroyo S, Baiges-Gaya G, Hernández-Aguilera A, Rodríguez-Tomàs E, Mercado-Gómez M, Menendez JA, Camps J, Joven J. **Chemokine (C-C motif) ligand 2 gene ablation protects low-density lipoprotein and paraoxonase-1 double deficient mice from liver injury, oxidative stress and inflammation.** Biochim Biophys Acta Mol Basis Dis. 2019 Mar 21. pii: S0925-4439(19)30080-8. doi: 10.1016/j.bbadis.2019.03.006. Impact factor: 4.328. Q1

- Hernández-Alvarez MA, Sebastián D, Vives S, Saška I, Bartoccioni P, Kakimoto P, PlanaN, 1 , Veiga S.R, Hernández V, Vasconcelos N, Gopalacharyulu P, Adrover A, Jové M, Pamplona R, Berenguer-Llergo A, Gordaliza I, Calvo E, **Cabré N**, Castro R, Kuzmanic A, Boutant M, Sala D, Hyotylainen T, Orešič M, Fort J, Errasti-Murugarren E, Orozco M, Joven J, Cantó C, Palacin P, Fernández-Veledo S, Vendrell J and Zorzano A**. Deficient endoplasmic reticulum-mitochondrial phosphatidylserine transfer causes liver disease**. Cell. 2019 May 2;177(4):881-895.e17. doi: 10.1016/j.cell.2019.04.010. Impact factor: 36.216. D1/Q1

- Arenas M, Rodríguez E, García-Heredia A, Fernández-Arroyo S, Sabater S, Robaina R, Gascón M, Rodríguez-Pla M, **Cabré N**, Luciano-Mateo F, Hernández-Aguilera A, Fort-Gallifa I, Camps J, Joven J. **Metabolite normalization with local radiotherapy following breast tumor resection**. PLoS One. 2018 Nov 16;13(11):e0207474.. Impact Factor: 2.776. Q2

- Hernández-Aguilera A, Fernández-Arroyo S, **Cabre N**, Luciano-Mateo F, Baiges-Gaya G, Fibla M, Martín-Paredero V, Menendez JA, Camps J, Joven J. **Plasma Energy-Balance Metabolites Discriminate Asymptomatic Patients with Peripheral Artery Disease**. Mediators Inflamm. 2018 Sep 20;2018:2760272. Impact factor: 3.545. Q2

- **Cabré N**, Luciano-Mateo F, Arenas M, Nadal M, Baiges-Gaya G, Hernández-Aguilera A, Fort-Gallifa I, Rodríguez E, Riu F, Camps J, Joven J, Domingo JL. **Trace element concentrations in breast cancer patients**. Breast. 2018 Oct 1;42:142-149. Impact factor: 3.494. Q1

- Garrido P, Rovira C, Cueto P, Fort-Gallifa I, Hernández-Aguilera A, **Cabré N**, Luciano-Mateo F, García-Heredia A, Camps J, Joven J, Garcia E, Vallverdú I. **Effect of continuous renal-replacement therapy on paraoxonase-1-related variables in patients with acute renal failure caused by septic shock**. Clin Biochem. 2018 Nov;61:1-6. Impact factor: 2.430. Q2

- Luciano-Mateo F, **Cabré N**, Nadal M, García-Heredia A, Baiges-Gaya G, Hernández-Aguilera A, Camps J, Joven J, Domingo JL. **Serum concentrations of trace elements and their relationships with paraoxonase-1 in morbidly obese women**. J Trace Elem Med Biol. 2018 Jul;48:8-15. Impact factor: 2.894. Q2

- Cuyàs E, Verdura S, Llorach-Pares L, Fernández-Arroyo S, Luciano-Mateo F, **Cabré N**, Stursa J, Werner L, Martin-Castillo B, Viollet B, Neuzil J, Joven. **Metformin directly targets the H3K27me3 demethylase KDM6A/UTX**. Aging Cell. 2018 May 8:e12772. Impact factor: 7.356. D1/Q1

- Iftimie S, García-Heredia A, Pujol-Bosch F, Pont-Salvadó A, López-Azcona AF, Hernández-Aguilera A, **Cabré N**, Luciano-Mateo F, Fort-Gallifa I, Castro A, Camps J, Joven J. **Serum Paraoxonase-1 Concentration as a Potential Predictor of Urinary Bladder Cancer Recurrence**. A Five Year Follow-Up Study. Arch Med Res. 2018 Feb;49(2):119-122. Impact factor: 1.895. Q3

- Rovira J, Hernández-Aguilera A, Luciano-Mateo F, **Cabré N**, Baiges-Gaya G, Nadal M, Martín-Paredero V, Camps J, Joven J, Domingo JL. **Trace Elements and Paraoxonase-1 Activity in Lower Extremity Artery Disease**. Biol Trace Elem Res. 2018 Nov;186(1):74-84. Impact factor: 2.431. Q3

- Arenas M, García-Heredia A, **Cabré N**, Luciano-Mateo F, Hernández-Aguilera A, Sabater S, Bonet M, Gascón M, Fernández-Arroyo S, Fort-Gallifa I, Camps J, Joven J. **Effect of radiotherapy on activity and concentration of serum paraoxonase-1 in breast cancer patients.** PLoS One. 2017. Impact Factor: 2.806. Q1 Nov 27;12(11):e0188633. Impact factor: 2.776. Q1

- Riera-Borrull M, García-Heredia A, Fernández-Arroyo S, Hernández-Aguilera A, **Cabré N**, Cuyàs E, Luciano-Mateo F, Camps J, Menendez JA, Joven J. **Metformin Potentiates the Benefits of Dietary Restraint: A Metabolomic Study.** Int J Mol Sci. 2017 Oct 28;18(11). pii: E2263.Imapct factor: 3.687. Q2.

- Martínez-García G, Pérez-Julián E, Agüí L, **Cabré N**, Joven J, Yáñez-Sedeño P, Pingarrón JM. **An Electrochemical Enzyme Biosensor for 3-Hydroxybutyrate Detection Using Screen-Printed Electrodes Modified by Reduced Graphene Oxide and Thionine.** Biosensors (Basel). 2017 Nov 11;7(4). pii: E50.

- Fort-Gallifa I, Hernández-Aguilera A, García-Heredia A, **Cabré N**, Luciano-Mateo F, Simó JM, Martín-Paredero V, Camps J, Joven J. **Galectin-3 in Peripheral Artery Disease. Relationships with Markers of Oxidative Stress and Inflammation**. Int J Mol Sci. 2017 May 4;18(5). pii: E973. Imapct factor: 3.687. Q2.

- Luciano-Mateo F, Hernández-Aguilera A, **Cabre N**, Camps J, Fernández-Arroyo S, Lopez-Miranda J, Menendez JA, Joven J. **Nutrients in Energy and One-Carbon Metabolism: Learning from Metformin Users**. Nutrients. 2017 Feb 10;9(2). pii: E121. Impact factor: 4.196. Q1.

- **Cabré N**, Camps J, Joven J. **Inflammation, mitochondrial metabolism and nutrition: the multi-faceted progression of non-alcoholic fatty liver disease to hepatocellular carcinoma**. Hepatobiliary Surgery Nutrition. 2016. doi: 10.21037/hbsn.2016.09.11

- Camps J, Hernández-Aguilera A, García-Heredia A, **Cabré N**, Luciano-Mateo F, Arenas M, Joven J. **Relationships between metformin, paraoxonase-1 and the chemokine (C-C motif) ligand 2.** Current Clinical Pharmacology. 2016. Impact factor: 3.584. Q1

- Hernández-Aguilera A, Fernández-Arroyo S, Cuyàs E, Luciano-Mateo F, **Cabré N**, Camps J, Lopez-Miranda J, Menendez JA, Joven J. **Epigenetics and nutrition-related epidemics of metabolic diseases: Current perspectives and challenges.** Food Chemical Toxicology. 2016. Impact factor: 3.584. Q1

- García-Heredia A, Riera-Borrull M, Fort-Gallifa I, Luciano-Mateo F, **Cabré N**, Hernández-Aguilera A, Joven J, Camps J. **Metformin administration induces hepatotoxic effects in paraoxonase-1-deficient mice.** Chemico-Biological Interactions. 2016. doi: 10.1016/j.cbi.2016.03.004. Impact factor: 2.577. Q2

- Hernández-Aguilera A, Sepúlveda J, Rodríguez-Gallego E, Guirro M, García-Heredia A, **Cabré N**, Luciano-Mateo F, Fort-Gallifa I, Martín-Paredero V, Joven J, Camps J. **Immunohistochemical analysis of paraoxonases and chemokines in arteries of patients with peripheral artery disease**. International Journal of Molecular Sciences. 2015. doi: 10.3390/ijms160511323. Impact factor: 2.862.Q2

LIST OF CONGRESS

- ***87nd European Atherosclerosis Society Congress (EAS).*** Luciano-Mateo F, **Cabré N**, Baiges-Gaya G, Rodríguez-Tomás E, Hérnadez-Aguilera A, Fernández-Arroyo F, Camps J, Joven J. **Systemic CCL2 overexpression promotes fibrosis and vascular alterations in a mouse model of accelerated aging.** Maastricht, Netherlands, 2019. Item Status: Accepted for oral presentation.

- ***EASL The International Liver Congress 2019.*** **Cabré N**, Chapsky DJ, Luciano-Mateo F, Baiges-Gaya G, Fernández-Arroyo F, Hérnadez-Aguilera A, Camps J, Rosa-Garrido M, Vondriska TM, Joven J. **Integrated analysis of DNA methylation and mRNA expression profiles to identify target gens in non-alcoholic fatty liver disease.** Vienna, Austria, 2019. Item Status: Accepted for poster presentation.

- ***EASL The International Liver Congress 2019.*** Luciano-Mateo F, **Cabré N**, Baiges-Gaya G, Rodríguez-Tomás E, Hérnadez-Aguilera A, Fernández-Arroyo F, Camps J, Joven J. **Metabolic inflammation: The role of chemokine C-C motif ligan 2 in the crosstalk between liver tissue and muscle**. Vienna, Austria, 2019. Item Status: Accepted for poster presentation.

- ***Cell Symposia Aging and Metabolism 2018.*** Luciano-Mateo F; **Cabré N**; Baiges-Gaya G; Mercado-Gómez M; Rezola-Artero I; Rodríguez-Tomás E; Hernandez-Aguilera A; Fernández-Arroyo S; Camps J; Joven J. **Overexpression of CCL2 promote systemic alterations in a mouse model of accelerated aging.** Sitges, Spain 2018. Item Status: Poster presentation.

- ***NAFLD Summit Congress 2018***. **Cabré N**; Luciano Mateo F.; Baiges Gaya G.; Fernádez Arroyo S.; Camps J.; Joven J. **Energy metabolism in obesity reveals that NASH requires targeting AMPK/mTOR – driven pathways.** Geneva, Switzerland, 2018. Item Status: Oral presentation

- ***NAFLD Summit Congress 2018.*** Luciano-Mateo F; **Cabré N**; Baiges-Gaya G; Hernández-Aguilera A; Fernández-Arroyo S; Camps J; Joven J. **High fat high sucrose intake underlies the progression of simple steatosis to nonalcoholic steatohepatitis.** Geneva, Switzerland, 2018. Item Status: Oral presentation

- ***EASL The International Liver Congress 2018.*** Luciano-Mateo, F.; **Cabré, N**.; Baiges-Gaya, G.; Hernández-Aguilera, A.; Fernández-Arroyo, S.; Camps, J.; Joven, J. **The multifactorial pathogenesis of nonalcoholic fatty liver disease: connecting inflammation and oxidation** Paris, France 2018. Item Status: Poster presentation.

- ***EASL The International Liver Congress 2018.*** **Cabré, N**.; Luciano-Mateo, F.; Baiges-Gaya, G.; Águila-Hervás, P.J.; Català-Blanco, M.; Hernández-Aguilera, A.; Fernández-Arroyo, S.; Camps, J.; Joven, J**. Effects of bariatric surgery on non-alcoholic fatty liver disease: The role of macrophage-mediated the systemic inflammation.** Paris, France 2018. Item Status: Poster presentation.

- ***86nd European Atherosclerosis Society Congress (EAS).*** Hernández-Aguilera, A.; Fernández-Arroyo, S.; Pantoja, C.; Mercado, M.; Luciano-Mateo, F.; **Cabré, N**.; Baiges, G.; Martin-Paredero, V.; Camps, J.; Joven, J. **Energy metabolism as a potential source of biological markers in abdominal aortic aneurysm** Lisboa, Portugal, 2018. Item Status: Poster presentation.

- ***86nd European Atherosclerosis Society Congress (EAS).*** **Cabré, N**.; Luciano-Mateo, F.; Baiges, G.; Fernández-Arroyo, S.; Hernández-Aguilera, A.; Camps, J.; Joven, J. **Bariatric surgery reverses DNA methylation modifying one carbon metabolism.** Lisboa, Portugal, 2018. Item Status: Oral presentation

- ***XIII Congrés Català de Ciències de Laboratori Clínic.*** Hernández-Aguilera, A.; Fernández-Arroyo, S.; Pantoja, C.; Mercado, M.; Fort-Gallifa I.; Luciano-Mateo, F.; **Cabré, N**.; Baiges, G.; Martin-Paredero, V.; Camps, J.; Joven, J.. **EL Metabolisme energètic com a potencial font de marcadors biològics en l'aneurisma d'aorta abdominal.** Reus, Spain, 2018. Item Status: Poster presentation

- ***XIII Congrés Català de Ciències de Laboratori Clínic.*** Baiges, G.; Hernández-Aguilera, A.; Pantoja, C.; **Cabré N**.; Luciano-Mateo, F.; Fort-Gallifa I.; Martin-Paredero, V.; Camps, J.; Joven, J. **Fragments de degradació de la matriu extracel·lular com a possibles marcadors biològics en l'aneurisma d'aorta abdominal.** Reus, Spain, 2018. Item Status: Poster presentation

- ***XIII Congrés Català de Ciències de Laboratori Clínic.*** **Cabré N**.; Luciano Mateo F; Hernández Aguilera A.; Fernández Arroyo S.; Baiges Gaya G.; García Heredia A.; Camps Andreu J.; Joven J. **El paper de l' α-cetoglutarat i el β-hidroxibutirat en la malaltia de l'esteatosi hepàtica no alcohòlica asociada a obesitat mòrbida: una aproximació metabolòmica**
  Reus, Spain, 2018. Item Status: Poster presentation

- ***EASL The International Liver Congress 2017.*** **Cabré N**.; Luciano-Mateo F; Hernández-Aguilera A.; Fernández-Arroyo S.; Baiges Gaya G.; García-Heredia A.; Camps Andreu J.; Joven J. **Role of α-ketoglutarate and β-hydroxybutyrate in morbid obesity-associated non-alcoholic fatty liver disease: metabolomic approach**. Amsterdam, Netherlands 2017. Item Status: Poster presentation

- ***EASL The International Liver Congress 2017.*** Luciano Mateo F; **Cabré N**. Casares; Hernández Aguilera A.; Baiges Gaya G.; García Heredia A.; Fernández Arroyo S.; Camps Andreu J.; Joven J. **The role of chemokine (C-C motif) ligand 2 and the diet influence in the energy metabolism**. Amsterdam, Netherlands 2017. Item Status: Poster presentation

- ***EASL The International Liver Congress 2017.*** Juul Nielsen M.; **Cabré N**.; Julie Leeming D.; Karsdal AM.; Joven J**. Serologically assessed extracellular matrix remodeling is affected by bariatric surgery in morbidly obese NAFLD patients with 12 months follow-up**. Amsterdam, Netherlands 2017. Item Status: Poster presentation

- ***12th International Meeting on Cholinesterases-Sixth International Conference on Paraoxonases .*** **Cabré N**, Lucino-Mateo F, Guirro M, Esther Rodríguez-Gallego E, Hernández-Aguilera A, García-Heredia A, Fernández-Arroyo S, Camps J, Joven J. **Inflammation and oxidation in class III obesity: the role of chemokine (C-C motif) ligand 2 and paraoxonase 1.** Elche, Spain 2015. Item Status: Poster presentation

- ***83nd European Atherosclerosis Society Congress (EAS).*** Esther Rodríguez-Gallego E, Mariné-Casadó R, Guirro M, Hernández-Aguilera A, Lucino-Mateo F, **Cabré N**, Fernández-Arroyo S, Camps J, Joven J. **Inflammation and metabolism: The role of chemokine (C-C motif) ligand 2.** Glasgow, UK 2015. Item Status: Poster presentation

- ***83nd European Atherosclerosis Society Congress (EAS).*** Hernández-Aguilera A, **Cabré N**, Luciano-Mateo F, Rodríguez-Gallego E, Guirro M, Fernández-Arroyo S, Mariné-Casadó R, Camps J, Joven J. **Expression of functional and silent receptors of CCL2 in human coronary arteries**. Glasgow, UK 2015. Item Status: Poster presentation